An investigation into the mechanistic behaviour of RAFT-mediated miniemulsion polymerizations.

By

Marie-Claire Hermant

Thesis presented in partial fulfillment of the requirements for the degree of

Master of Science (Polymer Science)

at the

University of Stellenbosch

Study leader: Prof. R.D Sanderson

Co-study leader: Dr J.B McLeary **December 2005**

Declaration

I, the undersigned, hereby declare that the work contained in this thesis is my own original work and that I have not previously in its entirety or in part submitted it at any university for a degree

Signature……Date……

Pectora roborant cultus recti

ABSTRACT

Polymerization using the reversible addition-fragmentation chain transfer (RAFT) process affords a researcher control over the molecular weight and polydispersity of the final polymer. Research is being carried out globally, using heterogeneous RAFT systems, as these systems offer superior industrial possibilities. Many emulsion systems fail when incorporating RAFT agents due to phase separation and colloidal instability. Exchanging conventional emulsion polymerizations with predispersed polymerization systems (i.e. miniemulsions) has shown many improvements. Evidence of uncontrolled aqueous phase polymerization (i.e. not mediated by the RAFT process) has however been found. This behaviour is similar to polymerization in a conventional emulsion polymerization system, but is not expected in miniemulsion polymerization.

In this study, the mechanisms and kinetics behind the formation of conventionally polymerized polymer within RAFT-mediated miniemulsion polymerization is investigated. Variables within the miniemulsion formulation such as the surfactant type, concentration, initiator hydrophobicity and RAFT agent structure are varied so as to determine relationships between the miniemulsion formulation and uncontrolled polymerization. The elimination of uncontrolled polymerization is achieved by means of the inclusion of aqueous phase radical traps.

Distinct relationships between the RAFT agent structure, particle size and initiator hydrophobicity were found. A model describing the radical escape from growing particles is proposed and validated.

OPSOMMING

Polimerisasie deur gebruik te maak van omgekeerde addisie-fragmentasie oordrag (OAFO) geïnduseerde sisteme het oor die afgelope tydperk baie populêr geword aangesien dit ‘n navorser toelaat om die molekulêre massa en polidispersiteit van die finale polimeer te beheer. Verdere navorsing word nou wêreldwyd uitgevoer met heterogene OAFO sisteme aangesien hierdie sisteme superieure industrïele moontlikhede na vore bring. Dit moet egter in ag geneem word dat verskeie emulsie sisteme faal sodra OAFO geïnkorporeer word as gevolg van fase-skeiding en kolloidale onstabiliteit. Deur gewone emulsie polimersiasies met mini-emulsies te vervang, is verskeie verbeterings opgemerk. Bewyse van onbeheerde waterfase polimerisasie (i.e. sonder enige OAFO inkorporasie) is reeds gevind. Hierdie resultate is vergelykbaar met die van ‘n konvensionele emulsie polimerisasie sisteem, maar nie met mini-emulsie polimerisasie nie.

In hierdie studie, is die meganismes en kinetika verantwoordelik vir die vorming van konvensioneel-gepolimeriseerde polimer tydens OAFO-geïnduseerde mini-emulsies ondersoek. Verskeie veranderlikes binne die mini-emulsie formulasie, b.v. die seep-tipe en konsentrasie, afsetter hidrofobisiteit en OAFO-agent struktuur, is gevarieer om die verwantskappe tussen mini-emulsie formulasies en onbeheerde polimerisasie vas te stel. Die eliminasie van onbeheerde polimerisasie deur gebruik te maak van water-fase radikaallokvalle is ook ondersoek..

Die verhouding tussen die OAFO-agent struktuur, partikel groote en afsetter hidrofobisiteit is vasgestel. ’n Model wat die ontsnapping van radikale van groeiende partikels beskryf is voorgestel en

ACKNOWLEDGEMENTS

"No man is an island, entirety in itself; every man is a piece of the continent." – John Donne

This expression I truly began to appreciate during the undertaking of my MSc study. The concept that academic excellence is rooted in a hermitic existence focused on one field or area of study is flawed. During the past year and a half, as well as the preceding 4 years of undergraduate studies, I have discovered the true depth of friendship and companionship that walks hand in hand with any great achievement. In these acknowledgements I would like to thank those who have supported me, motivated and even kept me sane.

Keeping long distance relationships intact requires significant input from both sides. I would like to thank all my friends in Pretoria for always contacting me, and being interested in my *Maties* life over the last five years. They especially made me feel very welcome when returning home by letting me back into their personal lives. The old Girls High crowd: Jeanne, Natalie, Lyndall, Andrea, Romy and Wendy will never leave my heart. Special mention goes to Susan, Angelique, Bronwyn and Louise (Dvah) who have been an unbelievable group of close friends. Our friendship has endured much and has grown to be a bond that will never fatigue. To the Stellenbosch crowd: Hanneke, Emma, Andi, Sarah, Lizelle, Rene, Gareth, Lloyd, Jaco, Heinke, Carl, Werner, Andreas, Vernon B., Nicholas, Morne and Fabio, I'd like to send thanks for making my Uni experience extremely memorable and for always being there when I needed cheering up or discipline to work. Housemates, roommates and flat mates play an enormous role in the development of one's personality during the young adult years. For all the wonderful times and even the small catfights I'd like to thank Louise (Woz), Tracy, Jo and Gretha. Special thanks goes to Saskia. Our friendship has gone through many ups and downs during the 5 years that we have lived together, but I know that it is a friendship that will never cease to exist. Special thanks also goes to Louise for being an unbelievable friend during our migration to the Cape. All these friends have formed *families* all over South Africa that have accepted me and brought me great joy.

Family forms a foundation immovable by most forces. The various families in my life have acted as support systems during the years that I have been away from my immediate family. I'd like to thank the Van Rooyens: Aui, Oupa, Tani Ina, Karin and Alexi; the Hermants: Karen, Laurent and especially Meme and Pepe; the Kirsteins: Sylvia, Volker, Dorthe and Arno; the Wilsons: Isabelle, Geoff, Nicholas and Sean. To my immediate family: Bernhard, Martin and Lisa, I'd like to send

thanks for the love that I have always felt even though sometimes the times were hard. And to my three “adopted” families: the van Wingerdens, the Stumpfs and the Versters, I’d like to send thanks for being my home away from home. I’m greatly indebited to these *families*.

When I entered my MSc, I was still naïve and confused about good laboratory practice, project management and even Polymer Science. My education in these three fields is thanks to those I came in contact with in the Division of Polymer Science at US. To the friends that I made there: Pauline, Lee-Sa, Stephan and Marius I’d like to send thanks for the many laughs at coffee and lunch breaks. The laboratory itself runs smoothly because of the hard work of two people that I owe many thanks to: Adam and Calvin. For their time put into the many GPC samples, as well as being friends outside the institute, I’d like to thank Dr Valerie Grumel, Dr Andre van Zyl and Gretha. Dr Jean McKenzie must be thanked for the NMR analyses, Dr Mohammed Jaffer for the TEM analyses and Dr Ewan Sprong for CHDF analyses. I’d also like to thank Dr Margie Hurndall for all the time spent editing my thesis. Without her help, the finalization of this work would have been much slower and far less efficient. To the various teachers, that I have had during my education at the institute, Dr Peter Mallon and Dr van Reenen, much thanks is owed. Working is not complete without a balanced amount of fun and games. For the good times, as well as constructive debates, I’d like to send many thanks to the Free Radical (OAFOXXX) research group at US: Andrew, Ingrid, Gwen, Vernon R., Achille, Howard, Eric, JC, Jacques, Nadine, Osama, Fozi and Reda. The amazing time I spent during my MSc year including our Friday expeditions to Bohemia (amongst many others) is largely due to their friendship. When I first entered the Free Radical labs at the end of my BSc, I was made to feel very welcome, albeit my ignorance and complete lack of the most general free radical knowledge, by “die manne”: Evan, Malan, Jaco (Lam) and James as well as Matthew. Many thanks to these colleagues, for all their patience and acceptance as well as the friendships that are still alive even through long distances. Special thanks goes to the leader of the RAFT group and my co-study leader Dr James McLeary (boss) who has been a great inspiration to me. There have been laughs, and even tears, but for all the time he put into assisting me with finally writing this thesis as well as the project itself I am ever grateful. I hope for many years to come that we can remain in contact, not just in the academic realm, but also as friends. Prof. R.D. Sanderson (Doc) must be thanked for supporting me from my first days at Polymer Science and always encouraging me to reach my full potential. I hope that we still remain in contact and even engage in collaborations in future projects. As my study leader, he has always been a source of new ideas and

insights. These people all formed a *family* in my academic as well as personal life over the last years, for which I am ever grateful.

The last three people I would like to thank are most definitely the closest and most dear people to me. My partner Dale has been a bastion of strength over the last three years. Many thanks are owed to him for surviving all the good and bad times. My parents, Tinka and Guillaume, besides giving me the opportunity to live as well as experience so many great things during my 23 years, have been a source of much joy and love. While many times I have lived far away from both of them, they have always made a great effort to make their love be felt over many kilometers. Through all the tough times of puberty and childhood, my parents have had the patience and love that could endure all. I'd like to thank them for all the clear-minded advice that they shared as well as the moral code that they instilled in me. I hope that I can live up to be the person that they strove to mould. Not only must they be thanked for the financial support of my academic training, but also the interest and encouragement accompanied it. Thank you very much for all the opportunities, but most importantly, the unconditional love.

All the people mentioned in this acknowledgement fall into various *family* classes that have been with me over the last years. I'd like to send one last thank-you to all mentioned and also those that might have been omitted that also formed integral parts in my life. And to all these people I'd like to dedicate the following saying:

"Feelings of worth can flourish only in an atmosphere where individual differences are appreciated, mistakes are tolerated, communication is open, and rules are flexible - the kind of atmosphere that is found in a nurturing family." **–** Virginia Satir

INDEX

Pectora roborant cultus recti

Pectora roborant cultus recti

Pectora roborant cultus recti

LIST OF FIGURES

Pectora roborant cultus recti

Pectora roborant cultus recti

LIST OF SCHEMES

Pectora roborant cultus recti

LIST OF TABLES

Pectora roborant cultus recti

List of Symbols

β	Probability of reaction within the aqueous phase
C_t	Rate of chain transfer
C_W^{sat}	Saturated aqueous phase concentration
C^{sat}	Saturated particle monomer concentration
C_w	Concentration of initiator in the aqueous phase
C_p	Concentration of initiator in the particles
C_m	Chain transfer constant
D_w	Diffusivity of monomeric radicals in the aqueous phase
d_p	Polymer density
f	Radical efficiency
FW_M	Molecular weight of monomer
FW_{RAFT}	Molecular weight of RAFT agent
ΔG	Gibbs free energy
I_o	Initial concentration of initiator
[I]	Concentration of initiator
j_{crit}	Length of *j*mer
k_{fm}	Chain transfer to monomer rate coefficient
k_d	Dissociation constant
k_{pi}	Addition of initiating radical to monomer rate coefficient
k_p	Propagation rate coefficient
k_t	Termination rate coefficient
k_{tc}	Termination by coupling rate coefficient
k_{td}	Termination by disproportionation rate coefficient
k_{EXIT}	Radical exit rate coefficient
k_{COMB}	Rate coefficient of geminate recombination
M_n	Number average molar mass
M_w	Weight average molar mass

$[M]_0$	Initial concentration of monomer
$[M]$	Concentration of monomer
$[\mathrm{M}\cdot]$	Concentration of propagating chains
$\overline{M_n}$	Number average molar mass
$\bar{n}$	Average number of radicals
N_c	Number of particles
N_A	Avogadro's number
P	Probability of desorption
$P_{LAPLACE}$	Laplace pressure
$\overline{P_n}$	Average degree of polymerization
$[RAFT]_o$	Initial concentration of RAFT agent
R_p	Rate of polymerization
R	Ideal gas constant
R_{COMB}	Rate of geminate recombination
t	Time
T	Temperature
W_0	Initial monomer weight
x	Monomer conversion
γ_{LL}	Interfacial energy
r	Radius of particle
z	Length of $z$mer

Pectora roborant cultus recti

List of Abbreviations

ATRP	Atom transfer radical polymerization
AIBN	Azobisisobutyronitrile
BPO	Benzoyl peroxide
BA	Butyl acrylate
CTA	Chain transfer agent
CBD	Cumyl dithiobenzoate
CVADTB	Cyanovaleric acid dithiobenzoate
CPDTA	Cumylphenyl dithioacetate
CCT	Catalytic chain transfer
CMC	Critical micelle concentration
CTAB	Cetyl trimethyl ammonium bromide
CHDF	Capillary hydrodynamic fractionation
DT	Degenerative transfer
DIBTC	s-Dodecyl-s'-isobutryic acid trithiocarbonate
DPTC	s-Dodecyl-s'-phenylethyl trithiocarbonate
DMSO	Dimethyl sulphoxide
DDI	Distilled deionized water
DLS	Dynamic light scattering
ESR	Electron spin resonance
FRP	Free radical polymerization
GPC	Gel-permeation chromatography
HPLC	High performance liquid chromatography
HLB	Hydrophobic-lipophilic balance
KPS	Potassium persulphate
LRP	Living radical polymerization
MWD	Molecular weight distribution
MW	Molecular weight
NMR	Nuclear magnetic resonance
PDI	Polydispersity index
PRE	Persistent radical effect

PD	Polydispersity
PEDTB	Phenyethyl dithiobenzoate
PSD	Particle size distribution
RAFT	Reversible addition-fragmentation transfer
RI	Refractive index
SFRP	Stable free radical polymerization
SDS	Sodium dodecyl sulphate
SEC	Size exclusion chromatography
THF	Tetrahydrofuran
TEM	Transmission electron microscopy
UHP	Ultra high purity
UV	Ultraviolet

Pectora roborant cultus recti

Chapter 1. : *Introduction and Objectives*

1.1. INTRODUCTION

Owing to our evolution as a consumer society, the industries that supply our consumables have had to continually place increasing demands on the raw materials that are used in the production of consumables. Products are required to perform more specialized tasks and withstand a wider range of stresses. This in turn places new and increasing demands on the types of raw materials used in manufacturing. This trend is most evident in an industry like that of polymer production. Due to the fact that modern polymers are mainly synthetic products, the scope for design is wide. It now falls on the shoulders of the polymer scientist to design monomers, polymerization techniques and/or compounding processes that will deliver products for specialized applications.

In this thesis, the author investigates a specialized polymerization technique, namely reversible addition-fragmentation chain transfer (RAFT), which was designed to meet the above-mentioned requirement i.e. design control. Basic monomers are utilized, but it is the polymerization technique that provides the element of design control. The use of free radical polymerization as an efficient polymerization technique will be investigated. A discussion of the development of controlled/living free radical polymerization will follow and finally, it will be illustrated how the utilization of heterogeneous media, and more specifically miniemulsion systems, provide a manufacturer with an efficient polymerization technique. This technique, like many techniques, however has shortcomings. These will be investigated and solutions explored.

Pectora roborant cultus recti

1.2. FREE RADICAL POLYMERIZATION

The process of free radical polymerization (FRP) was documented as far back as the beginning of the 20th century.[1] By the early 1930s, the basic radical initiation and subsequent chain growth was understood.[2] Research performed into the free radical process boomed for many years, only to be slightly hampered by the increased interest in Ziegler-Natta catalysts.[3,4] FRP and metallocene catalysis polymerization are chain-growth or addition polymerization techniques, but utilize different active centers. The free radical polymerization uses initiators that become incorporated in the chains whereas Ziegler-Natta utilizes catalysts, which do not become incorporated into the chain, but regulate the monomer addition.

FRP is used extensively as an industrial process. More than 70% of vinyl polymers, which themselves comprise 50% of all plastics synthesized, are synthesized by this technique.[5] This is due mainly to the fact that the technique is tolerant to many impurities[6] and can be performed at a range

of temperatures, which simplifies the apparatus required. A wide range of monomers can also be utilized in FRP. Many of these monomers cannot be polymerized by any other technique.[7] These factors allow the relatively simple manufacture of many basic raw polymers utilized in industry. The application of FRP in aqueous systems also makes it very popular for industrial use. Emulsion polymerization incorporating free radical techniques accounts for 40-50% of all FRP systems.[8] All these advantages may lead one to assume that FRP is the main means of producing commercial polymers. There is however one strong disadvantage working against FRPs success. Radicals are highly reactive compounds. They react instantaneously with other radicals and undergo chain transfer to solvent and/or monomer in the system.[6] This reactivity leads to unpredictable behaviour in a polymerization system. Termination of radicals at any point in the polymerization of individual chains leads to the production of chains of varied lengths. This in turn leads to an increase in the polydispersity index (PDI). Many applications of polymers require the polymer to have distinct mechanical properties. These properties vary greatly with a change in molecular weight distribution of the polymer. The lack of control in the FRP technique leads to polymers that lack the designs that industry is so adamant to achieve. Ionic (cationic[9] and anionic[10]) polymerization and group transfer polymerization[11] are both able to provide this control, but these systems require stringent reaction conditions that are difficult to maintain in industrial applications. During the late 1980s, successful methods by which to maintain control within a free radical polymerization system were identified. This lead to the birth of "living" free radical polymerization (LRP).

1.3. "LIVING" FREE RADICAL POLYMERIZATION

The first few techniques became apparent in the early 1980s.[12] The concept of reversibly reacting stable free radicals with the radical polymer chains already in the system was introduced. Nitroxides were first used as stable free radicals.[13] This was the beginning of stable free radical polymerization (SFRP). During the subsequent years, many other techniques were discovered. These include atom transfer radical polymerization (ATRP)[14,15], degenerative transfer[16] and reversible addition-fragmentation transfer (RAFT).[17] These techniques all have the common mechanism of trapping active radical centers in a transition state between dormancy and activity.

$$\text{Dormant} \underset{}{\overset{k_{Ct}}{\rightleftharpoons}} \text{Active}$$

Figure 1.1: Technique of reversible termination.

k_{Ct} is the rate coefficient of chain transfer. The rate of termination is second-order whilst propagation is first-order. This implies that by reducing the number of growing radicals, the termination also decreases. This is achieved by reversibly deactivating the growing radicals with a scavenger (stable free radicals). The rate of transfer controls the "activated time" of the growing radicals. All the techniques mentioned earlier are designed such that C_t is very high and allows the growing radical to propagate to a limited degree. When the scavenger is in excess (compared to the initiator), a large portion of the polymer chains will be terminated with this scavenger that can later be activated. In this way, a controlled growth is maintained over most of the propagating chains. The control that is lacking in conventional FRP has now been added. "Living" radical polymerization is now defined as having the following characteristics:

- Mathematical modeling of theoretical molecular weights provides the ability to predetermine final molecular weights
- Polymers with a low polydispersity index (<1,3)
- End-group functionality can be altered in a simple manner

This new technique also lends a new characteristic to conventional FRP. On completion of the polymerization the chains are capped in a dormant state but this state can be reversed. Thus the chains can be brought "to life" again by the addition of more monomer (and other compounds, depending on the system used). In this way, the LRP technique can be seen to be a "living" system, similar to ionic polymerization. With this in mind, a further characteristic can be added to the list mentioned above:

- Facile formation of block copolymers or other architectured copolymer structures.

As was mentioned earlier, FRP techniques can be applied to aqueous systems. Generally this is true for LRP, but the degree of success varies from technique to technique.

1.4. "LIVING" FREE RADICAL POLYMERIZATION IN EMULSION SYSTEMS

The nature of free radical polymerization makes it compatible with heterogeneous aqueous systems such as emulsion systems. Such emulsion systems include macro-emulsions, mini-emulsions, micro-emulsions and inverse emulsions. These all use an oil-and-water combination but vary in

latex formation and latex particle sizes. The interest that industry shows for these systems is due to a variety of factors:

- The bulk of the reaction mixture is water, which is more environmentally friendly than many of the solvents otherwise used in solution polymerization, and it can easily be removed.[8]

- The heat capacity of water is much higher than that of many common solvents used in solvent polymerizations.[18] Thus, the heat dissipation in heterogeneous aqueous systems is much more efficient than in bulk and solvent systems. This minimizes the exotherm due to the Tromsdorff effect.

- The final polymer product is in a latex form of low viscosity but has a high solids-content, and this form can easily be processed.

- The probability of radical termination can be reduced by the localization of radicals to small reaction loci.

The application of LRP in heterogeneous systems is unfortunately not as easy as in the case of homogeneous systems like bulk-polymerization and solution-polymerization. Nitroxide-mediated emulsion polymerizations were found to have problems in terms of final emulsion stability, and it was found that the system kinetics were very different from that of a classical emulsion polymerization.[19] ATRP emulsion systems have been shown to give problems with control due to poor partitioning of the active species into the reaction loci.[20] The same problems were also seen with degenerative transfer.[21] In the latter two cases, seeded emulsion systems exhibited improved final control of the polymerization. RAFT in emulsion systems also suffered similar failures in stability.[22,23]

There remains much research still to be done on all these techniques before an industrially favorable system is achieved.

1.5. BACKGROUND TO THE PROJECT

The previous sections have described the development of free radical polymerization, all the way to living free radical polymerization. The current push in academia is to establish the kinetics of all these LRP techniques in various media. Currently the heterogeneous systems are under the spotlight

because of the industrial interest. This thesis focuses on such a specific heterogeneous system, namely miniemulsions. The LRP technique focused on is the RAFT technique.

Miniemulsions were first introduced in the 1970s and were shown to be effective as a polymerization system when compared to conventional emulsion systems.[24] The interest in miniemulsions increased due to the fact that a wider variety of monomers could be utilized (especially those that could not be polymerized in other systems). The incorporation of LRP techniques into miniemulsions led to mixed successes in terms of the established control of the chain growth. The ideal formulation with which to obtain stability was what all researchers in the field were trying to pinpoint. An easy formulation that led to a stable miniemulsion that retained its stability for up to months after preparation was eventually found by fellow workers.[25] A certain class of RAFT agents, namely dithiobenzoates, was used for this. In the original RAFT patent, many different RAFT agents are described.[17] It introduced another class of RAFT agents, the trithiocarbonates, which have higher k_{Ct} values than the dithiobenzoates. The application of the trithiocarbonates has been studied in conventional emulsion systems[26] but little research has been done on their application in miniemulsion systems. It has however been reported that the use of trithiocarbonates in miniemulsions has led to the formation of secondary polymer distributions that show little control.[27] Uncontrolled secondary polymer distributions have previously been seen in seeded miniemulsion systems where cyanoisopropyl-dithiobenzoate was used as the RAFT agent.[28] The origin of these distributions was explained by the fact that in a seeded system the RAFT agents are securely fixed in the original particles. Any new particles forming in the polymerization grow without the mediation of the RAFT mechanism, and thus show little control.

Different RAFT agents lead to vastly different miniemulsion polymerisations.[28,29] The nature of these differences can most probably be ascribed to the different structures of these agents. Hence, the correlation between the structure of the RAFT agents and the final behaviour of the system would possibly provide insight as to how best to optimize the miniemulsion to produce the desired polymer.

In this project the author investigated the behaviour of four RAFT agents: two trithiocarbonates and two dithiobenzoates within a miniemulsions system. The influence that various parameters had on miniemulsion systems incorporating various RAFT agents will be given. From this, comprehensive kinetic models of various RAFT-mediated miniemulsion polymerizations were formulated.

1.6. OBJECTIVES

The overriding objective of this study was to gather information on the mechamistic behaviour of RAFT-mediated miniemulsion polymerizations and, if possible, to formulate a composition that would provide an ideal reaction. The ideals desired include living radical polymerization characteristics including latex stability, homogeneous particles with respect to size and composition and high rates of reaction.

Within a miniemulsion system there are many variables that can influence the kinetic behaviour of the polymerization system. These include the locus of chain initiation and the location of the propagating radical chains. The incorporation of RAFT agents complicates the kinetics even further by adding new variables that increase the intricacy of the miniemulsion systems such as the location and distribution of the RAFT agent as well as effects that the presence of the RAFT agents may have on the radical types and concentrations.

In order to investigate the mechanistic behaviour of RAFT-mediated miniemulsion polymerizations it was considered both useful and systematic to examine the numerous reaction variables individually, and determine their effects on the mechanism of polymer formation. A RAFT-mediated miniemulsion polymerization comprises a minimum of five components: RAFT agent, initiator, monomer, and continuous phase (water) and surfactant. Starting with these components as variables and adding addition components to the polymerizations, detailed information on the mechanism of polymerization could be deduced.

The flow chart in Figure 1.2 serves to simplify the approach taken in this project; it shows the main variables in RAFT-mediated miniemulsion polymerizations and their role in the polymerization.

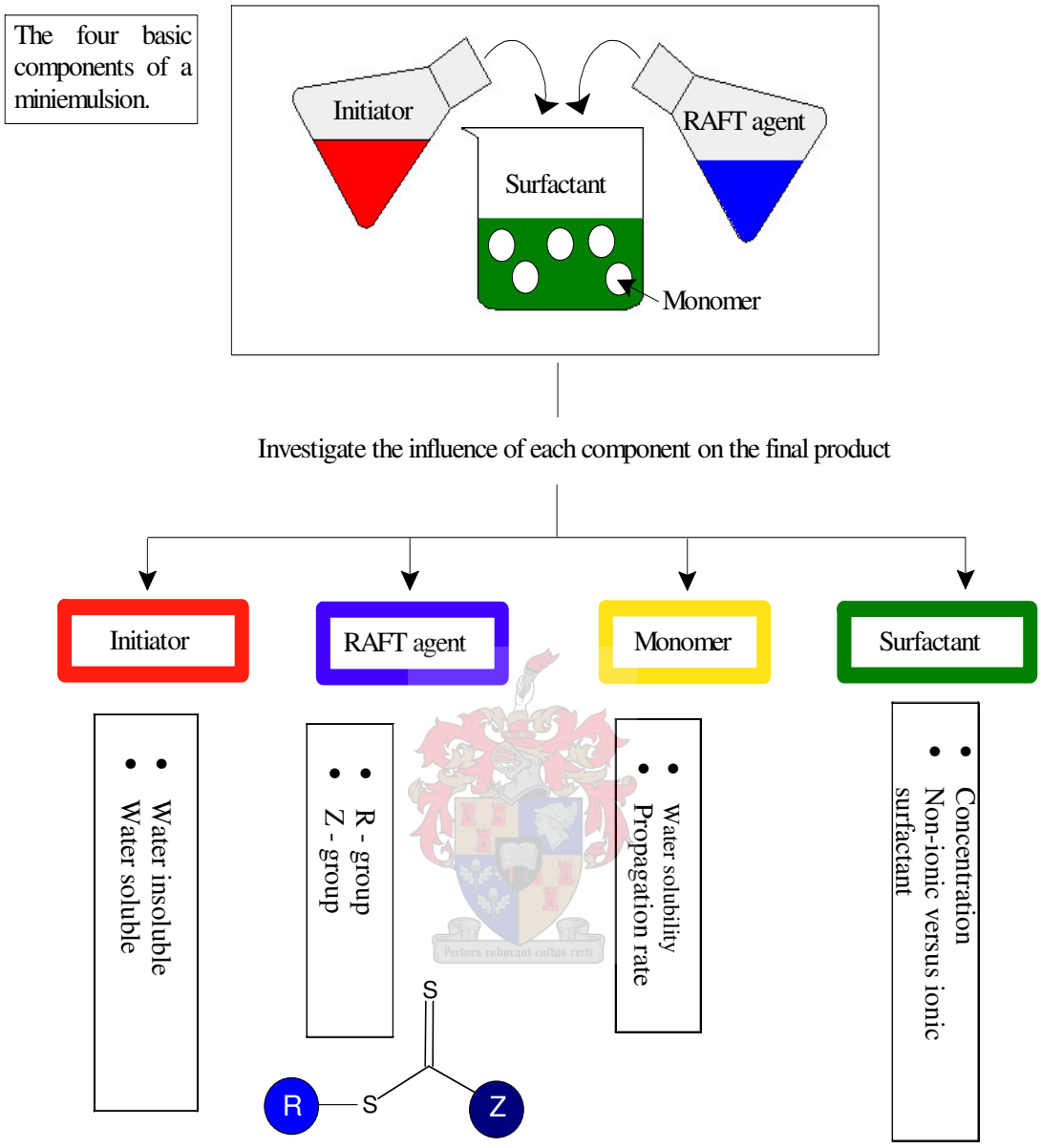

Figure 1.2: Flow chart indicating aspects to be considered in the project objectives (•).

The following specific variables were investigated:

1. **RAFT agent structure –** A serious of RAFT agents with differing:
    a. Stabilizing Z- group structure
    b. Leaving R- group structure

were synthesized and comparisons drawn between the effects of the different groups.

2. **Surfactant type** – Reactions were carried out utilizing:

    a. An ionic surfactant – SDS

    b. A non-ionic surfactant –Igepal®CO-990

    to investigate the effect of the type of latex stabilization on the kinetic behaviour.

3. **Surfactant concentration –** Concentrations were decreased so as to increase the droplet size and to investigate the role that this might have.

4. **Initiator hydrophobicity** – Reactions were performed utilizing:

    a. A water-soluble initiator – KPS

    b. An oil-soluble initiator – AIBN

5. **Monomer –** Styrene and butyl acrylate were used as monomers to investigate the role of the monomer hydrophobicity and rate of propagation.

The rate of polymerization was investigated for all polymerizations via gravimetry and semilogarithmic plots for conversion.

An additional miniemulsion component that was investigated, which is not part of the conventional RAFT-mediated miniemulsion formulation, is that of **aqueous phase radical traps**. The addition of these radical scavengers is known to influence the kinetic and mechanistic behaviour of RAFT-mediated miniemulsions and can deliver significant information with relation to the locus of chain initiation.

From the variation of the reaction components mentioned above and reaction conditions (temperature and homogenization) an understanding of the effects of each as well as insight into the design of an ideal latex formation is expected.

1.7. THESIS OUTLINE

- Chapter 1:

    A brief introduction and background to the evolution of controlled/"living" free radical polymerizations as well as their applications in heterogeneous aqueous systems is given.

The objectives of the research are also included.

- Chapter 2:

  A detailed literature review on the evolution of and present knowledge related to free radical polymerization, living free radical polymerization and emulsion polymerization, with special focus on miniemulsion systems, is presented

- Chapter 3:

  The experimental procedures used for RAFT agent synthesis, as well as the miniemulsion polymerizations are given. Analytical techniques used in polymer and latex characterization are also described.

- Chapter 4:

  This chapter acts as a bridge between the historical chapter (Chapter 2) and the experimental chapters (Chapter 5, 6 and 7). A detailed look into the possible mechanistic pathways of RAFT-mediated miniemulsion polymerizations are given. Conventional free radical miniemulsion polymerizations are also investigated.

- Chapter 5:

  The behavioural changes of miniemulsion systems with changes in the surfactant type and concentration are investigated. The initiator hydrophobicity as a parameter is also addressed.

- Chapter 6:

  The behavioural changes of miniemulsion systems with changes in the RAFT agent structure are investigated.

- Chapter 7:

  The use of aqueous phase radical traps in RAFT-mediated miniemulsions is investigated.

- Chapter 8:

  Taking the results of all experimental data into consideration, conclusions are made with respect to the RAFT mechanism in miniemulsion systems. Some recommendations for future work are also given.

Pectora roborant cultus recti

1.8. REFERENCES

(1) Staudinger, H. *From Organic Chemistry to Macromolecules*; Wiley-Interscience: New York, **1961**

(2) Flory, P. J. *Principles of Polymer Chemistr;*, Cornell University: Ithaca, New York, **1953**. p. 109

(3) Ziegler, K.; Holzkamp, E.; Breil, H.; Martin, H. *Angewandte Chemie* **1955**, *67*, 426

(4) Natta, G.; Pino, P.; Corradini, P.; Danusso, F.; Mantica, E.; Mazzanti, G.; Moraglio, G. *Journal of the American Chemical Society* **1955**, *77*, 1708

(5) Otsu, T. *Journal of Polymer Science: Part A: Polymer Chemistry* **2000**, *38*, 2121

(6) Moad, G.; Solomon, D. H. *The chemistry of Free Radical Polymerization*; Oxford: Pergamon, **1995**

(7) Stevens, M. P. *Polymer Chemistry, an Introduction*; 2nd ed., Oxford University Press: New York, **1990** p.189

(8) Gilbert, R. G. *Emulsion Polymerization: A Mechanistic Approach*; Academic Press: San Diego, **1995**

(9) Fukui, H.; Sawamoto, M.; Higashimura, T. *Macromolecules* **1993**, *26*, 7315

(10) Quirk, R. P.; Lynch, T. *Macromolecules* **1993**, *26*, 1206

(11) Sogah, D. Y.; Hertler, W. R.; Webster, O. W.; Cohen, G. M. *Macromolecules* **1987**, *20*, 1473

(12) Otsu, T.; Yoshida, M.; Tazaki, T. *Macromol. Chem. Rapid Commun.* **1982**, *3*, 133

(13) Moad, G.; Rizzardo, E.; Solomon, D. H. *Macromolecules* **1982**, *15*, 909

(14) Wang, J.-S.; Matyjaszewski, K. *Journal of the American Chemical Society* **1995**, *117*, 5614

(15) Kato, M.; Kamigaito, M.; Sawamoto, M.; Higashimura, T. *Macromolecules* **1995**, *28*, 1721

(16) Matyjaszewski, K.; Gaynor, S.; Wang, J.-S. *Macromolecules* **1995**, *28*, 2093

(17) Le, T. P.; Moad, G.; Rizzardo, E.; Thang, S. H. in PCT Int Appl World Patent 98/01478 **1998**

(18) Lide, D. R., Ed. *CRC Handbook of Chemistry and Physics*; CRC Press: Boca Raton **2004**

(19) Marestin, C.; Noel, C.; Guyot, A.; Claverie, J. *Macromolecules* **1998**, *31*, 4041

(20) Qiu, J.; Shipp, D.; Gaynor, S. G.; Matyjaszewski, K. *Polymer Preprints (Am Chem Soc Div Polym Chem)* **1999**, *40*, 418

(21) Lansalot, M.; Farcet, C.; Charleux, B.; Vairon, J.-P. *Macromolecules* **1999**, *32*, 7354

(22) Monteiro, M. J.; Hodgson, M.; de Brouwer, H. *Journal of Polymer Science: Part A: Polymer Chemistry* **2000**, *38*, 3864

(23) Uzulina, I.; Kanagasabapathy, S.; Claverie, J. *Macromol. Symp.* **2000**, *150*, 33

(24) Ugelstad, J.; El-Aasser, M. S.; Vanderhoff, J. W. *Journal of Polymer Science: Polymer Letters Edition* **1973**, *111*, 503

(25) McLeary, J. B.; Tonge, M. P.; De Wet-Roos, D.; Sanderson, R. D.; Klumperman, B. *Journal of Polymer Science: Part A: Polymer Chemistry* **2004**, *42*, 960

(26) Senyek, M. L.; Kulig, J. J.; Parker, D. K. The Goodyear Tyre & Rubber Company in US Patent 6,369,158 B1; **2002**

(27) McLeary, J. B. PhD thesis; University of Stellenbosch **2004**

(28) De Brouwer, H.; Tsavalas, J. G.; Schork, F. J.; Monteiro, M. J. *Macromolecules* **2000**, *33*, 9239

(29) Lansalot, M.; Davis, T. P.; Heuts, J. P. A. *Macromolecules* **2002**, *35*, 7582

Pectora roborant cultus recti

Chapter 2. : *Historical*

ABSTRACT

Complex polymerization systems like RAFT-mediated miniemulsion polymerizations were developed after extensive research into emulsion systems and living radical polymerization processes. The historical build up to and current developments in these two fields are discussed.

Scientific investigations are designed on the foundations of previous knowledge. To build an accurate description of any system's behaviour, it is first necessary to have a solid understanding of the tools with which one will create that description. These tools will include models of the mechanistic and kinetic behaviour of free radical polymerizations (controlled and conventional) as well as those of heterogeneous aqueous systems. It is these tools that will help to unravel the behavioural mysteries of RAFT-mediated miniemulsion systems. Ultimately, these tools should allow the author to achieve the objectives stated in Chapter 1.

2.1. FREE RADICAL POLYMERIZATION

At the end of the 19th century, there was a vast amount of investigation into the strange behaviour of some unsaturated compounds. It had been observed that exposure to light and/or heat caused physical changes in these compounds. Theories arose that described the new "macro-molecules" as molecular aggregates.[1] After much investigation, it was Staudinger[2] who, in 1920, described polymers as monomer units connected by primary valences. The behaviour of the physical changes taking place when placed in an oxygen atmosphere as well as the influence of peroxides led researchers to believe that it was radical peroxide fragments that acted as initiators in the reaction. This theory was confirmed after identifying the polymer end-groups to be peroxide fragments.[3] The process by which these macromolecules were forming was then identified as a radical addition growth or *polymerization*. Mechanistic and kinetic models and descriptions of this process have been evolving for many years.

Pectora roborant cultus recti

The current understanding of the mechanism of FRP follows that of a radical chain addition,[4] added to which additional side reactions take place. The primary chain-addition steps are: initiation, propagation and termination. The side reactions, called chain transfer reactions, lead to alternative polymer products. All these steps are shown schematically below:

STEP 1: Initiation

As the name implies, the generation of free radicals is imperative for the onset of polymerization. There are various means by which to introduce radicals into a system to initiate FRP: electromagnetic radiation, mechanical stress, sonic treatments and thermally decomposing compounds. Thermal initiators are widely used, and are characterized by an additive that decomposes when heated, releasing radicals. This is shown below:

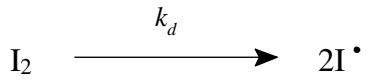

Scheme 2.1: Decomposition of a thermal initiator.

The resultant species are called the *primary radicals*.[5] The value k_d is unique for all initiators and is also dependant on the specific solvent and temperature of the system. Using a simple mathematical derivation, the rate of primary radical formation can be expressed as the decreased concentration of the initiator species:

$$[I_2] = [I_2]_o \cdot e^{-k_d \cdot t} \tag{2.1}$$

where $[I_2]$ is the initiator concentration, k_d the rate coefficient for the initiator decomposition and t time in seconds. Primary radicals then react with the monomer to form *initiating radicals*.[5] The process of their formation is shown below:

Scheme 2.2: Addition of primary radicals to monomer to form initiating radicals.

The process above is grossly simplified for it assumes that all primary radicals formed after decomposition react with monomer. The thermolysis of the initiator does not usually lead to a 100% yield of primary radicals due to rearrangements, fragmentation or side reactions (with solvent,[6] oxygen[7] and even other primary radicals[8]) that the radicals may undergo, leaving a range of terminated products.

The initiating radicals further react with monomer and are then called *propagating radicals*. The rate at which the primary radicals add to monomer is dependent on many experimental factors. It has however been shown that monomers are effective radical scavengers. There is a "measure" of the extent of monomer addition called the *initiator efficiency* (f):

$$f = \frac{[\text{Rate of initiation of primary radicals}]}{2[\text{Rate of initiator disappearance}]} \tag{2.2}$$

The value of *f* is typically not a constant since the side reactions mentioned earlier may occur with a greater probability as the monomer is depleted and the viscosity of the system increases. The initiator efficiency becomes an important factor when proceeding to the next step, propagation.

STEP 2: Propagation

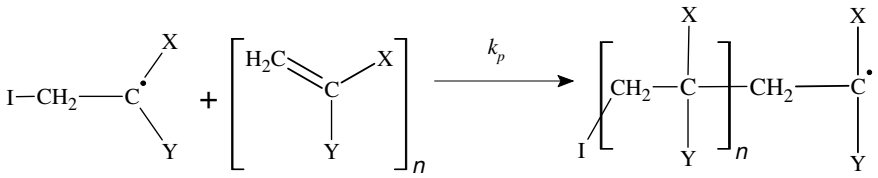

Scheme 2.3: Propagation of propagating radicals by monomer addition.

The scheme above illustrates the multiple monomer additions that can take place during the propagation of the polymer chain. The rates at which these additions take place are dependant on the monomer-propagating radical system. It is known that substituents on the propagating radical center can stabilize the radical thereby increasing its reactivity. It was thus assumed that this was the determining factor in the rate of monomer addition.[9] It has however been found that other factors such as steric, polar, electrosteric and bond-strength constraints can also play a big role in the rate of monomer addition.[9]

In the end, a value for each monomer is assigned that gives an indication of its "reactivity" and this is called the *propagation rate constant* (k_p) of that monomer. This describes the rate at which monomer is consumed in the system. This is expressed mathematically below:

$$\frac{-d[\mathrm{M}]}{dt} = k_p[\mathrm{M}\bullet][\mathrm{M}] \qquad (2.3)$$

where $[\mathrm{M}]$, $[\mathrm{M}\cdot]$ and k_p are the monomer concentration, propagating radical concentration and monomer addition rate coefficient. These values can be determined through methods such as calorimetry.[10] This is however an outdated method (1974) and many new methods have since been introduced that allow for vastly more accurate results. Most recently *pulsed laser photolysis* has been used to determine accurate k_p values.[11] It has been found that the propagation rate coefficient is not a constant value for the entire reaction. The first monomer additions were found to take place at accelerated rates and the rates decreased to a constant value after some 5 to 10 monomer additions. All these factors must be taken into consideration when examining the kinetics of free radical polymerization.

STEP 3: Chain transfer

Although it is not exactly correct to class this separately, since it is not an imperative step in free radical polymerization, it should be placed here so as to illustrate the "point-in-time" that these reactions may occur. Chain transfer takes place when a propagating radical transfers its unpaired electron to an accepting species through the abstraction of an atom from the accepting species. At any point during the propagation, propagating radicals may chain transfer to various species. Typical species transferred to are:

- Solvent
- Monomer
- Formed polymer
- Chain transfer agents

Transfer to monomer will cause the formation of new (and thus smaller) propagating chains. Transfer to formed polymer will simply relocate the active radical center, which will create branched chains of varying lengths. Chain transfer agents (CTA) are additives that are used specifically to reduce chain lengths. They are also used to influence and control the final chain length distribution. In all these circumstances, the number of active sites will not change but the molecular weight of the final polymer chain lengths will be altered. Solvents that are "transfer active" usually possess a weakly bonded group of atoms (for example hydrogen, chlorine and bromine). Rate of transfer is chain length dependent; but quite obviously, the system in question will determine the extent to which transfer will take place.

STEP 4: Termination

As has been stated before, radicals are highly reactive. At any point, two radicals may combine, bonding through their two unpaired electrons; or one radical may abstract a proton from another to form two dead polymer chains. This ends the life of these two radicals, and propagation of the chains ceases. This is illustrated below:

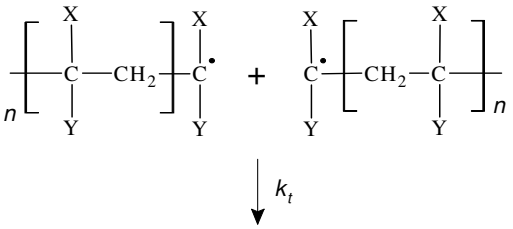

COMBINATION DISPROPORTIONATION

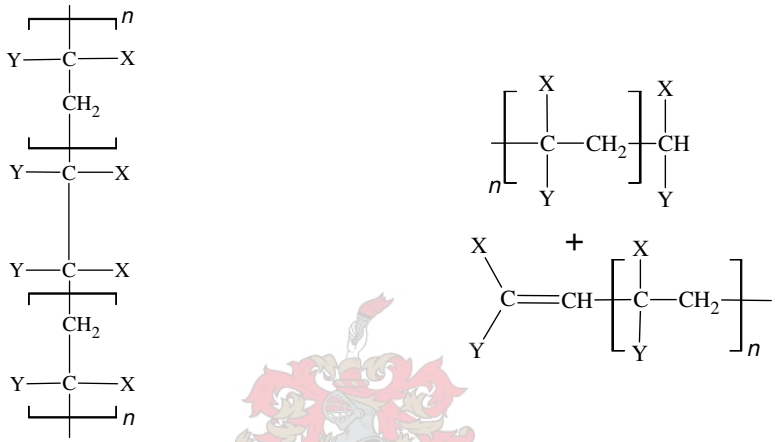

Scheme 2.4: Termination pathways for free radical polymerization.

It should be noted that these are not the only possible methods by which termination can take place. Reactions between propagating radicals and stable radicals (e.g. nitrogen, oxygen) or non-radical species (e.g. phenol, a quinone which forms stable radicals) will also terminate the chain, and are commonly called *inhibitors*. The bimolecular termination processes shown are however the most common. It can immediately be seen that the termination requires two radical chain ends to "find" each other. This implies that the termination of radical chains is diffusion controlled. The diffusivity of these ends is dependent on the chain size and shape and thus it can be deduced that the termination rate is chain length dependent.[12] This rate of termination can kinetically be expressed as the following:

$$\frac{-d[\mathrm{M}\bullet]}{dt} = 2k_t[\mathrm{M}\bullet]^2 \qquad (2.4)$$

where $[\mathrm{M}\cdot]$ and k_t are the propagating radical concentration and termination rate coefficient respectively. In this relationship, the *termination rate constant* (k_t) includes both the rates at which the two bimolecular termination paths, shown earlier, take place:

$$k_t = k_{tc} + k_{td} \tag{2.5}$$

where k_{tc} and k_{td} are the rate coefficients of combination termination and disproportionation termination respectively. These values are monomer dependent, and there has been a great effort to determine exact values for conventional systems such as styrene[13] and methyl methacrylate[14] polymerizations.

The final product of any industrial manufacturing process should be qualified by some means. For the polymerization process, the molecular weight and molecular weight distribution (MWD) are two of many variables that are used to describe the final polymer product. These variables will in turn influence many other physical properties of the product. The nature of the free radical polymerization process leads to many problems in trying to accurately determine these types of variables. The process can however be expressed kinetically so as to give a *rate of polymerization* (R_p) that includes all the four steps shown above. A simple mathematical manipulation of equation (2.4) gives:[15]

$$\ln\left(\frac{[M]_0}{[M]_t}\right) = k_p\left(\frac{f \cdot k_d}{k_t}\right)^{0.5} \cdot [I]^{0.5} \cdot t \tag{2.6}$$

where $[\mathrm{M}]_0$ and $[\mathrm{M}]_t$ are the monomer concentrations at time zero and time t respectively and $[I]$ the initiating radical concentration. The derivative of this equation gives a value of R_p. In this manipulation, it is assumed that the change in initiator concentration and average termination rates with time are negligibly small. The *average degree of polymerization* $\overline{P}_n$ describes the average chain length for a system. Assuming no transfer to solvent, initiator, polymer or transfer agents takes place, $\overline{P}_n$ is given as:[16]

$$\overline{P}_n = k_p[M]\left(\frac{1}{f \cdot k_d \cdot k_t \cdot [I]}\right)^{0.5} \tag{2.7}$$

With all this information at a researcher's disposal, polymers can easily be synthesized to meet certain criteria. The shortcoming of FRP lies in the diffusion-controlled termination reactions. This leads to a large chain distribution. The advent of living radical polymerization finally equipped a

researcher with the ability to control these two properties as well as many others. This will be further expanded on in Section 2.3

2.2. HETEROGENEOUS AQUEOUS SYSTEMS

In the polymer industry there is a continual search for increasingly effective systems to optimize product output. Besides this criterion, environmental concerns worldwide are requiring industry to evolve cleaner and safer infrastructures and processes. This has caused research and development to place the spotlight onto heterogeneous aqueous systems. In Chapter 1 the reasons for this change in direction are given.

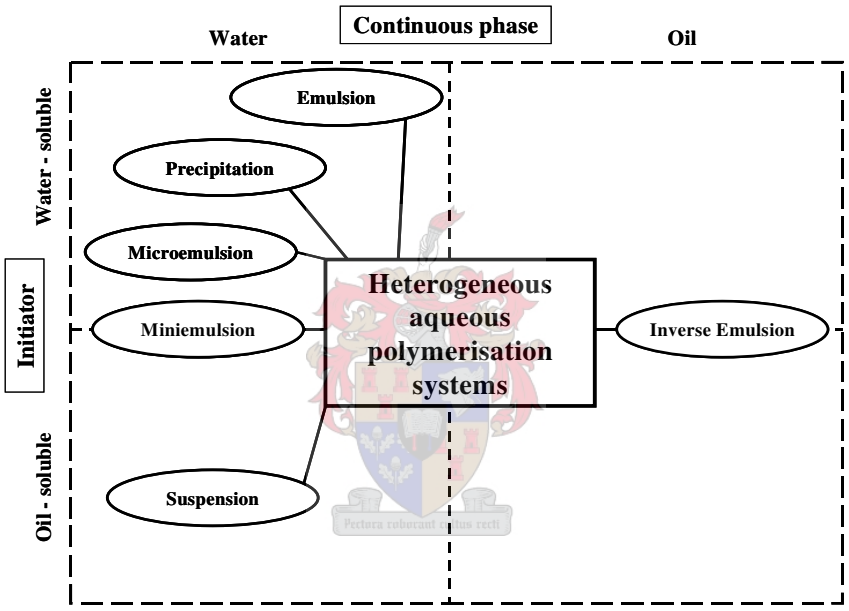

Figure 2.1: Various heterogeneous aqueous phase systems.

The first heterogeneous systems, namely emulsions, were introduced by Luther and Hueck, at the beginning of the Second World War, as a means to polymerize synthetic rubber.[16] From this starting point, many other heterogeneous systems were developed. The study of the kinetics behind each system has been arduous due to their complexity. Various examples of heterogeneous systems are given below, as well as their fundamental constituents:

EMULSION POLYMERIZATION

Emulsions are formed by a mixture of water, monomer, surfactant and a water-soluble initiator.[17] This mixture leads to the formation of micelles (surfactant aggregates that may contain monomer)

and large monomer droplets stabilized with surfactant. There are three main polymerization loci: inside the micelles, inside particles (polymer, monomer and surfactant structures) and in the aqueous phase. This implies three different mechanisms of polymerization with varying kinetics and behaviour that can potentially vary. The particle sizes range from 50 – 300 nm and droplet sizes from 1 – 10 μm.

PRECIPITATION

This technique utilizes a similar mixture as in the case of emulsions except that it lacks surfactant, and only water-soluble monomers can be polymerized. The monomer does not swell the formed polymer and thus the locus of polymerization is the particle-water interface. No droplets are formed in the initial mixture, but the final latex has particle sizes ranging from 50 – 300 nm.

MICROEMULSIONS

As the name suggests, microemulsions are simply "smaller" emulsions. A co-surfactant (e.g. hexanol) is added. The formed stable droplets are smaller than conventional monomer droplets, but larger than micelles; they are approximately 10 nm in size. These stabilized droplets are the main location for polymerization. The final latex particles are 10 – 30 nm in size.

MINIEMULSIONS

This system lies between emulsions and microemulsions on the "size of particle" scale (some overlap does exist). A similar reaction to microemulsions is utilized. Thermodynamically stable droplets are formed and are about 30 nm in size. The final latex particles are 30 – 100 nm in size. One of the main reasons why micro- and miniemulsions were developed is that water-insoluble monomers cannot be polymerized efficiently in conventional emulsion systems.

SUSPENSION

The reaction mixture for suspension polymerizations is similar to that of an emulsion except for the fact that an oil-soluble initiator is used. The locus of polymerization is also shifted to the monomer droplets. The droplet sizes are usually 1 – 10 μm in size and the final latex particles are greater than 1 μm.

INVERSE EMULSION

As the name suggests, an inverse emulsion is simply an emulsion in which the continuous and dispersed phases are reversed. Oil-soluble and water-soluble initiators can be used. The monomers polymerized are always water-soluble and the main locus of polymerization is the droplets that contain water and monomer. The droplet sizes are similar to that of an emulsion, but the final latex particles are much larger, ranging from $10^2 – 10^3$ nm in size.

Besides the obvious environmental benefit of converting the main medium of polymerization to something less harmful, like water, there are benefits that the heterogeneous systems also provide on a kinetic level. The formation of droplets in a continuous phase allows for *compartmentalization* of the various reaction loci in the system. This in turn leads to an increase in rate of polymerization.[18] This can be seen by looking at the kinetic expressions of the emulsion systems when compared to those of the respective bulk or solution systems. Below is a *rate of polymerization* (R_p) expression for a heterogeneous system:[17]

$$R_p = -\frac{d[M]}{dt} = \frac{k_p \cdot [M] \cdot \bar{n} \cdot N_c}{N_A} \tag{2.8}$$

where $\bar{n}$ is the average number of radicals per particle, N_c is the number of particles and N_A is Avagadros number. A mathematical manipulation (assuming that $\bar{n}$ remains constant over the reaction time) gives the *average degree of polymerization* ($\bar{P}_n$):[17]

$$\bar{P}_n = \frac{k_p \cdot [M] \cdot \bar{n} \cdot N_c}{2f \cdot k_d \cdot [I]} \tag{2.9}$$

In these equations, N_c represents the number of latex particles per unit volume and $\bar{n}$ the average number of radicals per particle. If one looks back to equations (2.6) and (2.7) and compares them to these two equations (2.8) and (2.9), it can be seen that by increasing the number of particles, both the rate of polymerization and average chain length are increased. If the oil: water phase ratio is kept constant, this would mean we would achieve increased propagation rates by decreasing the particle sizes.

2.2.1. EMULSION POLYMERIZATION

As mentioned earlier, emulsion systems were first introduced with the synthesis of synthetic rubber in mind. Emulsion systems have subsequently been expanded to incorporate free radical polymerization as well. The behaviour of FRP in emulsions has been under much investigation. This will be the main focus of this section.

2.2.1.1. The fundamental mechanism of emulsion polymerizations

In the brief introduction to emulsion polymerization it was stated that the main locus of polymerization is the monomer droplets stabilized by surfactant. On a more detailed level however, this is not actually the case. There are two other loci of polymerization, and these arise through other processes. All the mechanisms start from a common point: initiation. In this step, a water-soluble initiator thermally fragments to form initiating radicals in the aqueous phase. These undergo propagation with monomer that is dissolved in this phase to form propagating radical chains. From this point, the three mechanisms differ. These differences are given below:

Homogeneous nucleation:

The propagating radical chains can grow until a point at which they exceed their solubility limit. At this point they are called *j-mers*. For a set monomer system, the length that a propagating chain has to grow before it can be labeled a j-mer is defined as the j_{crit} value. This value can be estimated using the following equation:[19]

$$j_{crit} = 1 - \frac{55 KJmol^{-1}}{RT \ln C_W^{SAT}} \tag{2.11}$$

where the value C_W^{SAT} is the saturated aqueous phase concentration of monomer (in mol.dm^{-3}), R is the ideal gas constant and T the temperature. The j-mers precipitate out of the aqueous phase and become swollen by monomer, forming a particle. These particles are stabilized by the charged groups on the initiator fragments (on the chain ends). This simplified mechanism is called the "HUFT" (Hansen-Ugelstad-Fitch-Tsai) theory.[20] This theory has been revised since its establishment to include other factors like the coagulation of smaller particles.

Micellar nucleation:

It must be remembered that in an emulsion system there may be free surfactant molecules in the aqueous phase. At a certain concentration, called the *critical micelle concentration* (CMC), the surfactant molecules undergo structural rearrangement to form micelles (spherical structures, where the hydrophobic tails will aggregate inwards). These micelles will become swollen with monomer (since monomer is also hydrophobic). The propagating radical chains present in the aqueous phase cannot penetrate these micelles due to their insufficient *surface-activity*. At a specific length (arbitrarily defined as *z*) the surface-activity reaches a level where the chains can penetrate the micelles. At this specific length the chains are called *z-mers*. Propagation can continue inside the micelles that are now labeled particles. There is a certain degree of coagulation of these particles. This theory is based on the work of Smith and Ewart.[21] It has however undergone many rewrites, for example, to include the aqueous phase growth of the propagating chains. The value of z is given by the following equation:

$$z \approx 1 - \frac{23KJmol^{-1}}{RT \ln C_W^{SAT}} \qquad (2.12)$$

where C_{WSAT} is the saturated aqueous phase monomer concentration.

Droplet nucleation:

The mechanism of droplet nucleation is the same as that for micellar nucleation. The only difference lies in the fact that the instead of entering micelles, the z-mers enter stabilized (by surfactant) monomer droplets. The fact that droplet nucleation can, in most systems, be ignored lies in the fact that the total surface area afforded by the droplets is much less than that of the micelles due to the larger size of the droplets. It can thus be deduced that the probability that a z-mer enters a micelle is far greater than that of it entering a droplet. For this reason, in the most recent models for conventional emulsion systems, droplet nucleation is ignored.

These three, or to be correct (ignoring droplet nucleation) two, nucleation mechanisms will define the radical entry into the particles.

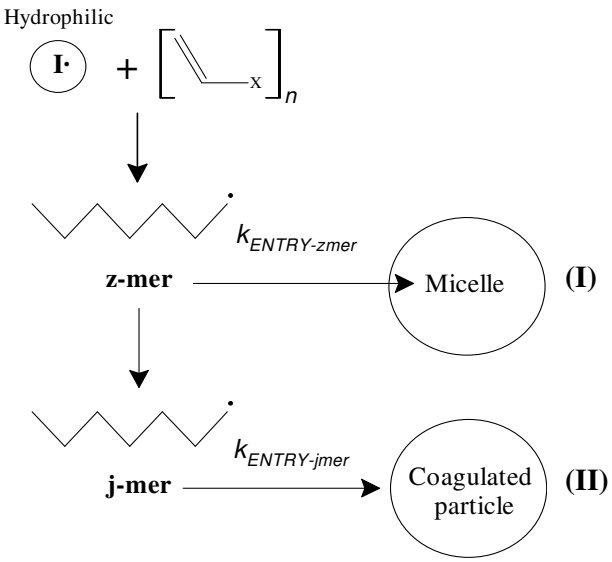

Figure 2.2: Two main mechanisms of particle formation via radical entry into a micelle (I) and the formation of a coagulated particle (II).

The entry of the propagating radicals into the particles has now been addressed. The existence of these various mechanisms of particle formation makes kinetic modeling extremely difficult. Models that try to simulate radical entries into particles are usually based on seeded systems that do not require the inclusion of the different mechanisms of particle formation. This however falls outside the scope of this investigation.

Looking beyond the particle formation, it is found that the radicals within the particles will undergo propagation within the particles until either they terminate or chain transfer to monomer or a chain transfer agent.[22] Chain transfer will lead to a dead polymer chain within the particle as well as a smaller radical species that can desorb from the particle into the aqueous phase. These desorbed radical species can either undergo aqueous phase propagation, termination, or may even reenter the particle. This is illustrated below:

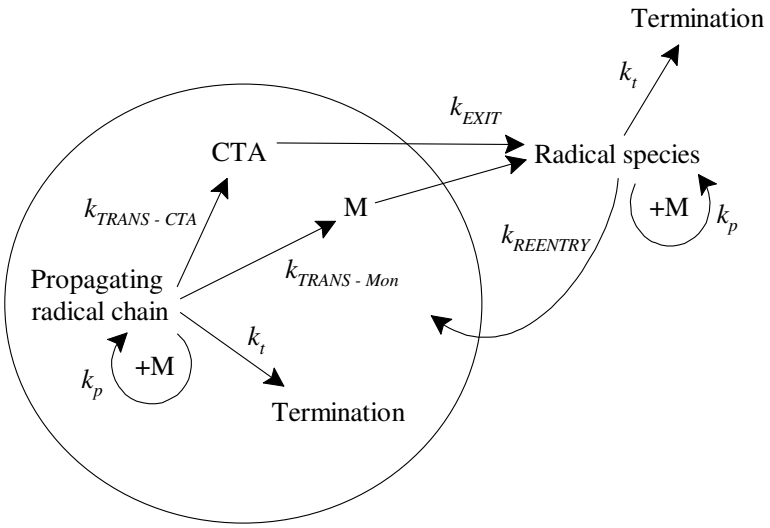

Figure 2.3: The fate of propagating radicals within a particle as well as the desorbed radical species.

The desorption of radical species from the particles is described by the following mathematical expression, which defines the *rate coefficient of radical exit* (k_{exit}):[23]

$$k_{exit} = k_{fm}[M]_p \beta \frac{P}{1-P(1-\beta)} \tag{2.13}$$

The values $[M]_p$, P, β and k_{fm} are respectively: the monomer concentration in the polymer particles, the probability of desorption, the probability of reaction within the aqueous phase and the rate of chain transfer to monomer. This equation has been found to be erroneous in some situations, but generally still holds in most instances. Rigorous modeling has produced a more accurate expression.[23] From this model, the following relationships are found to exist in an emulsion system:

- k_{exit} decreases with the number of particles in the system
- k_{exit} increases as the concentration of radicals in the aqueous phase increases
- k_{exit} increases as the particle size increases if a constant number of particles are maintained

It was also seen that radical exit, as well as entry into particles, is greatly affected by the type of stabilization used in the system. Highly charged lattices and dense "hairy" electrosteric stabilizers will decrease the rate of both these processes.[24]

2.2.1.2. An overview of the kinetics of emulsion polymerization

After looking at the mechanistic view of emulsions, a kinetic evaluation will equip a researcher with models to better understand and forecast the behaviour of the various systems. From equations (2.9) and (2.10) it is obvious that the average number of radicals per particle will influence the rate of polymerization as well as the average degree of polymerization. The average number of radicals per particle is in turn dependent on the relative rate of radical entry into the particles, rate of exit from the particles and the rate of bimolecular termination that takes place within the particles. The formation and growth of the particles happens in different "stages" of the polymerization. Three stages or intervals of the complete polymerization process have been defined.[25] These intervals are illustrated in Figure 2.4.

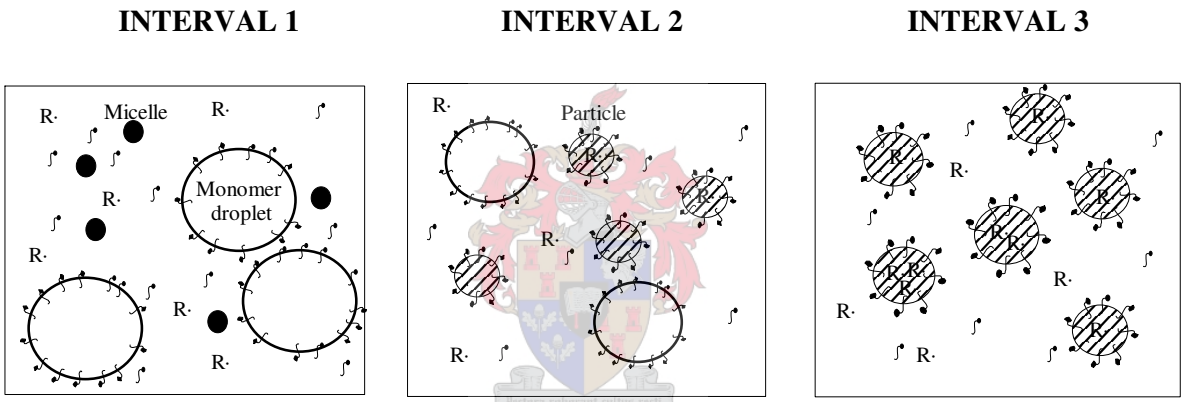

Figure 2.4: The three intervals of the emulsion polymerization model.

- Initiator fragments in the aqueous phase are entering micelles → increase in particle numbers = increased R_p
- Aqueous phase monomer concentration decreases but is replenished via the monomer droplets.

- Particle formation ceases.
- Constant monomer/polymer ratio maintained within particles due to balancing of *free energy of mixing* and *surface energy* effects. This is achieved by a continuous migration of monomer from monomer droplets to the latex particles.
- $\Delta[\mathrm{M}] = \Delta N_c = \Delta R_p = 0$

- All monomer droplets exhausted.
- As polymerization continues, the monomer-polymer ratio will decrease, and this causes a decrease in R_p
- Increased viscosity in particles may cause termination to decrease → R_p could increase

It should be noted that this interval segregation and mechanistic model holds true only for systems in which homogeneous nucleation can largely be ignored. The existence of micelles and free surfactant also implies that the system is above its CMC (this would also imply that the system might very well not undergo homogeneous nucleation). This model allows us to sketch a theoretical trend for the rate of polymerization:

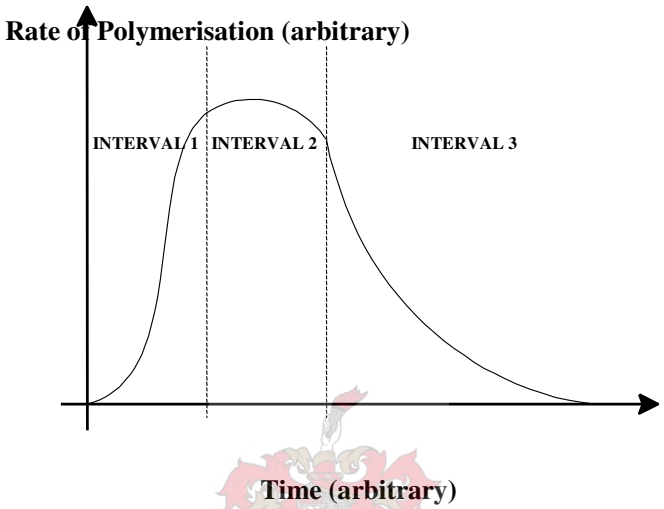

Figure 2.5: Kinetic behaviour of a common emulsion system illustrating the three intervals 1,2 and 3

Looking back at equation 2.10, it can be seen that the rate of polymerization is dependent on the monomer concentration in the particles and the number of particles. These two variables have been modeled above. R_p is however also dependent on the value $\bar{n}$. This value can be modeled in two different ways, which differ in the way that radicals terminate within the particles. These two models are described below:

Zero-one systems:

This describes a system in which the compartmentalization of the radicals will cause the instantaneous termination of two radicals that could be present in one particle simultaneously. Termination can thus be said to be non-rate determining. Thus, at any one time, there will exist only one or no radicals within the particle, hence the name "zero-one". The value $\bar{n}$ is thus less than or equal to 0,5. This model fails at higher conversions and is replaced by the next model.

Pseudo-bulk systems:

If the conditions in a system are such that two radical species can coexist within a particle without instantaneously terminating, the system resembles a bulk system and is specifically called a psuedo-bulk system. The termination of these chains is then diffusion controlled and rate determining. This model can actually lead to a different trend to that given in Figure 2.5. At higher conversions, the viscosity within the particles increases due to a lack of replenishing monomer from the aqueous phase that would dilute the formed polymer. This in turn will decrease the termination rate due to the longer lifetime of multiple radical chains within the particles. The rate of polymerization will then increase contrary to the trend given.

Both these models can contribute to a better understanding of the behaviour of emulsion systems. The situation is however further complicated when we introduce living radical polymerization into our present models.

2.2.2. MINIEMULSION POLYMERIZATION

The idea of dispersing large monomer droplets found in emulsions into only submicron droplets was introduced by Ugelstad *et al*. in 1973.[26] By increasing the droplet surface area through miniemulsification, the droplets become the main locus for particle formation. These droplets were typically stabilized with ionic surfactants and co-surfactants, which are mostly long-chain alkanes and fatty alcohols. Immediately after the introduction of miniemulsions, substantial research was carried out to investigate the formation and stability of the monomer droplets and latex particles[27] as well as the kinetics of miniemulsion systems.[28] The growth of knowledge in these two fields of miniemulsion systems is discussed below:

2.2.2.1. Stability of miniemulsion droplets and latex particles

The formation of stable particles begins with the process of dispersion of the droplets into submicron sizes.

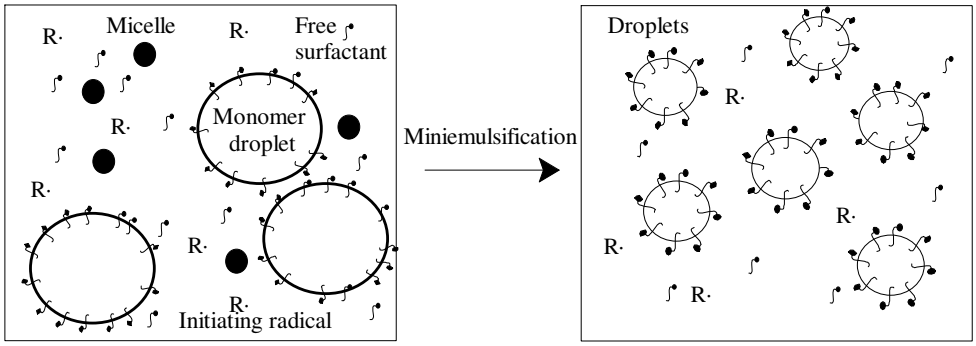

Figure 2.6: Formation of stable miniemulsion droplets via miniemulsification.

The miniemulsification is achieved by ultrasonicating the original emulsion mixture or by sending it through a high-pressure homogenizer. Both create a miniemulsion with homogeneous droplet sizes through a fission-fusion process. These submicron droplets are thermodynamically unstable and will coalesce as well as grow in size due to Ostwald ripening. These two stability problems are looked at below:

- The coalescence of the droplets is limited by the use of surfactant. Ionic surfactants such as sodium dodecyl sulphate (SDS) or cetyl trimethyl ammonium bromide (CTAB) repel other similarly charged droplets via an electrostatic force. Nonionic surfactants have also been used.[29] Non-ionic surfactants stabilize sterically rather than electrostatically and thus the particle sizes are usually large. It was also found that the rate of polymerization was lower than that seen for ionic surfactant systems and this was thought to be due to a retardation effect on the entry of oligomeric radicals into the droplets due to the hydration layer around these droplets.[24]

- Ostwald ripening describes the nature of smaller particles that decrease in size while larger particles increase in size. This is due to the increased water-solubility of monomer in the aqueous phase as the interfacial curvature increases.[30] The tendency for particles of radius *r* to shrink can be described by the *Laplace pressure* expression, where γ_{LL} is the interfacial energy and *r* the particle radius:

$$p_{LAPLACE} = \frac{2\gamma_{LL}}{r} \qquad (2.14)$$

This growth can be counteracted by the addition of a *co-surfactant* like cetyl alcohol and hexadecane. The term co-surfactant implies that the agent is surface active and acts along with the surfactant in reducing the interfacial energy of the particles. It has been found that co-surfactants do not have to be amphiphiles (both containing a hydrophobic and hydrophilic segment). Barely water-soluble co-surfactants have been found to be the most effective.[31] Hexadecane, a common co-surfactant, which is more accurately described as an *ultra-hydrophobe*, does not reside in the interfacial region but inside the particles.[32] The ultra-hydrophobe increases the *osmotic pressure* within the particle. The osmotic pressure within a particle is given as:

$$p_{OSMOTIC} = \frac{3T[M]}{4\pi r^2} \tag{2.15}$$

where T and $[M]$ are the temperature and the monomer concentration respectively. When a small fraction of monomer diffuses out of the particle, the osmotic pressure will increase. When the Laplace and osmotic pressures equalize, a state of stability is maintained. It was found that the particle sizes are not (or are very weakly) dependent on the amount of ultrahydrophobe and that the minimum ratio of monomer to ultrahydrophobe to build up sufficient osmotic pressure is 250:1.[33] Small amounts of high molecular weight polymer (e.g. polystyrene) have also been reported to act like a co-surfactant.[34]

It should also be noted that some co-surfactants, especially the fatty alcohols, further facilitate the prevention of coalescence. The incorporation of the hydroxyl groups into the interfacial region along with the surfactant will increase the barrier towards coalescence.[35]

Any system strives for a condition where the *Gibbs free energy* (ΔG) is at a minimum. The efficiency of a co-surfactant to change the ΔG_1 is given by the following equation:[36]

$$\Delta\overline{G}_1 = RT\left(\ln\phi_1 + \left(1 - \frac{1}{j_2}\right)\phi_2 + \phi_2^2\chi + \frac{2V_M}{rRT}\right) \tag{2.16}$$

where $\Delta\overline{G}_1$ is the partial molar free energy of mixing of the monomer in the particles, ϕ_1 and ϕ_2 are the volume fractions of the monomer and co-surfactant respectively, r is the particle radius, χ is the interaction parameter, V_M is the molar volume of the monomer and j_2 is the molar volume of the monomer to the molar volume of the co-surfactant. By setting the value of $(1/j_2)$ to 0, the swelling capacity of the particles can be calculated.

2.2.2.2. Mechanistic and kinetic models for miniemulsion systems

Since a miniemulsion system leads on from a conventional emulsion system, it can be assumed that their mechanistic models are similar. This is in part true, but miniemulsion systems behave differently due to the stability of the initial droplets. The particle sizes and size distributions do not change throughout the polymerization.[32] This would imply that no Ostwald ripening or coalescence has taken place and that all the particles that were present at the onset of polymerization are still present and no new particles have been formed. When comparing this scenario to that of an emulsion system, we see that no micellar or homogeneous nucleation may have occurred to form new particles. The droplets within a miniemulsion are of large enough total surface area (due to reduction in size) to absorb most of the surfactant, leaving little surfactant to form micelles or to stabilize new particles that might form. The larger surface area will also increase the probability of the propagating radical entry into the droplets. This will limit the amount of homogeneous nucleation. As was done for emulsion systems, the miniemulsion behaviour during polymerization can be sectioned into intervals as shown in Figure 2.7:[37]

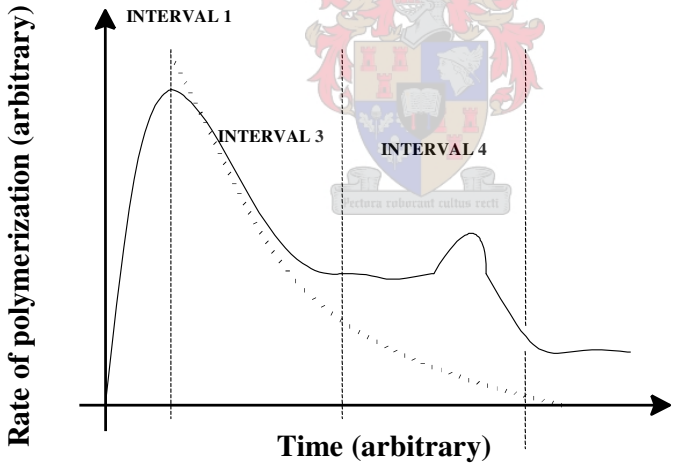

Figure 2.7: Kinetic behaviour of a typical miniemulsion system illustrating the three intervals 1,3 and 4

Each interval will be looked at separately below:

INTERVAL 1

- Miniemulsion systems "look" like the illustration on the right in Figure 2.6.
- Propagating radicals are entering the droplets within the system. Equilibrium is reached at the end of interval 1 and $\bar{n}$ is given as 0,5 if zero-one conditions apply.
- Although the duration of interval 1 is much shorter here than in an emulsion system, slow radical flux into the droplets prevents the simultaneous onset of propagation within the particles.

INTERVAL 3

- Completion of particle nucleation and $\bar{n} \approx 0{,}5$ during the interval.
- Each particle acts like an individual reactor and follows bulk polymerization kinetics (the trend for bulk polymerization is given as the dotted line in the figure).
- This duration of this interval is influenced by various variables, as is investigated below:

INTERVAL 4

- The increased viscosity inside the particles can lead to $\bar{n}$ increasing above 0,5. This is due to the Trommsdorff-Norrish effect and is similar to what may occur during interval 3 in a conventional emulsion system.
- Equation 2.15 showed that an increase in $\bar{n}$ leads to and increase in R_p thus the bulge (gel peak) in Figure 2.7.
- This gel peak is less defined for smaller particle sizes.

The main difference between emulsion and miniemulsion systems is clearly seen when one compares Figures 2.7 and 2.5. The lack of interval 2 in miniemulsion polymerizations is what leads to the retention of "particle identity" for the duration of the polymerization. The slow radical reflux into the droplets which causes longer interval 1 times can be caused by the following:

- The electrostatic layer that stabilizes the droplets can prevent propagating radical chains from entering the droplets.[37]
- Before a propagating radical chain can become surface-active and enter the droplets, the chain must be formed by propagation of the initiator fragments. Since most of the monomer is confined to the droplets, there is little monomer to form these propagating oligomeric radical chains. It has been shown that increasing the initiator concentration does not shorten interval 1 and from this it can be determined that droplet nucleation is the rate determining step and is only dependent on the monomer concentration in the aqueous phase.[38]

Tang *et al.* speculated that using sparsely water soluble initiators like azobisisobutyronitrile (AIBN) would eliminate these problems, which was in actual fact not the case.[39] The mechanism of oil-soluble initiators in miniemulsion polymerization has been a discussion point for some time. In

conventional emulsion systems, the use of oil-soluble initiators showed little difference from water-soluble initiators.[40] It has been determined that the initiator radicals that desorb from the droplets after fragmentation are the primary source of radicals in the aqueous phase that can initiate the formation of the surface-active propagating radical chains.[41] It was then established that a similar pattern occurred in miniemulsion systems.[42] The big problem lies in the fact that in the droplets the volume is small, causing instantaneous recombination of the radical fragments formed during initiator decomposition due to the inability of the two radicals to diffuse away from each other. This process is called *rate of geminate recombination* and is given as:

$$R_{COMB} = \frac{3k_{COMB}}{2\pi N_A r^3} \tag{2.17}$$

The rate of exit R_{EXIT} is given as:

$$R_{EXIT} = \frac{6D_W}{r^2}\frac{C_W}{C_p} \tag{2.18}$$

Where D_w is the diffusivity of monomeric radicals in the aqueous phase, and C_w and C_p are the concentrations of monomer in the aqueous phase and particles respectively. It can be seen that for smaller particles, initiator exit from the particles is more effective. It was found that by eliminating the contribution of aqueous phase initiation, propagation still proceeded, and that the aqueous phase initiation was not the only method of initiation. However, even for larger particles it was found to be the dominant mechanism.[42]

Looking back at equation 2.10, one can see that the particle size will influence the rate of polymerization. The effects that surfactant and co-surfactant have on the rate of polymerization were found to be as follows:

- Systems above their CMC have a slower rate of polymerization than that of a conventional system and vice versa.[43]

- Increased amounts of ultra-hydrophobe lead to a decrease in polymerization rate due to the decreased monomer concentration in the droplets.[44]

- A small amount of predissolved polymer increases the rate of polymerization due to a reduction in particle size as well as the increased viscosity in the particle, which limits radical exit.[34]

There are many other variables that will affect the particle size, for example the stirring speed, pH and monomer. The following expression can be used to obtain a general value for the particle size:

$$N_c = \frac{3W_0(1-x))}{4\pi\bar{r}^3 d_p} \tag{2.19}$$

where x is the monomer conversion, W_0 is the initial weight of monomer, $\bar{r}$ is the average unswollen particle radius and d_p the polymer density

2.2.3. AQUEOUS PHASE RADICAL SCAVENGERS IN MINIEMULSIONS

In many investigations into the mechanistic and kinetic behaviour of miniemulsion systems, aqueous phase radical scavengers have been utilized to eliminate radicals that may exit from droplets after fragmentation.[42] Typical aqueous phase radical scavengers used include sodium nitrite ($NaNO_2$) and 2,5-dihydroxy-1,4-benzene disulphonic acid.[39]

It has been shown that utilizing excess initiator in some systems has resulted in homogeneous nucleation within the miniemulsion system.[45] It was previously assumed that in a miniemulsion system there are no micelles due to the complete absorption of all the surfactant onto the droplet interfaces. This is however not the case in all systems.[46] If micelles are present, initiating radicals that accumulate in the aqueous phase and form surface-active propagating radicals may enter the micelles, forming new particles. Aqueous phase radical scavengers could be used to prevent the build-up of initiator fragments that could undergo propagation within the aqueous phase, thus limiting the amount of homogeneous and/or micellar nucleation.

2.3. LIVING RADICAL POLYMERIZATION

The mechanism of FRP techniques shows how uncontrolled behaviour can result. To ultimately introduce near perfect control the following parameters need to be met in any new adapted FRP system:

- Low concentration of propagating radicals → limits termination reactions
- Fast initiation → simultaneous growth of all propagating chains.

All these criteria are met by the addition of compounds that can reversibly react with propagating chains. These additives limit the number of irreversibly terminated chains to below 5% whilst not

affecting the reactivity rates of the conventional FRP equivalent.[47] Theoretically, the LRP system allows for the simultaneous initiation of all chains and, through the exchange between dormant and active states, decreases the difference in the lifetime of different propagating radicals.

The development of LRP was built on the knowledge that certain compounds interact with propagating radicals without interfering with the ultimate chain growth. This interaction simply limits the irreversible termination of these radical chains.[48] The equilibrium that is created by adding these "controlling agents" is illustrated below. By ensuring that the rates of transfer k_{tr} and k_{dtr} are sufficiently larger than the rate of propagation (k_p), chain growth is controlled.

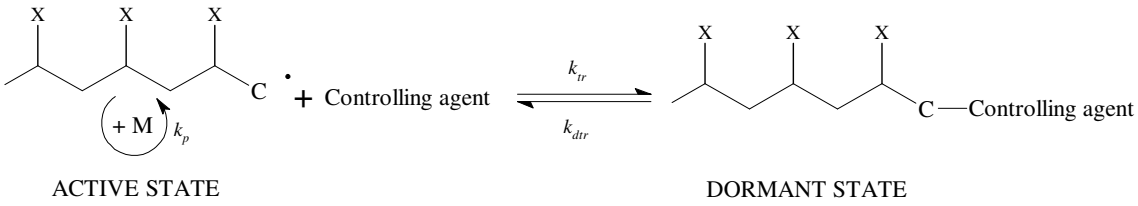

Scheme 2.5: The fundamental process of living radical polymerization techniques.

The evolution of the field of living radical polymerization is given in the timeline below:

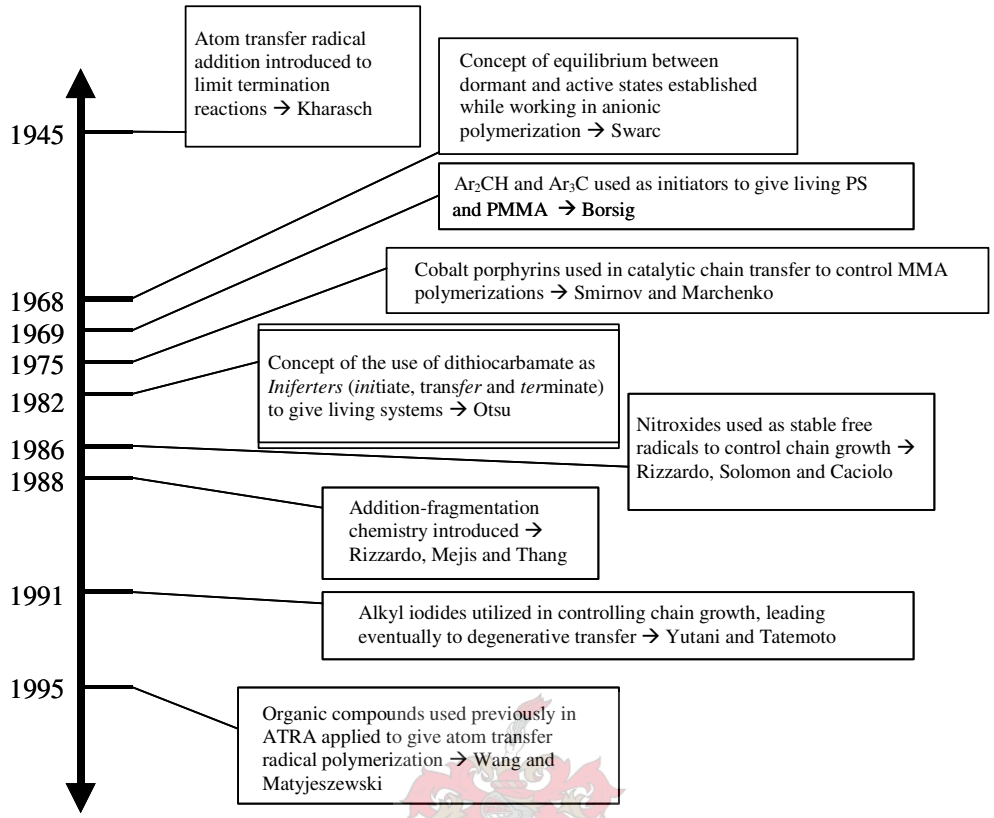

Figure 2.8: Timeline illustrating the evolution of the field of living radical polymerization.[49-56]

At present, all LRP systems are classified into one of two "mechanistic" classes.

- Class 1: The *reversible termination* processes, which includes stable free radical polymerization (SFRP) and atom-tansfer radical polymerization (ATRP).
- Class 2: The *reversible transfer* processes, which includes degenerative transfer (DT) and reversible addition-fragmentation transfer (RAFT).

These techniques all differ mechanistically to that illustrated in Scheme 2.5. Each technique has been applied to bulk, solvent and heterogeneous systems with varying success. In this thesis, the focus is on aqueous heterogeneous systems. The application of the various LRP systems in such media will thus be focused on in this chapter.

2.3.1. STABLE FREE RADICAL POLYMERIZATION

Rizzardo *et al*. first introduced SFRP in the 1980s.[53] The stable free radicals (X·) desired were nitroxides that, in the dormant form, gave alkoxyamines. It was found that certain alkoxy amines

functioned well in the role of initiator.[57] The nitroxide was added in the alkoxyamine form to the polymerization, which thermally cleaved to give the nitroxide radical and an active initiating fragment, which can undergo propagation.

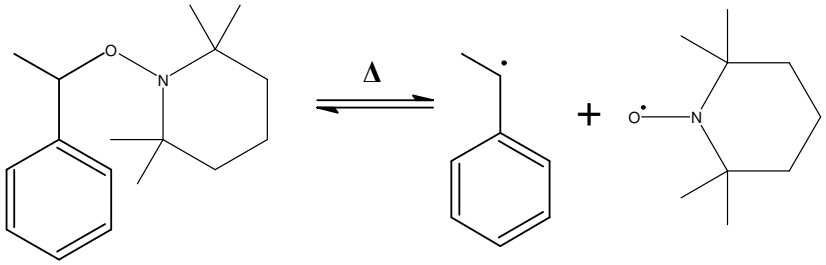

Figure 2.9: Reversible homolytic cleaving of styrene – 2,2,6,6-tetramethyl-1-piperidinyloxy (S-TEMPO) to give the stable free radical 2,2,6,6-tetramethyl-1-piperidinyloxy (TEMPO) and initiating styryl radical.

As is illustrated above, the equilibrium can only be maintained at raised temperatures (>120^{o}C). This system was shown to give products with slightly higher polydispersities than were observed for systems including traditional initiators like benzoyl peroxide (BPO), but lacked the low molecular weight tail common to FRP. The use of such high temperatures is unfavourable for many industrial applications, especially in aqueous heterogeneous polymerization systems. Various other alkoxyamine structures have been proposed that require temperatures of 70 – 110^{o}C.[58]

There is one major drawback of this LRP system: extended polymerization times. This is directly linked to the persistent radical effect *(PRE)*. PRE describes the build up of the nitroxide stable free radicals due to self-termination of the propagating radical chains. This in turn causes the accumulation of dormant polymer chains (a shift in equilibrium).[59] A few ways to overcome this failure of the system have been reported:

- incorporating slow decomposing, conventional initiators without interfering to a large extent with the control → Prevents build-up of persistent radicals[60] and
- introducing instability into the persistent radical structure or additives into the system that will react with the persistent radicals, thereby eliminating them.[61]

SFRP was the first LRP system used in seeded emulsion systems.[62] These systems yielded low molecular weights and large polydispersities. *Ab initio* systems gave successful results but coagulation always occurred to a certain extent in most systems.[63] Better particle stabilities were

obtained by replacing bicomponent initiating systems with negatively charged alkoxyamines.[63] SFRP was also applied in miniemulsions by many research groups with varying degrees of success.[64,65] Slower rates of polymerization as well as larger polydispersities were found when compared to bulk systems.[65] All these systems had still to be kept at raised temperatures (> 100°C), which led to autopolymerization of styrene and in turn a lack of control of the system. The use of macroinitiators (TEMPO capped polystyrene chains) did increase the control of the system.[66] Many systems showed stability problems and much research must still be carried out to solve this.

2.3.2. ATOM TRANSFER RADICAL POLYMERIZATION

In 1995, the system of ATRP was introduced.[56] A schematic representation of this system is shown in scheme 2.6; a covalent bond in a dormant species is cleaved by a redox process, followed by the subsequent atom transfer to the active propagating radical chain.

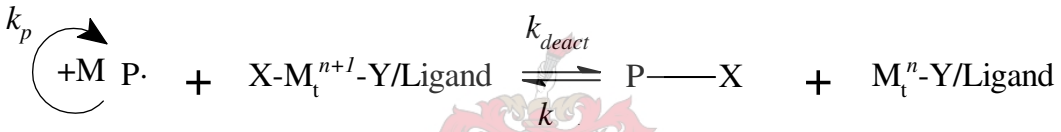

Scheme 2.6: Reversible atom transfer in a transition metal catalyzed ATRP system.

In this scheme, P· represents the propagating radical chain. ATRP has successfully been used to polymerize styrene's, (meth)acrylates, (meth)acrylamides and acrylonitrile.[67] Careful selection of the components in the system will lead to a successful system. The alkyl halide (R-X) initiators used in ATRP are chosen because, if the correct halide is used, the migration of the X atom species between the alkyl group and the propagating radical chain is rapid and selective. Halogens like chlorine, bromine[68] and iodine[69] have been found to be suitable for use in various transition-metal systems for specific monomers. The process of initiation is illustrated below:

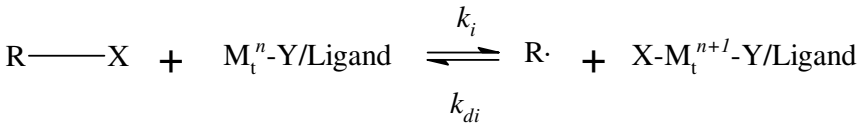

Scheme 2.7: The activation of the ATRP transition metal catalyst by an alkyl halide.

The choice of catalyst system will ultimately determine the dynamics of the interchange between the dormant and active states of the propagating radical chains. The main drawbacks of ATRP are its limited use in the polymerization of less stabilized monomers (vinyl halides, esters, etc) and

acidic monomers that react with the catalyst systems. ATRP has been applied in emulsion systems with limited success for every system.[70] Only ligands with sufficient hydrophobicity will bring the activator-deactivator system into the organic phase. This will allow for a fast enough equilibrium to be established to maintain controlled chain growth. Problems were encountered when some surfactants were found to interfere with the metal-complex system.[71] The use of cationic and non-ionic surfactants solved this problem.[72] ATRP was successfully applied to miniemulsion systems when a strongly hydrophobic ligand, like 5,5'-di(5-nonyl)-4,4'-bipyridine, and a water insoluble initiator were used.[73] Despite the fact that the copper complex is largely water soluble, the fast equilibrium between dormant and active state is maintained within the oil-phase. There was however evidence of poor stability of the particles.[74]

2.3.3. DEGENERATIVE TRANSFER

Alkyl halides were first introduced as controlling agents in the polymerization of fluorinated monomers.[55] Subsequently, many publications illustrate the use of DT in controlling FRP. The fact that low polydispersities were rarely achieved does however make it less favorable than the other LRP techniques already described.[75] The mechanism of the chain transfer illustrated in Scheme 2.8 is clarified below:

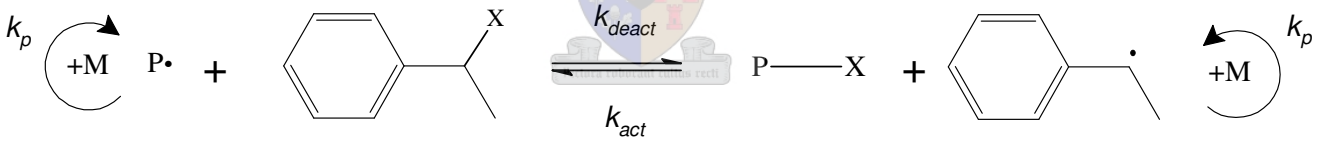

Scheme 2.8: Degenerative transfer using a 1-phenylethly iodide transfer agent.

In this schematic $P\bullet$ refers to the propagating radical chain. A kinetic investigation revealed that the total number of propagating radical chains in a DT system is always equal to the sum of the concentrations of the transfer agent and the concentration of the initiator.[76] This suggests that to have maximum control of the system, the initiator concentration needs to be kept as low as possible. This would then limit the amount of irreversible termination in the system.[76] Degenerative transfer applied in emulsion systems gave stable latexes as well as a living system.[77] Problems with non-linear growth of $\overline{P}_n$ have been identified and linked to low chain transfer constants. A slow diffusion rate of active chain transfer agents from the monomer droplets to the active particles due to the low solubility of the CTAs in the aqueous phase results in the low chain transfer rates. DT was the first

LRP system to be used in miniemulsion polymerizations.[77] 100% chain transfer efficiency was achieved and the molecular weights obtained corresponded well with the theoretically determined MWs. A linear increase in molecular mass could be achieved by feeding the monomer into the polymerization. The slow feed rate leads to much better results than in a corresponding batch emulsion polymerization.

2.3.4. REVERSIBLE ADDITION-FRAGMENTATION TRANSFER

The beginning of addition-fragmentation chemistry started with introducing chain-end functionality using methacroyl-terminated macromonomers synthesized via catalytic chain transfer (CCT).[78] The exchange reaction rates in this system were very low and only high polydispersities could be obtained in bulk polymerizations. The use of more reactive double bond species like dithioesters[79] and xanthates[80] afforded greater control and led to the exponential growth of reversible addition-fragmentation transfer systems. The general structure of "RAFT agents" is given below:

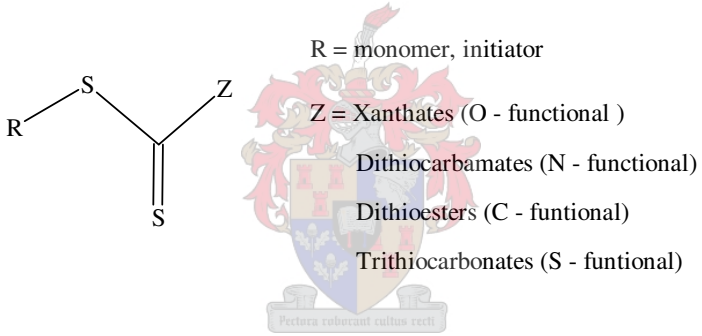

Figure 2.10: Structure of RAFT agents as well as common stabilizing Z- groups and leaving R- groups.

The structure of the leaving group R is usually related to the monomer being used in the polymerization system[81] or to initiators that have previously been shown to work successfully in conventional polymerization systems.[82] Specific RAFT agents work with maximum success in certain systems but not all systems (mostly monomer dependent). It is thus up to a researcher to choose a suitable RAFT agent for any defined system. The structure of the RAFT agent will influence the kinetics of the system due to varying reactivity of the leaving groups as well as the stabilizing nature of the Z groups. This influence can be understood when one examines the mechanism of the addition-fragmentation with specific focus on the rates of addition and fragmentation of the various species.

The mechanistic model of the RAFT process has undergone many changes and is still at this point in time under much debate. A generally accepted fundamental mechanism is given below:

INITIATION:

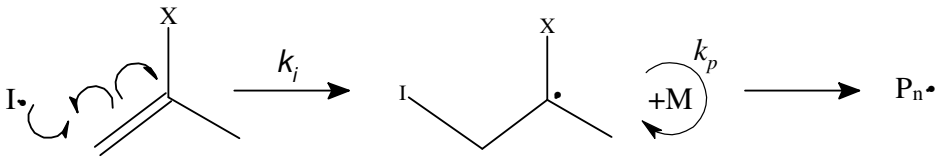

CHAIN TRANSFER:

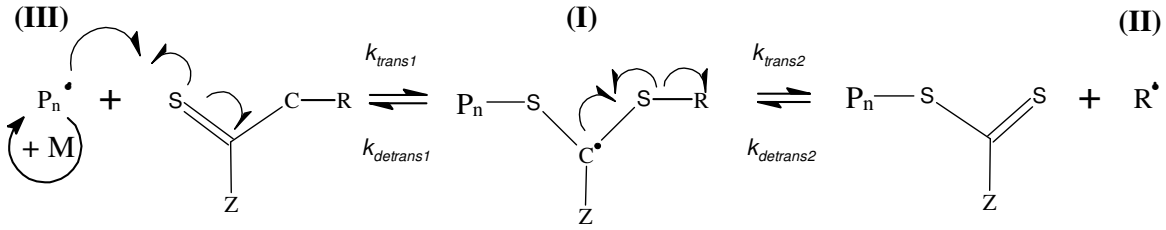

REINITIATION:

CHAIN EQUILIBIRUM:

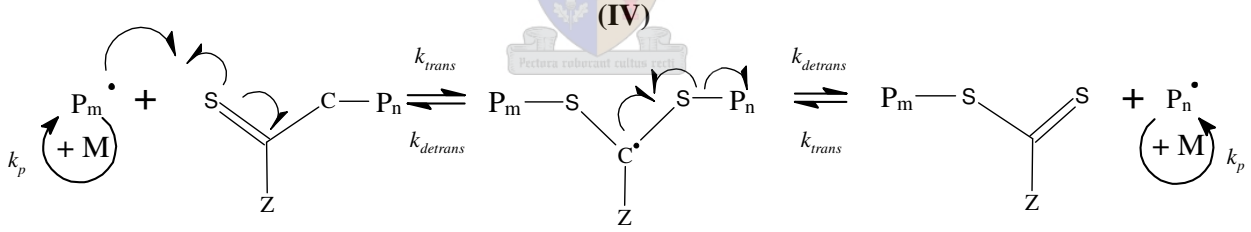

TERMINATION:

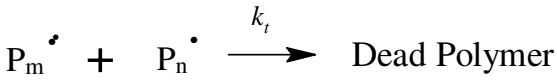

Scheme 2.9: Mechanism of reversible addition-fragmentation transfer.

The fact that the intermediate radical species **(IV)** has been observed via electron-spin resonance (ESR)[83] has led most research groups to believe this elementary mechanism to be an accurate description of the system. To ensure a step-wise growth of the propagating radical chains, the rate of addition of the propagating radical chains to the dithiocarbonyl double bond must be fast when

compared to the rate of propagation. Along with this fact, the termination must be suppressed, which is achieved by keeping the propagating radical concentration low.

$$k_{transfer} \rangle k_{propagationn}$$
$$\text{Probability of transfer} \rangle \text{Pr obability of termination} \tag{2.20}$$

The chain addition of monomer to the propagating radical chain leads to undesirable low molecular mass chains due to termination of fragmented radical chains. Added to this is the fact that common free radical initiators have an exponential decay and will provide free radicals throughout the polymerization. Chains can thus be initiated at all times in the polymerization, which leads to a population of shorter chains. These short chains terminate rapidly due to their ease of diffusion. This is an inherent problem with RAFT-mediated polymerizations and which, to date, has not been eliminated.

The structure of the RAFT agent used in any specific system not only influences the kinetics and behaviour of the system, it also changes the "living" character of the system when expanded to block copolymers. To create a second block, a second monomer is simply added to the system as well as additional initiator. The structure of the macro-RAFT agent (now called a macro-RAFT agent due to the polymer chain end-capped by the RAFT functional group) will influence the fragmentation rates and thus ultimately determine the ability of the polymer chain to fragment from the RAFT agent and for the new monomer unit to add into the RAFT agent. This is illustrated schematically below:

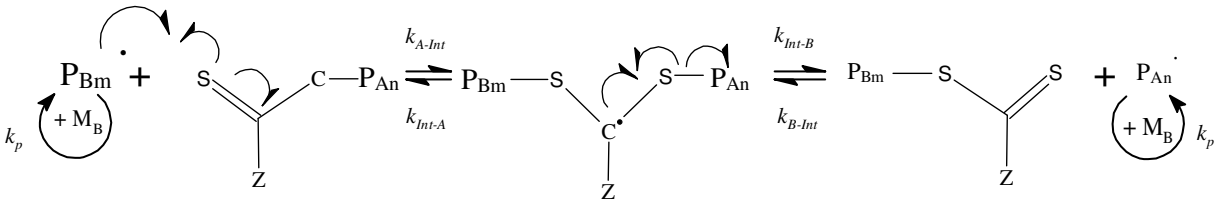

Scheme 2.10: Block copolymer synthesis via RAFT polymerization.

The propagating radical chain P_{Bm}• is formed by the initiation step shown previously in Scheme 2.9. The ability of this chain to add to the macro-RAFT agent without immediately fragmenting again will determine the success of the block copolymer formation. In other words:

$$k_{Int-B} > k_{Int-A} \tag{2.21}$$

This criterion can only be reached if the group P_{An} has a better or comparable leaving ability than the group P_{Bm}.[84] For example: acrylyl and styryl propagating radicals are poor leaving groups whereas methacyryl propagating radicals are good leaving groups. From this one can deduce that methacryl monomers will be used to synthesize the first block. Similar logic for other monomers will determine the sequence of addition.

The kinetics of LRP systems affords a researcher the ability to predict the final molecular mass of the polymer synthesized. For RAFT systems, the concentration of chains in the system after 100% conversion is given as:

$$[chains] = [RAFT] + 2 \cdot f \cdot ([I] - [I]_0) \tag{2.22}$$

The first term describes the RAFT capped living (but dormant) chains and the second term the chains derived from the decomposed initiator. From this one can calculate the theoretical molecular mass:[85]

$$\overline{M}_n theory = FW_{RAFT} + \frac{x[M]_0 FW_M}{[RAFT]_0} \tag{2.23}$$

$$\overline{M}_n theory = FW_{RAFT} + \frac{x[M]_0 FW_M}{[RAFT]_0 + 2 \cdot f \cdot [I]_0 (1 - e^{-kdt})} \tag{2.24}$$

Equation 2.23 excludes the contribution of initiator-derived chains to the final chain concentration whereas 2.24 includes this time-dependant concentration.

There are two mechanistic problems that are plaguing researchers in the field of RAFT polymerization: inhibition and retardation.[86] These two factors are evident in many RAFT systems but their intensities are dependent on the system. Inhibition and retardation lead to polymerization times being longer than theoretically expected. The reasons for this retardation are, with reference to Scheme 2.9:

- slow fragmentation of the intermediate radical species **(I)** as well as **(IV)**,
- slow re-initiation via the leaving fragment **(II)**,
- preferred addition of leaving fragment **(II)** to the RAFT agent compared to addition to monomer and

- preferred addition of the propagating radical chain **(III)** to the RAFT agent compared to addition to monomer.

It has also been speculated that termination of the intermediate propagating radical species **(I** and **IV)** may also lead to the retardation phenomena.[86] There is still much debate about this theory, but the detection of these terminated species using ^{13}C NMR spectroscopy has led to further evidence that this might actually be the case.[87] All these problems are linked to the mechanistic behaviour of the RAFT agents. By appropriately choosing efficient stabilizing and leaving groups, the retardation effects can be limited. Even with these failures, RAFT-mediated polymerization is still a versatile means to synthesize designed polymers. There is a range of "architectural tools" that RAFT-mediated polymerization provides:[88]

- polymers with low polydispersities can be synthesized (<1,2),
- RAFT functionality is retained on all chain ends and can be converted to another desired functionality e.g. a dithioester can be converted to a thiol group after treatment with a hydroxide or amine,
- gradient polymers can be synthesized by designing an appropriate feed rate of various monomers,
- star polymers can be synthesized using multi-arm dithio compounds,
- block copolymers are easily synthesized due to the livingness of system. Criteria set out earlier must however be met to maintain low polydispersities of the final block and
- triblock copolymers can be synthesized using difunctional RAFT agents.

All these "tools", along with the versatility of RAFT with respect to varying reaction conditions: monomers, initiators, solvents and temperatures, makes RAFT-mediated polymerization one of the most useful LRP systems. Currently, there is much research being done on the application of RAFT polymerization in heterogeneous aqueous systems like emulsions and suspensions.[89] The application of RAFT in water-based systems is a natural extension, since the RAFT process is in itself a robust system and does not require stringent conditions.

2.3.4.1. Reversible addition-fragmentation transfer in emulsion systems

The mechanism that operates in reversible transfer LRP techniques such as DT and RAFT should theoretically enable its application to emulsion systems. The reason for this is the fact that the transfer agent species remains at all times on a polymer chain. This lowers the probability of control agent species loss through desorption into the aqueous phase. The system will behave as though a simple chain transfer agent has been added. To maintain the control that the RAFT technique affords a researcher, the following points need to be addressed:

- The concentration of RAFT agents in the aqueous phase should be kept to a minimum as to prevent water-soluble oligomers forming, which will not nucleate droplets.
- Due to that fact that most common RAFT agents have limited phase mobility, the droplet-water interface must be large enough to ensure all droplets contain the RAFT agent and that it is consumed early in the polymerization.
- The exit rate coefficient of the leaving groups is dependent on the size of the particles, diffusion coefficient and partition coefficient of the species in the water phase.[20] This radical exit will lead to rate retardation. Seeded experiments have shown that the presence of transfer agents strongly affects the exit and even entry rates of radical species.[90]

Dithioester RAFT agents were the first RAFT agents used in emulsion systems[79] and later xanthates were also used.[93] Both systems gave good conversions and control although the dithioester RAFT agents produced polymers with narrower PDs. Rate retardation was observed in both systems[92,93] but the biggest problem encountered was the formation of a separate bulk phase at the onset of interval 2 for RAFT agents with a high transfer coefficient (C_t). This layer was identified as containing dormant, short polymer chains, swollen with monomer.[94] The formation of this layer was linked to the formation of low molecular mass dormant chains that, due to their slow diffusion into the particles, remain in the aqueous phase and eventually coalesce and form a coagulum.[95] Elimination of this destabilization and layer formation was achieved by the use of dithiobenzoate-end-capped styrene oligomers (macroRAFT agents) rather than conventional dithiobenzoate RAFT agents.[96]

2.3.4.2. Reversible addition-fragmentation transfer in miniemulsion systems

Many of the benefits of miniemulsion systems can be successfully applied to create optimal conditions for LRP techniques. The fact that for typical miniemulsion systems each droplet acts like an individual nano-reactor means that no transport of monomer through the aqueous phase is required. Any control agent components can be selectively kept inside the particles and transport through the different phases is not required.

The RAFT technique was the first LRP technique introduced into miniemulsion systems. The first investigations showed a lack of stability, similar to that seen in emulsion systems.[94] The destabilization was found to be higher with ionic surfactants (SDS and CTAB) and almost absent with nonionic surfactants.[94] Water-soluble and insoluble initiators behaved similarly as did most conventional monomers. Systems using RAFT agents with lower chain transfer coefficients (slower reacting) showed better success.[92] As was mentioned earlier, similar instability problems were also experienced with ATRP and SFRP techniques when applied to miniemulsion systems. This indicates that the cause of the instability does in fact not lie in the mechanistic behaviour of the techniques. The cause lies rather in the common fact that for these three techniques, during the early stages of polymerization, low molecular weight oligomers in dormant and/or active states are present. These oligomers will alter the kinetic model of radical desorption, termination and droplet nucleation.[94] The use of polymeric RAFT agents provides stability, indicating that the radical exit from the droplets might be the ultimate cause for instability.[93] The fact that nonionic surfactants reduce the degree of destabilization could be linked to the fact that the hydration layer prevents radical movement into and out of the particles.[24] A standard "recipe" for the creation of stable miniemulsions has now been established.[98]

The introduction of the RAFT technique into miniemulsion polymerizations was expected not to affect the rate of polymerization R_p due to the fact that the number of active chains is, in theory, constant throughout the reaction. This in fact is not the case and significant rate retardation is found. This problem was introduced in Section 2.3.4.1 and was linked to the RAFT agent itself. The fact that certain RAFT agents do show stronger rate retardation indicates that the fate of the intermediate radical species does influence the system kinetics.[97] Compounded with this problem is the fact that radical exit from the droplets is also plausible (as was seen for emulsion systems). After the first exchange reaction between the RAFT agent and a propagating radical chain, a short radical species R·, that is the initiator fragment, remains. This fragment may exit from the particle, and this rate of

exit is determined by its solubility in the aqueous phase, its ability to move through the stabilizing surfactant layer and its tendency to add back onto the RAFT agent. Equation 2.13 described the radical exit kinetically.

One of the problems with miniemulsion systems that will detract from the control afforded by the RAFT technique is that of micellar and homogeneous nucleation. It is generally accepted that most RAFT agents' diffusivity through the aqueous phase is limited.[91] Thus the droplets (and later particles) will be the only locus of controlled growth. This, however, is not always the case. A certain degree of micellar or homogeneous nucleation can occur.[46] This will lead to the formation of particles that lack a RAFT agent, which implies non-living polymer growth. To analyze the occurrence of uncontrolled growth, a technique to identify chains that contain the RAFT agent functionality is required. A duel-detector system namely refractive index (RI) – ultraviolet (UV), coupled to gel permeation chromatography (GPC) has been used to identify different polymers during a copolymer synthesis.[98] This technique can be utilized to differentiate between the polymer distributions that have retained the thiol carbonyl thiol (RAFT agent) functionality and those that have not, during the polymerization. The two distributions will then mechanistically have a different origin. The origin of any non-living polymer can also be investigated by using aqueous phase radical scavengers (introduced in Section 2.2.3). If the presence of these scavengers in a miniemulsion polymerization causes a change in the non-living polymer growth, then the mechanism behind this growth could be traced to the fact that there are propagating radicals within the aqueous phase. If there is no evidence of a change in non-living growth, then the origin should lie in a mechanistic phenomenon taking place within the oil-phase. Non-living polymer growth has been reported for copolymerizations of styrene and methyl methacrylate when the feed monomer ratio was 1:9.[99] A duel-detector system like that described above was utilized to monitor the styrene inclusion into the copolymer. It was reported that the non-living nature was due to coupling reactions, but this must still to be confirmed.

2.4. REFERENCES

(1) Schroeter, G. *Be.r* **1916**, *49*, 2698

(2) Staudinger, H. *From Organic Chemistry to Macromolecules*; Wiley-Interscience: New York, **1961**

(3) Kern, W.; Kammerer, H. *Makromoleckular Chem.* **1948**, *2*, 127

(4) Moad, G.; Solomon, D. H. *The Chemistry of Free Radical Polymerization*; First ed., Elsevier Science Ltd: Oxford, **1995**

(5) Solomon, D. H.; Moad, G. *Macromolecular Chem., Macromolecular Symp.* **1987**, *10*, 109

(6) Bednarek, D.; Moad, G.; Rizzardo, E.; Solomon, D. H. *Macromolecules* **1988**, *21*, 1522

(7) Maillard, B.; Ingold, K.; Scaiano, J. C. *Journal of the American Chemical Society* **1983**, *105*, 5095

(8) Moad, G.; Rizzardo, E.; Solomon, D. H.; Johns, S. R.; Willing, R. I. *Macromolecular Rapid Commun.* **1984**, *5*, 793

(9) Bamford, C. H. In *Comprehensive Polymer Science*; Sigwalt, P., Ed.; Pergamon: London, **1989**; Vol. 3, p 219

(10) Allen, P. E. M.; Partick, C. R. *Kinetics and mechanims of polymerization reactions*; Ellis Harwood: Chichester, **1974**

(11) Olaj, O. F.; Bitai, I.; Hinkelman, F. *Macromolecular Chem.* **1987**, *188*, 1689

(12) Heuts, J. P. A.; Davis, T. P.; Russell, G. T. *Macromolecules* **1999**, *32*, 6019

(13) Gleixner, G.; Olaj, O. F.; Breitenbach, J. W. *Makromolekular Chem.* **1979**, *180*, 2581

(14) Bizilj, S.; Kelly, D. P.; Serelis, A. K.; Solomon, D. H.; White, E. S. *Australian Journal of Chemistry* **1985**, *38*, 1657

(15) Matyjaszewski, K.; Davis, T. P., Eds. *Handbook of Polymer Chemistry*; John Wiley and Sons, Inc.: Hoboken, **2002**

(16) Luther, M.; Hueck, C. In U.S. Patent 1,864,078 **1932**

(17) Gilbert, R. G. *Emulsion Polymerization: A Mechanistic Approach*; Academic Press: San Diego, **1995**

(18) Ghielmi, A.; Storti, G.; Morbidelli, M.; Ray, W. H. *Macromolecules* **1998**, *31*, 7172

(19) Maxwell, I. A.; Morrison, B. R.; Napper, D. H.; Gilbert, R. G. *Macromolecules* **1991**, *24*, 1629

(20) Ugelstad, J.; Hansen, F. K. *Rubber Chemistry Technol.* **1976**, *49*, 536

(21) Smith, W. V.; Ewart, R. H. *Journal of Chemical Physics* **1948**, *16*, 592

(22) Asua, J. M. *Journal of Polymer Science: Part A: Polymer Chemistry* **2004**, *42*, 1025

(23) Asua, J. M. *Macromolecules* **2003**, *36*, 6245

(24) Vorwerg, L.; Gilbert, R. G. *Macromolecules* **2000**, *33*, 6693.

(25) Gardon, J. L. *Journal of Polymer Science Part A: Polymer Chemistry* **1968**, *6*, 2853

(26) Ugelstad, J.; El-Aasser, M. S.; Vanderhoff, J. W. *Journal of Polymer Science: Polymer Letters Edition* **1973**, *111*, 503

(27) Brouwer, W. M.; El-Aasser, M. S.; Vanderhoff, J. W. *Colloids Surfaces* **1986**, *21*, 69

(28) Delgado, J.; El-Aasser, M. S.; Vanderhoff, J. W. *Journal of Polymer Science: Polymer Chemistry Edition* **1986**, *23*, 2973

(29) Wu, X. Q.; Schork, F. J. *Journal of Applied Polymer Science* **2000**, *81*, 1691

(30) Kabalnov, A. S.; Shchukin, E. D. *Adv. Colloid Interface Sci.* **1992**, *38*, 69

(31) Luo, Y.; Tsavalas, J. G.; Schork, F. J. *Macromolecules* **2001**, *34*, 5501-5507

(32) Landfester, K.; Bechthold, N.; Forster, S.; Antonietti, M. *Macromolecular Rapid Commun.* **1999**, *20*, 81

(33) Delgado, J.; El-Aasser, M. S.; Silibi, C. A.; Vanderhoff, J. W. *Journal of Polymer Science Part A: Polymer Chemistry* **1990**, *32*, 777

(34) Miller, C. M.; Blythe, P. J.; Sudol, E. D.; El-Aasser, M. S. *Journal of Polymer Science Part A: Polymer Chemistry* **1994**, *32*, 2365

(35) Blythe, P. J.; Morrison, B. R.; Mathauer, K. A.; Sudol, E. D.; El-Aasser, M. S. *Macromolecules* **1999**, *32*, 6944

(36) Blythe, P. J.; Klein, A.; Sudol, E. D.; El-Aasser, M. S. *Macromolecules* **1999**, *32*, 6952.

(37) Bechthold, N.; Landfester, K. *Macromolecules* **2000**, *33*, 4682.

(38) Tang, P. L.; Sudol, E. D.; Adams, M. E.; Silebi, C. A.; El-Aasser, M. S. In *Polmyer Latexes: Preparation, characterization and application*; American Chemical Society: Washington DC **1992** p. 72

(39) Blythe, P. J.; Sudol, E. D.; El-Aasser, M. S. *Journal of Polymer Science: Part A: Polymer Chemistry* **1997**, *35*, 807

(40) Edelhauser, H.; Breitenbach, J. W. *Journal of Polymer Science* **1959**, *35*, 423

(41) Asua, J. M.; Rodriguez, V. S.; E.D., S.; El-Aasser, M. S. *Journal of Polymer Science: Part A: Polymer Chemistry* **1989**, *27*, 3569-358

(42) Luo, Y.; Schork, F. J. *Journal of Polymer Science: Part A: Polymer Chemistry* **2002**, *40*, 3200.

(43) Tang, P. L.; Sudol, E. D.; Adams, M.; El-Aasser, M. S.; Asua, J. M. *Journal of Applied Polymer Science* **1991**, *42*, 2019

(44) Rodriguez, V. S.; Asua, J. M.; El-Aasser, M. S.; Silibi, C. A. *Journal of Polymer Science Part A: Polymer Physics* **1991**, *29*, 483

(45) Chern, C. S.; Liou, Y. C. *Journal of Polymer Science Part A: Polymer Chemistry* **1999**, *37*, 2537

(46) Sajjadi, S.; Jahanzad, F. *Euopean Polymer Journal* **2003**, *39*, 785

(47) Matyjaszewski, K.; Ziegler, M. J.; Arehart, S. V.; Greszta, D.; Pakula, T. *Journal of Physical Organic Chemistry* **2000**, *13*, 775

(48) Swarc, M. *Carbanions, Living Polymers and Electron transfer process*,; Interscience: New York, **1968**

(49) Kharasch, M. S.; Jensen, E. V. *Science* **1945**, *102*, 128

(50) Borsig, E.; Lazar, M.; Capla, M.; Florian, S. *Angewandte Makromolekular Chemie* **1969**, *9*, 89

(51) Enikolopov, N. S.; Korolev, G. V.; Marchenko, A. P.; Ponomarev, G. V.; Smirnov, B. R.; Titov, V. I. In Russian Patent 664,434, **1980**

(52) Otsu, T.; Yoshida, M.; Tazaki, T. *Macromolecular Chemistry, Rapid Commun.* **1982**, *3*, 133

(53) Solomon, D. H.; Rizzardo, E.; Cacioli, P. In U. S. Patent 4,581,429, **1986**

(54) Rizzardo, E.; Mejis, G. F.; Thang, S. In World Patent 884304, **1988**

(55) Yutani, Y.; Tatemoto, M. In European Patent 489370, **1991**

(56) Wang, J.-S.; Matyjaszewski, K. *Journal of the American Chemical Society* **1995**, *117*, 5614

(57) Hawker, C. J.; Hedrick, J. L. *Macromolecules* **1995**, *28*, 2993

(58) Muira, Y.; Nakamura, N.; Taniguchi, I. *Macromolecules* **2001**, *34*, 447

(59) Fischer, H. *Macromolecules* **1997**, *30*, 5666-5672

(60) Greszta, D.; Matyjaszewski, K. *Journal of Polymer Science: Part A: Polymer Chemistry* **1997**, *35*, 1875

(61) Georges, M. K.; Veregin, R. P. N.; Kazmaier, P. M.; Hamer, G. K.; Saban, M. D. *Macromolecules* **1994**, *27*, 7228

(62) Bos, S. A. F.; Bosveld, M.; Klumperman, B.; German, A. L. *Macromolecules* **1997**, *30*, 324

(63) Marestin, C.; Noel, C.; Guyot, A.; Claverie, J. *Macromolecules* **1998**, *31*, 4041-4044

(64) Farcet, C.; Lansalot, M.; Charleux, B.; Pirri, R.; Vairon, J.-P. *Macromolecules* **2000**, *33*, 8559

(65) Prodpan, T.; Dimonie, V. L.; Sudol, E. D.; El-Aasser, M. S. *Polymer Materical Science Engineering* **1999**, *80*, 534

(66) Keoshkerian, B.; Macleod, P. J.; Georges, M. K. *Macromolecules* **2001**, *34*, 3594

(67) Matyjaszewski, K. *Chemical European Journal* **1999**, *5*, 3095

(68) Davis, K.; O'Malley, J.; Paik, H. J.; Matyjaszewski, K. *Polym Prepr (Am Chem Soc Div Polym Chem)* **1997**, *38*, 687

(69) Kotani, Y.; Kamigaito, M.; Sawamoto, M. *Macromolecules* **1999**, *32*, 2420

(70) Qiu, J.; Shipp, D.; Gaynor, S. G.; Matyjaszewski, K. *Polymer Preparations (Am Chem Soc Div Polym Chem)* **1999**, *40*, 418

(71) Chambard, G.; de Man, P.; Klumperman, B. *Macromolecular Symposia* **2000**, *50*, 45

(72) Jousset, S.; Qiu, J.; Matyjaszewski, K.; Granel, C. *Macromolecules* **2000**, *34*, 5951.

(73) Matyjaszewski, K.; Qiu, J.; Tsarevsky, N. V.; Charleux, B. *Journal of Polymer Science: Part A: Polymer Chemistry* **2000**, *38*, 4724.

(74) Matyjaszewski, K.; Shipp, D. A.; Qiu, J.; Gaynor, S. *Macromolecules* **2000**, 33, 2296

(75) Gaynor, S. G.; Wang, J.-S.; Matyjaszewski, K. *Macromolecules* **1995**, *28*, 8051

(76) Matyjaszewski, K.; Gaynor, S.; Wang, J.-S. *Macromolecules* **1995**, *28*, 2093

(77) Lansalot, M.; Farcet, C.; Charleux, B.; Vairon, J.-P. *Macromolecules* **1999**, *32*, 7354

(78) Moad, C. L.; Moad, G.; Rizzardo, E.; Thang, S. H. *Macromolecules* **1996**, *29*, 7717

(79) Chiefari, J.; Chong, Y. K. B.; Ercole, F.; Krstina, J.; Jeffery, J.; Le, T. P. T.; Mayadunne, R. T. A.; Meijs, G. F.; Moad, C. L.; Moad, G.; Rizzardo, E.; Thang, S. H. *Macromolecules* **1998**, *31*, 5559

(80) Destarac, M.; Charmot, D.; Franck, X.; Zard, S. Z. *Macromolecular Rapid Commun.* **2000**, *21*, 1035

(81) Tang, C.; Kowalewski, T.; Matyjaszewski, K. *Macromolecules* **2003**, *36*, 8587

(82) Thang, S. H.; Chong, Y. K. B.; Mayadunne, R. T. A.; Moad, G.; Rizzardo, E. *Tetrahedron Letters* **1999**, *40*, 2435

(83) Calitz, F. M.; Tonge, M. P.; Sanderson, R. D. *Macromolecules* **2003**, *36*, 5

(84) Chong, B. Y. K.; Le, T. P. T.; Moad, G.; Rizzardo, E.; Thang, S. H. *Macromolecules* **1999**, *32*, 2071

(85) Moad, G.; Chiefari, J.; Chong, B. Y.; Krstina, J.; Mayadunne, R. T.; Postma, A.; Rizzardo, E.; Thang, S. H. *Polymer International* **2000**, *49*, 993

(86) Monteiro, M. J.; de Brouwer, H. *Macromolecules* **2000**, *34*, 349

(87) Calitz, F. M.; McLeary, J. B.; Mckenzie, J. M.; Klumperman, B.; Sanderson, R. D.; Tonge, M. P. *Macromolecules* **2003**, *36*, 9687

(88) Rizzardo, E.; Chiefari, J.; Chong, Y. K.; Ercole, F.; Krstina, J.; Jeffery, J.; Le, T.; Mayadunne, R.; Mejis, G. F.; Moad, G.; Thang, S. H. *Macromolecular Symposia* **1999**, *143*, 291

(89) Le, T. P.; Moad, G.; Rizzardo, E.; Thang, S. H. In World Patent 98/01478, **1998**

(90) Smulders, W.; Gilbert, R. G.; Monteiro, M. J. *Macromolecules* **2003**, *36*, 4309

(91) Charmot, D.; Corpart, P.; Adam, H.; Zard, S. Z.; Biadatti, B. G. *Macromolecular Symposia* **2000**, *150*, 23-32

(92) Monteiro, M. J.; Hodgson, M.; de Brouwer, H. *Journal of Polymer Science Part A: Polymer Chemistry* **2000**, *38*, 3864

(93) Monteiro, M. J.; Sjoberg, M.; Van Der Vlist, J.; Gottgens, C. M. *Journal of Polymer Science: Part A: Polymer Chemistry* **2000**, *38*, 4206

(94) De Brouwer, H.; Tsavalas, J. G.; Schork, F. J.; Monteiro, M. J. *Macromolecules* **2000**, *33*, 9239

(95) De Brouwer, H. PhD thesis; Eindhoven University of Technology; **2001**

(96) Vosloo, J. J.; De Wet-Roos, D.; Tonge, M. P.; Sanderson, R. D. *Macromolecules* **2002,** 35, 4899

(97) McLeary, J. B.; Tonge, M. P.; De Wet-Roos, D.; Sanderson, R. D.; Klumperman, B. *Journal of Polymer Science Part A: Polymer Chemistry* **2004**, *42*, 960

(98) Lansalot, M.; Davis, T. P.; Heuts, J. P. A. *Macromolecules* **2002**, *35*, 7582

(99) Luo, Y.; Liu, X. *Journal of Polymer Science Part A: Polymer chemistry* **2004**, *42*, 6248

Pectora roborant cultus recti

Chapter 3. : *RAFT agent synthesis, miniemulsion formulations and preparation, and characterization of polymer and latexes.*

ABSTRACT

The synthesis of four the RAFT agents used in various miniemulsion polymerizations in this thesis is first described. The standard miniemulsion formulation as well as a table describing all the polymerizations referred to in Chapters 4 –7 is given. The preparation of the miniemulsions is also examined. Lastly, the analytical techniques used to characterize the various polymers and latexes are addressed.

3.1. RAFT AGENT SYNTHESIS

The general structure of all RAFT agents used in this study was given in Figure 2.10. In Section 2.3.4, it was proposed that the structure of the RAFT agent could potentially have a significant effect on its mechanistic behaviour. This structurally dependent behaviour could be linked to the nature of the R- and/or Z- groups of the RAFT agent. Focusing on the leaving R- group, characteristics such as water solubility, diffusivity and reactivity (towards monomer and the RAFT agent) will influence the RAFT equilibrium established within the particles of a miniemulsion. This equilibrium will also be influenced by the degree of stabilization of the intermediate radical, provided by the Z- group.

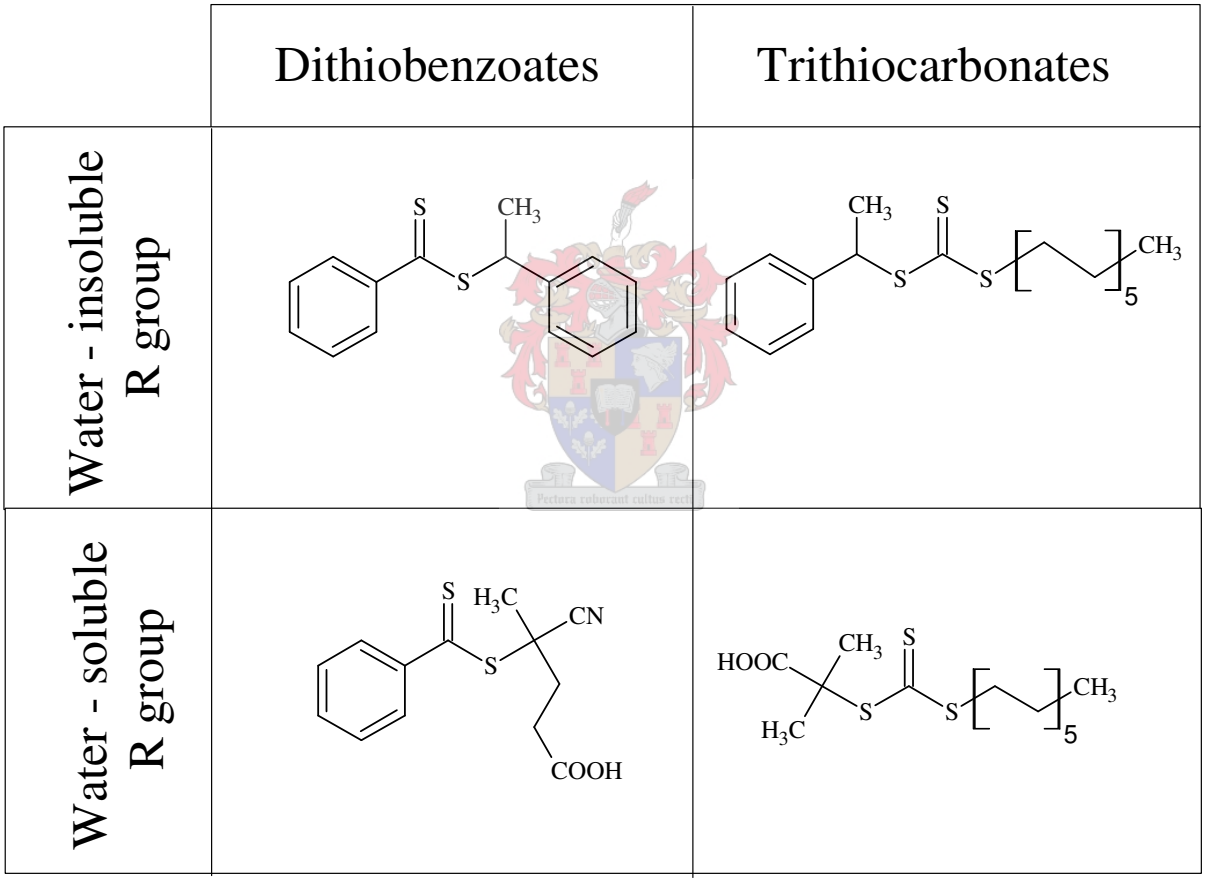

Figure 3.1: The four RAFT agents synthesized in this study.

To create an accurate model that will describe the effect that these variables (nature of R- and Z-groups) will have on the RAFT-mediated miniemulsion polymerization, a range of RAFT agents needs to be investigated. For this purpose, four RAFT agents were synthesized. They fall into two groups: dithiobenzoates and trithiocarbonates, as shown in Figure 3.1.

3.1.1. DITHIOBENZOATES

Dithiobenzoates are described by the common RAFT agent structure given in Figure 2.10, where the Z- group of the RAFT agent is a phenyl group and the R- group is an alkyl or aryl group. These RAFT agents are synthesized by forming dithioesters from dithiobenzoic acids. The two dithiobenzoates synthesized in this study were: cyano-valeric acid dithiobenzoate (CVADTB) and 1-phenylethyl dithiobenzoate (PEDTB). Both syntheses require a common starting material, namely dithiobenzoic acid. For the sake of simplicity, the preparation of the dithiobenzoic acid will be presented in Section 3.1.1.1, followed by separate synthetic pathways for the final RAFT agents.

3.1.1.1. Synthesis of dithiobenzoic acid

A Grignard reaction allows for the carbon-carbon formation between a halogenated compound and an electrophile such as aldehyde, alkyl halide, ester or isocyanate.[1] This process has been successfully used to synthesize dithiobenozic acid of high purity.[2] The organic halogen and electrophile used in the synthesis of dithiobenzoic acid were bromobenzene and carbon disulphide (CS_2) respectively. The complete synthesis is shown in Schemes 3.1 and 3.2:

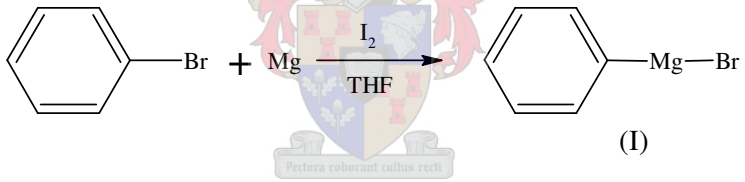

Scheme 3.1: Preparation of the Grignard agent (I) using bromobenzene as the organic halide.

Iodine is used *in situ* to activate the magnesium substrate. The addition of iodine is assumed to form a catalytic amount of magnesium iodide or to etch the surface of the magnesium turnings.[1]

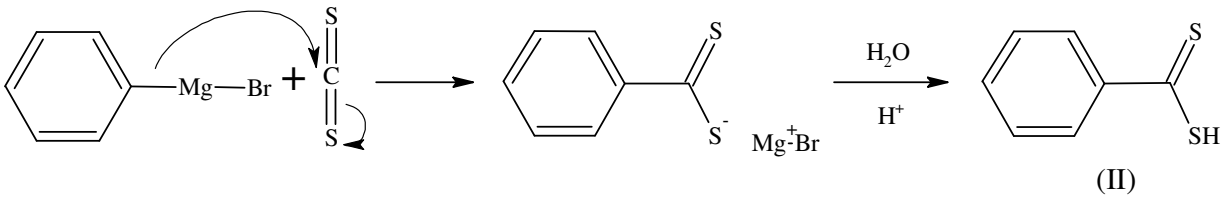

Scheme 3.2: Nucleophilic addition of (I) to CS_2 to give dithiobenzoic acid (II).

Experimental

Magnesium turnings (Aldrich, 3 g, 0.123 mol) were placed in a 250 ml three-neck reaction vessel along with a catalytic amount of iodine (Aldrich, 1 crystal) and a magnetic stirrer bar. A condenser

closed with a calcium chloride drying tube and two dripping funnels, was fitted. Great care was taken to ensure that all the apparatus was dry before assembly. Anhydrous conditions were maintained throughout the Grignard reaction. Bromobenzene (Aldrich, 18.4 g, 0.117 mol) was placed in one dripping funnel and dry, distilled THF (distilled from $LiAlH_4$, 50 ml) in the other.

A small volume (± 2 ml) of THF was added to allow sufficient mixing of the magnesium turnings. A few drops of bromobenzene were added and the reaction was heated very slightly. The onset of the reaction is marked by the disappearance of the yellow-brown iodine colour. At this point the vessel was submerged in an ice-bath. The remaining bromobenzene was added dropwise. The reaction colour changed to green-grey. Additional THF was added when the viscosity of the reaction mixture increased. After 20 min the ice bath was removed and the reaction was left to run to completion, as indicated by the complete cooling of the reaction mixture.

After the Grignard agent was formed, the reactor was placed in an ice-bath. CS_2 (Aldrich, 9.17 g, 0.12 mol) was placed in an empty dripping funnel, replacing one of the used dripping funnels. The CS_2 was added dropwise to ensure that the exothermic reaction did not become uncontrolled (complete addition over 20 min). Additional THF was added if the reaction mixture became viscous. The addition of the CS_2 led to a colour change from green-grey to red. After all the CS_2 was added, the Grignard mixture was neutralized by the addition of 100 ml cold, distilled, deionized water. The neutralization was exothermic and the reactor was kept in the ice-bath until no reaction heat evolved. The mixture was filtered to remove unreacted magnesium turnings. The filtrate was then transferred to a 1*l* separating funnel and acidified by the addition of 20 ml 33% HCl (ACE). The acidification led to the red colour being replaced by a deep purple colour of the dithiobenzoic acid. The mixture was washed twice with diethyl ether and the organic layer was dried over anhydrous magnesium sulphate. The diethyl ether was removed by rotary evaporation, leaving the unpurified acid. The dithiobenzoic acid is unstable and was stored at -5^{o}C. It was found that in this way the acid could be stored for some weeks without major loss of product.

3.1.1.2. Synthesis of cyanovaleric acid dithiobenzoate from dithiobenzoic acid

The dithiobenzoic acid intermediate (II) is converted into bis(thiobenzoyl) disulphide via a redox coupling reaction.[3] Dimethyl sulphoxide is reduced to (methylthio) methane. The reaction is catalyzed by iodine:

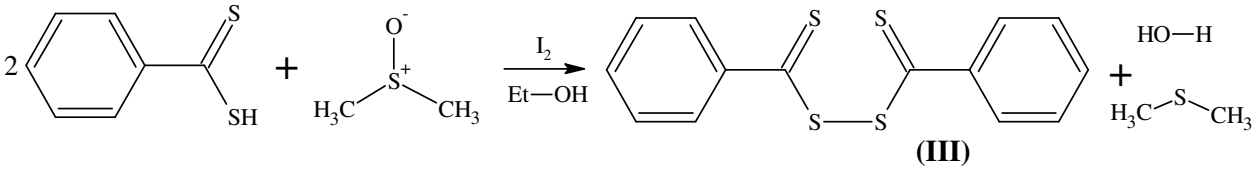

Scheme 3.3: Formation of bis(thiobenzoyl) disulphide (III) from dithiobenzoic acid.

The final step is that of a radical reaction between the bis(thiobenzoyl) disulphide and an appropriate initiator commonly used in free radical polymerizations.[3] The choice of initiator depends on the desired leaving group of the final RAFT agent. In the case of CVADTB, the leaving group is that of cyano-valeric acid or cyano-pentanoic acid. The initiator used in the reaction is thus that of 4,4'-azo-bis(4-cyanovaleric acid). The initiator fragmentation and fragmentation products are shown in Scheme 3.4:

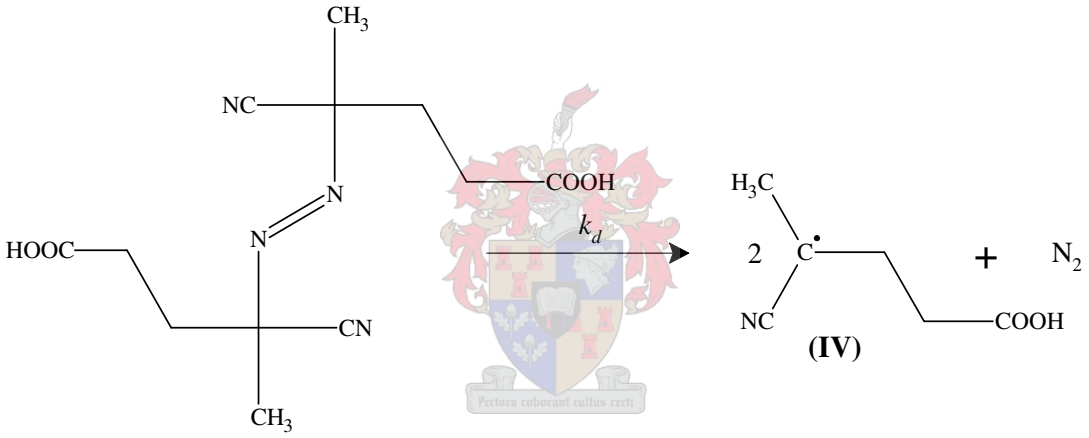

Scheme 3.4: Decay of 4,4'-azo-bis(4-cyanovaleric acid).

These initiator fragments then react with the disulphide molecules to give the final cyanovaleric acid dithiobenzoate:

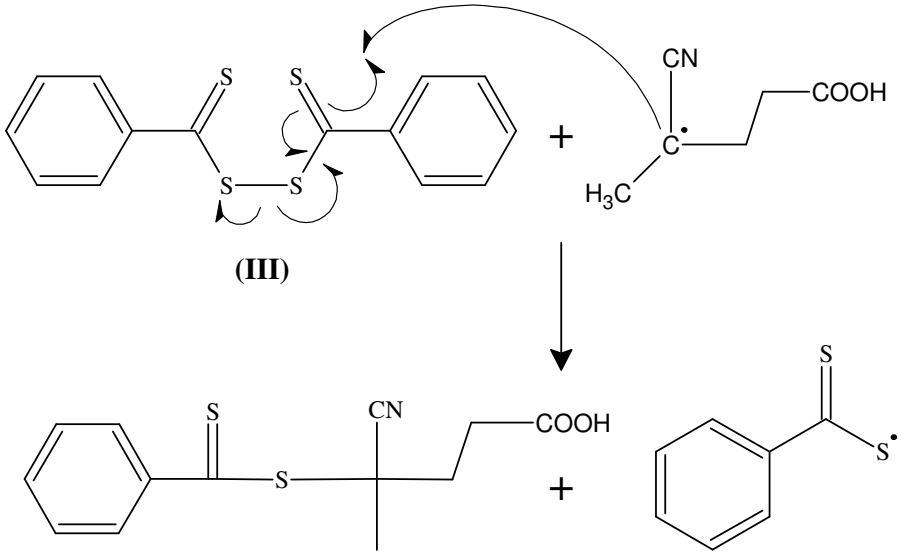

Scheme 3.5: Radical addition of initiator fragment to bis(thiobenzoyl) disulphide (III).

For all radical reactions, the time until completion depends on the rate of decay of the initiating radical species, given by k_d. Any initiating species has a defined *half-life*, which is the time taken for the initiator concentration to halve. To estimate the time needed for the radical reaction shown in Scheme 3.5 to reach completion, five times the half-life of the initiator was taken; this was about 12 hours at 85°C. It was found that extending the reaction beyond this leads only to the formation of degradation products and a decrease in yield of the RAFT agent. The reaction is performed under an inert atmosphere, e.g. UHP nitrogen, to eliminate the inhibiting effect of oxygen on the radical reaction.

Experimental

Dithiobenzoic acid (34.63 g, 0.224 mol) was placed in a 250 ml two-neck reactor vessel along with a magnetic stirrer bar and a catalytic amount of iodine. Approximately 5 ml of absolute ethanol was added. A condenser was fitted to one neck and a dripping funnel to the other. DMSO (Saarchem, 17.52 g, 0.224 mol) was placed in the dripping funnel. The reactor was placed in an ice-bath to prevent excessive heat build-up during the DMSO addition, as well as to promote the crystallization process. The DMSO was added dropwise, and the last few drops caused crystals to appear. The crystals were filtered off and washed with cold ethanol. The filtrate was also stored at –5°C to promote additional crystal formation. The crystals were of high stability and could be stored for many weeks.

For the radical reaction, a 250 ml three-neck flask with a magnetic stirrer bar was placed in an oil-bath at 85°C. The bis(thiobenzoyl) disulphide crystals (27.86 g, 0.091 mol) and 4,4'-azo-bis(4-cyanovaleric acid) (Sigma-Aldrich, 25.50 g, 0.091 mol) were placed in the reactor along with about 20 ml ethyl acetate. The reaction mixture was purged with UHP nitrogen for 10 min. The reaction was kept under an inert atmosphere for the duration of the reaction.

After 12 hours the reaction was stopped. All solvent was removed by rotary evaporation. The RAFT agent was purified by column chromatography using silica gel as stationary phase and a mixture of 2:2:6 heptane:pentane:ethyl acetate as mobile phase (R_f = 0.625). The final product crystallized during vacuum drying. Verification of purity and structure was determined by ^{1}H-NMR ($CDCl_3$): 1.95, s, 3H → methyl; 2.4 -2.8, m, 4H → methylene; 7.3 – 8.0, m, aromatic and 99% purity. The yield for the complete reaction (i.e. including the synthesis of the bis(thiobenzoyl) disulphide crystals) was calculated to be 65%. The GPC chromatogram, UV absorbance spectrum and ^{1}H NMR spectrum of CVADTB are shown in Appendix A.

3.1.1.3. Synthesis of 1-phenylethyl dithiobenzoate from dithiobenzoic acid

The synthesis of 1-phenylethyl dithiobenzoate was first introduced in the original RAFT patent.[4] Dithiobenzoic acid, synthesized by the technique described earlier, was simply reacted with styrene in a Markovnikov nucleophilic addition reaction.[3] The reaction is given in Scheme 3.6:

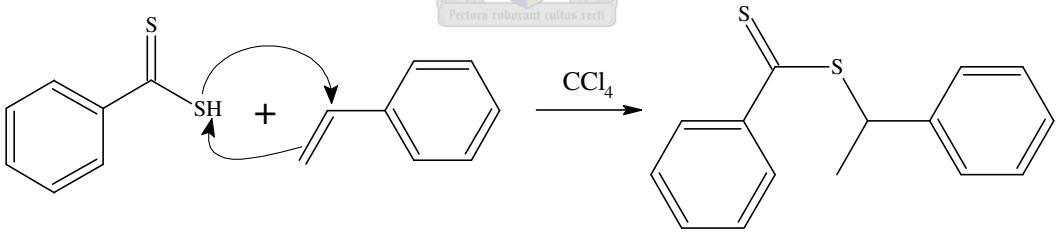

Scheme 3.6: Synthesis of 1-phenylethyl dithiobenzoate.

An acid catalyst, such as para-toluene sulfonic acid, can also be used in the reaction. In the original RAFT patent however, the catalyst was not included.

Experimental

The dithiobenzoic acid (34.63 g, 0.225 mol) and a molar equivalent of styrene (Plascon Research Center, University of Stellenbosch, distilled, 23.38 g, 0.225 mol) were placed in 250 ml three-neck flask containing a magnetic stirrer and 30ml carbon tetrachloride (Saarchem). The reaction was run

at 70°C for 6 hours. An oily product was obtained after rotary evaporation. Column chromatography was used to purify the RAFT agent. Silica gel was used as stationary phase and hexane as eluent (R_f = 0.5). Verification of purity and structure was determined by ^{1}H-NMR ($CDCl_3$): 0.9, d, 3H → methyl H; 5.3, q, 1H → methine H; 7.2 – 8.0, m, 10H → aromatic H and purity of 90%. The GPC chromatogram, UV absorbance spectrum and ^{1}H NMR spectrum of PEDTB are shown in Appendix B.

3.1.2. TRITHIOCARBONATES

Trithiocarbonates are described by the common RAFT agent structure given in Figure 2.10, where the stabilizing Z- group is an alkyl thiol and the R- leaving group is an alkyl or aryl group. The two trithiocarbonates synthesized in this project were: S-dodecyl-S'-isobutyric acid trithiocarbonate (DIBTC) and S-dodecyl-S'-phenylethyl trithiocarbonate (DPTC). The synthesis entails the nucleophilic addition of an organic sulphide anion (that will become the stabilizing Z- group) to carbon disulphide to form a trithiocarbonate anion. The anion undergoes further nucleophilic addition to the species that will become the leaving R- group. Attaching the water-soluble and water-insoluble leaving groups requires different synthetic procedures.

3.1.2.1. Synthesis of S-dodecyl-S'-isobutyric acid trithiocarbonate

The creation of a trithiocarbonate structure is simplified by the fact that sulphur anions have a large selectivity for nucleophilic addition to CS_2. This leads to the formation of a trithiocarbonate anion intermediate. First, dodecyl mercaptan is treated with sodium hydroxide, and then reacted with CS_2 to give a stable dodecyl trithiocarbonate anion:

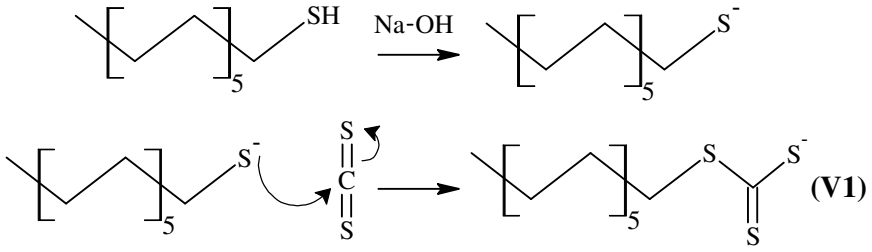

Scheme 3.7: Formation of dodecyl trithiocarbonate anion (VI).

The reaction of the sodium hydroxide and mercaptan is complicated by the fact that they form two separate phases when added together. Phase-transfer methods can overcome this problem by creating a "pathway" for ions from the water phase to move into the organic phase.[5] This is

achieved by the action of phase transfer catalysts like tricapryl methyl ammonium chloride. The structure of this catalyst is shown in Figure 3.2:

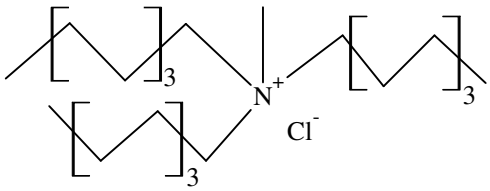

Figure 3.2: Structure of tricapryl methyl ammonium chloride.

The substituents on the quaternary ammonium salt are such that the compound is afforded organic solubility. When the phase-transfer catalyst moves across the interfacial barrier, in order to maintain the electrical neutrality of the phases, a counter-ion is "pulled along". The net result is the transfer of anions into the organic phase.[5]

The dodecyl trithiocarbonate anion is then nucleophilically added to a cyclic intermediate formed by the chloroform, acetone and sodium hydroxide. This intermediate product is shown in Scheme 3.8:

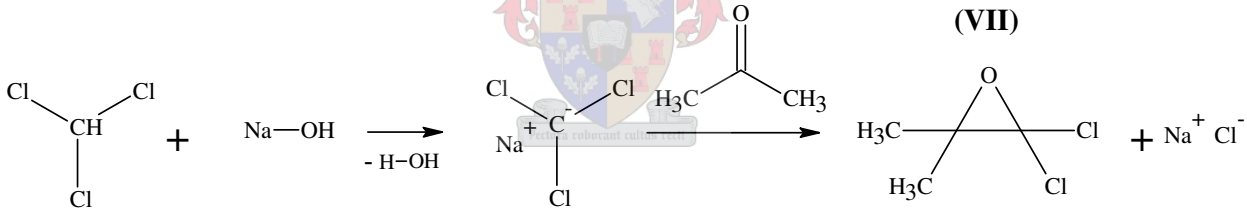

Scheme 3.8: Formation of the cyclic intermediate (VII).

The reaction between the cyclic intermediate (VII) and the dodecyl trithiocarbonate (VI) yields the final DIBTC structure:

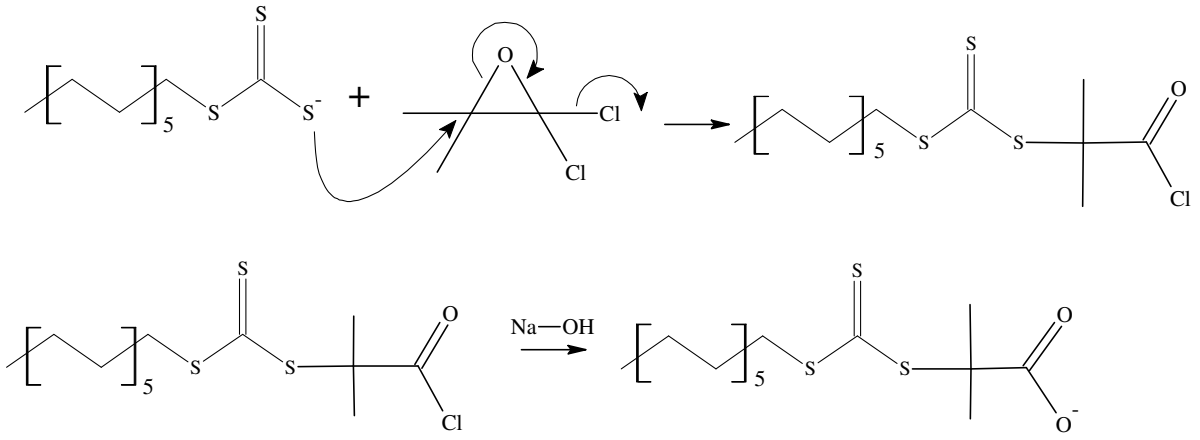

Scheme 3.9: Nucleophilic addition of dodecyl trithiocarbonate anion to the cyclic intermediate to give DIBTC.

The reaction route illustrated in Scheme 3.8 is as described by Lai *et al.*[6]

Experimental

1-Dodecanthiol (Aldrich, 8.05 g, 0.043 mol) was placed in a 250 ml three-neck reactor vessel along with acetone (SAARChem, 20.1 g), Aliquat 336 (tricapryl methyl ammonium chloride, Fluka, 0.63 g) and a magnetic stirrer bar. A gas feed was added and UHP nitrogen was purged throughout the reaction. A dropping funnel and a condenser were attached to the remaining two necks. The reactor was kept in an ice-bath. A sodium hydroxide solution (50%) (ACE, 4 g, 0.05 mol) was placed in the dropping funnel and added dropwise over 20 min. The reaction was then left for an additional 15 min.

Carbon disulphide (Aldrich, 3.5 g, 0.046 mol) and acetone (4.01 g) were placed in the empty dropping funnel. The CS_2 – acetone mixture was added over 20 min to the contents of the round-bottom flask. The reaction mixture turned from an opaque, milky white colour to a bright, transparent yellow. Chloroform (Labchem, 7.1 g, 0.06 mol) was then added in one portion. A second quantity of sodium hydroxide solution (50%) (ACE, 16 g, 0.2 mol) was added dropwise over 30 min. The reaction was left to react overnight.

The reaction mixture was added to ± 600 ml water in a 1*l* beaker and 10 ml HCl (33%, ACE) was added to this. The mixture was stirred at high revolutions for an hour. A thick yellow precipitate formed. This solid was filtered off and dissolved in 500 ml isopropanol in a 1*l* beaker. The isopropanol solution was filtered to remove any precipitate. The insoluble yellow precipitate was

identified as S,S'-bis(dodecyl) trithiocarbonate, the esterification product of the dodecyl trithiocarbonate anion and unreacted mercaptan:

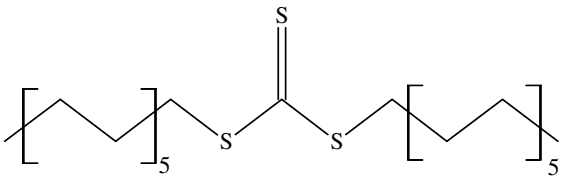

Figure 3.3: The structure of S,S'-bis(dodecyl) trithiocarbonate.

The filtrate was concentrated by rotary evaporation and the concentrate added to cool hexane. Yellow crystals formed and were filtered off. Verification of structure and purity was given by ^{1}H-NMR ($CDCl_3$): 0.9, t, 3H → terminal methyl; 1.2-1.4, m, 20H → alkyl methylene; 1.72, s, 6H → isobutyric acid methyl groups; 3.3, t, 2H → methylene adjacent to sulphur group; 13.1, s, 1H → acid. The yield of this reaction was calculated to be 53%. The GPC chromatogram, UV absorbance spectrum and ^{1}H NMR spectrum of DIBTC are shown in Appendix C.

3.1.2.2. Synthesis of S-dodecyl-S'-phenylethyl trithiocarbonate

The synthesis of DPTC commences at the same point as that of DIBTC. The dodecyl trithiocarbonate anion (VI in Scheme 3.7) is formed and this is followed by nucleophilic addition of the anion to an organic halide. The reaction between (VI) and the alkyl halide, which in the case of DPTC is 1-phenylethyl bromide, is given in Scheme 3.10:

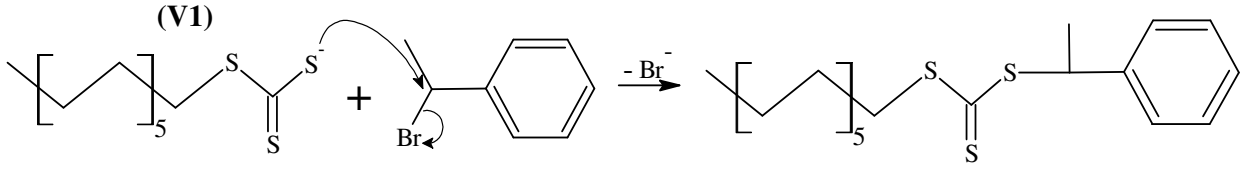

Scheme 3.10: The reaction between the dodecyl trithiocarbonate anion (VI) and 1-phenylethyl bromide.

This synthesis is based on the method of Degani *et al.*[7]

Experimental

A 250 ml three-neck round-bottom flask, equipped with a magnetic stirrer bar was charged with, carbon disulphide (Aldrich, 1.9 g, 0.025 mol), Aliquat 336 (Fluka, 0.05 g), dodecyl mercaptan (Aldrich, 3.855 g, 0.019 mol) and KOH solution (10%) (ACE, 11.09 g, 0.019 mol). A nitrogen feed

was added through one neck and the system was purged for 10 min. A dry dropping funnel was placed in the second neck. The reaction mixture was stirred at room temperature for 15 min. 1-(bromoethyl)benzene (Acros, 4.6265 g, 0.025 mol) was placed in the dropping funnel, then was added all at once. The reaction mixture was heated to 70^{o}C and left to run to completion over 30 min.

After cooling, the reaction mixture was washed with petroleum ether. The organic layers were combined and dried over anhydrous magnesium sulphate. The product was obtained after rotary evaporation. Column chromatography was performed to purify the RAFT agent. Silica gel was used as the stationary phase and the eluent mixture comprised 2:3:0.05 hexane:petroleum ether:diethyl ether. Verification of structure and purity was done by ^{1}H-NMR ($CDCl_3$): 0.9, t, 3H → terminal methyl; 1.2 – 1.5, m, 18H → alkyl methylene; 1.7, m, 2H → 2nd last alkyl methylene; 1.8, d, 3H → methyl; 3.35, t, methylene adjacent to sulphur group; 5.25, q, 1H → methane; 7.2 – 7.4, m, 5H → aromatic. The purity was calculated to be 95%. The yield of the reaction was calculated to be 57%. The GPC chromatogram, UV absorbance spectrum and ^{1}H NMR spectrum of PEDTB are given in Appendix D.

3.2. MINIEMULSION POLYMERIZATION PROCEDURE

The method of miniemulsion polymerization was illustrated in Figure 2.6. An initial emulsion mixture is prepared. The final miniemulsion is formed by the miniemulsification of this emulsion. The default formulation for all polymerizations in this study is given below, along with the method of preparation of the miniemulsion.

Like any conventional emulsion, the pre-emulsion is prepared by the coarse mixing of an oil and water phase. One of the prerequisites for the formation of stable miniemulsions not found in a conventional emulsion formulation is a cosurfactant or, more specifically, an ultra-hydrophobe. This forms part of the oil phase along with the monomer, oil-soluble initiator (AIBN, Riedel De Haen) and RAFT agent. Hexadecane (Aldrich) was the ultra-hydrophobe used in all the formulations in this study. The water phase consisted of distilled and deionized water (DDI water) and surfactants SDS (BDH) or Igepal®CO-990 (Aldrich). These two phases were prepared separately and then combined in a 250 ml long-form beaker. The mixture was stirred at 1000 rpm for 1 hour, using a magnetic stirrer bar and magnetic plate. The default formulation was as follows:

- Water phase:
    - DDI water - 40 ml
    - Surfactant - 1 g
- Oil phase:
    - Monomer - 10 ml
    - Initiator - 6.0×10^{-6} mol
    - RAFT agent - 4.5×10^{-4} mol
    - Ultrahydrophobe - 0.43 g

The mass of surfactant remained the same when either the nonionic or the anionic surfactants were used. For the polymerization in which the water-soluble initiator potassium persulphate (KPS, SARCHEM) was used, the initiator was dissolved in the water phase rather than the oil phase. Where applicable, aqueous-phase radial traps were dissolved in the water phase. The number of moles of radical trap equals that of the number of moles of initiator in the system. Thus the mass of Fremy's salt (Aldrich) used as radical trap was 0.033 g and the mass of sodium nitrite (Holpro) used as radical trap was 0.008 g.

This pre-emulsion was sonicated to form the final stable miniemulsion mixture. The sonication was performed using a Sonics and Material Vibra cell Autotune ultrasonic processor 750 VCX. The sonication time was set at 10 min, with a set amplitude of 80% and a cut-off probe temperature of 50^{o}C. The final energy output required to form stable latexes was 100 kJ. The latex was then transferred to a 250 ml three-neck round-bottom flask fitted with a septum, condenser and nitrogen feed. The mixture was purged with nitrogen for 10 min, hereafter nitrogen was allowed to flow through the apparatus for the remaining reaction time. The reaction flask was placed in a preheated oil-bath (75^{o}C), at which time the polymerization commenced. Samples were drawn via the septum using a needle. These were dried so as to remove all volatile components (water and monomer). All conversions were determined gravimetrically. The final latex mixture was stored for further analysis.

Detailed formulations of each experiment are tabulated in Table 3.1. AIBN was used as initiator except where indicated. Superscript [a] indicates that KPS was used as initiator in the place of AIBN (concentration held constant). Superscript [b] indicates the addition of Fremy's salt in the

miniemulsion formulation and [c] the addition of $NaNO_2$ in the formulation (concentrations of both equal to initiator concentration).

Table 3.1: Miniemulsion formulations for polymerizations investigated in this study.

RAFT agent	Reaction number	Monomer	Surfactant	RAFT agent concentration ($mol.dm^{-3}$)	Surfactant concentration ($g.dm^{-3}$)
CVADTB	A1	Styrene	SDS	0.0499	25.078
	A2	Butyl acrylate	SDS	0.0498	24.838
	A3	Styrene	Igepal®CO-990	0.0446	25.200
	A4	Butyl acrylate	Igepal®CO-990	0.0446	25.750
DIBTC	B1	Styrene	SDS	0.0500	25.250
	B2	Butyl acrylate	SDS	0.0498	25.395
	B3	Styrene	Igepal®CO-990	0.0501	24.978
	B4	Butyl acrylate	Igepal®CO-990	0.0500	25.073
	B5	Butyl acrylate	SDS	0.0499	12.675
	B6	Styrene	SDS	0.0510	12.675
	B7[a]	Butyl acrylate	SDS	0.0499	25.583
	B8	Butyl acrylate	Igepal®CO-990	0.0508	24.975
	B9[b]	Butyl acrylate	Igepal®CO-990	0.0498	25.370
	B10[c]	Butyl acrylate	Igepal®CO-990	0.0499	25.175
	B11[c]	Styrene	Igepal®CO-990	0.0498	25.440
PEPDTB	C1	Butyl acrylate	SDS	0.0499	26.068
	C2	Styrene	SDS	0.0517	25.000
	C3	Butyl acrylate	Igepal®CO-990	0.0508	26.283
	C4	Styrene	Igepal®CO-990	0.0514	25.340
DPTC	D1	Butyl acrylate	SDS	0.0511	25.008
	D2	Styrene	SDS	0.0523	25.070
	D3	Butyl acrylate	Igepal®CO-990	0.0508	26.650
	D4	Styrene	Igepal®CO-990	0.0506	25.230
	E1	Butyl acrylate	SDS	0	26.215
	E2	Butyl acrylate	Igepal®CO-990	0	25.373
	E3	Styrene	SDS	0	25.340
	E4	Styrene	Igepal®CO-990	0	27.128

3.3. CHARACTERIZATION OF POLYMER AND FINAL LATEX

Various analyses were performed on the samples taken throughout the polymerizations as well as on the final latexes. Details of these analytical techniques are given in Sections 3.3.1-3.3.5.

3.3.1. GEL PERMEATION CHROMATOGRAPHY (GPC)

Size exclusion chromatography (SEC) or gel permeation chromatography (GPC) was utilized to monitor the evolution of the molar masses. A refractometer was used as the detector for this analytical method. The GPC instrument consisted of a Waters 717 plus Autosampler, Waters 600E System controller and the Waters 610 fluid unit. The detector was a Waters 410 differential refractometer, used at 35°C. Tetrahydrofuran (HPLC-grade) purged with IR-grade helium was used as eluent at a flow rate of 1 $mL.min^{-1}$. The columns used were two PLgel 5 µm Mixed-C columns and a pre-column (PLgel 5 µm guard). The column oven was kept at 30°C and the injection volume was 100 µl. The system was calibrated with narrow polystyrene standards ranging from 800 to 2 x 10^6 $g.mol^{-1}$. The GPC was coupled to a UV detector set to monitor a wavelength of 320nm.

3.3.2. DYNAMIC LIGHT SCATTERING (DLS)

Particle sizes were determined using a Malvern Instruments Zetasizer 1000 HAS with a fixed scattering angle of 90° at 25°C. Data processing was performed using an automatic distribution function, which enables multi-modal distributions to be analyzed. Samples for DLS were prepared as follows: a small amount of latex was diluted using a 1 mmol NaCl solution. The instrument was calibrated using polystyrene nanospheres (200 nm). The calibration samples were prepared using a 10 mmol NaCl solution. For certain samples, accurate polydispersity values could not be calculated due to machine failure.

3.3.3. TRANSITION EMISSION MICROSCOPY (TEM)

TEM pictures were taken using a Leo 912 TEM apparatus equipped with a digital camera. Machine time was generously provided by the Electron Microscopy Unit at the Physics Department of the University of Cape Town. Samples were prepared as follows: a small amount of latex was applied to a gold grid. Excess latex was washed off with distilled water. The samples were then stained using a 2% uranyl acetate solution. Polymers that absorb this stain, like poly(butyl acrylate), appear black on the TEM images. Those that do not, like poly(styrene), appear white with a black edge.

3.3.4. ULTRAVIOLET SPECTROSCOPY (UV)

UV chromatograms were obtained using a Perkin Elmer Lambda 20 UV/VIS Spectrometer. Auto-zeroing was performed using THF references. The samples were prepared as follows: varying masses (ranging from 0.1 to 0.5 g) of the solid to be scanned were dissolved in 5 ml THF. Quartz cuvettes where then filled with the solution. A scan profile was set to scan from 200 to 600 nm in a single ramp profile.

3.3.5. CAPILLARY HYDRODYNAMIC FRACTIONATION (CHDF)

Capillary hydrodynamic fractionation was performed on the final latexes of the various miniemulsion polymerizations is order to determine the particle size distribution of the latexes. Analyses were performed using a Matec Applied Science CHDF 1100 and calibration was performed using polystyrene standards. Machine time was generously provided by the Key Centre for Polymer Colloids, University of Sydney. Samples were prepared as follows: a small amount of latex was diluted in a 1 mM NaCl solution. The weight average CHDF data can be compared to the DLS data. This is due to the fact that DLS calculates a weighted average particle size (larger particles will cause a shift of the Z *(*average*)* to value larger than the number average particle size). CHDF analysis could unfortunately not be performed on all the latexes prepared for this project due to limited machine time.

Pectora roborant cultus recti

3.4. REFERENCES

(1) Furniss, B. S.; Hannaford, A. J.; Rogers, V.; Smith, P. W. G.; Tatchell, A. R., Eds. *Vogel's Textbook of Practical Organic Chemistry*, Fourth ed.; Longman Group Limited: London, **1978**

(2) De Brouwer, H. PhD thesis; Eindhoven University of Technology; **2001**

(3) Oae, S.; Yaghihara, T.; Okabe, T. *Tetrahedron* **1972**, *28*, 3203

(4) Le, T. P.; Moad, G.; Rizzardo, E.; Thang, S. H. In World Patent 98/01478, **1998**

(5) Starks, C. M.; Owens, R. M. *Journal of the American Chemical Society* **1973**, *95*, 3613

(6) Lai, J. T.; Filla, D.; Owens, R. M. *Macromolecules* **2002**, *35*, 6754

(7) Degani, I.; Fochi, R.; Gatti, A.; Regondi, V. *Synthesis* **1986**, 894

Chapter 4. : *RAFT-mediated miniemulsion polymerizations and conventional free radical miniemulsion polymerizations*

ABSTRACT

The mechanistic models of miniemulsion polymerizations and the RAFT process were examined in Chapter 2. An amalgamated mechanistic process for RAFT-mediated miniemulsion polymerizations will be discussed in this chapter. This will be followed by an investigation into conventional FRP in miniemulsions.

In Chapter 2, the fundamentals of the kinetic and mechanistic aspects of miniemulsion polymerizations and the RAFT process were described. The amalgamation of these two process leads to a far more complex system. In this chapter, an overview of the various mechanistic pathways and their kinetic descriptions will be given so as to create a framework for the reader to refer to with respect to the more intricate concepts associated with the RAFT process and miniemulsion system, as discussed in the subsequent three chapters. Conventional free radical miniemulsion polymerization will also be addressed and these polymerizations will act as a "reference" against which the various RAFT-mediated miniemulsions in Chapters 5 – 7 can be compared.

4.1. MECHANISTIC PATHWAYS FOR RAFT-MEDIATED MINIEMULSION POLYMERIZATIONS

The mechanistic pathways for conventional free radical polymerizations in emulsions were addressed in Section 2.2.1.1. Figure 2.2 illustrated the particle formation (nucleation) mechanisms. These mechanisms were simplified after switching to a heterogeneous (miniemulsion) system. The RAFT process was addressed in Section 2.3.4 and the mechanistic pathways were illustrated in Figure 2.9. These mechanistic steps are made more complex with the introduction of multiple phases. Each species within the various equilibria will have a unique solubility that will influence the phase in which the majority of the species will reside. Over and above the different phases of the miniemulsion, the surfactant in the formulation forms a stabilizing hydration layer that will influence the rate at which species might move between the two phases. The mechanistic pathways are described by kinetic equations. These equations involve various parameters that will be investigated in the subsequent chapters. By pinpointing the kinetic behaviour of the various species within the miniemulsion system, the mechanistic processes that are operating can be determined. Scheme 4.1 illustrates the complex radical movement within the RAFT-mediated miniemulsion. Rate constants are defined so as to facilitate discussions in Chapters 5 – 7.

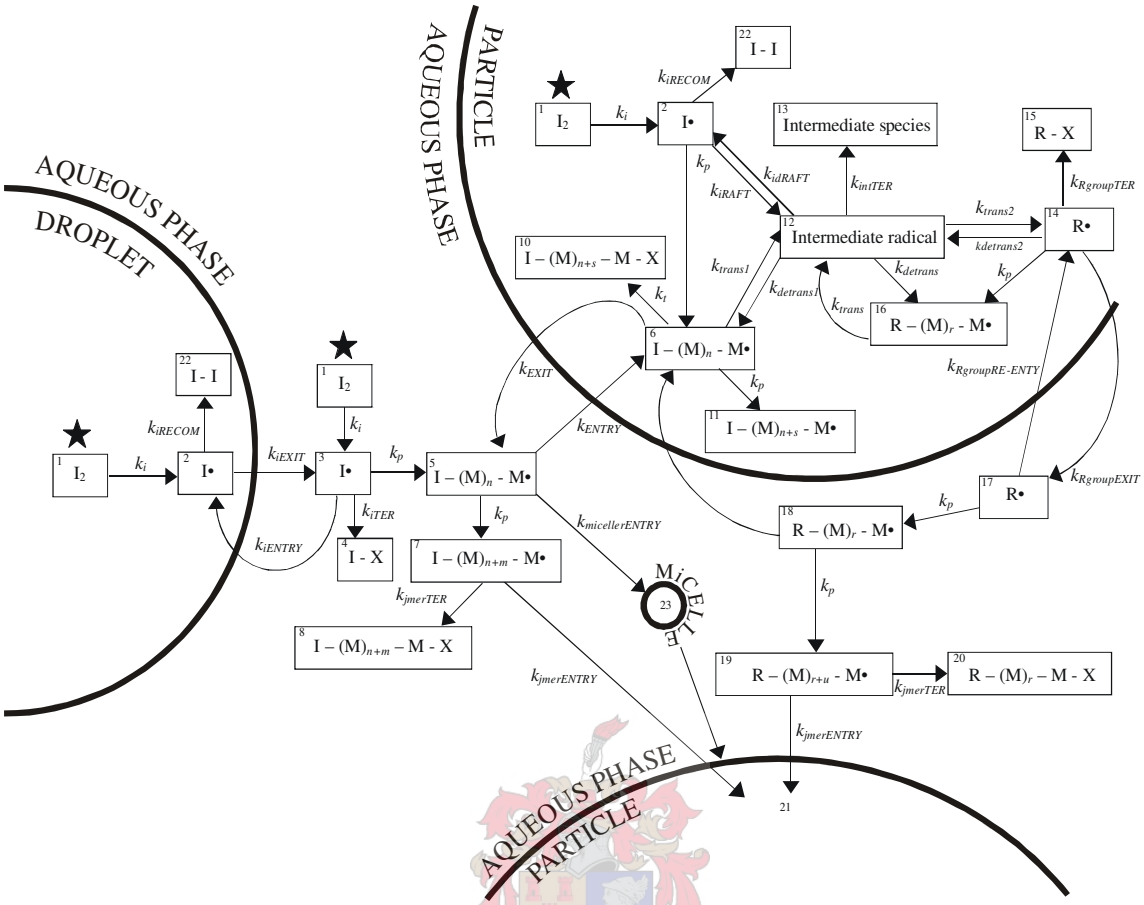

Scheme 4.1: The various radical movements and mechanistic pathways for a RAFT-mediated miniemulsion polymerization.

Scheme 4.1 is a complex flow chart and is based on a RAFT-mediated miniemulsion initiated with an oil-soluble initiator. The "starting" points are marked with stars. From each starting point many mechanistic pathways are indicated, each with their own unique rate coefficients. Table 4.1 provides the legend to Scheme 4.1, indicating the various species labeled 1 to 23 (superscripts). The definitions of the various rate coefficients are given in Table 4.2.

Table 4.1: Descriptions of the various species labeled in Scheme 4.1.

Label	Species description
1	Oil-soluble initiator
2	Initiating radicals in oil phase
3	Initiating radicals in aqueous phase
4	Terminated initiating radicals
5	Z-mers (formed from initiating radicals)
6	Z-mers that have nucleated droplets
7	Z-mers that have not nucleated droplets
8	Terminated oligomeric radicals ($n + m > z$)
9	J-mers (formed from initiator radicals)
10	Terminated z-mers (formed from initiating radicals)
11	Propagating radicals (oligomers formed by z-mers)
12	Intermediate radical formed after the *Initialization* step of the RAFT process
13	Terminated intermediate radical
14	Radical leaving group
15	Terminated radical leaving group
16	Propagating radicals (oligomers formed by the radical leaving group)
17	Exited radical leaving group
18	Z-mers (formed from the radical leaving group)
19	J-mers (formed from the radical leaving group)
20	Terminated z-mers (formed from the radical leaving group)
21	J-mers that have formed a secondary particle
22	Terminated products from geminate recombination
23	Nucleated micelle

Pectora roborant cultus recti

Table 4.2: Definitions of the rate coefficients given in Scheme 4.1.

Rate coefficient subscript	Reaction pathway/s	Description
i	1 → 2	Initiator decomposition
iEXIT	2 → 3	Initiating radical exit
iENTRY	3 → 2	Initiating radical entry
iRECOM	2 → 22	Product of geminate recombination
iTER	3 → 4	Initiating radical termination
iRAFT	2 →12	Initiator radical addition to RAFT agent
idRAFT	12 → 2	Initiator radical fragmentation from RAFT agent
p	3 → 5; 5 → 7; 6 → 11; 2 → 6; 14 → 16; 16 → 11; 17 → 18; 18 → 19	Propagation
jmerTER	7 → 8; 19 → 20	J-mer termination
jENTRY	7 → 21; 19 → 21	Secondary particle formation
ENTRY	5 → 6; 18 → 6	*Z*-mer entry
EXIT	6 → 5	*Z*-mer exit
t	6 → 10; 16 → 10	Termination
micellarENTRY	6 → 23	Micellar nucleation by z-mer
trans1	6 → 12	Z-mer addition to RAFT agent
detrans1	12 → 6	Z-mer fragmentation from RAFT agent
intTER	12 → 13	Intermediate radical termination
trans2	12 → 14	Leaving group fragmentation from RAFT agent
detrans2	14 → 12	Leaving group addition to RAFT agent
RgroupTER	14 → 15	Leaving group termination
trans	16 → 12	Oligomer addition to RAFT agent
detrans	12 → 16	Oligomer fragmentation from RAFT agent
RgroupEXIT	14 → 17	Leaving group exit
RgroupENTRY	17 → 14	Leaving group entry

There are certain important points that need to be addressed with respect to the various rate coefficients above. These points are given below, where the rate coefficient subscripts are given in italics.

i, iEXIT, iENTRY, iRECOM, iRAFT, idRAFT and *iTER*:

The initiator decomposition rate *i* is defined, for a certain initiator (1), by the Arrhenius equation.[1] The rate at which these initiating radicals (2) exit the droplets will depend on the droplet size.[2] Larger particles lead to lower exit rate coefficients. Geminate recombination of azo-initiators leads to inert species (22). The probability of this taking place is higher for smaller particles, where the initiators cannot diffuse away from each other at a fast enough rate.[2] The process of geminate recombination could be disrupted by the presence of RAFT agents. The addition of initiating radicals to the thio carbonyl thio group is almost instantaneous. This is more likely to take place in the larger droplets due to the decreased probability of exit (*iEXIT*) for the initiating radicals. If this is indeed the case, the oil-phase initiation could become the predominant nucleation mechanism. The probability that an initiating radical will re-enter the particle it exited from is highly unlikely due to its increased diffusivity in the aqueous phase.[3] Termination within the aqueous phase will be dependent on the radical concentration within this phase. Initiator that dissolves within the aqueous phase can also undergo decomposition and initiate z-mer formation. Asua *et al*. have speculated that this contribution to initiation is minimal.[4]

p:

The propagation rate coefficient is a constant value for any monomer. The k_p values for styrene and butyl acrylate at 20^{o}C are 3,4 x 10^4 L.mol^{-1}s^{-1} for butyl acrylate and 160 dm^3.mol^{-1}s^{-1} for styrene.[5] The rate at which the polymer will grow in either of the two phases is directly proportional to the monomer concentration within that phase. The C_W^{sat} value at 50^{o}C is 6.4 x 10^{-3} mol.dm^{-3} for butyl acrylate and 4.3 x 10^{-3} mol.dm^{-3} for styrene.[1] The rate at which polymer will form in any phase will be determined by the balancing of the k_p and monomer concentration. This is particularly important during the nucleation period (Interval I). The rate at which z-mers are formed in the aqueous phase will determine the nucleation rate. One important observation is that the increased monomer solubility will lead to a longer

z-mer length (i.e. value of z).[1] The nucleation rate will therefore rely on the compromise between a faster z-mer formation and longer z-mer length.

MicellarENTRY:

If the aqueous phase surfactant concentration is above CMC, micelles will be found in the miniemulsion. Z-mers (6) can enter these micelles (23) and propagate to form secondary particles (21). As a polymerization progresses, growing particles will absorb free surfactant from the aqueous phase leading to a reduction in the number of micelles. Micellar nucleation is highly unfavorable in a RAFT-mediated miniemulsion due to the fact that polymer forming within these particles will form via conventional FRP.[6]

jmerENTRY and *jmerTER:*

Z-mers that continue to grow in the aqueous phase can reach j_{crit} and form j-mers. These oligomeric radicals can form secondary particles by coagulation. Higher aqueous-phase monomer concentrations and poor nucleation will increase the probability of j-mer formation. It should be noted that if there is a high concentration of free surfactant at the onset of polymerization (above CMC), micelles are likely to aggregate. In this instance, micellar nucleation is far more probable than homogeneous-coagulative particle formation. Landfester *et al.*[7] showed that at the onset of polymerization (in which the surfactant is 50 wt% with respect to monomer) the free surfactant concentration is below CMC. This implies that the number of micelles will be minimal in the miniemulsions prepared in this study. Micellar nucleation is likely to become prevalent if the radical concentration within the aqueous phase is high. The competition between micelles and particles for radicals within the aqueous phase will determine the relative nucleation probabilities.

ENTRY and *EXIT:*

The rate of z-mer entry into the droplets and particles will depend on the interaction between the z-mer and the hydration layer around the droplet and the total monomer droplet surface area.[2] The rate of exit of a z-mer that is in a particle will depend on the reactivity of the radical to the RAFT agent, as well as the probability of radical termination and/or propagation. Chain transfer to the RAFT agent (C_{tr}) is very high for the trithiocarbonates[8] and dithiobenzoates[9]

used in this study. This implies that the probability of exit of the z-mers is likely to be low after initialization. Once the RAFT equilibrium has been established, z-mers that enter the active propagating state can however exit.

t:

Termination within the aqueous phase will depend on the concentration of radicals within the phase. If the miniemulsions follow *pseudo-bulk* kinetic behaviour, it is likely that the radical termination will be lower when compared to a miniemulsion that follows *zero-one* kinetics.[1] For *zero-one* systems, termination is not diffusion controlled and thus is not rate determining. Diffusion-controlled termination is typical for *pseudo-bulk* systems. The radical concentration within the particles will depend on the radical generation within the aqueous phase and the entry of radicals into the particles. If the chain transfer to the RAFT agent is efficient, the rate of termination in the particles should be reduced by trapping the propagating radicals in a dormant state.

trans1, detrans1, trans2, detrans2, trans and *detrans:*

These rate coefficients all relate to the RAFT equilibrium that is established within the particles. Their values are all linked to the stability of the various radical species within the equilibrium. As mentioned in Section 2.2.1.1, the chain transfer of z-mers (6) to the RAFT agent (*trans1*) is high enough to assume that all radicals entering any droplet will interact with the RAFT agent. The fragmentation releasing the z-mer will depend on the intermediate radical (12) stability. The four RAFT agents have R- groups that are good leaving groups, which will counteract this fragmentation. The fragmentation of the radical leaving group (14) (*trans2*) is favoured. The re-addition of the radical leaving group could take place, but re-fragmentation of the leaving group will proceed far faster than chain transfer. Monomer addition to this radical leaving group will generate oligomeric radicals (16) that will once again chain transfer to the RAFT agent, which is now a macroRAFT agent (RAFT end-capped z-mer). The RAFT equilibrium is then set up between species 12, 6 and 16, the last two of which will undergo single monomer additions before once again forming the intermediate radical. Intermediated radical termination has been speculated[10] but terminated intermediated species are yet to be observed.[11]

RgroupTER, RgroupEXIT and *RgroupENTRY:*

The probability of R- group exit is higher than that of the z-mers due to the smaller size of the group. The radical leaving groups will be highly reactive and are more likely to propagate or exit than terminate. The probability of exit is far higher for smaller particles. Particles from which radical exit has taken place will contain dormant RAFT end-capped chains. These will remain dormant until a new z-mer (or other radical fragment) enters that particle and re-initiates the macroRAFT agent. This cycle is likely to continue until all the radical leaving groups have exited from the particles and re-entered in the form of z-mers. The rate at which the R- groups exit the particles will depend on the reactivity, solubility and stability of the R- group. Increased solubility in the aqueous phase implies increased exit; increased reactivity implies that propagation is more probable thus fewer exit events will take place. Re-entry of the leaving group back into the particle could take place, but will become more unlikely as the concentration of radicals within the aqueous phase increases. An influx of radical leaving groups into the aqueous phase will cause an increase in termination. Radical leaving groups within the aqueous phase can undergo propagation to form z-mers that can enter particles or unnucleated droplets. These z-mers can also continue to grow and form j-mers. Micellar nucleation by the z-mers formed by the R- group is also possible.

Many of the mechanistic pathways that could possibly take place in a RAFT-mediated free radical polymerization within a miniemulsion have now been discussed. By defining various parameters and laying down a few definite values, understanding the mechanistic behaviours of the miniemulsions investigated in Chapters 5–7 should be simpler.

4.2. CONVENTIONAL FREE RADICAL MINIEMULSION POLYMERIZATIONS

These polymerizations will be used as references against which all other RAFT-mediated polymerizations in the subsequent chapters can be compared. The miniemulsions described in the next two sections (4.2.1 and 4.2.2) follow the standard formulation given in Chapter 3 with the exception that no RAFT agents were included. Section 4.2.1 deals with butyl acrylate miniemulsions and Section 4.2.2 deals with styrene miniemulsions. The polymerization labeling

(e.g. E1) was given in Table 3.1. Kinetic analysis is given by first-order rate plots, determined gravimetrically. The evaluation of polymer characteristics such as molecular weight and polydispersity with were determined by size exclusion chromatography (SEC). Particle size analysis was performed by transmission electron microscopy (TEM), capillary hydrodynamic fractionation (CHDF) and dynamic light scattering (DLS).

4.2.1. BUTYL ACRYLATE MINIEMULSIONS

Polymerizations E1 and E2 were investigated. The surfactants used were SDS and Igepal®CO-990 respectively. The first-order rate plots for both polymerizations are given in Figure 4.1:

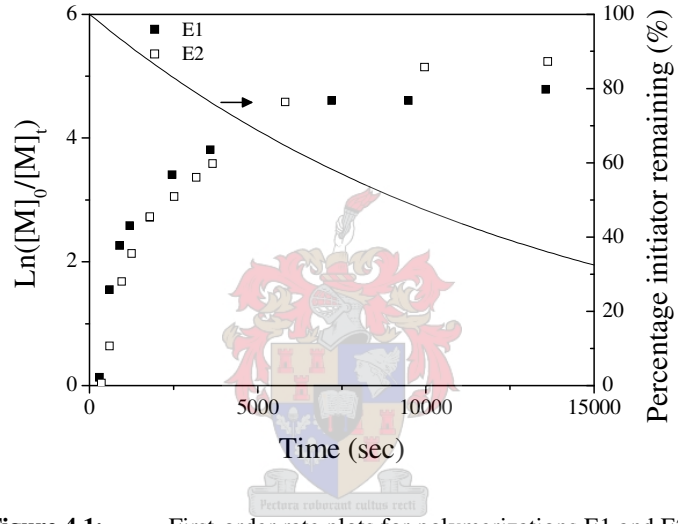

Figure 4.1: First-order rate plots for polymerizations E1 and E2.

The conversion after 3 hours was approximately 98% for E1 and 100% for E2. The length of Interval I was similar for E1 and E2. This was unexpected due to the fact that in E2 the non-ionic surfactant could retard the entry of the z-mers.[2] The crudeness of the profile of the plots in Figure 4.1 does however not provide accurate means to determine any distinct difference in kinetic trend during interval I. E1 and E2 both showed a clear interval III, which is characterized by an exponential decrease in reaction rate.[12] In this interval, termination remained chain-length dependent to a certain degree[13] but the rate-determining step of termination at this point was the diffusion of radicals into the particles. For this reason, the rate of reaction decrease was more gradual for the larger particles (E2), in which the radicals are required to diffuse across a larger distance.

The GPC chromatograms of E1 and E2 are given in Figure 4.2:

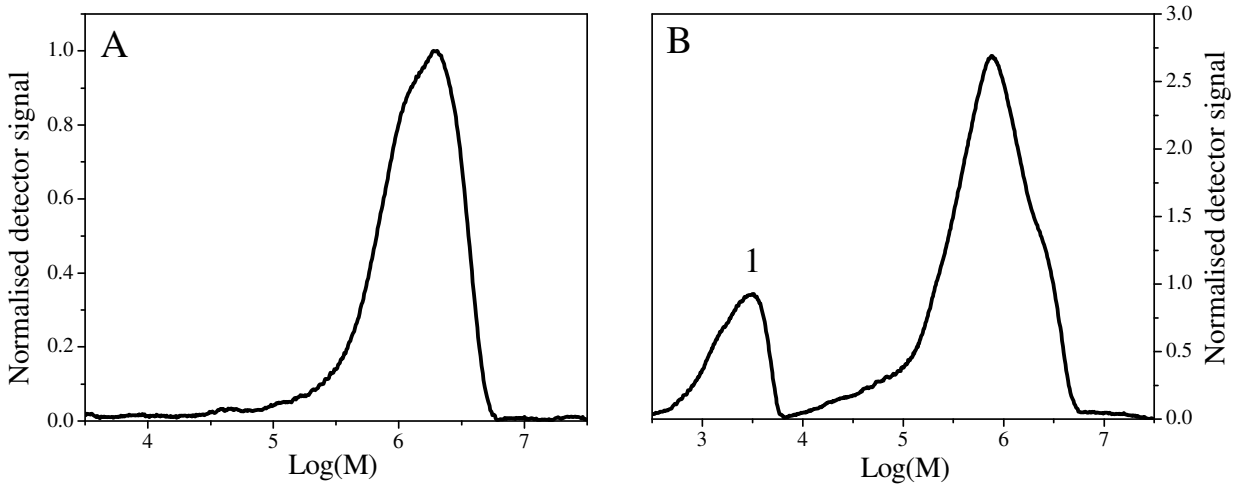

Figure 4.2: GPC chromatograms for polymerizations A.) E1 and B.) E2.

It should be noted that the shapes of these chromatograms are misleading. Due the extremely high molecular weight of the polymer, only a small fraction of polymer passed through the filtration step of the sample preparation and was examined by size exclusion. This implies a very low concentration of polymer, which leads to a poor signal-to-noise (S/N) ratio. The poor resolution is compounded by the fact that the polymer is eluting close to the exclusion limit. The shape is thus not an accurate description of the distribution of chain lengths eluting from the GPC column. For chromatogram B, the distribution labeled 1 is that of the surfactant (similar elution volumes). The number average molecular weights of polymerizations E1 and E2 are 1 863 000 and 581 700 $g.mol^{-1}$ respectively.

Considering that the surfactants used in E1 and E2 will interact differently with the z-mers within the aqueous phase, leading to unique z-mer entry rate coefficients, the nucleation period for each polymerization should be different. Longer nucleation times imply that the nucleated particles will contain chains of varying lengths, and thus have larger PDI values. The shape of chromatogram B indicates that there are a variety of chain lengths. The first-order rate plot given in Figure 4.1 indicates a slightly longer nucleation period for E2, which could explain the larger PDI. Further evidence substantiating this explanation is evident from particle size analyses performed, the results of which are given in Tables 4.3 and 4.4:

Table 4.3: DLS results for polymerizations E1 and E2

Reaction	RAFT	Monomer	Surfactant	Z (average)	Polydispersity
E1	-	Butyl acrylate	SDS	89.1	0.01
E2			Igepal®CO-990	140.9	0.009

The results from dynamic light scattering experiments indicate that both latexes have narrow particle size distributions (low values for polydispersity). SDS molecules are much smaller than the bulky polymeric non-ionic molecules. The smaller ionic "head" of the SDS molecule can pack in an orderly fashion, leading to a compact ionic layer. The non-ionic surfactant has a long polymeric "tail" that can solubilize in the organic phase. This solubilization within the organic phase decreases the amount of surfactant that is available for stabilization, resulting in larger particles.[14] This explains why it is repeatedly seen that the non-ionically stabilized miniemulsions have larger *average particle sizes.* The narrow particle size distribution indicates that all the particles in the miniemulsion were nucleated in a short time period and grew at similar rates.

Table 4.4: CHDF results for polymerizations E1 and E2

Reaction	Z (Number average)			Z (Weight average)		
	Mean	Max	Standard deviation	Mean	Max	Standard deviation
E1	73.2	72.7	18.6	85.9	86	17.3
E2	101	98.8	25.3	120.5	115.2	31.9

CHDF analysis provides a more accurate means of examining the particle size distribution of the final latex. The *weight* and *number average standard deviation* values are slightly higher for E2 according to CHDF analysis. From this information, it seems possible that the nucleation time for E2 was slightly longer than E1.[15] The length of interval I cannot be accurately determined using first-order rate plots.

4.2.2. STYRENE MINIEMULSIONS

Polymerizations E3 and E4 were investigated. The surfactants used were SDS and Igepal®CO-990 respectively. The first-order rate plots are given in Figure 4.3:

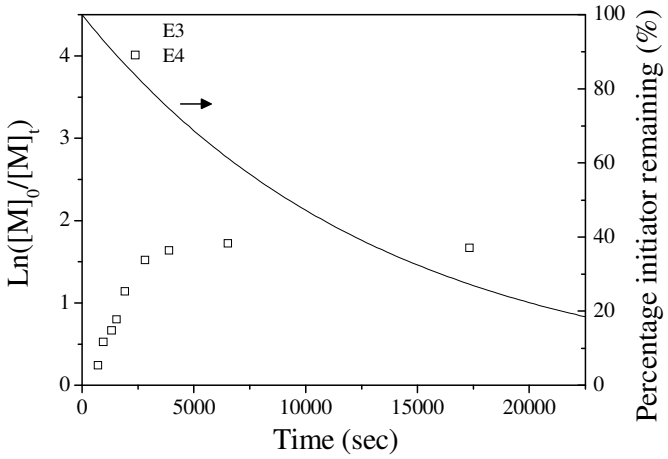

Figure 4.3: First-order rate plots for polymerizations E3 and E4.

The conversion after 3 hours was 98% for B3 and 78% for E4. Interval I appeared to be the same length for E3 and E4. The rate of reaction during this interval also appeared to be similar. The drop in reaction rate during interval III was more gradual for E3 compared to E4. Bechthold *et al.* reported clear cases in which interval IV (autoacceleration) was observed in conventional styrene miniemulsions in which the particles were larger than 150 nm.[12] This was not observed for non-ionically-stabilized miniemulsion (E4) due to the fact that the particle sizes were insufficiently large (as will be seen in Table 4.6).

The GPC chromatograms of E3 and E4 are given in Figure 4.4:

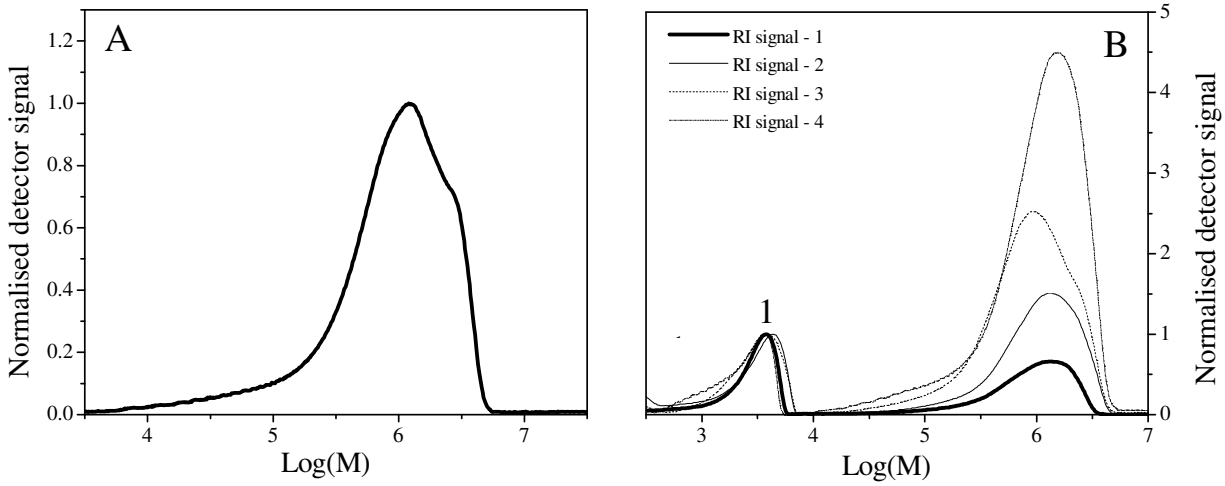

Figure 4.4: GPC chromatograms for polymerizations A.) E3 and B.) E4.

The conversions of the samples shown were as follows: for E3 98% and for E4: (1) – 21%, (2) – 40%, (3) – 55% and (4) – 77%. The samples in chromatogram B were normalised to the surfactant (marked as 1). The strange trace shapes are linked to a poor S/N ratio. From chromatogram B it could be observed that the molecular weight of the polymer did not change much with an increase in conversion. With an increase in conversion it can be said that the number of chains increased relative to the surfactant due to the fact that the increase on RI signal is purely due to an increase in concentration of eluted polymer and not molecular weight of the eluted polymer. The *number average molecular weight* at 90% conversion was higher for E3 than for E4 (825 418 $g.mol^{-1}$ and 581 689 $g.mol^{-1}$ respectively).

The results from the DLS analysis are given in Tables 4.5:

Table 4.5: DLS results for polymerizations E3 and E4

Reaction	RAFT	Monomer	Surfactant	Z (average)	Polydispersity
E3	-	Styrene	SDS	69.7	0.004
E4			Igepal®CO-990	121.6	0.011

The results of DLS analysis of polymerizations E3 and E4 show similar trends to results for polymerizations E1 and E2. The particle sizes for E3 and E4 were however smaller. This change in average particle size has been observed for miniemulsions utilizing monomers with differing solubilities. Hansen *et al.*[16]showed that more hydrophilic monomers lead to smaller particle sizes, which is not the case in the present investigation. The particle size distribution of E3 is narrower than that of E1, and the reverse is true for E4 and E2. These differences were probably due to statistical error in the size determination. The slight differences in the nucleation time and GPC chromatograms could indicate that there were few easily detectable mechanistic differences between the four systems. CHDF results are given in Table 4.6:

Table 4.6: CHDF results for polymerizations E3 and E4

Reaction	Z (Number average)			Z (Weight average)		
	Mean	Max	Standard deviation	Mean	Max	Standard deviation
E3	47.6	42.1	13.9	60	54.7	15.7
E4	74.4	50.5	26.5	98.9	102.2	24

From the *standard deviation* values it is possible to see that for polymerizations where butyl acrylate and styrene are used as monomer, the particle size ranges are similar. The CHDF chromatograms of the final latex of E3 is given in Figure 4.5:

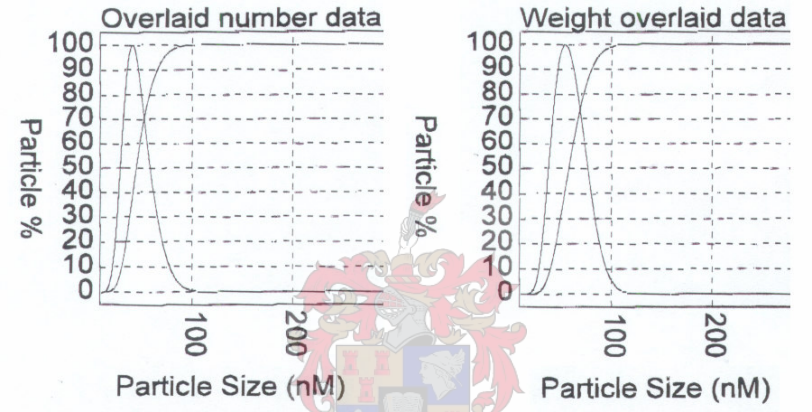

Figure 4.5: CHDF chromatograms of the final latex of polymerization E3.

A narrow distribution of particle sizes can be seen in both the CHDF (Figure 4.5) and TEM (Figure 4.6) results.

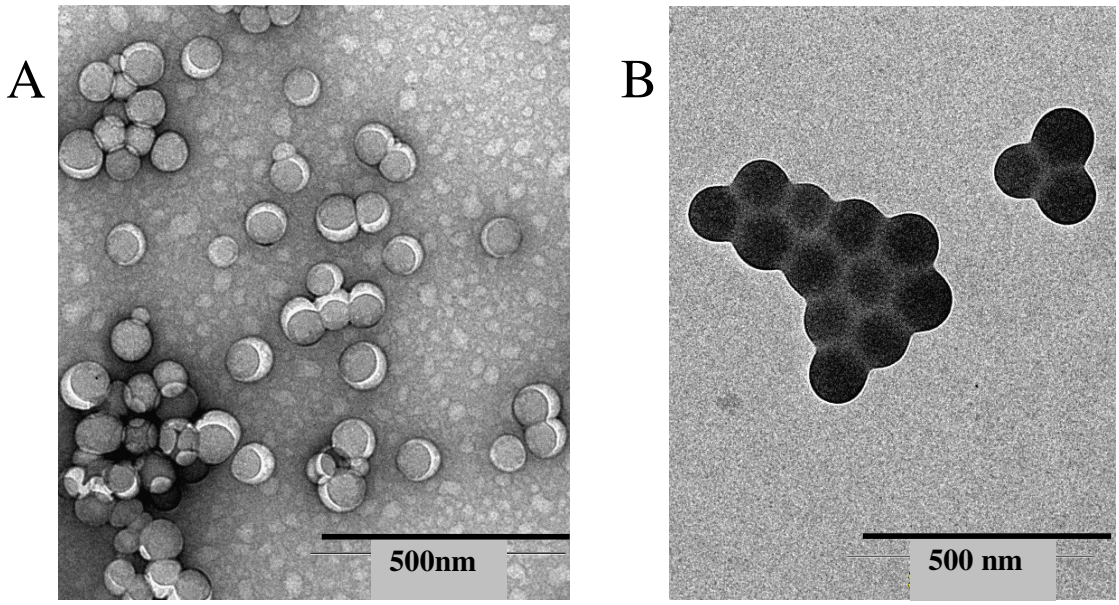

Figure 4.6: TEM micrographs of the final latexes for A.) E3 and B.) E4.

The slight difference in PSD could be linked to the different kinetic profiles, especially that of the termination rates.

4.2.3. BEHAVIOUR OF CONVENTIONAL FREE RADICAL POLYMERIZATIONS: CONCLUSIONS

The behaviour of conventional miniemulsion polymerizations is well documented.[12,17,18] In this section, control polymerizations were investigated so as to create an understanding of the various parameters that influence the kinetic and mechanistic nature of conventional miniemulsions. The behaviour of radicals within a miniemulsion during conventional polymerizations is much simpler than during RAFT-mediated miniemulsion polymerization. By first establishing the behaviour within the simpler system, expanding the models to more complex systems should be simpler. Comparing Sections 4.1.1 and 4.1.2, it is apparent that within one miniemulsion polymerization, by simply changing the monomer polymerized, the kinetic models that best describe the behaviour of the polymerization change dramatically. The two kinetic models used to describe FRP in heterogeneous media; *pseudo-bulk* and *zero-one* kinetics, can be applied to the systems given in Section 4.2.[1] Transition between the two kinetic models has been observed in particles in which the average particle radius was varied.[13] *Zero-one* kinetics has been reported to model styrene emulsion polymerizations to a large degree of accuracy.[19] It has been found that butyl acrylate emulsions

generally follow *pseudo-bulk* kinetics except for very small particles.[20] In this section, an attempt was made to classify the four polymerizations E1 – E4 into kinetic classes. The two main differences between the four polymerizations is the rate of reaction and molecular weight profile. Differing kinetic models will account for the differences. These differences are addressed below:

1. Rate of reaction.

The rate of reaction during interval I is dependent on the rate of z-mer formation and rate of entry of these z-mers into the monomer droplets. The rate of z-mer formation will be highest for the BA miniemulsions due the higher C_W^{sat} value and k_p value for BA monomer as compared to styrene monomer. Higher monomer solubility also leads to a greater value of *z*. The order of magnitude by which the k_p value is larger for BA as compared to styrene (200 times) is much higher than for the C_W^{sat} value (2 times). In the discussion in Section 4.1 about the rate coefficient in the aqueous phase, it was stated that monomers with higher solubilities and propagation rates lead to increased particle numbers (nucleation).[1] Oil-phase initiation will influence the reaction rate by increasing the number of propagating chains. This should however only take place in larger particles. The interaction of z-mers with the hydration layer of the stabilizing surfactant will influence the nucleation efficiency during interval I. The thick hydration layer of the surfactant will retard the entry of hydrophobic z-mers into the monomer droplets from the aqueous phase.[2] From this it can be speculated that the non-ionically stabilized miniemulsions will experience significant rate retardation.

Minimal information regarding the rate of reaction (especially during interval I) can be extracted from the gravimetric data due to the inaccuracy of the measurement (limited number if data points). The R_p during interval I appears to be similar for the two butyl acrylate miniemulsions (E1 and E2) and the two styrene miniemulsions (E3 and E4). Thus it is proposed that the z-mer entry rate is similar for both the non-ionically (E4) and ionically (E3) stabilized styrene miniemulsions, and slightly higher for the BA miniemulsions. This latter case is linked to the increased rate of z-mer formation. If there is significant retardation of the z-mer entry due to the non-ionic surfactant, then the high rate of z-mer formation could override this retardation, keeping the reaction rate high (as is seen for E1 and E2). The lower z-mer formation rate for styrene would most likely amplify the slow z-mer entry and result in rate retardation. As was stated, little difference between the ionically stabilized (E3) and non-ionically stabilized (E4)

miniemulsions was seen. A further point to consider is the matter of the total surface area. The total monomer droplet surface area is directly proportional to the nucleation rate.[2] Utilizing Igepal®CO-990 as a surfactant leads to miniemulsions with initial monomer droplets with larger average particle sizes and thus less monomer droplet surface area. The smaller total surface area of the non-ionically stabilized droplets as well as the thick hydration layer should imply that these miniemulsions will have substantial rate retardation. This appears not to be the case, and it can therefore tentatively be stated that the entry rate (k_{ENTRY}) is not the rate-determining step in the four polymerizations investigated.

2. Molecular weight profile.

The larger difference in final molecular weight for the styrene miniemulsions (E3 and E4) maybe linked to the difference in conversion of the samples. The fact that the conversion difference (12%) is quite small compared to the molecular weight difference (1.5 times larger for E3) implies that the molecular weight difference could be linked to a second reason. The molecular weight difference between the BA miniemulsions (E1 and E2) is much larger (1 280 400 g.mol^{-1}). Higher molecular weight polymer will result from a decreased initiator concentration[8] i.e. the higher the $\bar{n}$ value, the more propagating radicals there are, and the shorter the chains will be. The entry and exit of radicals from the particles, as well as possible generation of radicals due to oil-phase initiation, will affect this value. It is speculated that the radical entry was not rate determining for the polymerization and, due to the larger particle size, radical exit is unlikely. Oil-phase initiation may increase the concentration of propagating radicals, but simultaneously, will increase the rate of termination within the particles. An increased termination rate was seen for the non-ionically stabilized styrene miniemulsion (E4) but, due to the particle size (150 nm), it was assumed that oil-phase initiation would be minimal. The explanation for this phenomenon could lie in the radical kinetic behaviour within the particles or in the fact that the particle size and number will affect the value of $\bar{n}$. Few, larger particle will lead to an increase in number of radicals per particle. This in turn will lead to short chains.

3. Pseudo-bulk versus zero-one.

Pseudo-bulk behaviour implies that the $\bar{n}$ value can possibly be found to be greater than 0.5 in any average particle within a miniemulsion. This means that if a z-mer enters a nucleated droplet (particle), then instantaneous termination is not the most probable fate of the oligomeric radical. It does however imply that the probability of chain termination will increase as more and more radicals enter the particle. Thus, the rate of termination will be low at the onset of propagation and increase with time. If it is assumed that the non-ionically stabilized miniemulsions follow *pseudo-bulk* kinetics, then the sudden increase in termination rate for the styrene miniemulsion (E4) can be explained. This sudden increase is not seen for the BA miniemulsion (E2) since the rate would have been high from the onset of the polymerization due to the greater influx of z-mers into the particles (higher rate of z-mer formation). Conversely, if it is assumed that the smaller particles follow *zero-one* kinetics, the longer chain lengths and more gradual termination rates can be explained.

Parameters such as z-mer formation rate, entry rates, oil-phase initiation and kinetic behaviours have been addressed in this section. It is proposed that the larger, non-ionically stabilized miniemulsions typically follow *pseudo-bulk* kinetics while the smaller, ionically stabilized miniemulsions follow *zero-one* kinetics. The z-mer entry rate (k_{ENTRY}) appears not to be a rate-determining factor whilst the rate of z-mer formation is. These proposed models create a base from which more complex miniemulsions can be constructed and then more accurately described.

4.3. REFERENCES

(1) Gilbert, R. G. *Emulsion Polymerization: A Mechanistic Approach*; Academic Press: San Diego, **1995**

(2) Asua, J. M. *Journal of Polymer Science: Part A: Polymer Chemistry* **2004**, *42*, 1025

(3) Nomura, H.; Suzuki, K. *Industrial and Engineering Chemistry Research* **2004**, *48,* 2561

(4) Asua, J. M.; Rodriguez, V. S.; Sudol, E. D.; El-Aasser, M. S. *Journal of Polymer Science Part A: Polymer Chemistry* **1989**, *27*, 3569

(5) Beuermann, S.; Buback, M. *Progress in Polymer Science* **2002**, *27*, 191

(6) De Brouwer, H.; Tsavalas, J. G.; Schork, F. J.; Monteiro, M. J. *Macromolecules* **2000**, *33*, 9239

(7) Landfester, K.; Bechthold, N.; Forster, S.; Antonietti, M. *Macromolecula Rapid Commun.* **1999**, *20*, 81

(8) Lai, J. T.; Filla, D.; Shea, R. *Macromolecules* **2002**, *35*, 6754.

(9) Le, T. P.; Moad, G.; Rizzardo, E.; Thang, S. H. In World Patent 98/01478, **1998**

(10) Kwak, Y.; Goto, A.; Tsujii, Y.; Murata, Y.; Komatsu, K.; Fukuda, T. *Macromolecules* **2002**, *35*, 3026

(11) Venkatesh, R.; Staal, B. B. P.; Klumperman, B.; Monteiro, M. J. *Macromolecules* **2004**, *37*, 7906

(12) Bechthold, N.; Landfester, K. *Macromolecules* **2000**, *33*, 4682

(13) Prescott, S. W.; Ballard, M. J.; Gilbert, R. G. *Journal of Polymer Science Part A: Polymer Chemistry* **2005**, *43*, 1076

(14) Piirma, I.; Chang, M. *Journal of Polymer Science Polymer Chem. Edition* **1982**, *20*, 482

(15) Sudol, E. D.; El-Aasser, M. S. In *Emulsion Polymerization and Emulsion Polymers*; Lovell, P. A.; El-Aasser, M. S., Eds.; Wiley: New York, **1997**; p 699

(16) Hansen, F. K.; Hveem, J. *Journal of Colloid Interface Science* **1999**, *210*, 144

(17) Landfester, K. *Macromolecular Rapid Commun.* **2001**, *22*, 896

(18) Do Amaral, M.; Asua, M.; Jose´, M. *Journal of Polymer Science: Part A: Polymer Chemistry* **2004,** 42, 4222

(19) Casey, B. S.; Morrison, B. R.; Maxwell, I. A.; Gilbert, R.; Napper, D. H. *Journal of Polymer Science Part A: Polymer Chemistry* **1994**, *32*, 605

(20) Maeder, S.; Gilbert, R. G. *Macromolecules* **1998**, *31*, 4410

Chapter 5. : *The influence that the surfactant type, surfactant concentration, and initiator hydrophobicity on RAFT-mediated miniemulsion polymerizations*

ABSTRACT

Two of the fundamental components of a RAFT-mediated miniemulsion are the surfactant and initiator. Each surfactant type has a unique stabilization mechanism that will ultimately determine the hydration layer on the monomer droplet – water interface. This layer will influence radical movements between the two phases. The concentration of the surfactant will determine the monomer droplet surface area as well as the aqueous phase surfactant concentration. These factors will also influence the nucleation rates and nucleation mechanisms. Oil-phase initiators as well as water-soluble initiators can be used in miniemulsions. The differing locations of initiator decomposition will influence the aqueous phase radical concentration.

All these factors will influence the formation of droplets and secondary particles. Their roles, in conjunction with the RAFT process, in the formation of secondary particles are investigated in this chapter.

Pectora roborant cultus recti

The kinetic and mechanistic behaviour of a RAFT-mediated miniemulsion is dependent on the movement of the various radical species between the aqueous and oil phases. Parameters such as the location of initiating radical formation (initiator decomposition), rate of z-mer formation, efficiency of nucleation and radical exit from the polymerization loci substantially influence the overall behaviour. The influence that the surfactant and initiator have on RAFT-mediated miniemulsion polymerization is the focus of interest in this chapter. Changing the surfactant will influence the nucleation efficiency and radical exit from the nucleated particles.[1] The behaviour of systems utilizing hydrophilic and hydrophobic initiators will also be addressed. Changing the primary location of initiator fragmentation will influence the radical concentration in each phase.

All the miniemulsions, except where specified, were prepared following the miniemulsion polymerization procedure given in Section 3.2. The polymerization labels (for example A1) are provided in Table 3.1. The analyses of the polymerizations and the analyses of the final latexes are supplied for each reaction. Kinetic analysis is provided by first-order rate plots. The conversion versus time data needed for these plots was determined gravimetrically. The evaluation of the evolution of polymer characteristics such as molecular weight and polydispersity with conversion were determined by SEC. Particle size analysis was performed by TEM, CHDF and DLS.

5.1. SURFACTANTS

Two types of surfactants were used in this study: an ionic surfactant, sodium dodecyl sulphate (SDS), and a non-ionic surfactant, Igepal®CO-990.

5.1.1. SODIUM DODECYL SULPHATE (SDS)

The critical micelle concentration for SDS is 1.18 mM.[2] SDS is one of the most commonly used ionic surfactants for emulsion and miniemulsion polymerizations.[3] The structure of SDS is given in Figure 5.1:

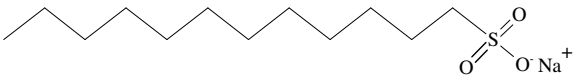

Figure 5.1: Structure of sodium dodecyl sulphate (SDS).

SDS shows no UV absorbance in the wavelength range of 200 to 600 nm. Due to the low molecular weight of the surfactant and its low solubility in THF, it is not possible to identify the surfactant on a standard GPC chromatogram.

5.1.2. IGEPAL®CO-990

Non-ionic surfactants stabilize sterically rather then electrostatically.[4] The ability of a non-ionic surfactant to stabilize an aqueous heterogeneous system is determined by its *hydrophilic-lipophilic balance* (HLB). The HLB of a surfactant is defined by the solubility of the surfactant in the water phase of a water and oil mixture. For HLB values <10, the surfactant is oil-soluble, and the emulsion formed will be a water-in-oil emulsion. For values >10, the surfactant is water soluble and the emulsion formed will be an oil-in-water emulsion.[5] The HLB value for Igepal®CO-990 is 19. Igepal®CO-990 displays a CMC value of 12.75mM.[6] The structure of Igepal®CO-990 is given in Figure 5.2:

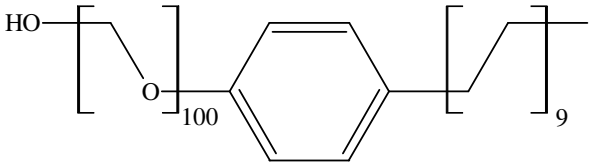

Figure 5.2: Structure of Igepal®CO-990.

The UV absorbance spectrum of Igepal®CO-990 in THF is given in Figure 5.3:

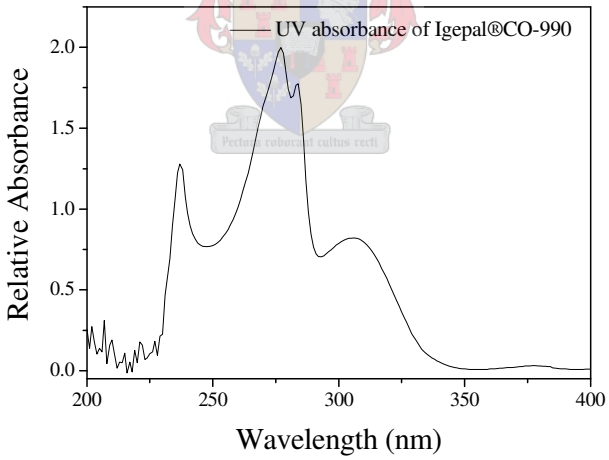

Figure 5.3: UV absorbance spectrum for Igepal®CO-990.

The GPC chromatogram of Igepal®CO-990 is given in Figure 5.4:

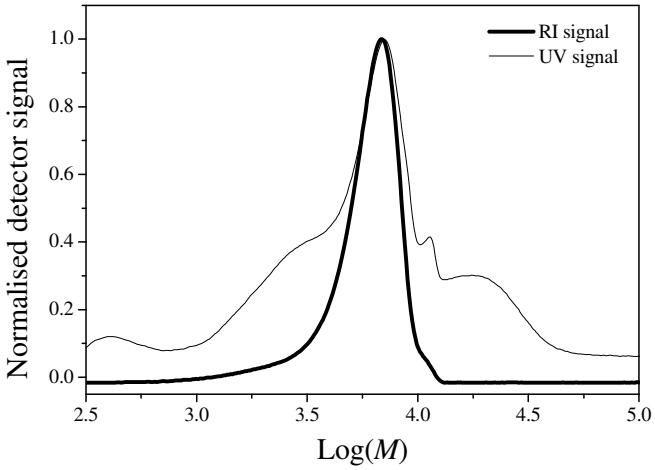

Figure 5.4: GPC chromatogram of the nonionic surfactant Igepal®CO-990.

The chromatogram of Igepal®CO-990 does not show a neat RI-UV overlay. This is most likely due to the very low signal-to-noise ratio, which causes the resolution to be very poor. This is indicative of a very low signal and thus absorbance at 320 nm for the polymeric surfactant. With this in mind, even although according to the UV absorbance spectra given in Figure 5.3 the surfactant will be detected at 320 nm, the signal will be very weak.

5.1.3. INFLUENCE OF THE SURFACTANT TYPE

The type of stabilization mechanism will influence the structure of the hydration layer which forms at the water-oil interface.[1] The density of surfactant units and the packing structure is predetermined by the nature and structure of the surfactant molecules. The behaviour of the interfacial region with respect to radical entry and exit influences the kinetics of the polymerization reaction. In this section a comparison is made between the polymerizations of miniemulsions stabilized by SDS and those stabilized by Igepal®CO-990 to determine the nature of the dependence of the mechanics of the RAFT-mediated miniemulsion polymerization on the surfactant type. The influence that the surfactant type may have on the concentration of secondary particles is also investigated.

Section 5.1.3.1 deals with CVADTB (a) and DIBTC (b) mediated styrene miniemulsions. This is followed by Section 5.1.3.2, which deals with CVADTB (a) and DIBTC (b) mediated butyl acrylate miniemulsions. A summary and conclusion of all the experimental data is given in Section 5.1.3.3.

5.1.3.1. Styrene miniemulsion polymerizations

Styrene miniemulsion polymerizations were performed with two surfactants and two RAFT agents.

a) Cyanovaleric acid dithiobenzoate (CVADTB)

Polymerizations A1 and A3 were investigated. The surfactants used were SDS and Igepal®CO-990 respectively. The kinetic rate plots for both are given in Figure 5.5:

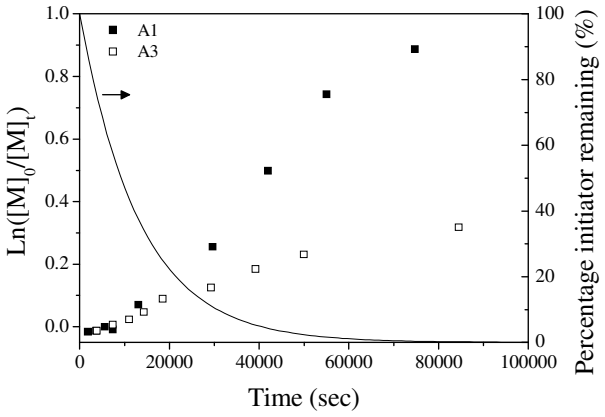

Figure 5.5: First-order rate plots for polymerizations A1 and A3.

The conversion of polymerization A3 after approximately 24 hours is 27% and A1 is 30%. It is evident that for A1 the rate of reaction during interval I is lower than A3. There appears to be an inhibition period for A1, implying that propagating radical loss is taking place at a higher rate during this interval. After this inhibition period, the rate increase during interval I is faster for A1. The nucleation period for both A1 and A3 is similar (8 hours). The value of R_p during this interval is similar for both A1 and A3. The onset of interval III (marked by the decrease in reaction rate) is similar for A1 and A3. The decrease in reaction rate during this interval is more gradual for A3. This implies that the rate of termination is not as high for A3.

The GPC analysis of A3 proves problematic due to the fact that the sample molecular weights are very low. The surfactant in the system has a molecular weight of 4 625 g.mol^{-1}. The theoretical $\overline{M}_n$ calculated from equation 2.12 at a conversion of 27% is only 5 344 g.mol^{-1}. Thus, in the GPC trace, it is difficult to distinguish between the surfactant and polymer eluting from the column. The results of GPC analysis are given in Figure 5.6:

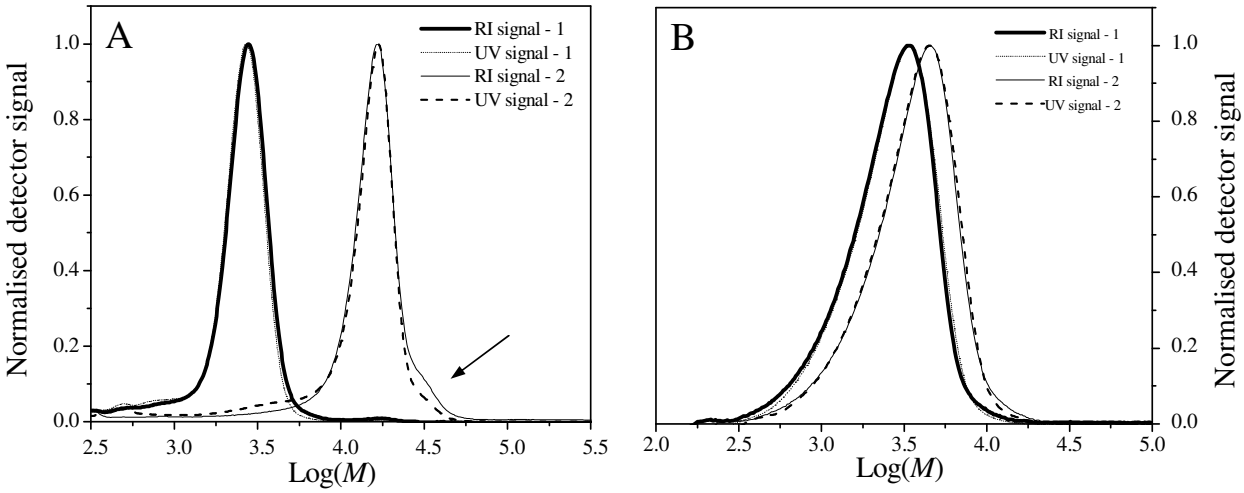

Figure 5.6: GPC chromatograms of the polymerizations A.) A1 and B.) A3. Sample conversions for A are: (1) – 20% and (2) – 27% and B are: (1) – 6% and (2) – 60%).

The RI-UV overlay for both chromatograms indicates that RAFT agents are incorporated in all the chains. The polydispersity for the SDS system is far lower than that of the non-ionically stabilized polymerization (1.14 for A1 versus 1.4 for A3). A low molecular weight tail can be seen in the chromatogram on the right. This is distinctive for a RAFT-mediated polymerization.[7] The traces illustrated in chromatogram B are from samples that have a much lower conversion when compared to those of chromatogram A. The *experimental number average molecular weight* is 13 949 g.mol^{-1} for A1 and while the predicted (utilizing Equation 2.12) value is 4 174 g.mol^{-1}. There is a slight shoulder on the RI sample 2 for chromatogram A (marked with an arrow). There is however no such shoulder on UV trace 2. Termination of RAFT end-capped polymer chains via coupling could result in these high molecular weight chains that exhibit a faint UV absorbance (faint due to a very low concentration of the thio carbonyl thio functionality).

The particle analysis results of polymerizations A1 and A3 are as follows:

Table 5.1: DLS results for polymerizations A1 and A3

Reaction	RAFT	Monomer	Surfactant	Z (average)	Polydispersity
A1	CVADTB	Styrene	SDS	82.7	0.063
A3			Igepal®CO-990	172.5	0.187

Results tabulated in Table 5.1, show that the non-ionic surfactant leads to particles being greater in size as well as having a larger distribution of sizes. The smaller ionic "head" of the SDS molecule can pack in an orderly fashion, leading to a compact ionic layer. The non-ionic surfactant has a long

polymeric "tail" that can solubilize in the organic phase. This solubilization within the organic phase decreases the amount of surfactant that is available for stabilization, resulting in larger particles.[8] Considering the fact that the non-ionic surfactant has its own unique molecular weight distribution, it is conceivable that not all the particles will have equal inclusion of the polymeric tails due to the varying tail lengths. Differing surfactant aggregates (conformations) has been reported for Igepal®CO-990 and could also account for the wider spread in particle sizes.[6] This can explain the increased *polydispersity* value. An increased polydispersity is also indicative of poor nucleation of the original monomer droplets of the miniemulsion. CHDF results are given in the following table:

Table 5.2: CHDF results for polymerizations A1 and A3

Reaction	Z (Number average)			Z (Weight average)		
	Mean	Max	Standard deviation	Mean	Max	Standard deviation
A1	60.4	56.9	17.6	74.5	74.7	17
A3	79.3	73.9	29.3	130.8	89.4	77.1

For A1, the *weight average mean particle size* in Table 5.2 is similar to the *Z (average)* shown in Table 5.1. The mean and maximum values are similar and the *standard deviation* value is low, indicating a narrow, singular peak. This can be seen in Figure 5.7:

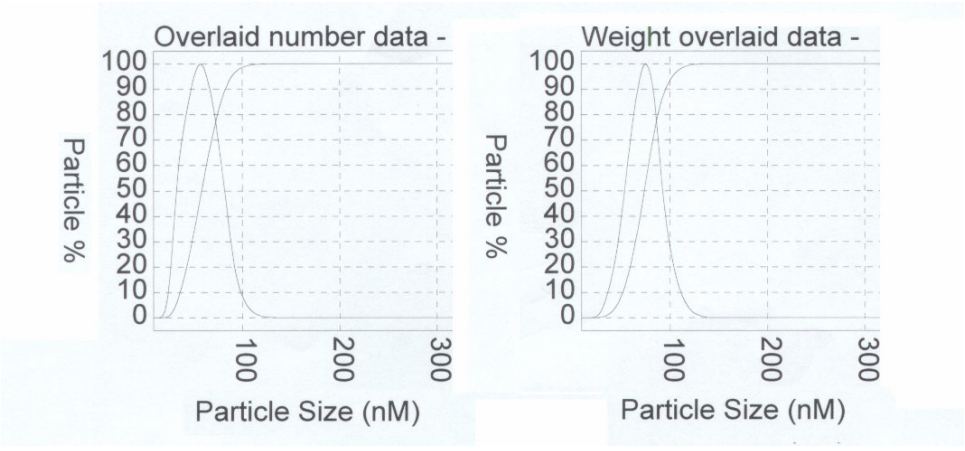

Figure 5.7: CHDF chromatograms for the final latex of A1.

These results are substantiated when examining the TEM results of the final latex of A1, shown in Figure 5.8.

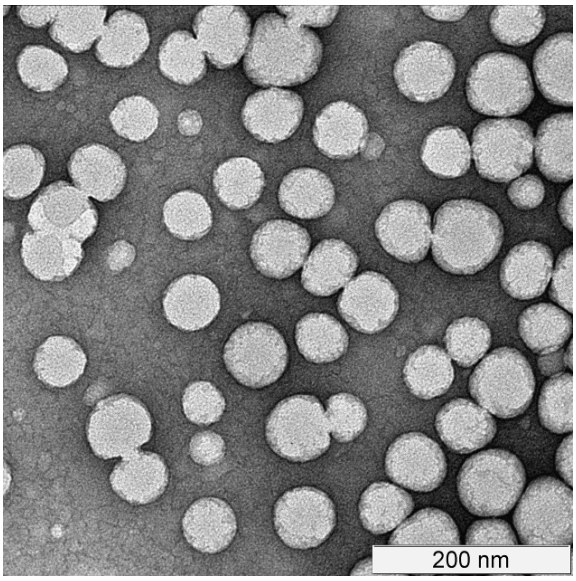

Figure 5.8: TEM micrograph of final latex for polymerization A1.

Figure 5.8 shows that most of the particles are of similar size. The weight average CHDF results for A3 do not agree as well as those determined with DLS. The *weight average mean* and *maximum particle sizes* (determined with CHDF) are quite different for A3, indicating that there is a wide range of particle sizes (specifically more small particles and a few larger particles).

b) S-Dodecyl-S'-isobutyric acid trithiocarbonate (DIBTC)

The polymerizations of styrene mediated by DIBTC (reactions B1 and B3) are investigated in this section. The surfactants used for the two reactions were SDS and Igepal®CO-990 respectively. The kinetic rate plots for both reactions are given in Figure 5.9:

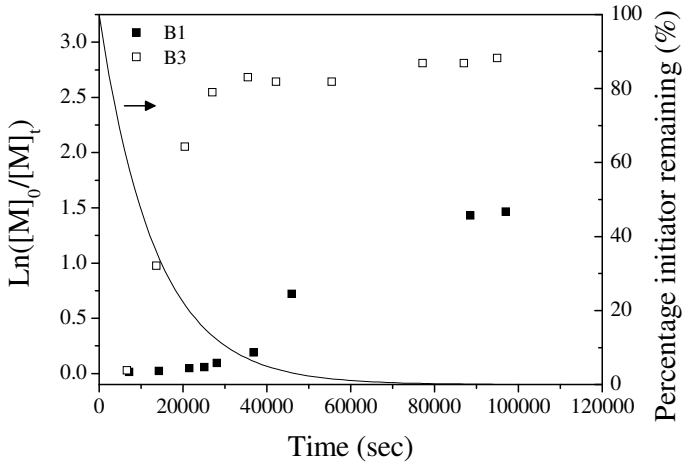

Figure 5.9: First-order rate plots for polymerizations B1 and B3.

The rate of polymerization trend seen for this set of reactions is quite different to that seen for CVADTB mediated polymerizations as described in Section 5.1.3.1.a. After 24 hours, the conversion for B1 is 67% compared to 93% for B3. The duration of interval I (nucleation time) is much longer for B1, and the rate of reaction during this period is much lower. There even appears to be an inhibition period for B1, which implies that radicals are irreversibly terminated during this time. Interval III is clear for both, however in the case of B1 this interval appears at a later time (most likely due to the long duration of interval I).

The GPC chromatograms of the polymerizations B1 and B3 are given in Figure 5.10.

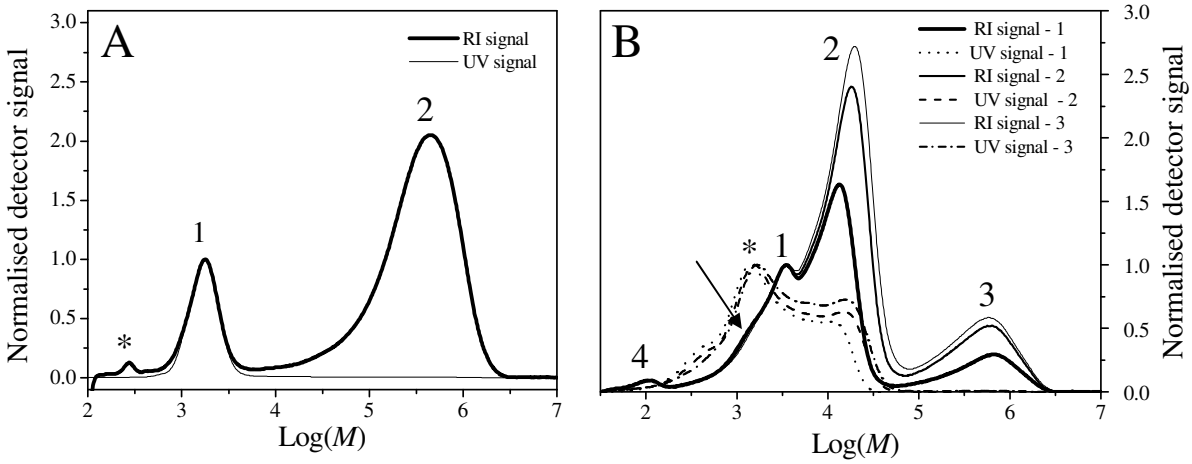

Figure 5.10: GPC chromatograms for the polymerizations A.) B1 and B.) B3. Sample conversion for A is: 67% and those for B are: (1) – 62%, (2) - 87% and (3) – 95%

Chromatogram A above (polymerization B1) shows a large distribution (labeled as 2) that does not show any UV absorbance. This implies that these chains lack the thiol carbonyl thiol functionality. These chains are irreversibly terminated and have polymerized conventionally, leading to the large polydispersity for the distribution. There appears a smaller peak at a molecular weight of 1 444 $g.mol^{-1}$ in the RI trace (labeled as 1). The UV signal overlays neatly with this distribution and implies that these are living RAFT end-capped chains. The *number average molecular weight* for the controlled distribution for B1 (distribution 1) is much lower than the theoretical value (experimental value of 1 444 $g.mol^{-1}$ versus the predicted value of 12 720 $g.mol^{-1}$). There appears to be a small distribution (marked with an asterisk) at a molecular weight similar to that of the RAFT agent. This suggests that while most of the RAFT agents are consumed, many of the RAFT end-capped chains grow at reduced rates due to starvation of monomer.

The chromatogram of the Igepal®CO-990 polymerization (B3) is more complex. The RI traces show four distinct distributions. The distribution labeled as 1 is that of the surfactant. The second distribution (labeled as 2) is fairly narrow although it overlaps with the surfactant peak. This peak increases in intensity with conversion. The shift of the peak height to higher peak molecular weights is also apparent, which implies that this is a living polymer distribution. This is confirmed by the presence of UV absorbance (at 320 nm). The intensity of the UV absorbance peak is not a true indication of the concentration of RAFT agents due to the fact that all the traces were normalised to the peak height of the surfactant peak. It is noted that the UV and RI traces overlap perfectly for the second distribution, and that the peak height increases along with the RI peak as well as shifting to higher molecular weights. The *peak molecular weight* for the controlled distribution is slightly higher than the predicted $\overline{M}_n$ value (experimental M_p is 19 543 $g.mol^{-1}$ whilst the theoretical $\overline{M}_n$ value is 16 534 $g.mol^{-1}$). The third distribution (labeled as 3) is a much broader and less intense peak. It shows no distinct UV absorbance, which implies a lack of thiol carbonyl thiol functionality and a conventional radical polymerization mechanism that explains the broadness of the distribution as well as the exceptionally high *peak molecular weight*. The most prominent peak in the UV trace (marked with an asterisk) does not overlay with any distinct RI distribution. It does however fall in the region in which there appears to be a shoulder on the surfactant peak (marked with an arrow). This distribution is possibly due to short, dormant chains that are end-capped with RAFT agents. The molecular weight of these chains is similar to the RAFT end-capped chains (distribution labeled as 1) seen in the chromatogram for B1. The origin of these chains is unclear, but it can be speculated that these chains either started growing late in the reaction or were formed during

interval I, but remained in a dormant state for the remaining part of the polymerization. The fact that with an increase in conversion, the molecular weight of these chains does not change implies that the latter explanation is most likely true. The distribution labeled as 4 corresponds to the RAFT agent present in the system. It appears that there are small quantities of unconsumed RAFT agents. The presence of these unreacted RAFT agents explains the abnormally high molecular weights for the controlled distribution (2).

Particle size analyses can provide insight into the nucleation mechanisms operating within the latex of the miniemulsion. The results from DLS and CHDF analyses are given in Table 5.3 and 5.4:

Table 5.3: DLS results for polymerizations B1 and B3

Reaction	RAFT	Monomer	Surfactant	Z (average)	Polydispersity
B1	DIBTC	Styrene	SDS	50.7	0.343
B3			Igepal®CO-990	163.6	0.017

The difference in the *Z (average)* value for the two reactions is due to the inclusion of the non-ionic surfactant into the particles. The *polydispersity* trend is however different to that seen when comparing the CVADTB mediated polymerizations (A1 and A3). It appears that the particle size distribution is much larger for B1 (ionic) than B3 (non-ionic). It is likely that droplet nucleation is not the only nucleation mechanism at play in either of these polymerizations. The CHDF results are given below:

Table 5.4: CHDF results for the polymerizations B1 and B3

Reaction	Z (Number average) (nm)			Z (Weight average) (nm)		
	Mean	Max	Standard deviation	Mean	Max	Standard deviation
B1	40.3	35.6	9.8	47.9	42.4	11.7
B3	92.6	47	41.5	142.7	145.7	42

The *standard deviation* values are however vastly different for each polymerization. According to CHDF, the particle size distribution for B1 is much narrower than for B3. The longer nucleation period for B1 is simply due to inhibition taking place, and does not lead to an apparent increase in the PSD. The results for B3 show that there is a large population of small particles, but that there are also larger particles. The number of larger particles is about 30% less than that of the smaller

particles, as can clearly been seen from the number average chromatogram of B3 shown in Figure 5.11.

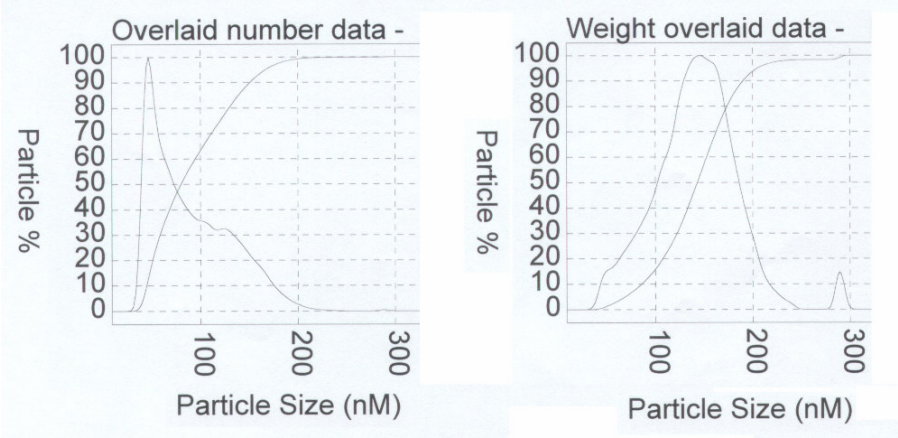

Figure 5.11: CHDF chromatogram of the final latex of polymerization B3.

The TEM micrograph of B3 given in Figure 5.12 shows a wide range of particle sizes.

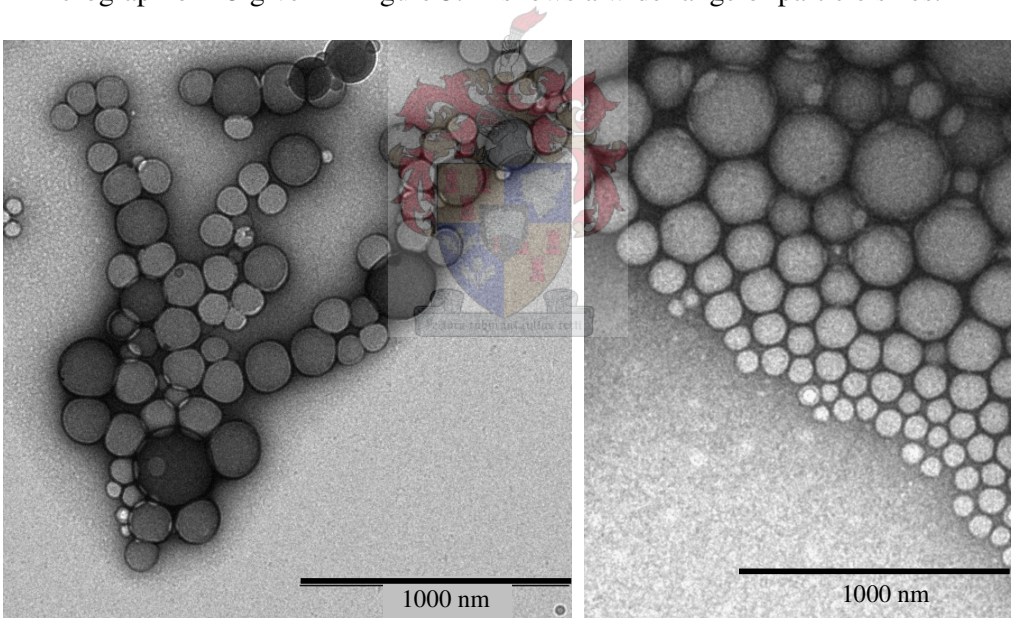

Figure 5.12: TEM micrographs of the final latex of polymerization B3.

The origin of these varying particle sizes is the complex particle formation within the polymerization. According to the GPC chromatogram in Figure 5.9 (B), there are chains that are RAFT terminated and chains that have no RAFT functionality. These chains must reside in different particles and these particles must have formed via different mechanisms. Additionally, there is a species of shorter chains that are end-capped with RAFT agents, but appear to be dormant. The controlled polymer particles formed from conventional droplet nucleation. The TEM micrograph

shows many particles of approximately 130 nm in size. Taking into account that for polymerization B1 it is clear that there is primarily uncontrolled polymer in the latex, and that the particle size distribution is very narrow (and averaged around 35 nm), it is proposed that the similar size particles for B3 also formed in a similar mechanism. In other words, the smaller particles evident in B3 most likely originate from polymer that is polymerized either in micelles or in the aqueous phase (to later form particles through homogeneous-coagulative particle formation). The conventional polymerization taking place within these particles, is defined by high propagation and termination rates. This implies that the particles will form in a short time span. The smaller particle sizes of the secondary particles stem from the fact that the initial micelles are very small. The RAFT-mediated polymerization taking place in the particles formed by droplet nucleation is much slower, but the rate of termination is also lower. Monomer diffusion into the particles (Ostwald ripening) can take place, leading to the larger particle sizes. Larger particles within the latex of polymerization B3 most likely formed by droplet nucleation, which, from their nucleation, are larger than the secondary micelles.

5.1.3.2. Butyl acrylate miniemulsion polymerizations

Butyl acrylate miniemulsion polymerizations were performed with two surfactants and two RAFT agents.

c) CVADTB

Polymerizations A2 and A4 were investigated. The surfactants for the reactions were SDS and Igepal®CO-990 respectively. The first-order kinetic rate plots for both are given in Figure 5.13:

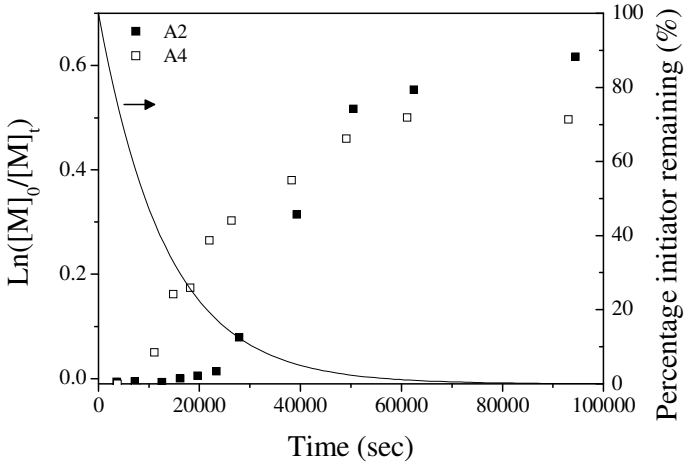

Figure 5.13: First-order rate plots for the polymerizations A2 and A4.

The conversion after 24 hours for A2 is 46% and for A4 is 39%. The nucleation time (interval I) appears to be much longer for A2 and even shows evidence of an inhibition period. The onset of interval III is much earlier for A4, and the duration of this interval appears longer due to a gradual decrease in rate of polymerization.

GPC analysis, the results of which are shown in Figure 5.14, reveals similar molecular weight profiles for both polymerizations, albeit slight differences in controlled and uncontrolled polymer concentrations.

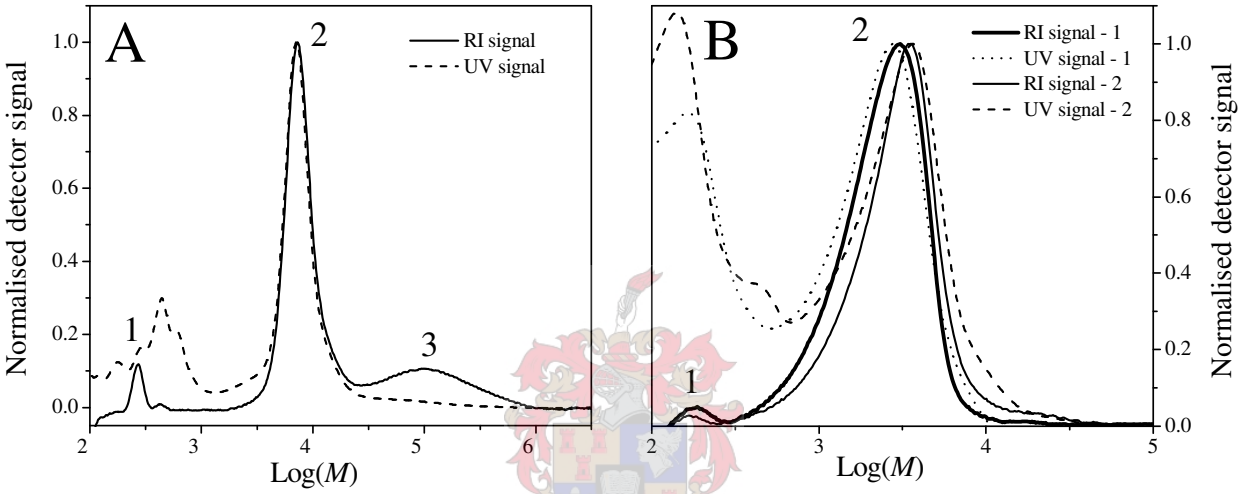

Figure 5.14: GPC chromatograms of the polymerizations A.) A2 and B.) A4. Sample conversion for A2 is 40% and those for A4 are: (1) – 15% and (2) – 40%.

The chromatogram for the ionically stabilized miniemulsion (A2) shows three distributions. The first small distribution (labeled as 1) has a strong UV absorbance and has an elution volume similar to that of the RAFT agent. The second distribution (labeled as 2) shows thio carbonyl thio functionality, whilst the third (labeled as 3) lacks RAFT functionality. This implies that the second and third distributions are controlled and uncontrolled respectively. The experimental *number average molecular weight* for the controlled distribution is 10 252 g.mol^{-1} which is much higher than the theoretical value of 6 902 g.mol^{-1}. This is possibly due to the unreacted RAFT in the latex. Chromatogram B (the non-ionically stabilized miniemulsion) shows two distributions. The first (labeled as 1) corresponds to the RAFT agent CVADTB. This distribution has a strong UV absorbance as 320 nm, which verifies this identification. The second distribution (labeled as 2) is the surfactant as well as the polymer within the latex. These two distributions cannot be distinguished from each other due to their similar elution volumes (the molecular weight of the

polymer at 39% conversion is theoretically 4 000 $g.mol^{-1}$ whilst that of the surfactant is 4 625,72 $g.mol^{-1}$). No uncontrolled distribution can be identified for polymerization A4.

From the vastly different kinetics during interval I, revealed by the first-order kinetic plots, it is expected that the particle size distribution (PSD) for the final latexes will be unique. DLS results in Table 5.5 indicate that the non-ionically stabilized latex of A4 has larger *average particle sizes*:

Table 5.5: DLS results for the polymerizations A2 and A4

Reaction	RAFT	Monomer	Surfactant	Z (average)	Polydispersity
A2	CVADTB	Butyl acrylate	SDS	117.5	0.052
A4			Igepal®CO-990	226.7	0.115

The increased *polydispersity* for A4 could be linked to a longer interval III (longer termination interval). The CHDF analysis results are given in Table 5.6:

Table 5.6: CHDF results for the polymerizations A2 and A4

Reaction	**Z (Number average)**			**Z (Weight average)**		
	Mean	**Max**	**Standard deviation**	**Mean**	**Max**	**Standard deviation**
A2	68.8	33.1	30.3	102.8	89.6	28.3
A4	121.9	92	55.8	230.7	133.9	109.9

The data obtained from CHDF and given in Table 5.6 illustrates clearly that the distribution of particle sizes for both A2 and A4 is broad. The CHDF chromatograms of A2 are given in Figure 5.15.

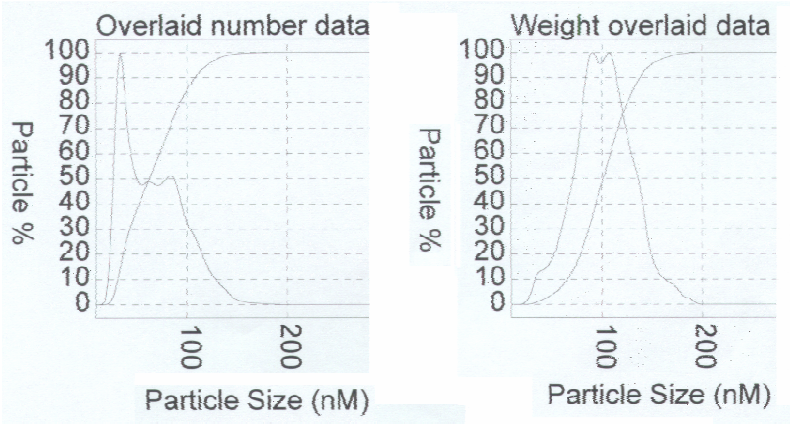

Figure 5.15: CHDF chromatograms of A2.

From the *overlaid number data* chromatogram it is observed that there is a large species of particles, around 30 nm in size. A second species of larger particles also exists. A similar chromatogram is seen for polymerization B3 (Figure 5.10). The results for A4 indicate that there is a very wide range of particle sizes. These strange results may be due to latex instability or faulty analysis (particle coalescence during sample preparation). The chromatograms of A4 are given in Figure 5.16:

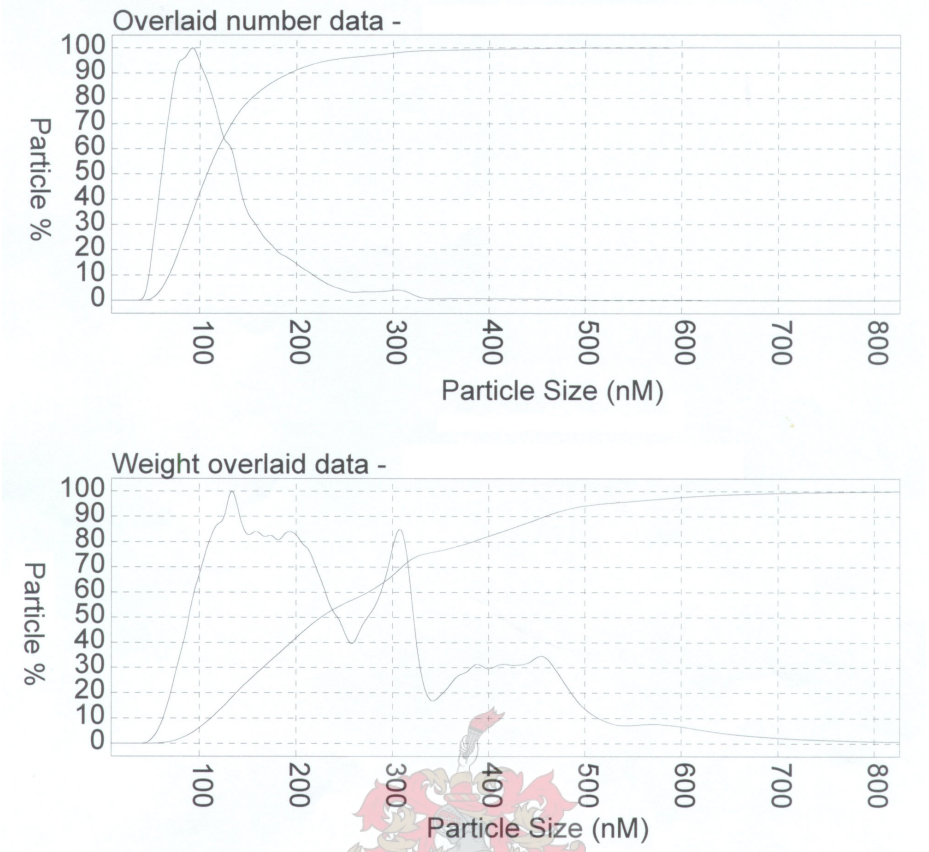

Figure 5.16: CHDF chromatograms of A4.

The large PSD for A4 may be a result of poor droplet nucleation. Large amounts of unreacted RAFT agents add weight to this hypothesis.

d) DIBTC

Polymerizations B2 and B4, carried out using surfactants SDS and Igepal®CO-990 respectively, are presented. The first-order kinetics plots for both polymerizations are given in Figure 5.17:

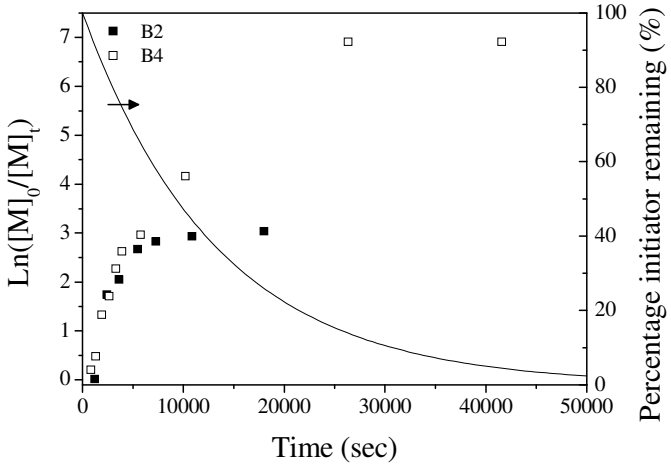

Figure 5.17: First-order rate plots for the polymerizations B2 and B4.

The conversion at 24 hours for B2 is 96% and for B4 is 100%. The nucleation period for B2 and B4 cannot accurately be determined from the data given above, but the respective rates of reaction and duration of the period appear to be very similar. The onset of interval III is similar for B2 and B4, but the rate at which the reaction rate decreases is lower for B4.

In Figure 5.18, the GPC chromatograms of these two polymerizations are given:

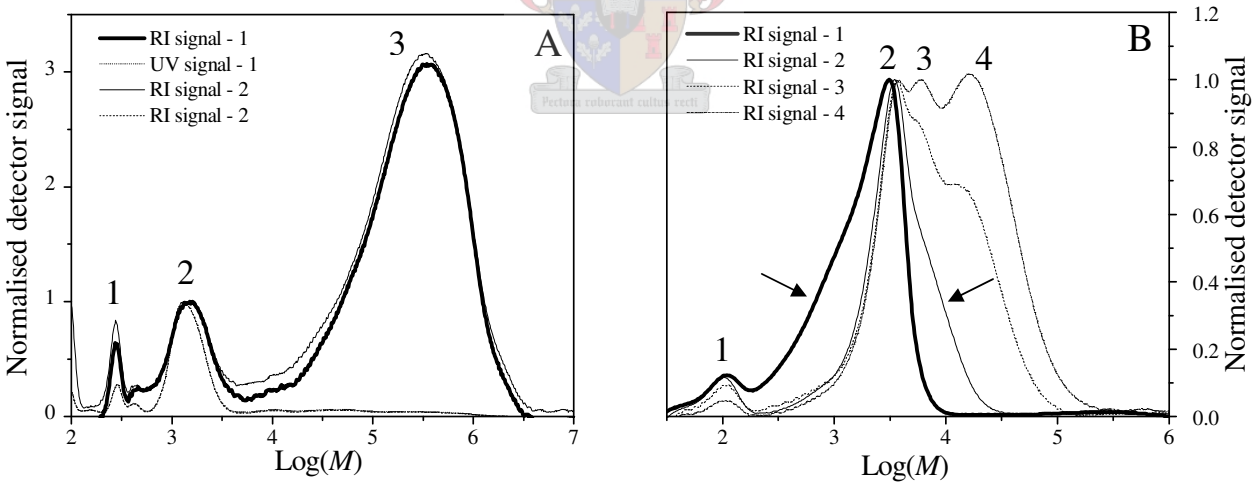

Figure 5.18: GPC chromatograms of the polymerizations A.) B2 and B.) B4. Sample conversions for B2 are: (1) - 80% and (2) - 87% and B4 are: (1) – 18%, (2) – 38%, (3) – 73% and (4) – 100%.

The RI-UV overlay for B2 is given but, for clarity, the overlay for B4 has been omitted. A single sample (RI signal – 4 in chromatogram B, Figure 5.18) overlay is given in Figure 5.19:

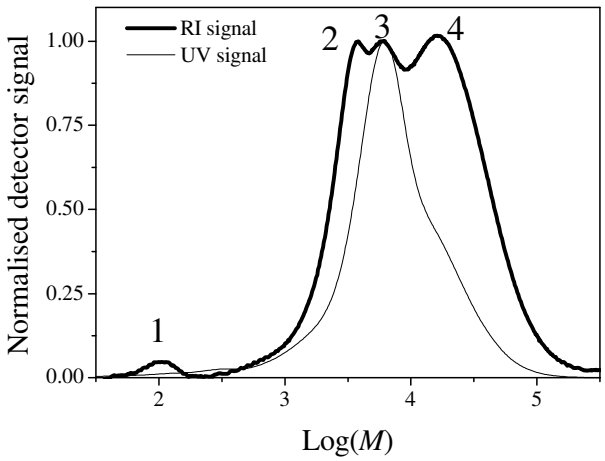

Figure 5.19: GPC chromatogram of polymerization B4 showing the RI–UV overlay of sample – 4.

The chromatogram of the ionically stabilized miniemulsion (A) given in Figure 5.18 shows three distributions for both samples 1 and 2. The first distribution corresponds to unreacted RAFT agent within the latex. The third distribution (labeled as 3) in both chromatograms has no UV signal, whilst the second distribution (labeled as 2) shows a perfect RI-UV overlay. This implies that the third distribution is uncontrolled and the second is controlled. Chromatogram (A) looks similar to that seen for the respective styrene polymerization (B1 in Figure 5.10). In the chromatogram for the non-ionically stabilized miniemulsion B4 (Figure 5.18 B), we see that the first two samples (signals - 1 and 2) show a single tailing distribution (labeled as 2) as well as a small distribution (labeled as 1) at an elution volume the same as that of the RAFT agent. Distribution 1 is unreacted RAFT agent still present in the latex. The second distribution in sample 1 appears to have a shape that results from the superposition of two distributions, of which one is a smaller peak at a lower molecular weight (marked with an arrow) and the second a larger peak at a higher molecular weight. The second sample shows the same superposition except that the smaller peak (still marked with an arrow) has now shifted to a molecular weight higher than that of the larger peak. The larger peak has a retention time similar to that of the surfactant. Samples 3 and 4 begin to show all the distributions. The second distribution (labeled as 2) is constant in intensity, but the third and fourth distributions increase with conversion. Distribution 3 increases in molecular weight as does 4, however only to a limited degree. The RI-UV overlay shown in Figure 5.19 shows that the third distribution absorbs UV irradiation at a wavelength of 320 nm and it can thus be said to be RAFT-mediated (controlled), whilst the fourth distribution is uncontrolled.

The concentrations of uncontrolled and controlled polymer in the latexes of the two polymerizations imply that there are multiple nucleation mechanisms operating. This was investigated via DLS and CHDF:

Table 5.7: DLS results for the polymerizations B2 and B4

Reaction	RAFT	Monomer	Surfactant	Z (average)	Polydispersity
B2	DIBTC	Butyl acrylate	SDS	48.2	0.268
B4			Igepal®CO-990	163.1	0.056

The *Z (average)* values for the respective BA and styrene miniemulsions are similar. There is however a large difference in *Z (deviation)* value for each final latex. The CHDF analysis results are presented in Table 5.8:

Table 5.8: CHDF results for the polymerizations B2 and B4

Reaction	Z (Number average)			Z (Weight average)		
	Mean	Max	Standard deviation	Mean	Max	Standard deviation
B2	36.3	33.3	8.2	42.3	37.9	9.9
B4	109.9	101.1	35.7	167.5	130.1	87.1

The results for B2 show that the *standard deviation* value for both *weight average* and the *number average* is much lower than that obtained by DLS. The same disagreement between results was seen for the DLS and CHDF data for B1 (in Tables 5.3 and 5.4). The results for B2 (ionic surfactant) in Table 5.8 indicate that there is a very narrow distribution of small particles in the system. The results for B4 (non-ionic surfactant) indicate quite the opposite. The weight average data show a very wide distribution of particles sizes. From the difference in number average mean and weight average mean it is known that the majority of particles are approximately 100 nm in size, with a few larger particles present in the latex. The CHDF chromatogram of B4 is given in Figure 5.20:

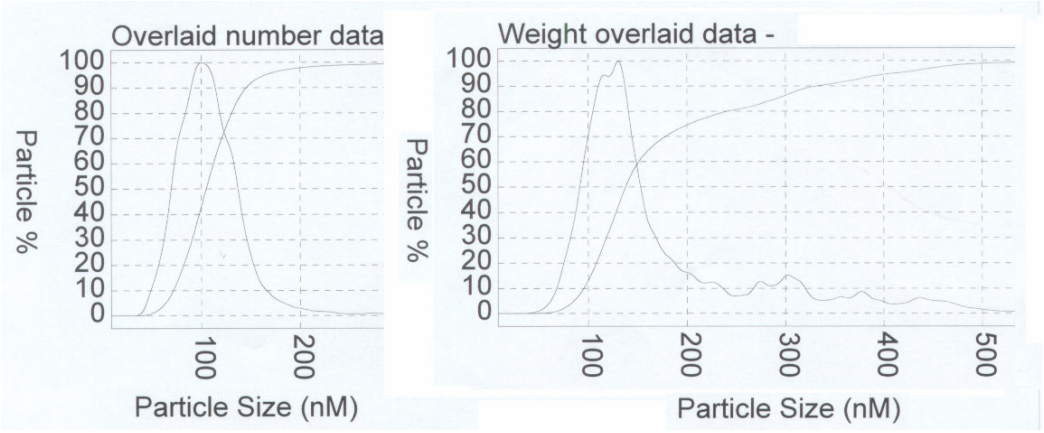

Figure 5.20: CHDF chromatogram of the final latex of polymerization B4.

The TEM micrograph for B4 is shown in Figure 5.21, illustrating the size distribution of the final latex:

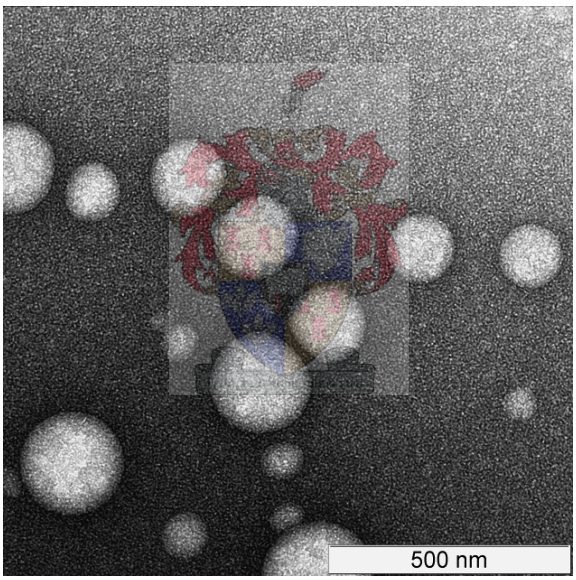

Figure 5.21: TEM micrograph of the final latex of polymerization B4.

5.1.3.3. Ionic versus non-ionic surfactants: Summary and conclusions

The influence that a specific surfactant might have on the radical behaviour of a RAFT-mediated miniemulsion polymerization can only accurately be described with reference to the model described in Chapter 4. This model assumes that any RAFT agents within a miniemulsion will remain within the initial monomer droplets. Any polymerization that does not take place within these droplets will follow conventional free radical polymerization kinetics. The decomposition of the initiator will be the primary source of radicals and these radicals will reside either within the

particles (oil-phase initiation) or the aqueous phase (aqueous-phase initiation). The polymerization systems investigated in this section (5.1.3) will theoretically follow the mechanistic model given in Section 2.2.2.2. It can thus be stated that any polymerization not taking place within the monomer droplets must have been initiated by radicals that escaped the droplets and did not re-enter them, or by initiating radical fragments that undergo propagation within the aqueous phase and fail to enter the droplets. Determining which of these two mechanisms is responsible will ultimately allow for the complete removal of any conventional polymerization from the system.

All eight polymerizations investigated in this section (5.1.3) have unique behaviour when compared to conventional miniemulsion polymerizations. Distinct rate retardation during interval I proves that propagating radical loss from the polymerization loci is taking place. Poor nucleation can result in z-mers reaching j_{crit} and further propagating conventionally within the aqueous phase. Dormant RAFT end-capped chains indicate that certain droplets are being nucleated but then remain dormant. Multiple nucleation mechanisms must result from unusual radical movements between the aqueous and oil phases. These factors will now be discussed individually:

1. **Rate retardation.**

   The rate of reaction is dependent on the concentration of radical species in the locus of polymerization (first-order dependence) as well as the propagation rate constant of the radical – monomer system and concentration of monomer in the phase in which polymerization is taking place. If radicals are lost from the locus, retardation of the reaction rate will be observed. From the miniemulsion schematic given in Chapter 4 (Scheme 4.1), it is clear that radical loss from the particles can occur, leading to dormant species within the particles. The extent to which radicals are lost from the particles is dependent on the concentration of these radicals, their solubility in each phase, as well as their reactivity with other components in each phase. After the initialization step between a RAFT agent and z-mer (within the particles), a radical leaving group is generated and this group may exit from the particle. Retardation due to the use of chain transfer agents with high transfer constants has been reported and it was stated that the retardation is due to exit of the leaving group radical from the droplets.[9] It should be stressed that due to the fact that rate retardation also takes place in homogeneous systems, radical exit is not the only possible contributor to the phenomenon. This results in a dormant RAFT end-capped chain as well as a radical within the aqueous phase. The RAFT-mediated miniemulsions examined in this section showed varying degrees of rate retardation. Assuming that after a few

monomer additions the probability of radical exit is greatly reduced due to strong repulsion from the hydration layer of the surfactant, it can be assumed that the behaviour and movements of these small radical leaving groups will define the retardation of any RAFT-mediated miniemulsion.

The radical leaving groups for CVADTB and DIBTC are the cyanovaleric acid and isobutyric acid groups respectively. The water solubility of these two groups will be slightly different. Resonance stabilization of the respective tertiary radical centers of the cyanovaleric acid group will cause this radical to be far more stable. It has been determined that the chain transfer efficiency for the trithiocarbonates is very high, but, more importantly, the low stabilization of the intermediate radical leads to an increased fragmentation rate during the initialization step. An increase in radical leaving group concentration in the particles will follow. These three variables (solubility, reactivity and concentration) make modeling the varying behaviour of radical exit quite cumbersome. An increase in rate retardation during interval I for the DIBTC mediated styrene miniemulsions (B1 and B3) compared to those mediated with CVADTB (A1 and A3) implies that more radical leaving groups are being terminated in the aqueous and oil phases for the DIBTC mediated polymerizations. The higher solubility of the isobutyric acid radical group as well as the increased likelihood of radical exit (increased concentration in particles) of this group could explain the increased rate retardation. The butyl acrylate miniemulsions do not however show a similar trend. For both non-ionically (A4) and ionically (A2) stabilized CVADTB BA miniemulsions there is distinct rate retardation, whilst the DIBTC mediated derivatives (B4 and B2 respectively) have no rate retardation during interval I. The increased monomer solubility of butyl acrylate as well as the higher propagation rate coefficient for BA implies that radicals that do end up in the aqueous phase have a higher probability of propagation and subsequent particle nucleation, thus less rate retardation. Termination of exited radicals can also explain the retardation for the styrene polymerizations (B1 and B3). This theory is substantiated by the GPC data for polymerizations B4 and B2 that confirmed that conventional free radical polymerization was taking place within secondary particles formed within the aqueous phase.

Asua *et al.*[1] reported poor entry of z-mers into droplets stabilized with non-ionic surfactants. This retardation of entry rate was linked to the thick, hairy hydration layer created by the non-ionic surfactant around the droplets. This, over and above the fact that the total monomer droplet surface area is smaller, would lead to increased interval I lengths and lower rates of

reactions during this interval for the non-ionically stabilized miniemulsion. From the first-order plots given in this section, this is clearly not the case. The CVADTB and DIBTC mediated styrene and BA miniemulsions all showed a decrease in rate retardation during interval I for the non-ionically stabilized miniemulsions. This indicates that the thick hydration layer does not impede the entry of surface active z-mers into the droplets.

Differences in the reaction rate between the miniemulsions stabilized by the two different surfactants could also be linked to possible oil-phase initiation that might take place in the larger particles. If this is indeed the case, then the reaction rate could be higher for the non-ionically stabilized miniemulsions, taking into account that the rate of termination could also be higher. Discerning between differences in reaction rate due to oil-phase initiation and radical exit is a problematic task. From the DIBTC mediated BA polymerization, it appears that the reaction rates are similar during interval I. For the other six polymerizations, no accurate deductions can be made. The introduction of RAFT agents adds a whole new dimension to oil-phase initiation. The addition of the initiating radical species to the RAFT agents in the particles is very fast and might even disrupt the geminate recombination that normally takes place.[10] The subsequent monomer additions will happen at rates that are influenced by the RAFT agent structure, as has been reported.[11] A slower rate of the first monomer addition could lead to an inhibition period. This fact, in conjunction with possible oil-phase initiation, could explain the inhibition period for the CVADTB mediated BA polymerization. If oil-phase initiation is taking place within the larger droplets stabilized with the non-ionic surfactant, the concentration of unreacted RAFT agents should be low. The CVADTB mediated, non-ionically stabilized butyl acrylate polymerization shows a higher concentration of unreacted RAFT agents compared to the respective ionically stabilized miniemulsion, which implies that oil-phase initiation is probably minimal. Possible oil-phase initiation is further investigated in Section 5.1.4.

2. Unreacted RAFT agents.

It is assumed that droplet nucleation is efficient, which will lead to complete consumption of the RAFT agents within the system. It is clear from the GPC chromatograms for certain of the polymerizations that there are still quantities of unreacted RAFT agent within the latex. The rate at which the z-mers form will be higher for a BA polymerization. An increase in z-mer concentration should theoretically lead to an increased efficiency in nucleation. The GPC data for the CVADTB mediated BA polymerizations (A4) however shows an increased

concentration of unreacted RAFT agents compared to the styrene counterpart (A3). This implies that the nucleation efficiency is poor for both monomers. The differences in concentrations of unreacted RAFT agents between certain polymerizations could lie in the ability of certain radicals to nucleate droplets. The concentration of initiating radicals forming within the aqueous phase is a constant amongst the eight polymerizations as this is independent of the RAFT process. Thus differences in the radical concentration in the aqueous phase are due to radicals that originated from the nucleated particles. Radical leaving groups undergo exit from the particles leading to a higher aqueous phase radical concentration and consequently more termination. Once a steady state is reached between the initiating radical formation (those exiting from the droplets into the aqueous phase) and leaving group radical exit from the particles, the rate of nucleation will increase. At this point, the higher rate of z-mer formation for the BA miniemulsion should theoretically lead to increased nucleation. A higher concentration of unreacted RAFT proves this not to be the case. Increased radical exit in the case of the BA polymerization leads to less growing particles. The lack of many growing particles leads to a higher concentration of free surfactant and thus the likelihood of there being micelles in the aqueous phase is high. Z-mers within the aqueous phase can enter micelles and form secondary particles. The rate of entry into the micelles is much higher than that of entry into monomer droplets due to the larger surface area of the micelles. Less droplet nucleation implies a higher RAFT agent concentration. This is further investigated in Section 5.1.4.

Pectora roborant cultus recti

The four butyl acrylate polymerizations all show more unreacted RAFT agent than their styrene counterparts. Due to the increased concentration of monomer in the aqueous phase for the BA polymerizations as well as the increased propagation of butyl acrylate, the formation of z-mers is far faster. Even though the solubility of BA is higher, which implies a longer z-mer length, the speed of the z-mer production implies that particle nucleation will occur at an increased rate.

3. Multiple nucleation mechanisms.

Conventional miniemulsion polymerizations show narrow particle size distributions, which indicate simultaneous particle formation and growth of all the particles within the latex. It has been shown that homogeneous nucleation and micellar nucleation lead to broader particle size distributions. The particle size data presented for the eight RAFT-mediated polymerizations in Sections 5.1.3.1 and 5.1.3.2 showed a wide range of size distributions. From the presence of unreacted RAFT in the latexes of many of the miniemulsions, it is clear that droplet nucleation

is inefficient. The GPC chromatograms for many of the miniemulsions show clear signs of conventionally polymerized polymer. This polymer will form in particles nucleated through a secondary process. This fact, along with extended droplet nucleation times, will lead to broad particle size distributions. The varying degrees of droplet and secondary particle formation will depend on the radical movement between the aqueous and oil phases.

The narrowest particle size distributions are seen for the ionically stabilized DIBTC mediated styrene (B1) and butyl acrylate (B2) polymerizations. The latexes for both of these polymerizations show extensive uncontrolled polymerization, suggesting that two nucleation mechanisms are at play. The narrow PSD can be linked to the fact that most of the particles will still be formed by one dominant mechanism (most probably micellar nucleation) due to limited polymerization taking place within the particles derived from nucleated droplets. The propagation within these secondary particles will proceed far faster than the controlled polymerization taking place in the droplet-derived particles. The small initial micelle size will lead to smaller final particles sizes compared to droplet-derived particles. The polymerizations for which little uncontrolled polymer was detected, namely the CVADTB mediated styrene polymerizations (A1 and A3), also showed narrow PSDs, which are also linked to the fact that one primary nucleation mechanism (droplet nucleation) is at play. Wider PSDs are observed for polymerizations in which multiple nucleation mechanisms are operating, for example the non-ionically stabilized DIBTC mediated styrene (B3) and butyl acrylate (B4) polymerizations. The one exception to this trend is that of the non-ionically stabilized CVADTB mediated butyl acrylate polymerization (A4) in which no uncontrolled polymer was observed but it had the widest PSD. This can be linked to longer particle nucleation periods or *zero-one* kinetics. If the particles within the latex of A4 follow *zero-one* kinetics, low $\bar{n}$ values could lead to broad PSDs.[3]

4. Dormant RAFT end-capped chains.

RAFT end-capped oligomers were observed for all except the non-ionically stabilized butyl acrylate miniemulsion (B4). It is proposed that these chains form immediately after z-mers nucleate droplets. After the initialization step between the z-mer and the RAFT agent, the radical leaving group is released which can exit from the newly formed particle, leaving a dormant RAFT end-capped z-mer within the particle. The particle was most likely starved of monomer, via Ostwald ripening, and failed to grow. The increasing surface area of the growing

particles will lead to competition between these and the dormant particles for z-mers in the aqueous phase. Less z-mer entry into the dormant particles (which could have led to their reactivation) will result. The reduced radical exit coupled to the increased nucleation rate explains why these chains are not observed for B4.

It has been seen that for miniemulsions mediated by the RAFT agents CVADTB and DIBTC, by changing the stabilizing surfactant and particle size, a large difference in overall behaviour is observed. This is linked to the altered behaviours of radical species within the miniemulsion. The main question posed in this section is: does the surfactant influence the concentration of conventionally polymerized polymer and, if so, what does that imply about the origin of the radicals forming this polymer? The uncontrolled polymer must form secondary particles devoid of any RAFT agents. Radicals that can possibly initiate this polymerization must be present in the aqueous phase and could either be initiator fragments or other radicals that desorb from the particles. The partition of the initiator fragments between the oil and aqueous phase should be the same for all the ionically stabilized miniemulsions. The partition could theoretically be different for all the non-ionically stabilized miniemulsions.[1] If this is indeed the case and it is assumed that the uncontrolled polymer originates from initiator fragments in the aqueous phase then, for the SDS stabilized miniemulsions, more uncontrolled polymer should be observed. This is true for all but the CVADTB mediated styrene miniemulsions. The main conclusion that can be made here is that the structure of the RAFT agent and surfactant will influence the radical "environment" of the miniemulsion. This in turn alters the nucleation mechanisms that will operate.

The main "source" of the secondary polymer has yet to be determined. For polymerizations where substantial exit leads to altered nucleation mechanisms, high concentrations of secondary polymer are observed. By keeping the surfactant type and RAFT agent constant and then changing the monomer droplet surface area, a more detailed understanding of the mechanistic pathways can be built.

5.1.4. INFLUENCE OF THE SURFACTANT CONCENTRATION

The concentration of the surfactant in the system will determine the final number of particles that form and total monomer droplet surface area. The mathematical expression below is derived from the Smith-Ewart model:[3]

$$N_c(t=\infty) = 0.70\left(\frac{k_d[I]}{K}\right)^{2/5}(a_S[S])^{3/5} \tag{5.1}$$

where [*S*] is the surfactant concentration, a_S is the surface area of one surfactant molecule, *K* is the coefficient of transfer to monomer or CTA and N_c is the number of particles. Laboratory data has however shown that deviations from this model are frequent.[3] The results of investigations into the effect that the surfactant concentration has on the rate of polymerization as well as the molecular weight distribution are given and discussed here. Reducing the surface area of the monomer droplets will greatly influence the rate at which radicals enter and exit these droplets. By decreasing the monomer droplet surface area, the rate of radical exit is limited and the extent to which this will influence the uncontrolled polymer formation can be investigated.

The polymerizations investigated in this section are divided into the styrene minemulsions (5.1.4.1) and butyl acrylate miniemulsions (5.1.4.2). The surfactant for all the polymerizations is SDS and the RAFT agent is DIBTC.

5.1.4.1. Styrene miniemulsion polymerizations

The first order rate plots for polymerizations B1 and B6 are given in Figure 5.22. In polymerization B6 the SDS concentration has been halved.

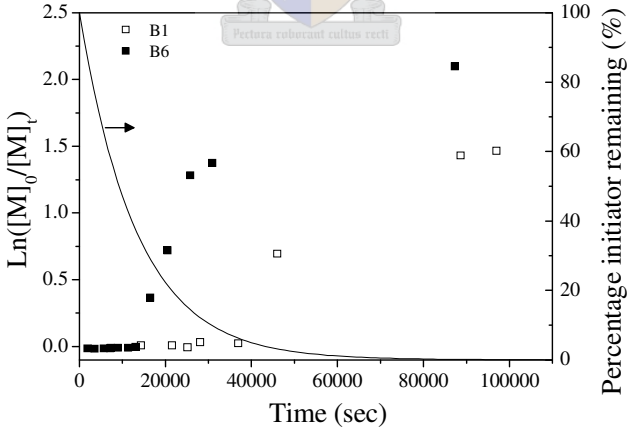

Figure 5.22: First-order rate plots for the polymerizations B6 ([SDS] = 1.75 mmol) and B1 ([SDS] = 3.5 mmol).

The conversion of polymerization B6 after 24 hours is 87%, which is slightly higher than that of B1. Inhibition is taking place during interval I in both B1 and B6, however the period is much shorter for B6. The rates for B1 and B6 appear to be similar after their respective inhibition periods. The duration of interval III appears longer for B6. This was seen for the non-ionically stabilized

miniemulsions discussed in Section 5.1.3.3 and could be linked to the fact that the particles are larger, which might induce *pseudo-bulk* kinetics, for which termination is chain-length dependent.

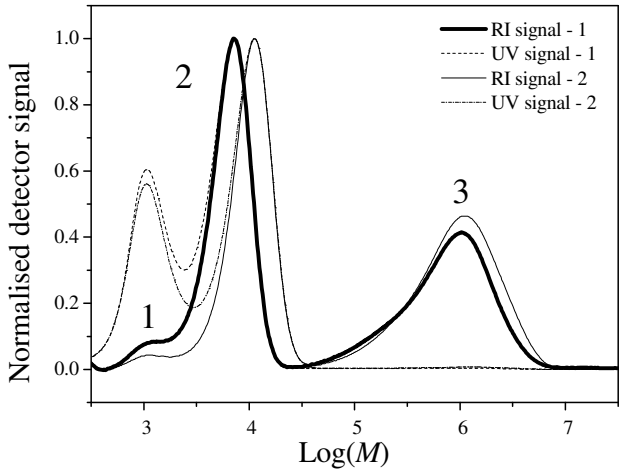

Figure 5.23: GPC chromatogram for the polymerizations B6 ([SDS] = 1.75mmol). Sample conversions are: (1) – 20% and (2) – 42%.

The chromatogram in Figure 5.23 has been normalised to the controlled distributions (labeled 2). The RI-UV overlay verifies that this is a controlled distribution whilst the broader distribution (labeled as 3) lacks the thio carbonyl thio functionality and is uncontrolled. The presence of a much smaller distribution (labeled as 1) of a molecular weight $\approx$1000 g.mol^{-1} that has a strong UV absorption at 320 nm is also apparent. This indicates that there are shorter chains within the miniemulsion that contain the RAFT agent, but they are most likely in a dormant state. The shoulder decreases in size with conversion, indicating that some of these dormant chains are being activated and continue propagating. This phenomenon has been illustrated earlier for the non-ionically stabilized DIBTC mediated styrene miniemulsions (Section 5.1.3.1a).

A GPC chromatogram overlay of a sample from polymerization B6 and the control reaction B1 is given in Figure 5.24 to aid the comparison of the molecular weight distribution evolution for the two reactions.

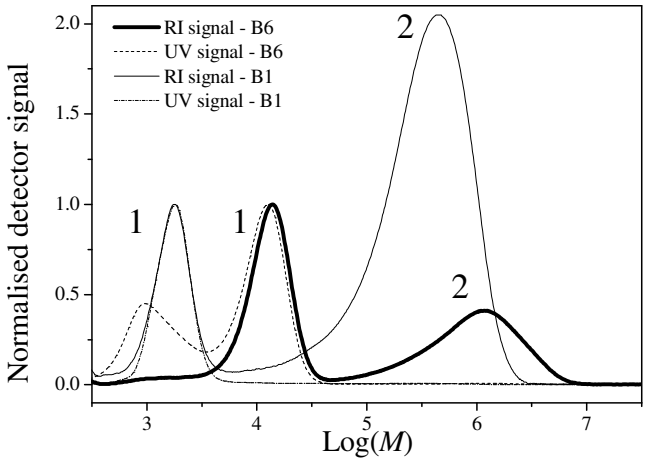

Figure 5.24: Comparison of GPC chromatograms of samples from B1 and B6 with a conversion of 60%.

The chromatogram in Figure 5.24 was normalised so as to illustrate the relative sizes of the second, uncontrolled distributions (labeled as 2) between the two polymerizations. It is evident that there is a larger degree of uncontrolled polymerization for B1 than for B6. The controlled chains (labeled as 1) in B6 are longer than in B1 (also labeled as 1) ($\overline{M}_n$ values are 11 091 and 1 444 g.mol^{-1} for B6 and B1 respectively). The theoretical value is 12 725 g.mol^{-1}. The uncontrolled chains for B6 compared to B1 are also longer in length (the peak molecular weights for B6 and B1 are 1 233 928 and 485 478 g.mol^{-1} respectively)..

Results of DLS particle size analyses for B6 and B1 are given in Tables 5.9 and 5.10.

Table 5.9: DLS results for the polymerizations B1 and B6

Reaction	RAFT	Monomer	Surfactant	Z (average)	Polydispersity
B1	DIBTC	Styrene	SDS	50.7	0.343
B6				92.1	X

The lower the concentration of surfactant within a system, the smaller is the surface area that the surfactant can stabilize.[12] Thus the particle sizes within a system in which the surfactant concentration has been halved will be bigger. This is substantiated by the results observed in Table 5.9. Unfortunately, the *polydispersity* value for B6 could not be determined due to equipment failure.

5.1.4.2. Butyl acrylate miniemulsion polymerization

The first-order rate plot given in Figure 5.25 is for the polymerizations B2 and B5 (B5 is the polymerization in which the SDS concentration was halved).

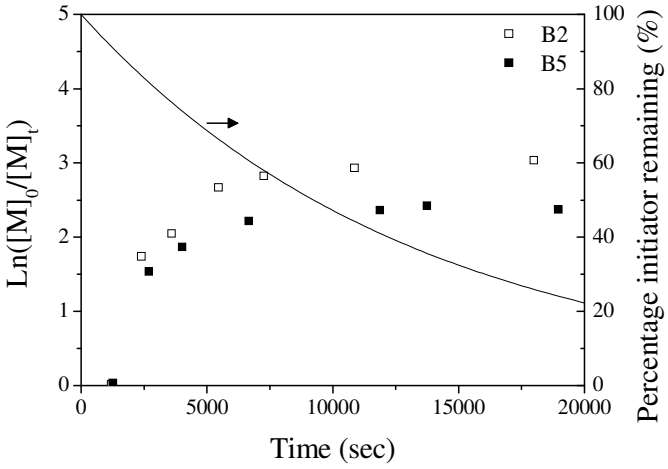

Figure 5.25: First-order rate plots for the polymerizations B5 ([SDS] = 1.75 mmol) and B2 ([SDS] = 3.52 mmol).

The conversion after 24 hours is 91% for B5, which is similar to that of B2 (96%). The nucleation period and the rate of reaction are similar for both polymerizations. One apparent difference is the gradient of the rate of reaction during interval III; it appears steeper for B5.

The GPC chromatograms in Figure 5.26 illustrate A.) the molecular weight and molecular weight distribution evolution for B5 and B.) a comparison of samples for B5 and B2 of 90% conversion:

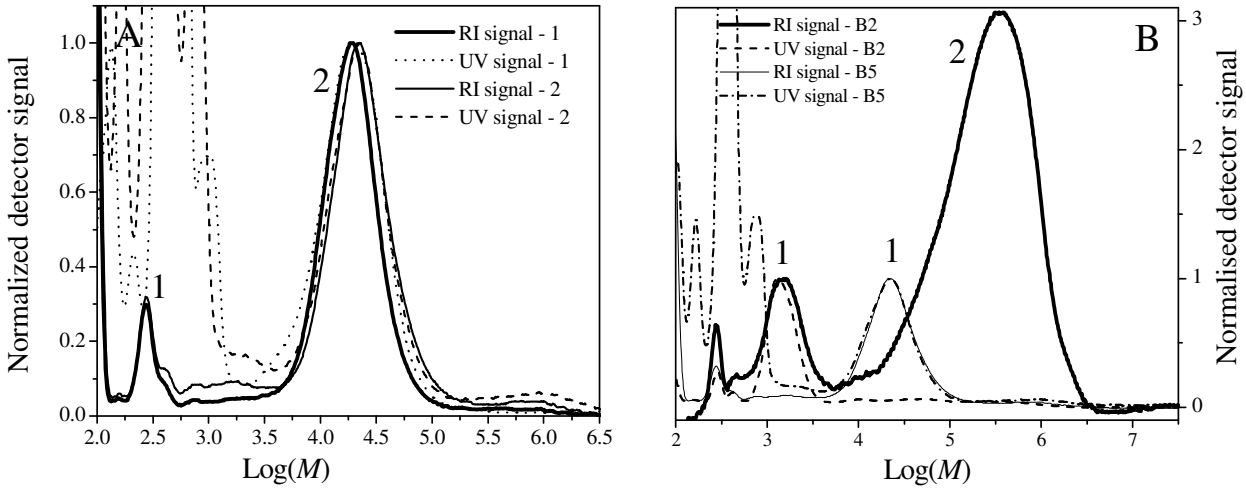

Figure 5.26: GPC chromatograms of A.) polymerization B5 ([SDS] = 1.75 mmol) for which the sample conversions are: (1) - 78% and (2) - 91%; and B.) a comparison of a sample of 90% conversion of both B2 and B5.

The RI-UV overlay in Figure 5.26 (A) shows evidence of two distributions, both of which contain the trithiocarbonate functionality. There is no evidence of the second uncontrolled distribution that was clearly seen for B2 in Figure 5.18 (A) and Figure 5.26 (B). The first distribution (labeled as 1) has a very strong UV absorbance and has an elution volume corresponding to that of the RAFT agent. From the intensity of the UV signal it appears that the concentration of unreacted RAFT agents is fairly significant. The second distribution (labeled as 2) shows a fitting RI-UV overlay, indicating that it is a controlled distribution. The *number average molecular weight* for the controlled distribution is 22 387 $g.mol^{-1}$, which is higher than the predicted value of 16 485 $g.mol^{-1}$. This difference in experimental and theoretical values is probably due to the concentration of unreacted RAFT agent found in the polymerization, as this leads to an altered monomer:RAFT agent ratio. The RAFT agent loss amounts to 30% which corresponds to a 27% loss of particles due to Ostwald ripening.

Chromatogram (B) has been normalised so that the controlled distribution (labeled as 1) of both polymerizations is the same height. For this reason, no comparison between the heights of these two distributions can be made. The concentration of the uncontrolled distribution (labeled as 2) for B2 is much larger than the controlled peak. There is a large difference in molecular weights for the controlled distribution for both B2 and B5. This is due in B2 to the differing concentrations of unreacted RAFT and the loss of monomer to the uncontrolled polymerization.

The large difference in concentrations of uncontrolled and controlled polymer implies a secondary nucleation mechanism. This was investigated by particle size analysis.

Table 5.10: DLS results for the final latexes of polymerizations B5 and B2

Reaction	RAFT	Monomer	Surfactant	Z (average)	Polydisperisty
B2	DIBTC	Butyl acrylate	SDS	48.2	0.268
B5				91.1	X

The results in Table 5.10 are similar to those of B1 and B6 (styrene polymerizations in Section 5.1.4.1). The particles sizes of the final latex of polymerization B2 are smaller, which indicates that radical exit from the particles could occur with an increased likelihood, but also implies that the initiator fragments are more likely to nucleate the initial droplets due to the larger monomer droplet surface area in the case of smaller particles.

5.1.4.3. Surfactant concentration: Summary and conclusions

The altering of the droplet surface area led to substantial changes in the final miniemulsion latex. From first glance at the GPC chromatograms for the two polymerizations in which the surfactant concentration was halved (B5 and B6) it is clear that less uncontrolled polymer formed in the miniemulsion polymerization with larger particle sizes. Another alarming fact is the similarity in rate of reaction during interval I for the four polymerizations (B1, B2, B5 and B6). Assuming zero-one kinetics, the rate of reaction is dependent on the monomer droplet surface area,[16] thus it can be assumed that the rate of reaction will be higher for B2 (smaller particles). The first-order kinetic plot for the styrene miniemulsions (B1 and B6, the latter having half the surfactant concentration) shows only a slight difference in the inhibition period that appears during interval I. After this period, the gradients at which the reaction rates increase are similar. The same can be said for B2 and B5 (the latter having half the surfactant concentration). If oil-phase initiation does not occur, similar rates of polymerization imply similar radical entry coefficients, which are unexpected, due to the large difference in particle surface area. Oil-phase initiation can take place in the larger particles and would lead to R_p values similar to those of the smaller particles in which aqueous-phase initiation occurs. Determining the extent to which either initiating mechanism operates in the miniemulsion is complex.

The rate of radical exit is dependent on the particle size and is given as Equation 2.18. This equation states that as the particle size increases, the probability of radical exit decreases. This fact will greatly influence the rate retardation and nucleation mechanisms operating in the miniemulsion. Similar to the manner in which the summary of Section 5.1.3.3 was presented, four main points will be addressed here with respect to the four polymerizations investigated in this section. One additional point will be addressed: the origin of uncontrolled polymer.

1. Rate retardation and inhibition.

The rate of reaction during interval I will differ for the two monomer polymerizations due to differing $C_{sat}{}^{W}$ and k_p values. The rate will also vary according to the loss of radicals from polymerization loci. For the styrene polymerizations (B1 and B6) a slight inhibition period can be observed. This is caused by radical loss from the system through termination. Initiating radicals can undergo termination before forming surface-active z-mers or radicals (such as the radical leaving group) that can exit from the particles and terminate in the aqueous phase,

yielding dormant chains. If initiating radicals undergo aqueous phase termination, the absence of inhibition for the butyl acrylate polymerizations can be explained by the increased rate of z-mer formation and nucleation. The inhibition periods for the styrene miniemulsions with larger (B6) and smaller (B1) droplet sizes are significantly different. By increasing the monomer droplet surface area, the probability that surface-active z-mers undergo droplet nucleation is increased. However, from the rate plots for B1 and B6 it is apparent that the inhibition period is longer for the system in which the surface area is larger. This implies that loss of initiating radicals or z-mers from the aqueous phase is not the sole cause of the inhibition, but rather increased aqueous-phase termination.

If radicals exit the particles after nucleation (i.e. before propagating to a length in which exit is not viable), they can undergo termination within the aqueous phase. The probability of radical exit is increased for miniemulsions in which the particle sizes are small. This can explain the difference in inhibition periods for B6 and B1. The smaller particles of B1 could lead to increased radical exit and thus increased termination of these radicals in the aqueous phase. The butyl acrylate polymerizations will logically undergo the same extent of radical loss from the particles but there is no inhibition period observed for these polymerizations. The higher solubility of BA monomer coupled to the increased rate of propagation will lead to the propagation of exited radicals. Z-mers will still form and enter particles, leading to a slightly shorter inhibition period. This process is far slower for styrene, leading to a decreased nucleation rate, and thus a more distinct inhibition period. The very slight difference in retardation in reaction rate between the butyl acrylate polymerizations with smaller (B2) and larger (B5) particles implies that even though more radicals are undergoing exit for B2, the increased probability of propagation (lower termination due to lower aqueous phase radical concentration) in the aqueous phase will counteract this rate-retarding effect.

The rate of polymerization in conventional miniemulsion polymerizations is directly proportional to the monomer droplet surface area.[13] This implies that the gradient at which the reaction rate increases will be much higher for B1 and B2 than B5 and B6. Although an accurate determination of the behaviour of the reaction rate during interval I cannot be established with the available data, it does appear that the gradients of the change in reaction rate are similar for the two styrene polymerizations, and slightly lower (as expected) than that of the two butyl acrylate polymerizations (which are also similar). The kinetic descriptions given above with respect to the polymerizations investigated indicate that, regardless of the surface area of the

monomer droplets, the z-mer entry rate into the droplets is not the overall rate-determining factor. The crudeness of gravimetric analysis makes it impossible to accurately determine whether or not there is an inhibition period for the BA miniemulsions.

2. Unreacted RAFT agents.

Unreacted RAFT agents are observed in different concentrations for all four polymerizations described in Section 5.1.4. The lowest concentration of RAFT agents was observed for the polymerizations with smaller particle size (B1 and B2). This is understandable, considering that the larger the monomer droplet surface area is the greater the probability of particle nucleation. The inhibition period observed arises from the increased termination due to the increased radical flux into the aqueous phase. Theoretically, the radical exit and entry (flux) will reach a steady state at a point that all the droplets are nucleated (all particles will contain RAFT end-capped z-mers). This is however not the case, since there is clear evidence of unnucleated droplets.

The ratio of the concentration of unreacted monomer in the BA and styrene polymerizations for both smaller and larger particle sizes indicates that there is less unreacted RAFT agent in the final latexes of the styrene polymerizations. The radical exit into the aqueous phase should be similar for the styrene and BA miniemulsions. Radical exit will not occur for only a small number of particles and these particles will continue to undergo propagation. Monomer diffusion (Ostwald ripening) into these particles will happen at a faster rate for BA than for styrene (water solubility). These particles will grow and act as radical sinks. These larger particles will compete with the unnucleated particles for radicals and especially surfactant-like z-mers from the aqueous phase, resulting in less particle nucleation. The process is slower for styrene polymerization due to a lower monomer solubility and thus slower Ostwald ripening. Less competition for aqueous phase radicals will result, leading to increased droplet nucleation. Increased nucleation also leads to increased adsorption of free surfactant from the aqueous phase. Less soluble surfactant or possibly even micelles will be present in the styrene polymerization, leading to a lower probability of secondary particle growth. From the GPC data for the BA systems in Section 5.1.4, it is clear that this is indeed the case.

The size of the particles from which the radical exit will take place will greatly influence the concentration of exited radicals. Larger particles result in fewer exits and thus a lower concentration in the aqueous phase. This results in less nucleation and higher concentrations of

unreacted RAFT agent. For the styrene miniemulsion polymerization of the larger particle size (B6), the increased nucleation rate (albeit slower than that of the smaller particles) due to the slower Ostwald ripening leads to increased droplet nucleation and less unreacted RAFT agents. Efficient consumption of the RAFT agents leads to similar predicted and experimental $\overline{M}_n$ values. Butyl acrylate polymerization B5 (larger droplets) shows more unnucleated droplets, which is linked to the faster Ostwald ripening of the growing particles in the miniemulsion. Poor RAFT agent consumption for B5 leads to an experimental value of $\overline{M}_n$ which is higher than predicted.

3. **Multiple nucleation mechanisms.**

Without sufficient data concerning particle size distributions of the various latexes, few conclusions can be drawn with respect to the nucleation mechanisms in operation in the system. It can however be speculated that the PSDs for the smaller particles (B1 and B2) will be narrower since, primarily, conventionally polymerized polymer is observed in the GPC chromatograms. This polymer will form in newly created particles through a secondary mechanism. Mixed latexes, like that for the styrene polymerization B6 (with larger particle sizes), will have a broader distribution of particle sizes.

4. **Origin of uncontrolled polymer.**

The hypothesis stated at the beginning of this section (5.1.4), that the origin of the conventionally polymerized polymer remains unknown, has now been disproved. It was seen that by decreasing the monomer droplet surface area the concentration of uncontrolled polymer decreased. The nucleation efficiency for both the larger and smaller particles was seen to be similar, and it was proposed that substantial exit of radicals from the nucleated particles was taking place, leaving dormant short RAFT end-capped chains. Propagation of these radicals takes place within the aqueous phase forming oligomers that are surface active and can enter the unnucleated droplets, nucleated particles and/or micelles. By decreasing the surfactant concentration, the aqueous phase surfactant concentration after homogenization can theoretically be lower than previously. This implies that fewer micelles will be present, and thus a decreased probability of secondary particle formation will prevail. For the smaller particles, by decreasing the aqueous phase monomer concentration (styrene monomer) the concentration of uncontrolled polymer and the concentration of unreacted RAFT agent also decreases, implying

more nucleation. For the larger particles, by increasing the solubility of the monomer, nucleation is limited and the concentration of unreacted RAFT is higher.

The behaviour of the radicals that exit the nucleated particles influence the radical concentration within the aqueous phase, which in turn will influence the nucleation of droplets as well as the probability of secondary particle formation. Larger particles can lead to increased oil-phase initiation. Increased consumption of the RAFT agent should follow from this, but as has been seen in Section 5.1.4 this is not the case. The role of the initiating fragments as an origin for the uncontrolled polymer can be investigated by the use of a water-soluble initiator, as will be done in Section 5.2.

5.2. INITIATORS

The behaviour of water-soluble and insoluble initiators has been debated for some time.[13] The main point of debate is the main locus of initiation for each. It is obvious that for the water-soluble initiators, the initiating radical molecules reside only in the aqueous phase. For the oil-soluble initiators, the initiating molecules partition between the aqueous phase and the oil phase.[14] If there is an increase in the concentration of conventionally polymerized polymer, then it might be assumed that initiating radicals within the aqueous phase are a possible source of uncontrolled polymer.

To investigate the effect of utilizing an initiator of differing solubility, standard miniemulsions were prepared and polymerized using different initiators: potassium persulphate (KPS), which is water-soluble; and 2,2'-azobis(isobutyronitrile) (AIBN), which is hardly water-soluble.

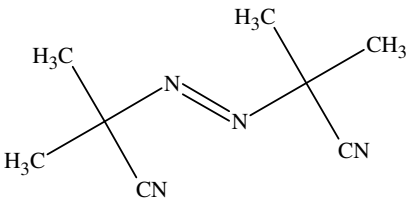

Figure 5.27: Structure of AIBN.

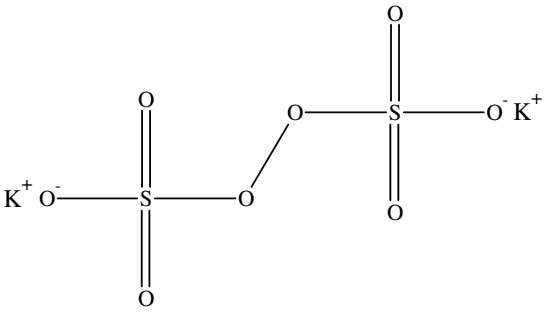

Figure 5.28: Structure of KPS.

Styrene miniemulsion polymerizations were first discussed in Section 5.2.1, followed by the butyl acrylate miniemulsion polymerizations (Section 5.2.2). SDS was the surfactant for all four polymerizations and the RAFT agent was DIBTC.

5.2.1. STYRENE MINIEMULSIONS

The first-order rate plots for B1 (AIBN) and B8 (KPS) are given in Figure 5.29:

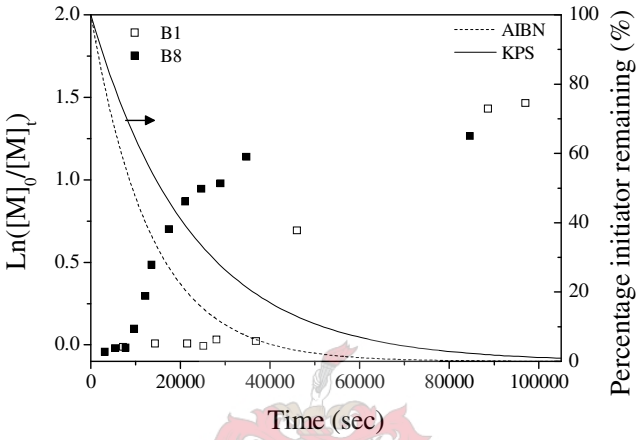

Figure 5.29: First-order rate plots for polymerizations B8 (KPS) and B1 (AIBN).

The conversion of B8 after 24 hours is 70%, which is approximately the same as that of B1. This agrees with published data for similar emulsion polymerizations.[10] The inhibition period observed for B1 is much shorter than for B8. The rates of polymerization appear similar for B1 and B8 after their respective inhibition periods. The GPC chromatogram of B8 is given in Figure 5.30 (A) and a single sample RI-UV overlay is given in Figure 5.30 (B):

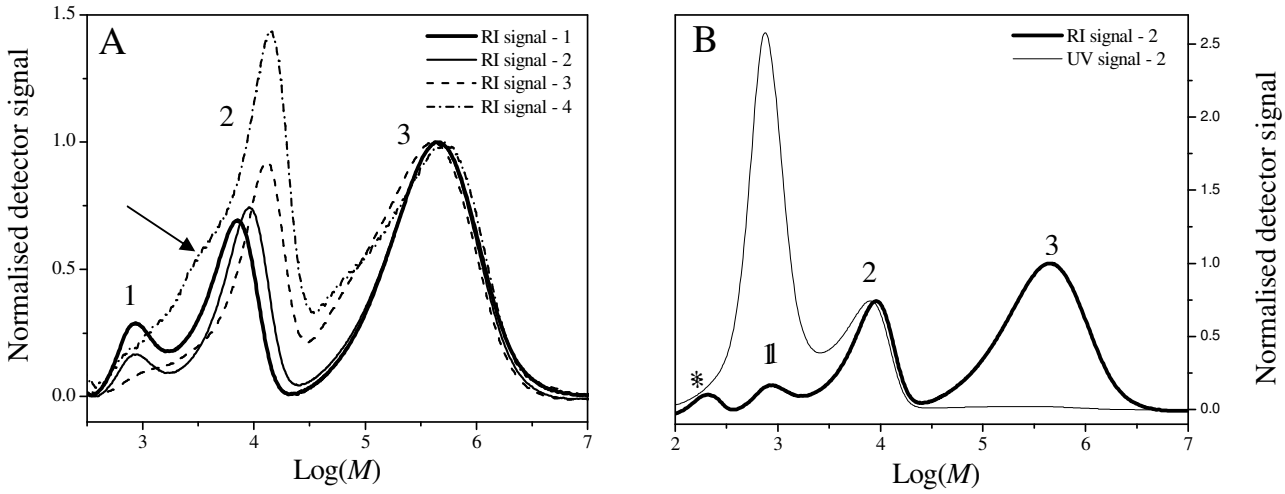

Figure 5.30: GPC chromatogram for polymerization A.) B8 (KPS) and B.) sample 2 of B8 showing the RI-UV overlay. Sample conversions for B8 are: (1) – 25%, (2) – 38%, (3) – 67% and (4) – 71%.

The normalisation in Figure 5.30 (A) is done relative to the third broader distribution (labeled as 3) so as to illustrate the increasing second, narrower peak. The ratio of the intensities of the third (uncontrolled) to the second (controlled) polymer distributions illustrates that the uncontrolled polymer is formed early in the reaction (already at 25% conversion). GPC chromatograms show that this is not the case for AIBN initiated polymerization. The uncontrolled distribution detected in these latexes increases in intensity for the duration of the polymerization. From the RI-UV overlay given in Figure 5.30 (B) it is possible to identify the third broader peak as the uncontrolled distribution due to that fact that it shows no UV absorbance. The first (labeled as 1) and second (labeled as 2) distributions contain the RAFT functionality. The first peak is similar to that seen in Figure 5.10 and is most likely due to short RAFT end-capped chains. The distribution increases in molecular weight with conversion, which implies that the chains are still living. These growing shorter chains are possibly the reason for the lower molecular weight shoulders (marked with an arrow) on the controlled distribution (2) at higher conversions. The *peak molecular weight*, 14 841 g.mol^{-1}, for the controlled distribution is much higher than the *number average molecular weight*, 4 958 g.mol^{-1}, and this is due to a broad distribution largely because of the existence of short chains. The M_p is very close to the predicted value of 13 318 g.mol^{-1}. A small distribution (marked with an asterisk) could be due to unreacted RAFT agent. An overlay of a sample from both B1 and B8 is given in Figure 5.31 to compare the difference in molecular weight distributions for each polymerization. The conversion of the two samples is B8 – 67% and B1 – 95%.

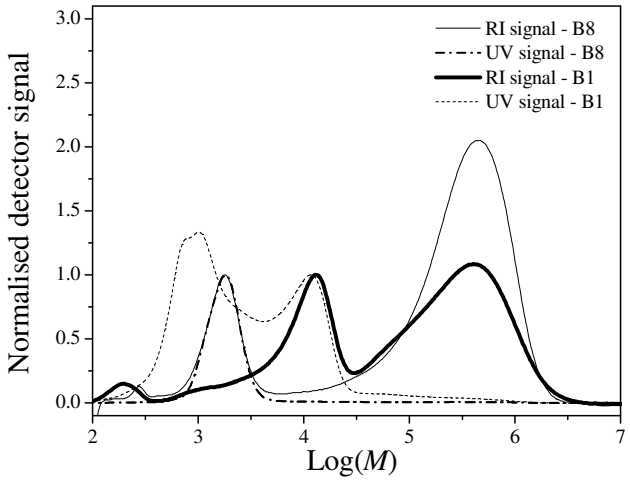

Figure 5.31: GPC chromatograms of samples of both B1 (AIBN) and B8 (KPS), showing the RI-UV overlay.

The normalisation was done in such a manner that the controlled distribution (labeled as 2) for each sample is of the same height. From this overlay it is possible to see that polymerization B1 has a much larger uncontrolled distribution (labeled as 3).

The particle size analysis results for B1 and B8 are in given Tables 5.11 and 5.12:

Table 5.11: DLS results for polymerizations B1 and B8

Reaction	RAFT	Monomer	Initiator	Z (average)	Polydispersity
B1	DIBTC	Styrene	AIBN	50.7	0.343
B8			KPS	73.1	X

The *polydispersity* value for B8 could unfortunately not be determined due to technical problems encountered. The slight difference in *Z(average)* values for the two polymerizations can be linked to the varying nucleation mechanisms.

5.2.2. BUTYL ACRYLATE MINIEMULSIONS

The first-order kinetic plots for the B2 (AIBN) and B7 (KPS) are given in Figure 5.32:

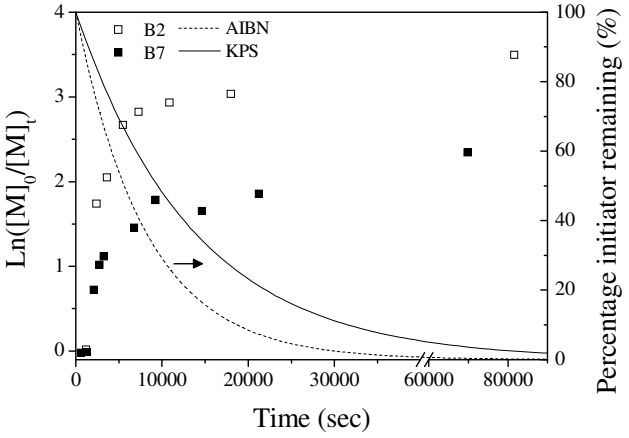

Figure 5.32: First-order rate plots for the polymerizations B7 and B2.

The conversion after 24 hours for B7 is 90%, which is similar to that obtained for the same polymerization using AIBN (B2). Unlike reactions B1 and B8, the nucleation time for both reactions seems to be similar. Accurate descriptions of interval I for the BA polymerizations cannot be constructed due to the high propagation rate. The onset of interval III appears similar for both polymerizations. There is a slight difference in the gradient of reaction rate during interval III. The rate decrease of reaction B7 appears faster than B2. The GPC chromatogram of this polymerization is given in Figure 5.33:

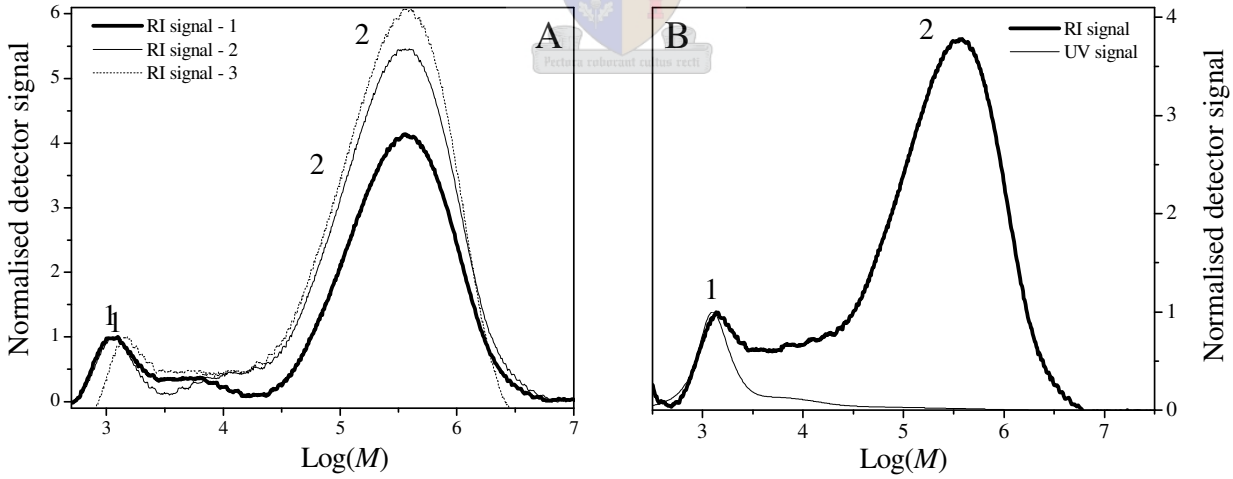

Figure 5.33: GPC chromatogram for A.) B7 and B.) a single sample - 1 from B7 illustrating the RI-UV overlay. Sample conversions for B7 are: (1) – 51%, (2) – 63% and (3) – 90%.

Chromatogram (A) in Figure 5.33 shows that for B7 there is a large, broad distribution (labeled as 2) and from chromatogram B we can also see that it lacks any UV absorbance at 320 nm, and thus

polymerized in an uncontrolled fashion (lacking the thio carbonyl thio functionality). The smaller distribution (labeled as 1) shows a UV absorbance, and polymerized in a controlled fashion. This controlled distribution has a *number average molecular weight* of 1 756 g.mol^{-1}, far below that of the predicted value of 16 915 g.mol^{-1}, as will be expected because of the uncontrolled polymerization.

An overlay of a sample from both B7 and B2 is given in Figure 5.34 to illustrate the difference in molecular weight distribution when using different initiators.

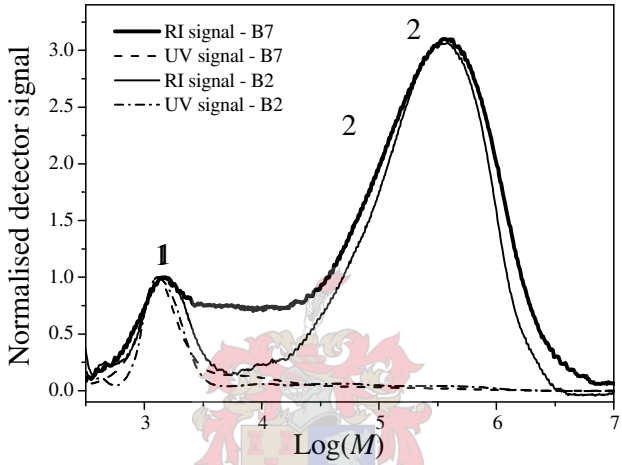

Figure 5.34: GPC chromatograms of samples with a conversion of 62% for both B7 (KPS) and B2 (AIBN).

The RI-UV overlay in Figure 5.34 shows one distribution (labeled as 2), which lacks the thio carbonyl thio functionality. This distribution is thus uncontrolled. The neat RI-UV overlay for the distribution labeled as 1 implies it is a controlled distribution. These are most likely dormant, short RAFT end-capped chains. The experimental *number average molecular* weights for both B7 and B2 for the controlled distribution are much lower than the predicted values. The fact that the two samples overlay so well indicates that the mechanistic behaviour of each polymerization is very similar. The uncontrolled distribution appears to have a higher PDI for the KPS initiated polymerization. This could be linked to the slower initiator decomposition.

The particle size analysis data is given in Table 5.12:

Table 5.12: DLS results for the final latexes of polymerizations B7 and B2

Reaction	RAFT	Monomer	Surfactant	Z (average)	Polydispersity
B2	DIBTC	Butyl acrylate	SDS	48.2	0.268
B7				61.3	X

The *polydispersity* value for B7 could unfortunately not be determined due to technical problems encountered.

5.2.3. WATER SOLUBLE VERSUS WATER INSOLUBLE INITIATORS: SUMMARY AND CONCLUSIONS

The solubility of the initiator used in a miniemulsion polymerization will affect the main site of *z*-mer formation. The water-soluble initiator will fragment within the aqueous phase, which implies that the radical concentration within the aqueous phase should be higher, which could lead to a higher termination rate within the aqueous phase. Furthermore, it implies that the rate of *z*-mer formation will be higher. From the data collected it is seen that the reaction rate profiles for the AIBN and KPS initiated polymerizations are similar, which implies that the propagating radical concentration are similar. The reaction rates during interval I are similar, indicating minimal differences in rate retardation. The main points of interest are that the inhibition period is reduced compared to that of styrene polymerizations and that the relative concentration of uncontrolled polymer increased with the more water soluble acrylate monomer.

1. Inhibition.

The styrene polymerizations B1 (AIBN initiated) and B8 (KPS initiated) have inhibition periods in interval I of vastly different lengths. The longer inhibition period for B1 implies that more termination of radicals is taking place within the aqueous phase, which is highly unexpected due to the lower radical concentration in the aqueous phase for the oil-soluble initiator. One plausible explanation is that the higher solubility of the KPS initiator fragments leads to the subsequently longer z-mer. A greater *z* value for KPS implies slower propagation of z-mers and increased probability of z-mer termination. By slowing down the nucleation rate, the consumption of the RAFT agents is reduced. The exit of radical leaving groups will also be slower, leading to less termination within the aqueous phase and a shorter inhibition period. Capek *et al*. found that KPS and AIBN initiated polymerizations showed similar nucleation

rates.[15] This discredits the suggested explanation. Another possible scenario also explains the differing trends in the uncontrolled polymer distribution intensity seen in the GPC chromatograms for B1 (AIBN) and B8 (KPS); the higher concentration of initiating radicals within the aqueous phase associated with KPS could lead to an increased probability of secondary particle formation. If this is indeed the case, then at a low conversion the concentration of uncontrolled polymer should be relatively high. The nucleation of droplets will occur simultaneously, resulting in an influx of radical leaving groups into the aqueous phase. This will result in an increase in termination within the aqueous phase, and the rate of the formation of secondary particles will decrease. The particles for which radical exit did not occur and/or those particles, which were reactivated, will continue growing, leading to an increase in controlled polymer concentration. Thus, at a point in the polymerization, the concentration of uncontrolled polymer will reach a constant value, whilst the concentration of controlled polymer will continue to increase. The growing particles compete with secondary particles for monomer and free surfactant in the aqueous phase, leading to reduced polymerizations within the secondary particles (due to their smaller surface area). This hypothesis is substantiated by the GPC data collected.

Minimal inhibition is observed for the butyl acrylate polymerizations and the difference between the AIBN and KPS initiated miniemulsions is small. Assuming that the radical behaviour is similar to that described above, the similarity in inhibition period length as well as the ratio of the concentrations of uncontrolled to controlled polymer with an increase in conversion can be explained with regard to the competing nucleation mechanisms. The competition for aqueous phase radicals between unnucleated droplets and nucleated particles was described in Section 5.1.3.3, with regard to the Ostwald ripening of nucleated particles. This phenomenon was speculated to be the cause of the increased secondary particle or micellar nucleation for BA miniemulsions. This could explain the continuous secondary particle formation for the KPS initiated miniemulsions (B7) as well as the absence of the inhibition period for the AIBN initiated miniemulsions (B2). Increased micellar nucleation early in the polymerization overrides the inhibitory effect of increased termination due to the higher aqueous phase radical concentration, thus explaining the absence of an inhibition period for B2. It also explains the continual formation of uncontrolled polymer for B7.

2. Controlled versus uncontrolled polymer concentrations.

The butyl acrylate polymerizations B2 and B7 show little difference in their GPC chromatograms. The reaction rate profiles are similar, which implies that the kinetics and mechanisms operating in the miniemulsions are similar. The only distinct difference between B2 and B7 is the low molecular weight tail of uncontrolled polymer for the B7. The higher concentration of radicals in the aqueous phase for the water-soluble initiator will lead to increased termination of the propagating oligomers that will go on to form secondary particles. This will result in a wide distribution of chain lengths and will account for the low molecular tail in the GPC chromatogram.

The ratios of controlled and uncontrolled polymer concentrations for the styrene polymerizations (AIBN – B1 and KPS – B8) are vastly different. A plausible explanation for the differing ratios of controlled to uncontrolled polymer concentrations was addressed in Section 5.2.3, point 1, with reference to the inhibition periods. The onset of the formation of secondary particles was held as the reason. In conclusion, for the styrene miniemulsions, the differing multiple nucleation mechanisms could explain the differing polymer molecular weight ratios.

Secondary particles can be formed via micellar nucleation (increased probability over homogeneous-coagulative particle nucleation due to a large micellar surface area and thus z-mer entry rate). The probability of micellar nucleation will depend on the monomer droplet surface area compared to the micelle surface area. Ideally oil-phase initiation will not lead to micellar nucleation (geminate recombination). The concentration of initiating radical fragments will influence the nucleation (of micelles and droplets). For KPS, the high aqueous-phase initiating radical concentration will lead to an increased probability of micellar nucleation. As can clearly be seen from the GPC chromatogram overlays for the styrene miniemulsions B1 (AIBN) and B8 (KPS) as well as the butyl acrylate miniemulsions B2 (AIBN) and B7 (KPS), switching to a water-soluble initiator does not result in more uncontrolled polymer. This implies that it is not only the initiating radicals in the aqueous phase that will influence the secondary particle formation. In Sections 5.1.3 and 5.1.4 discussions on the varying nucleation mechanisms of differing RAFT-mediated polymerizations revealed that the behaviour of the radical leaving group of the RAFT agent could influence the formation of secondary particles. The exit of the radical leaving group was identified as a crucial factor in the formation of the secondary particles. By increasing the aqueous phase radical concentration via the use of a water-soluble initiator, termination of these exited radicals is

increased. The slower propagation of z-mers in the aqueous phase for styrene miniemulsions leads to increased termination, which results in short terminated chains (which are observed) as well as less uncontrolled polymer, whilst the faster z-mer formation for the butyl acrylate polymerizations leads to less pronounced termination and increased uncontrolled polymer formation.

The water-soluble initiator KPS appears to operate in two ways in the RAFT-mediated miniemulsions investigated in this section. The high aqueous phase radical concentration leads to increased nucleation during the first few percentage conversion. Once droplet nucleation occurs and the influx of radical leaving groups into the aqueous phase increases, the initiating radicals act now as a "radical scavenger" terminating radicals in the aqueous phase, that could lead to subsequent secondary particle nucleation.

5.3. REFERENCES

(1) Asua, J. M. *Journal of Polymer Science: Part A: Polymer Chemistry* **2004**, 42, 1025

(2) Velikov, K. P.; Velev, O. D.; Marinova, K. G.; Constantinides, G. N. *Journal of the Chemical Society, Faraday Trans*. **1997**, 93, 2069

(3) Gilbert, R. G. *Emulsion Polymerization: A Mechanistic Approach*; Academic Press: San Diego, **1995**

(4) Wu, X. Q.; Schork, F. *J. Journal of Applied Polymer Science* **2000**, 81, 1691

(5) Wu, J.; Xu, Y.; Dabros, T.; Hamza, H. *Colloids and Surfaces A: Physiochemical and Engineering Aspects* **2004**, 232, 226 - 237

(6) Boissier, C.; Lofroth, J.; Nyde, M. *Langmuir* **2001**, 17, 8368

(7) McLeary, J. B. PhD thesis; University of Stellenbosch, **2004**

(8) Piirma, I.; Chang, M. *Journal of Polymer Science Polymer Chemistry Edition* **1982**, 20, 482

(9) Bessels, R. In PhD thesis; Technische Universiteit Eindhoven; **2004**

(10) Tonge, M. P.; McLeary, J. B.; Vosloo, J. J.; Sanderson, R. D. *Macromolecular Symposia* **2003**, 193, 289

(11) McLeary, J. B.; Mckenzie, J. M.; Tonge, M. P.; Sanderson, R. D.; Klumperman, B. *Chemical Communications* **2004**, 1950

(12) Landfester, K.; Bechthold, N.; Tiarks, F.; Antonietti, M. *Macromolecules* **1999**, 32, 5222

(13) Blythe, P. J.; Klein, A.; Phillips, J. A.; Sudol, E. D.; El-Aasser, M. S. *Journal of Polymer Science Part A: Polymer Chemistry* **1999**, 37, 4449

(14) Capek, I.; Barton, J.; Karpatyova, A. *Makromolecular Chemie* **1987**, 188, 703

(15) Capek, I. *Advanced Colloid Interface Science* **2001**, 91, 295

Pectora roborant cultus recti

Chapter 6. : *The influence that the R- and Z- group structure of the RAFT agent has on RAFT-mediated miniemulsion polymerizations*

ABSTRACT

The RAFT process introduces new complexities into the reaction mechanisms at play in the miniemulsion. The effect that each variable group of the RAFT agent structure has on the final miniemulsion behaviour is investigated in this section.

The structure of a specific RAFT agent utilized in RAFT-mediated miniemulsion polymerizations influences the behaviour of the polymerization.[1] The cause of this influence lies in the mechanism of the RAFT process as well as the processes in a miniemulsion. In this chapter, the relationship between the RAFT agent's structure and the rate of polymerization, as well as the evolution of the molecular weight and molecular weight distribution with conversion, are investigated. The chapter is divided into two sections. The first will examine the influence of various stabilizing Z- groups. The second will examine the influence of various leaving R- groups. All miniemulsion polymerizations follow the formulation and procedure as stated in Section 3.2, except where specified. The polymerization numbering (e.g. A1) and polymerization conditions are given in Table 3.1 As in Chapter 5, the kinetic analysis of reactions and size analysis of the final latexes are supplied for each polymerization. Kinetic analysis is provided by first-order rate plots. Conversions were determined gravimetrically. Polymer characteristics, such as molecular weight and polydispersity, were determined by SEC. Particle size analysis was performed by TEM, CHDF and DLS.

6.1. Z- GROUP DEPENDENCE

The RAFT equilibrium established within the particles of a miniemulsion will influence the radical behaviour in the polymerization, as seen in Section 5.1. The rates of radical exit (k_{EXIT}), reaction with monomer (k_p) and termination (k_t) within the oil-phase depend on the relative concentrations of radical species within the oil-phase. The RAFT equilibrium is established in a thermodynamically favorable way, which is highly dependent on the relative stability of all the radical species within the equilibrium (i.e. the intermediate radical, oligomeric radical and radical leaving group). The structure of the Z- group will influence the stability of the intermediate radical and the various rate coefficients linked to the equilibrium (*trans, trans1, trans2, detrans, detrans1* and *detrans2*).[2] The extent to which this stabilization will affect the net radical behaviour of the miniemulsion polymerizations is investigated within this section. The two Z- groups that will be investigated are the phenyl and dodecyl-thiol groups, illustrated in Figure 6.1:

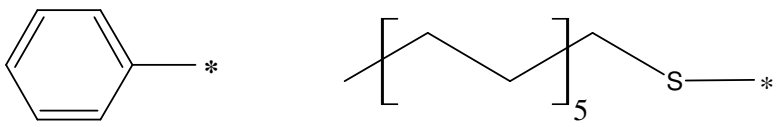

A B

Figure 6.1: The stabilizing groups investigated: (A) phenyl and (B) dodecyl thiol

The asterisks in Figure 6.1 indicate the linkage point of the Z- group to the thio carbon of the RAFT agent. The RAFT agents compared were 1-phenylethyl dithiobenzoate (PEDTB) and S-dodecyl-S'-phenylethyl trithiocarbonate (DPTC). The structures of these two RAFT agents were shown in Figure 3.1. The leaving group of these two RAFT agents is the 1-phenyl ethyl group.

These polymerizations will be compared to the control polymerizations given in Section 4.2. The default surfactant used for the four polymerizations is SDS. The PEDTB and DPTC mediated butyl acrylate miniemulsions will be described in Section 6.1.1 and followed by the PEDTB and DPTC mediated styrene miniemulsions in Section 6.1.2.

6.1.1. BUTYL ACRYLATE MINIEMULSION POLYMERIZATIONS

The first-order rate plots for polymerizations C1 (PEDTB) and D1 (DPTC) are given in Figure 6.2.

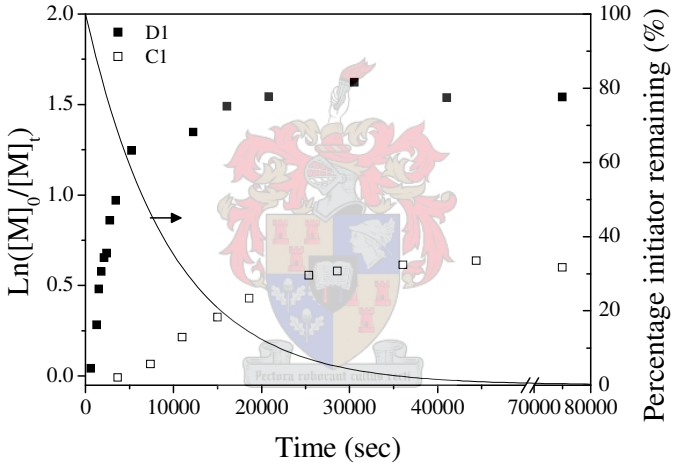

Figure 6.2: First-order rate plots for polymerizations D1 and C1.

For D1 the conversion after 24 hours is 80% and for C1 it is 50%. From these plots it appears that the nucleation times for the polymerizations are very different. The nucleation time for C1 is just under 3 hours whilst D1 has a nucleation time similar to that of the control polymerization E1 (see Figure 4.1). The rate of reaction is much faster for D1 than C1 during interval I. Interval III can clearly be identified for both polymerizations, but there is no evidence of interval IV for either reaction. The GPC chromatograms of these polymerizations are given in Figure 6.3:

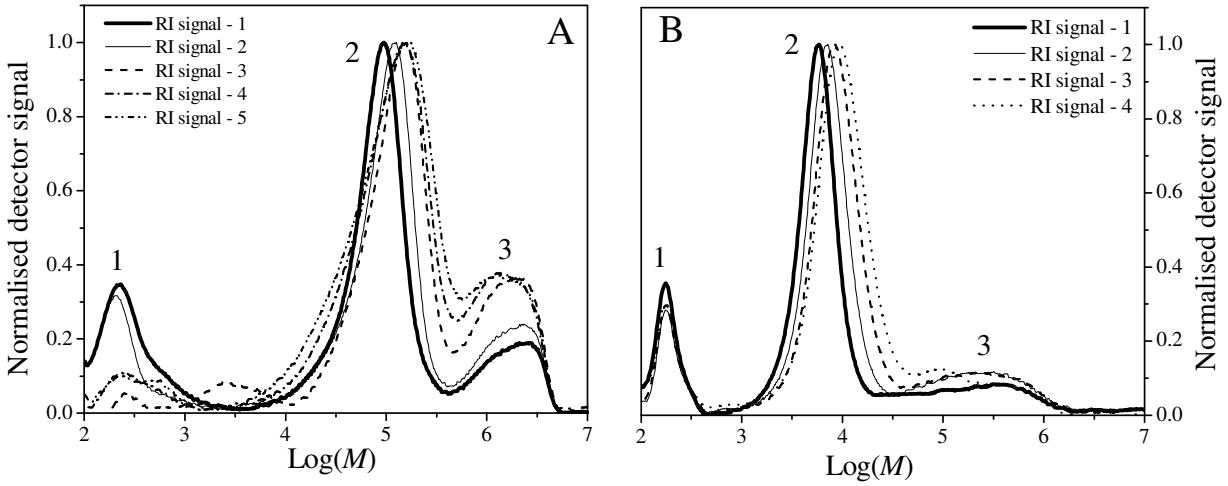

Figure 6.3: GPC chromatograms for polymerizations A.) D1 and B.) C1. Sample conversions for A are: (1) – 24%, (2) – 38%, (3) – 49%, (4) – 62% and (5) – 75% and B are: (1) – 27%, (2) – 34%, (3) – 42% and (4) – 51%.

A single sample from both chromatogram A and B in Figure 6.3 are given in Figure 6.4 below to illustrate the RI-UV overlay.

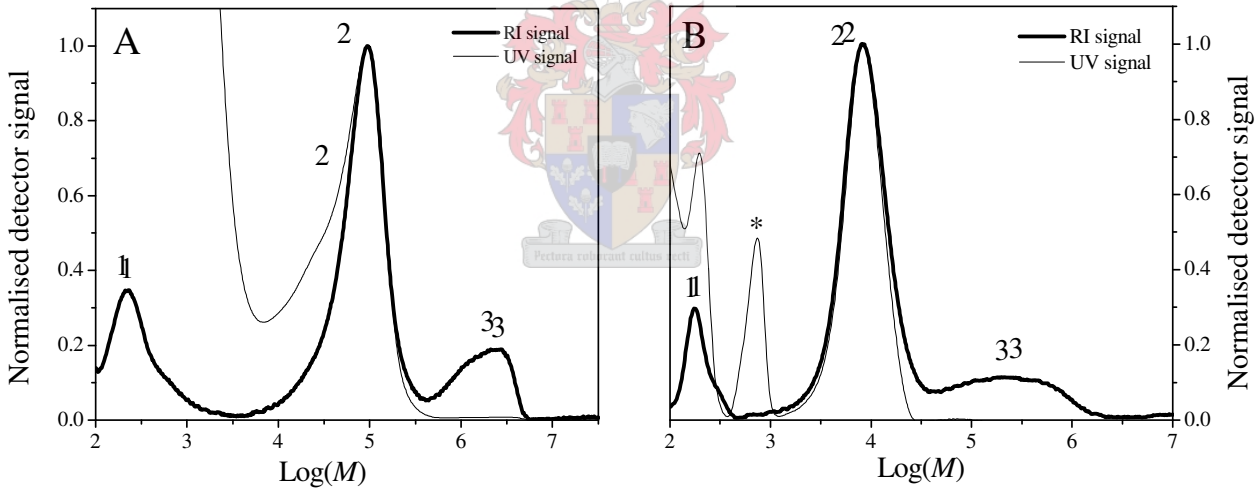

Figure 6.4: GPC chromatograms showing the RI-UV overlay for a single sample given in Figure 6.3: (A) sample 1 of D1 and (B) sample 3 of C1.

The GPC chromatograms for both polymerizations indicate that there is evidence of uncontrolled polymerization taking place. In D1, from Figure 6.4 (A), three distinct distributions can be seen. The first distribution (labeled as 1) decreases in intensity with conversion. The *peak molecular weight* for the second distribution (labeled as 2) is increasing with conversion whilst that of the third distribution (labeled as 3) is constant. From the RI-UV overlay given in Figure 6.4 (A), it is possible to positively identify the three distributions. Distribution 2 shows a UV absorbance at 320 nm and

thus contains the thio carbonyl thio functionality. The third distribution (3) lacks this absorbance and thus lacks this functionality. The strong UV absorbance at a *peak molecular weight* of approximately 300 g.mol^{-1} corresponds to the RAFT agent (labeled as 1). It is evident that much of the RAFT agent remains unreacted in the system. The fact that the intensity of this distribution decreases with conversion could mean that the droplets in which these RAFT agents reside are being nucleated at a later stage of the reaction. Considering that nucleation periods typically run until about 20-40 % conversion[3] it is possible that nucleation is still taking place within the latex of D1 and that the RAFT agent is being consumed. The *number average molecular weight* of the controlled distribution (2) is much higher than the targeted weight (43 886 g.mol^{-1}, versus the 14 242 g.mol^{-1} targeted weight) for sample 5. This means that 32% of the RAFT agent is lost and that 32% of the particles are not renucleated and lose monomer to Ostwald ripening.

In Figure 6.3 (B), the chromatogram for C1 shows three distributions similar to those of D1, except for the fact that the third distribution (labeled as 3) has a lower intensity compared to the second distribution (labeled as 2). Distribution 2 increases in molecular weight with conversion. The RI-UV overlay in Figure 6.4 (B) indicates that distribution 3 is uncontrolled whilst distribution 2 is controlled. The first distribution (labeled as 1) corresponds to the RAFT agent. There is less absorbance seen for the unreacted RAFT in C1 than D1 and this indicates that there is less unreacted RAFT in C1. This can be stated due to the quantitative nature of UV as a detector (concentration of UV absorbent species is directly proportional to the absorbance according to the Beer-Lambert equation). In Figure 6.4 (B) there is evidence of short chains (less than 1 000 g.mol^{-1}) containing the thio carbonyl thio functionality (labeled with an asterisk). The *number average molecular weight* ($\overline{M}_n$) for the controlled distribution in the sample 4 for C1 is 10 727 g.mol^{-1} whilst the targeted weight is 9 796 g.mol^{-1}.

The results of the particle size analyses for polymerizations D1 and C1 are given in Tables 6.1 and 6.2:

Table 6.1: DLS results for polymerizations for the final latexes of D1 and C1

Reaction	RAFT	Monomer	Surfactant	Z (average)	Polydispersity
D1	DPTC	Butyl acrylate	SDS	243.1	0.089
C1	PEDTB		SDS	72	X

Compared to those of the control reaction (E1), these values show large differences for the RAFT agent DPTC. C1 shows similar *Z (average)* values to E1.

Table 6.2: CHDF results for the final latexes of polymerizations D1 and C1

Reaction	Z (Number average)			Z (Weight average)		
	Mean	Max	Standard deviation	Mean	Max	Standard deviation
D1	97.5	33.3	79.6	266.7	304.9	92.6
C1	64.8	64.7	19.4	81.2	74.4	20

C1 shows a narrow distribution of sizes according to both the *number average* and *weight average* data. The particle sizes are similar to those of E1, and the distributions almost as narrow. The duration of interval I is slightly longer for C1 than E1. The results for D1 are very different from those for E1. A comparison between the *number average* and *weight average particle size* values as well as the *standard deviation* values reveals that there is a wide variety of particle sizes. According to the *number average mean* and *max* values, there are a number of smaller particles with sizes around 35 nm. From the *weight average mean* and *max* values there is evidence of larger particles. The larger *standard deviation* value (relative to that of E1) indicates a much less efficient droplet nucleation process, or possible coagulation of particles. The *weight overlaid* CHDF chromatogram for D1 indicates that there are particles up to 470 nm in diameter. The range of particle sizes is indicative of secondary nucleation mechanisms like micellar nucleation and/or homogeneous-coagulative nucleation. The CHDF chromatograms for C1 are given in Figure 6.5:

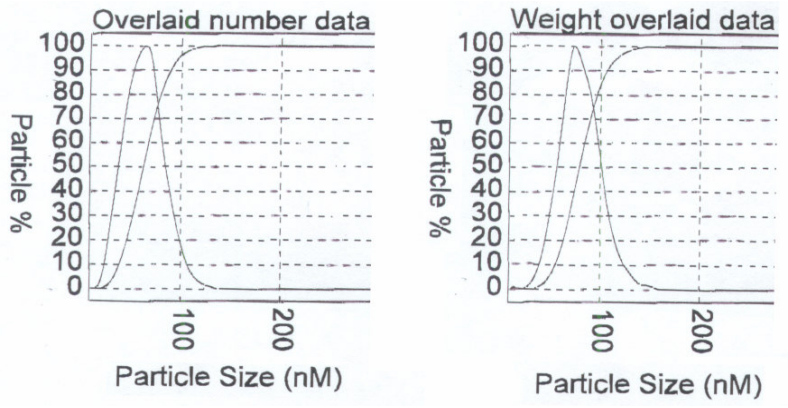

Figure 6.5: CHDF chromatogram of the final latex of polymerization C1.

The *standard* deviation values for C1 are only slightly higher than those for E1, which indicates that there are similar mechanisms operating in both polymerizations. The range of particle sizes is shown in the TEM micrograph for the final latex of C1 in Figure 6.6:

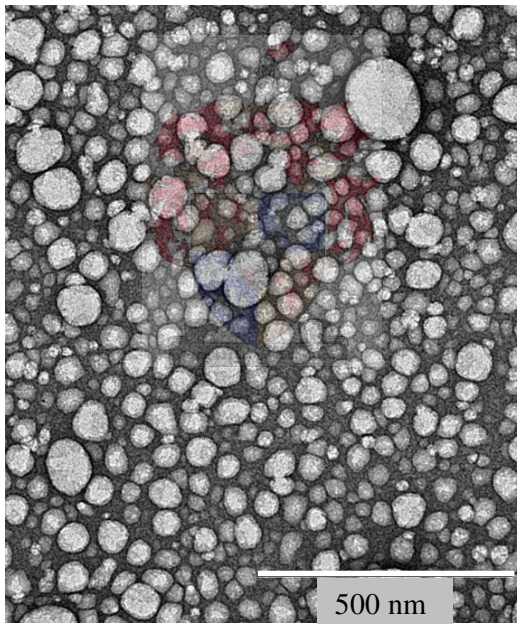

Figure 6.6: TEM micrograph of the final latex of polymerization C1.

The TEM micrograph confirms the wide size variation and supports the reasons presented (see the large particle in the top right corner).

6.1.2. STYRENE MINIEMULSION POLYMERISATION

The first-order rate plots for polymerization D2 (DPTC) and C2 (PEDTB) are given in Figure 6.7.

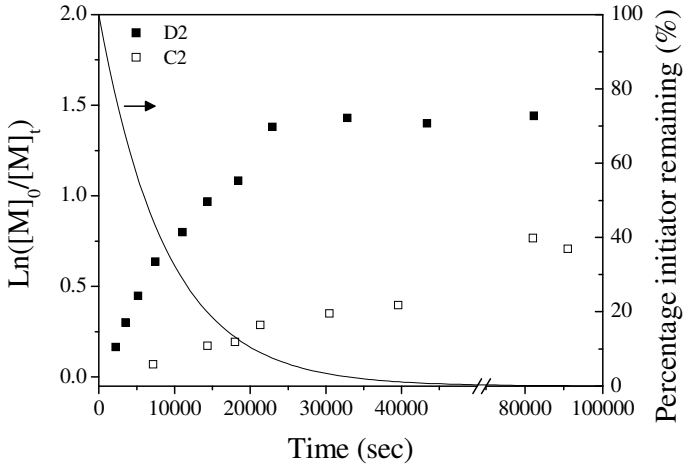

Figure 6.7: First-order rate plots for polymerizations D2 and C2

The final conversions for D2 and C2 are 76% and 50% respectively. The duration of interval I is shorter for polymerization D2 than for C2, but is still longer than that of control polymerization E3 i.e. there is rate retardation (as expected for RAFT polymerizations) during interval I for both D1 and C1. The rate of polymerization during interval I is faster for D2. Interval III appears to be longer for C2 and the rate at which the reaction rate decreases is much higher for D2.

The GPC chromatograms of these polymerizations are given in Figure 6.8:

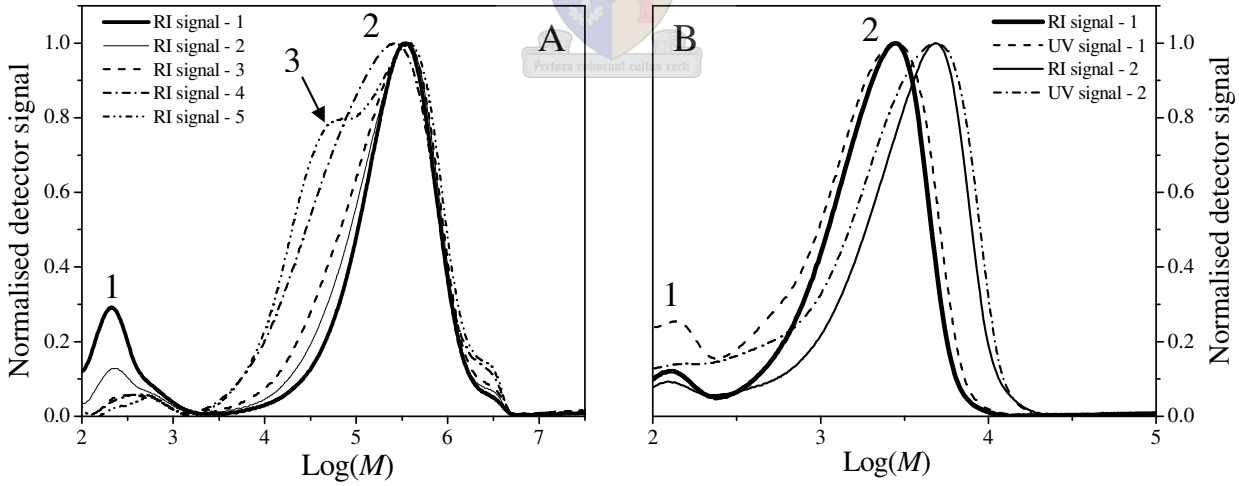

Figure 6.8: GPC chromatograms of polymerizations A.) D2 and B.) C2. Sample conversions for A are: (1) – 25%, (2) – 36%, (3) – 47%, (4) – 61% and (5) – 74% and B are: (1) – 24% and (2) – 32%.

The GPC chromatogram of a single sample (5) from D2 is given in Figure 6.9 to illustrate the RI-UV overlay:

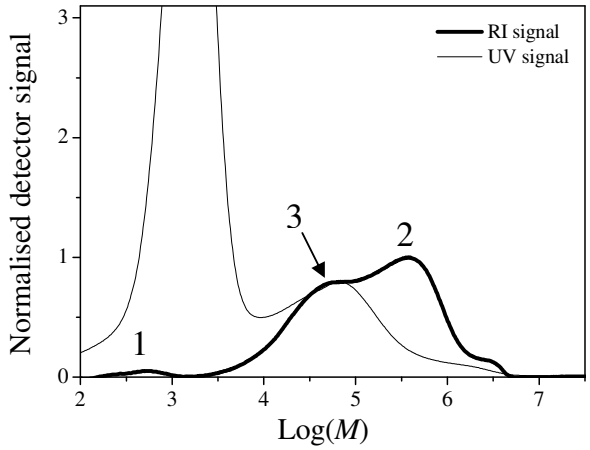

Figure 6.9: GPC chromatogram of polymerization D2, sample 5.

From Figure 6.8 (A) we can explain the molecular weight distribution evolution for D2. At approximately 300 g.mol^{-1} we see a small distribution (labeled as 1) that decreases in size with an increase in conversion. This distribution corresponds to the RAFT agent that remains unreacted in the system. The fact that distribution 1 decreases with conversion indicates that RAFT agents are consumed continuously during the reaction and not instantaneously at the beginning of the reaction. The same was seen for D1 and C1. The second distribution (labeled as 2) changes shape with conversion, and for sample 5 it seems that a third distribution (labeled as 3), appears next to distribution 2. The RI-UV overlay given in Figure 6.9 reveals that the shoulder (3) on the left hand side of the second distribution (2) has a strong UV absorbance at 320 nm. This implies that distribution 3 is a controlled distribution. There is a very strong absorption on the RAFT agent peak (labeled as 1), similar to D1. Distribution 2 shows little UV absorbance, which indicates that it lacks the thio carbonyl thio functionality and originates from an uncontrolled polymerization. Due to the overlap between the uncontrolled distribution (2) and the controlled distribution (3), an accurate value for the *number average molecular weight* ($\overline{M}_n$) cannot be calculated. The *peak molecular weight* (M_p) for distribution 3 of sample 5, given in Figure 6.9, is 67 832 g.mol^{-1}, which is much larger than the predicted $\overline{M}_n$ of 12 783 g.mol^{-1}. The slight bulge on the higher molecular weight shoulder of D2 is probably due to the exclusion limit inherent to the column (different, very high molecular weight polymers that will elute simultaneously).

The chromatogram for C2 in Figure 6.8 (B) is much simpler. The RI-UV overlay indicates the existence of a small RAFT agent peak (labeled as 1), which decreases in intensity with conversion. This distribution is much narrower than the distributions seen for D2, D1 and C1. This might indicate that in this system most of the RAFT agents are consumed early in the reaction. The second

distribution (labeled as 2) shows a perfect UV overlay, which indicates the presence of the thio carbonyl thio functionality. This polymer was polymerized in a controlled manner. There is no evidence of any uncontrolled distribution. The *number average molecular weight* of the controlled polymer in sample 2 for C2 is 4 829 $g.mol^{-1}$, which is similar to the predicted value of 5 742 $g.mol^{-1}$.

The particle analyses results are given below in Tables 6.3 and 6.4:

Table 6.3: DLS results of the final latexes of polymerizations D2 and C2

Reaction	RAFT	Monomer	Surfactant	Z (average)	Polydispersity
D2	DPTC	Styrene	SDS	119.8	0.007
C2	PEDTB		SDS	107.9	0.044

From the DLS measurements in Table 6.3 it is clear that the average particle size is similar for both latexes. The *polydispersity* is slightly larger for C2. When comparing these results to those obtained for the BA miniemulsion polymerizations D1 and C1, a distinct difference is observed. The final latex of D1 shows a much larger average particle size than that of D2. The *polydispersity* is also much lower. The average particle size of C2 is however larger.

Table 6.4: CHDF results of the final latexes of polymerizations D2 and C2

Reaction	Z (Number average)			Z (Weight average)		
	Mean	Max	Standard deviation	Mean	Max	Standard deviation
D2	65.9	40.4	27.9	99.5	100.2	29
C2	50.5	37.5	21	86.4	48.3	39.4

A comparison between the D2 *number average* and *weight average* values indicates that the majority of particles are small, but the presence of larger particles increases the *weight average particle size*. The low *weight average standard deviation* value implies a narrow distribution, which corresponds well to the *polydispersity* value obtained via DLS. There is evidence of smaller particles, but the fact that the weight average standard deviation value is larger for C2 indicates that there are a few particles that are much larger than any particles seen in D2. These conclusions are made with reference to the CHDF chromatograms shown in Figure 6.10:

A

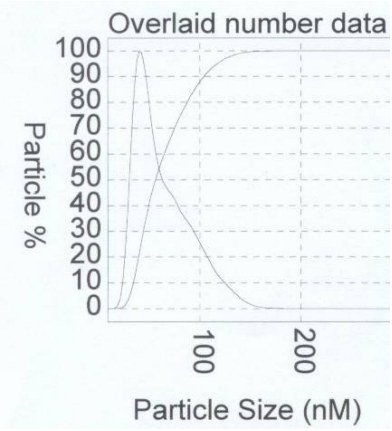

B

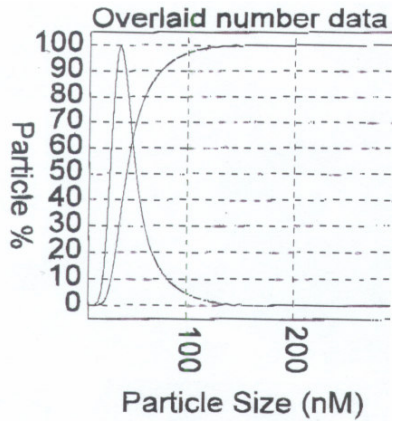

Figure 6.10: CHDF chromatograms of the final latexes of polymerizations A.) D2 and B.) C2.

6.1.3. THE ROLE OF THE Z- GROUP: CONCLUSIONS

The comparisons constructed in this section were structured so as to compare miniemulsions incorporating two different RAFT agents. The agents have similar leaving groups, but unique stabilizing groups. The structure of the RAFT agent will influence variables such as the rate coefficients of the RAFT equilibrium, which in turn will influence the concentration of the various radical species within the particles. When comparing the RAFT-mediated polymerizations to the control polymerizations, it is clear that there are deviations from the conventional miniemulsion models. The three distinct differences, which were detected and described in Section 6.1.1 and 6.1.2, will be addressed here. These points are:

1. Rate retardation.

The rate of polymerization during interval I was found to be high in the control polymerization. The duration of interval I was also found to be less than 30 min. For all four polymerizations: D1, D2, C1 and C2, rate retardation was observed during interval I. This could be caused by the loss of radical species from the locus of polymerization, insufficient droplet nucleation or the trapping of the propagating radical species in a dormant state. These two processes could also be working simultaneously in any of the miniemulsions. The dithiobenzoates are known to retard bulk polymerizations due to the fact that the intermediate radical stability is very high.[4] This implies that for the PEDTB mediated polymerizations, the concentration of radical oligomers within the particles will be lower (the concentration of the intermediate species being very high) than in the case of the DPTC mediated polymerizations. This fact will affect the rate of polymerization in two ways. An increased intermediate radical concentration and fast-

addition/slow-fragmentation equilibrium implies that the propagating chain grows slowly. The retarding nature of RAFT agents with different stabilizing groups has been reported previously by Barner-Kowollik *et al*.[5] They reported that there is a distinct difference in the retarding nature of the RAFT agents cumyl dithiobenzoate (CBD) and cumylphenyl dithioacetate (CPDTA) which have stabilizing groups that stabilize the intermediate radicals to varying degrees. The more unstable intermediate radical for the trithiocarbonate RAFT agent (DPTC) will lead to faster addition and fragmentation and thus less rate retardation. One benefit from the slower equilibrium is that the active propagating time of the radical oligomer (and, in the initial fragmentation step, the radical leaving group) is short, reducing the probability of exit from the particle. Radical species that do escape from the RAFT equilibrium into the aqueous phase will alter the aqueous phase radical concentration, leading to increased z-mer formation as well as termination. A steady-state between z-mer formation and termination will eventually be established in the aqueous phase, dependent on the decay of the initiator in the system.

If radical exit does increase termination within the aqueous phase, it can be expected that the DPTC mediated polymerizations will show the most rate retardation. This was however not the case. When comparing the rate retardation for the DPTC and PEDTB mediated polymerizations, it must be remembered that the higher propagation rate for polymerizations mediated with DPTC will compete with the rate retardation due to increased radical exit. Since the leaving groups of both RAFT agents are similar, the difference in concentration of radicals entering the aqueous phase will only be due to the fragmentation rate (k_{trans2}) of the RAFT agent. Differing radical fluxes into the aqueous phase will lead to different nucleation rates. This is addressed in point 2.

2. Unreacted RAFT agents within latex.

The presence of unreacted RAFT agents was identified in all four polymerizations described in this section. For the two DPTC mediated polymerizations, the concentration of the unreacted RAFT agent decreased with time, whilst for the PEDTB mediated butyl acrylate polymerization the concentration appeared to remain constant. The PEDTB mediated styrene miniemulsion had the least unreacted RAFT agent and the concentration decreased with conversion. The unreacted RAFT resides in unnucleated droplets. This implies that the nucleation efficiency during interval I was low for all the polymerizations, but that the unnucleated particles can be nucleated later in the polymerization. RAFT agents that are consumed long after the onset of

polymerization will result in the molecular weight broadening of the controlled distribution. The PEDTB mediated styrene polymerization showed the largest PDI and this could be linked to a long nucleation time. The PEDTB mediated butyl acrylate miniemulsion (C1) had an unreacted RAFT agent concentration that was far higher than the respective DPTC mediated polymerization (D1). This implies that in C1 there are unreacted RAFT agents, but similar predicted and experimental $\overline{M}_n$ values for the controlled distributions requires that the RAFT agent:monomer ratio remains constant during the polymerization. The two DPTC mediated polymerizations both showed evidence of unreacted RAFT agent as well as differences between the predicted and experimental $\overline{M}_n$ values. The largest difference was observed for the butyl acrylate polymerization (D1). It should however be remembered that an accurate $\overline{M}_n$ value for the styrene polymerization (D2) could not be accurately determined. The concentration of the unreacted RAFT agent decreased with conversion. This slow consumption indicated that droplet nucleation was still taking place after 40% conversion. This can explain the large difference in predicted and experimental $\overline{M}_n$ values.

3. Multiple nucleation mechanisms.

The CHDF chromatograms for the control polymerizations (E1 and E3) revealed that there was a very narrow spread of particle sizes. This is common to miniemulsion polymerizations in which one nucleation mechanism prevails. The GPC chromatograms for the four RAFT-mediated polymerizations described in this section indicated that there was probably more than one nucleation mechanism operating or that the nucleation efficiency was poor and that particles were continuously being nucleated during the polymerizations. The DPTC mediated polymerizations (D1 and D2) showed the widest spread of particle sizes (particle size distribution or PSD). The fact that both these polymerizations showed relatively low rate retardation during interval I suggested that the different particle sizes are probably due to multiple nucleation mechanisms operating rather than long nucleation times. The butyl acrylate polymerization (D1) had the largest PSD of the two DPTC mediated polymerizations, but the styrene polymerization (D2) had the highest concentration of uncontrolled polymer. The uncontrolled polymer formed in D2 appears to have formed early in the polymerization due to a constant uncontrolled distribution intensity. Poor homogenization can lead to the aqueous phase surfactant concentration being above the CMC, which implies that, at the onset of the polymerizations, micelles are probably present in the aqueous phase. Z-mers will either nucleate these micelles or give rise to new ones and cause the uncontrolled polymer. The conventional

FRP taking place in the micelles is very fast and monomer diffusion into the growing particles will cause the micelles to swell. The smaller initial micelle size will lead to a final particle size that is smaller than particles formed via droplet nucleation. Particles formed by droplet nucleation are much larger than particles that start as micelles, even though the swelling rate will be slower due to the reduced rate of polymerization within the particle (RAFT-mediated). For the DPTC mediated butyl acrylate polymerization (D1) the reverse is true. The uncontrolled polymer appeared to be forming continuously during the polymerization. This implies that micellar and droplet nucleation was occurring simultaneously, leading to wider PSDs. For the PEDTB mediated polymerizations (C1 and C2), the PSDs are narrow. For the styrene polymerization (C2), there appeared to be a slightly wider spread in sizes, which might indicate that the nucleation time was longer; this will also explain the larger PDI values for the controlled distribution. Multiple nucleation mechanisms were highly unlikely due to the absence of any uncontrolled polymer. The presence of uncontrolled polymer in the butyl acrylate polymerization (C1) did not appear to increase the PSD as significantly as was seen for the DPTC mediated BA polymerization (D1). This implies that the uncontrolled and controlled particles were nucleated over a similar time period.

The discussion in points 1–3 suggests that radical species behaviour within the particles is critical. The RAFT equilibrium will influence rate retardation due to slower propagation rates and altered radical exit events. The concentration of radical leaving groups that may exit the particles and undergo secondary reactions such as aqueous phase propagation and nucleation of unnucleated droplets is of primary concern. In conclusion: DPTC mediated polymerizations lead to increased radical leaving group concentration, thus increasing the probability of radical leaving group exit ($k_{RgroupEXIT}$). For the DPTC mediated butyl acrylate polymerization (D1), the faster addition-fragmentation equilibrium leads to higher propagation rates in the particles from which radical exit did not take place. These particles will grow, absorbing free surfactant from the aqueous phase as well as drawing monomer out of unnucleated particles. Ostwald ripening will lead to competition for radicals in the aqueous phase between the unnucleated droplets and the growing particles. This leads to the slow consumption of RAFT agents and the higher $\overline{M}_n$ values. The styrene polymerization (D2) has a high concentration of conventionally formed polymer, which implies that micellar nucleation is prevalent. Radical exit will be slightly slower for D2 compared to D1 due to slower nucleation. The rate of propagation within the particles will also be lower due to the lower k_p value of styrene. This implies that the growth of particles from which radical exit has not taken

place will be slower, leading to less extraction of free surfactant from the aqueous phase. Micellar nucleation can thus occur more frequently, leading to higher concentrations of uncontrolled polymer. Droplet nucleation increases as the free surfactant concentration drops to a point where no more micelles are present or can easily be formed, leading to an increase in concentration of controlled polymer as a function of the degree of polymerization. This leads to a decrease in unreacted RAFT agent with conversion. The use of PEDTB will lead to less radical exit events. The PEDTB styrene mediated polymerization (C2) shows little unconsumed RAFT agent, but since the exit and re-entry process is slow (due to a low concentration of radical leaving groups after the initial fragmentation step), the unreacted RAFT agents were slowly consumed, leading to large difference in predicted and experimental $\overline{M}_n$ and large PDI values. For the PEDTB butyl acrylate polymerization (C1) the slow radical flux does not lead to increased droplet nucleation, but rather to uncontrolled polymer. Faster Ostwald ripening (due to a higher monomer solubility) of the growing particles leads to increased competition between the nucleated and unnucleated droplets for z-mers in the aqueous phase. In this way, the radical entry (k_{ENTRY}) into unnucleated droplets decreases, leading to unreacted RAFT agents. The growing micelles (uncontrolled polymer) as well as the particles (controlled polymer) will draw monomer from unnucleated droplets. The slow propagation rate of the particles formed by droplet nucleation leads to less swelling by monomer compared to the growing secondary particles (micellar nucleation). This leads to low monomer concentrations within the particles and low $\overline{M}_n$ values, even though the concentration of unreacted RAFT agent is high.

Pectora roborant cultus recti

6.2. R- GROUP DEPENDENCE

In Section 6.1, the role of the Z- group was investigated. The stabilization that the Z- group affords the intermediate radical species within the particles was found to affect the radical behaviour of the miniemulsion polymerization. The nature of the radical leaving group should therefore also affect the behaviour of the miniemulsion polymerization. This radical R- group can undergo side reactions within the oil phase as well as the aqueous phase. The nature of these side reactions as well as their frequency will depend on the structure of the R- group as well as the concentration of the radical R-group within the particles and aqueous phase. The relationship between the R- group structure and miniemulsion polymerization behaviour will be investigated in this section. Three leaving groups will be compared. These are illustrated in Figure 6.11:

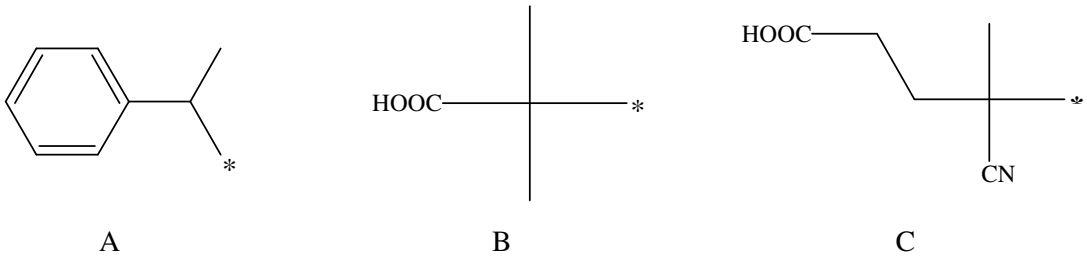

Figure 6.11: The leaving groups investigated in determining the R- group dependence are: (A) 1- Phenyl ethyl, (B) Isobutyric acid and (C) Cyanovaleric acid.

The asterisk indicates the position at which the R- group is connected to the carbon of the thio carbonyl thio group. In Section 6.2.1, a comparison of leaving group A to B will be given. This will be followed by a comparison of leaving group A and C in Section 6.2.2. All these polymerizations will be compared to the control reactions described in Chapter 4. First-order rate plots, GPC chromatograms and particle size analyses values for some polymerizations reported on in previous sections are repeated in the subsequent sections here, to allow for clear comparison.

6.2.1. 1- PHENYLETHYL VERSUS ISOBUTYRIC ACID

In this comparison, the two RAFT agents DPTC and DIBTC will be compared. The stabilizing group for these two agents is the dodecyl thiol group and the respective leaving groups are the 1-phenylethyl and isobutyric acid groups. Section 6.2.1.1 deals with DPTC and DIBTC mediated butyl acrylate polymerizations stabilized with both SDS and Igepal®CO-990. Section 6.2.1.2 deals with DPTC and DIBTC mediated styrene polymerizations stabilized with SDS and Igepal®CO-990.

6.2.1.1. Butyl acrylate miniemulsion polymerizations

Polymerizations D1 (DPTC) and B2 (DIBTC) in which SDS was used as surfactant were compared. The first-order rate plots for D1 and B2 are given in Figure 6.12.

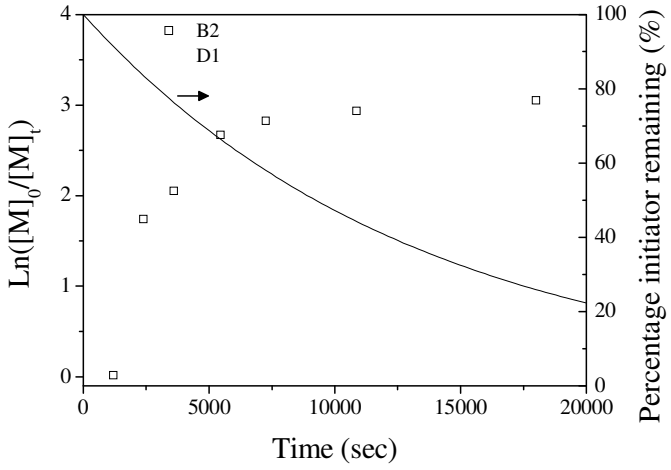

Figure 6.12: First-order rate plots for polymerizations D1 and B2.

The final conversion for D1 is 80%, whilst for B2 it is 90%. Interval I appears slightly longer for B2. The rate of polymerization trend cannot accurately be determined due to insufficient data points, but is does appear that there is an inhibition period for B2. After this period, the R_p increases rapidly. No such inhibition period can clearly be seen for D1, but it appears that the polymerization rate increases more gradually during interval I. The duration of interval III appears similar for both polymerizations, and no interval IV can be positively identified.

A GPC chromatogram overlay of a single sample from D1 and B2 is given in Figure 6.13. The conversion for the samples given is approximately 75%.

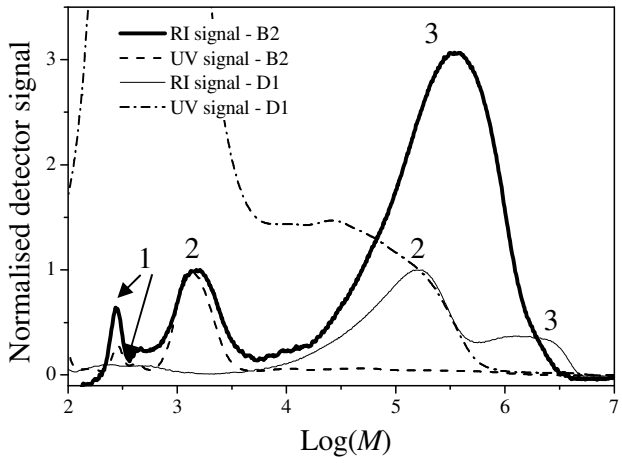

Figure 6.13: GPC chromatogram of samples of 75% conversion for D1 and B2.

Both the chromatograms above have been normalised to the controlled distribution (labeled as 2) of each chromatogram. The distribution labeled as 1 corresponds to unreacted RAFT agents. The lack of UV absorption for the distribution labeled as 3 for both D1 and B3 indicates that this is an uncontrolled distribution. The *number average molecular weight* of the controlled distribution is much higher for D1 than for B2 (43 886 g.mol^{-1} versus 1 883 g.mol^{-1} respectively) even though the conversion in the polymerizations is similar. The predicted $\overline{M}_n$ value for this conversion is 14 242 g.mol^{-1}. From the overlay it is evident that there is vastly more secondary, uncontrolled polymer (3) within the latex for B2 than for D1.

The two corresponding polymerizations in which Igepal®CO-990 is used as surfactant are D3 (DPTC) and B4 (DIBTC). The first-order kinetic plots for these polymerizations are given in Figure 6.14:

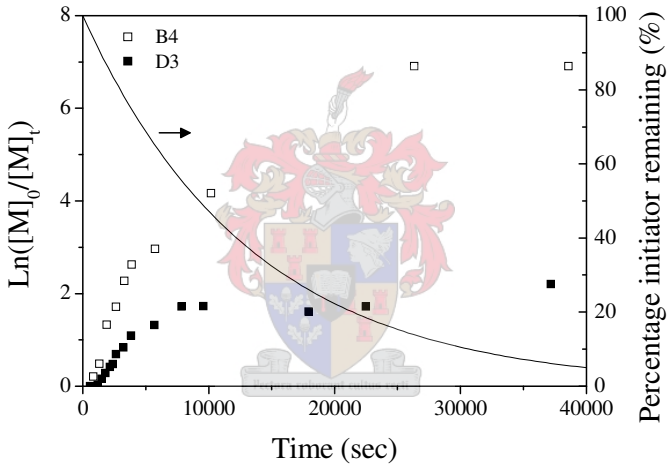

Figure 6.14: First-order rate plot for polymerizations D3 and B4.

The conversion after 24 hours for D3 is 88%, which is lower than that for B4 (100%). Interval I appears longer for D3 than B4 and R_p is lower for D3 during this interval. Interval III can clearly be seen for D3 and B4.

The GPC chromatogram for polymerization D3 is given in Figure 6.15 (A). A single sample (sample 4) is given in Figure 6.15 (B) to show the RI-UV overlay for D3:

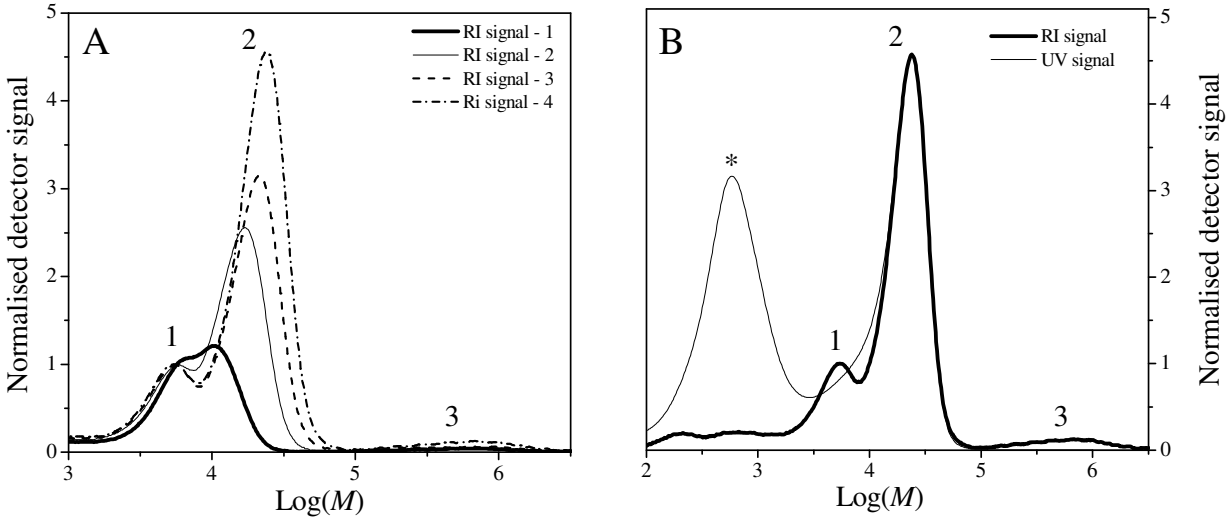

Figure 6.15: GPC chromatograms of A.) D3 and B.) sample 4 of D3 showing the RI-UV overlay. Sample conversions for D3 are: (1) – 24%, (2) – 37%, (3) – 49% and (4) – 56%.

The first distribution (marked with a 1) is the surfactant. The controlled distribution (labeled as 2) shows a clear UV absorbance, and increases in molecular weight with conversion. The *number average molecular weight* for this distribution cannot accurately be determined due to the overlap with the surfactant distribution (1), but the *peak molecular weight* is 23 926 g.mol^{-1} for sample 4. The predicted $\overline{M}_n$ value for this conversion is 11 146 g.mol^{-1}. There is a strong UV absorbance (marked with an asterisk in Figure 6.15 (B) at an elution volume similar to the RAFT agent DPTC). The width of this UV peak implies that there are probably short RAFT end-capped chains as well as unreacted RAFT agent. The RI signal in both chromatograms shows a very faint third distribution (marked with a 3), which does not show any UV absorbance. This implies there is some uncontrolled polymerization taking place. A GPC chromatogram overlay of a sample of a conversion of 75% for both polymerizations B4 and D3 is provided in Figure 6.16.

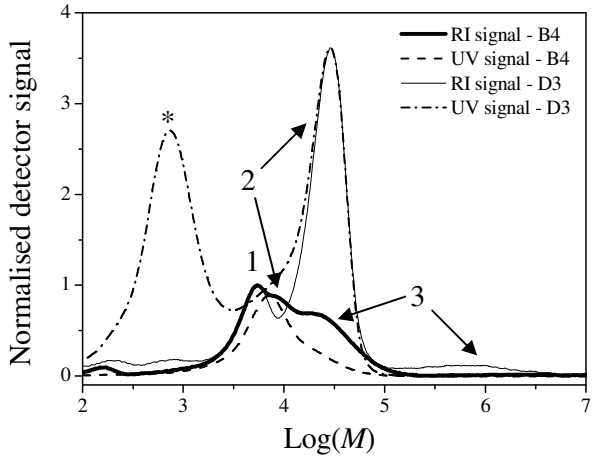

Figure 6.16: GPC chromatograms of a sample of 75% conversion for both D3 and B4.

From the overlay in Figure 6.16 it can be see that there is a distinct difference in control within the two polymerizations. The two chromatograms were normalised to the surfactant peak (labeled as 1). A direct comparison between the heights of the other distributions in the chromatogram is thus possible. The difference in height between the controlled distributions (labeled as 2 for both chromatograms) is substantial, and it is obvious that in the DPTC mediated polymerization (D3) there are very low concentrations of uncontrolled polymer as compared to B4. What is quite unusual is that within the system in which there is the most control (D3) there is also the most unreacted RAFT agent. The *number average molecular weight* for the controlled distribution (2) of B4 cannot be determined due to the overlap of the surfactant (1) and uncontrolled polymer (3) distributions. The *peak molecular weight* of the controlled distribution is larger for D3 than B4 (23 988 g.mol^{-1} for D3 versus 5 345 g.mol^{-1} for B4). The predicted $\overline{M}_n$ value at this conversion is 11 146 g.mol^{-1}.

Particle size analysis was performed on D1, B2, B4 and D3. The results are given in Tables 6.5 and 6.6.

Table 6.5: DLS results for the final latexes of polymerizations D1, B2, D3 and B4

Reaction	RAFT	Monomer	Surfactant	Z (average)	Polydispersity
D1	DPTC	Butyl acrylate	SDS	243.1	0.089
B2	DIBTC			48.2	0.268
D3	DPTC		Igepal®CO-990	294.1	0.09
B4	DIBTC			163.1	0.056

From these results it is evident that the average particle sizes for the DPTC mediated polymerizations are much larger than those mediated by DIBTC. The isobutyric acid radical leaving group that initiates z-mers could impart a certain degree of surface activity to the z-mer. The carboxylic acid functionality was shown by Ferguson *et al.*[6] to provide amphiphatic behaviour to a dithiobenzoate RAFT agent. The radical leaving group could behave in a similar manner and will result in increased particle surface areas (i.e. smaller particles).

Table 6.6: CHDF results for the final latexes of polymerizations D1, B2, D3 and B4.

Reaction	Z (Number average)			Z (Weight average)		
	Mean	Max	Standard deviation	Mean	Max	Standard deviation
D1	97.5	33.3	79.6	266.7	304.9	92.6
B2	36.3	33.3	8.2	42.3	37.9	9.9
D3	143.7	57	105.8	331.3	320.6	100.4
B4	109.9	101.1	35.7	167.5	130.1	87.1

The *polydispersity* values determined with DLS are slightly different from the *standard deviation* values determined with CHDF. The CHDF chromatogram for B4 was given in Figure 4.20 and the TEM micrograph for B4 in Figure 4.21. For B2 and B4 it can be stated that the particle size distribution is much narrower when DIBTC is used as mediator. B4 contains a species of larger particles, whilst B2 has a very narrow particle size distribution. This information alone indicates that there are varying nucleation mechanisms operating within each polymerization. The *number average* chromatographs for D1 and D3 are given in Figure 6.17:

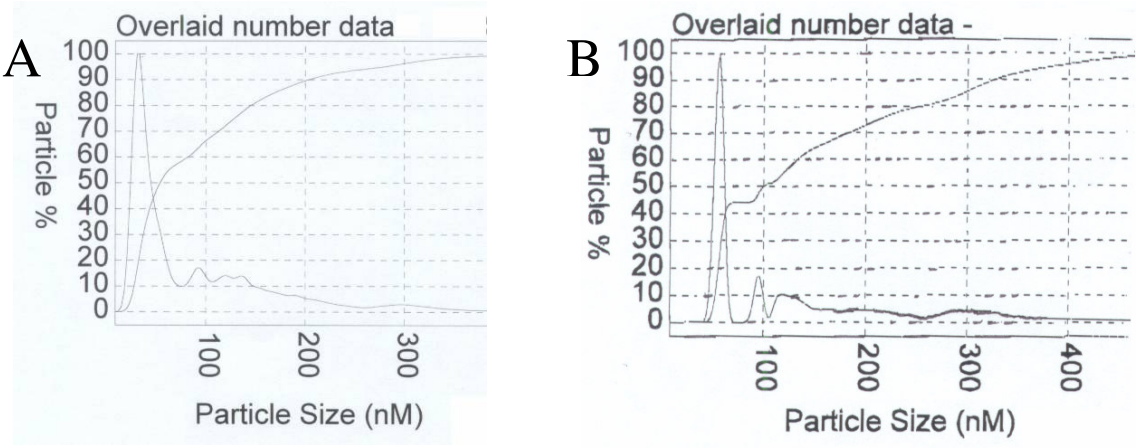

Figure 6.17: CHDF *number average* chromatograms for polymerizations (A) D1 and (B) D3.

The chromatograms in Figure 6.17 are similar except in the case of D3 where the main peak is shifted to larger particle sizes when nonionic surfactants are utilized in D3. The main peak is broader for D1, which is understandable, as according to the GPC data obtained for both, there is a greater concentration of uncontrolled polymer in D1, which implies multiple nucleation mechanisms. In both D1 and D3, particles over 200 nm were detected; these are probably due to particles that have coalesced. This indicates colloidal instability of the latex. This has been observed in polymerizations B4 and A4 (as well as C3, which will be addressed later in this chapter). All these systems are butyl acrylate polymerizations. It has been observed that the TEM images recorded for these polymerizations have given evidence of extensive film formation. This is due to the low T_g value of butyl acrylate polymers that leads to an increased likelihood of film formation at room temperature.[7] If there is a lay-over time between sample preparation and data acquisition, then film formation is probable. The same might be said for the CHDF analysis. It is probable that the larger particles form by coalescence that takes place during sample preparation. Latex instability that occurs during sample preparation could be due to the interaction of the dilute salt solution and the surfactant supported particles. If destabilization of the surfactant hydration layers occurs, then the particles could coalesce. Soft particles can undergo coalescence during CHDF analysis, leading to large particle sizes.[8]

6.2.1.2. Styrene miniemulsion polymerization

Polymerizations D2 (DPTC) and B1 (DIBTC), in which the surfactant is SDS, were compared. The first-order rate plots for B1 and D2 are given in Figure 6.18.

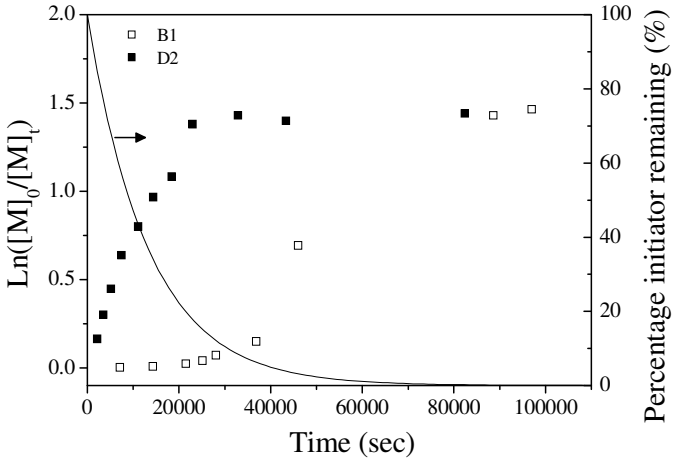

Figure 6.18: First-order rate plots for polymerizations D2 and B1.

The final conversion for polymerization D2 is 76 % whilst for B1 it is 67%. From this plot it is evident that the nucleation time for D2 is much shorter than for B1. An inhibition period is observed for B1 after which the rate of polymerization increases rapidly. No such inhibition can be seen for D2. Interval III appears to have a similar rate of R_p decrease.

GPC chromatogram overlays of single samples for D2 and B1 are given in Figure 6.19:

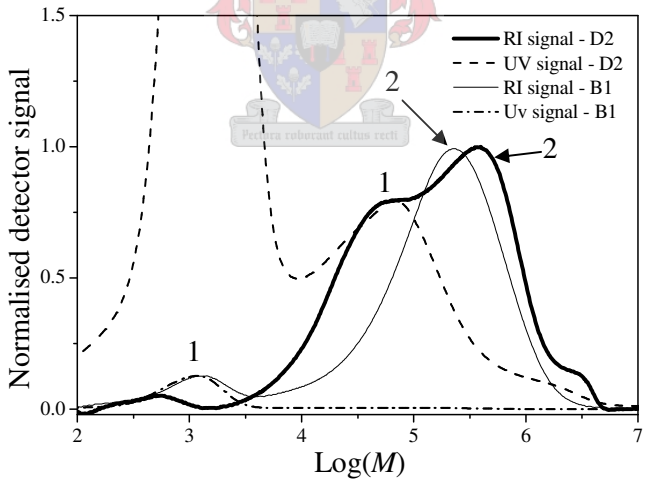

Figure 6.19: GPC chromatograms of samples of 70% conversion for D2 and B1.

The chromatograms have been normalised to the uncontrolled distribution (labeled as 2). The controlled distribution in both distributions is labeled as 1. It is apparent that if the chromatograms were normalised to the controlled distribution, then the uncontrolled distribution for B1 would be substantially greater in intensity than that of D2. The controlled distribution of B1 lies close to a similarly sized distribution in the chromatogram of D2 (labeled with an asterisk). This distribution

in D2 appears to be unreacted RAFT that is present in the system (this is verified by a clear UV absorbance). The *peak molecular weight* for the controlled distribution of the DPTC mediated polymerization (D2) is 67 832 g.mol^{-1} whilst the *number average molecular weight* for the same distribution for the DIBTC mediated polymerization (B1) is 1 444 g.mol^{-1}.

The two corresponding polymerizations in which Igepal®CO-990 is used as surfactant are D4 (DPTC) and B3 (DIBTC). The first-order rate plots for both are given in Figure 6.20:

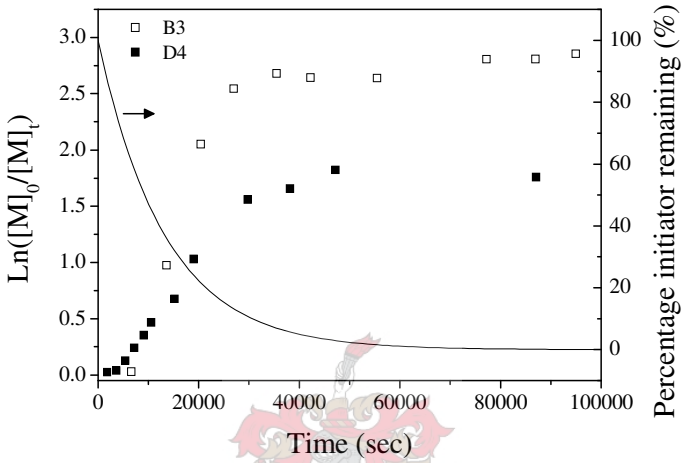

Figure 6.20: First-order rate plots for polymerizations D4 and B3.

The conversion after 24 hours for D4 is 86%, which is lower than the 93% for B3. The rate of polymerization is higher for B3, but there also appears to be an inhibition period for B3, which is not clearly seen for D4. R_p increases gradually for D4 and interval III appears to be a lot longer for D4.

The GPC chromatogram of polymerization D4 is given in Figure 6.21 (A) as well as one for a single sample to clearly illustrate the RI-UV overlay (B):

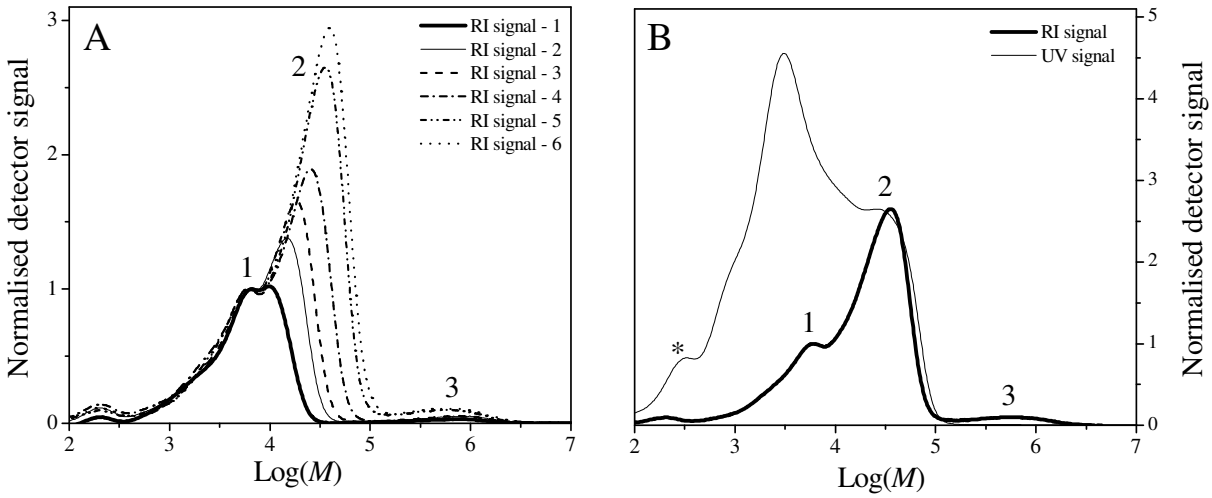

Figure 6.21: GPC chromatograms of (A) polymerization of D4 and (B) sample 6 of D4 showing the RI-UV overlay. Sample conversions for D4 are: (1) – 21%, (2) – 29%, (3) – 37%, (4) – 49%, (5) – 64% and (6) – 80%.

In the RI-UV overlay in chromatogram B the most intense distribution can be identified as the controlled distribution (labeled as 2). The *peak molecular weight* of this peak is 41 418 g.mol^{-1} while the predicted $\overline{M}_n$ value is 14 084 g.mol^{-1}. The UV signal is very strong over the surfactant peak (labeled as 1). From previous chromatograms of polymerizations in which Igepal®CO-990 was used as well as the UV scan (at 320 nm) for the surfactant (given in Figure 4.1), it was seen that the surfactant has minimal UV absorbance. It can thus be speculated that the strong signal might be due to shorter RAFT end-capped chains. The low molecular weight shoulder in the UV signal (marked with an asterisk) coincides with the RAFT agent distribution. A small distribution (marked as 3) can be seen at molecular weights of about 10^6 g.mol^{-1}. This has no apparent UV signal, implying it is uncontrolled polymer. The GPC chromatogram overlays of single samples for B3 and D4 are given in Figure 6.22:

Pectora roborant cultus recti

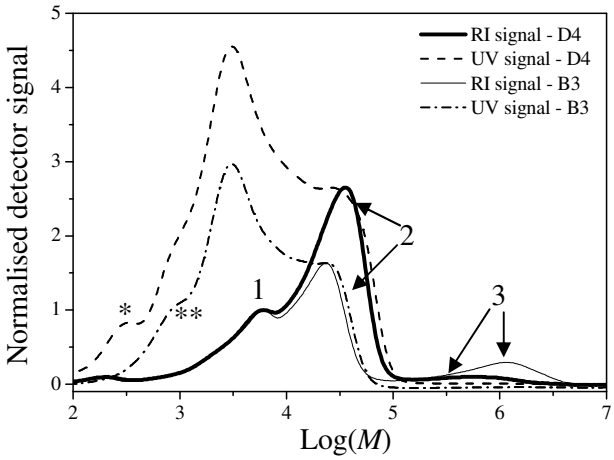

Figure 6.22: GPC chromatograms of a sample of 63% conversion for both D4 and B3.

Both chromatograms are normalised to the surfactant distribution (labeled as 1). The predicted $\overline{M}_n$ at this conversion is 11 436 g.mol^{-1} whilst the *peak molecular weight* for the controlled distribution (labeled as 2) in D4 is 38 047 g.mol^{-1} and for B3 is 23 604 g.mol^{-1}(the exact $\overline{M}_n$ cannot be calculated for either of the controlled distributions for D4 and B3). The distribution labeled as 3 shows no UV absorbance at 320 nm and is thus uncontrolled polymer. The UV absorption over the low molecular weight shoulders of the surfactant and controlled polymer peaks is seen in B3 as well as D4. The highest point of this peak is the same for D4 and B3. These are probably short dormant RAFT end-capped chains. There appears to be a shoulder on these distributions as well (labeled with an asterisk for D4 and a double asterisk for B3). In D4, the shoulder falls at the molecular weight of the RAFT agent. The shoulder for B3 appears to be slightly larger in molecular weight, implying that it is not unreacted RAFT, but very short dormant RAFT end-capped chains. The controlled distribution for D4 is much greater in intensity (indicating an increased concentration of controlled polymer) and the uncontrolled distribution is much less in intensity for D4 (indicating less uncontrolled polymer).

Particle size analysis was performed on D2, B1, B3 and D4. The results are given in Tables 6.7 and 6.8.

Table 6.7: DLS results for the final latexes of polymerizations D2, B1, B3 and D4

Reaction	RAFT	Monomer	Surfactant	Z (average)	Polydispersity
D2	DPTC	Styrene	SDS	119.8	0.007
B1	DIBTC			50.7	0.343
D4	DPTC		Igapl®CO-990	182.4	0.041
B3	DIBTC			163.6	0.017

The particles for the DPTC mediated polymerizations are larger than those for the DIBTC mediated polymerizations.

Table 6.8: CHDF results for the final latexes of polymerizations D2, B1, B3 and D4

Reaction	Z (Number average)			Z (Weight average)		
	Mean	**Max**	**Standard deviation**	**Mean**	**Max**	**Standard deviation**
D2	65.9	40.4	27.9	99.5	100.2	29
B1	40.3	35.6	9.8	47.9	42.4	11.7
D4	142.9	150.7	34.4	163.6	168.5	28.3
B3	92.6	47	41.5	142.7	145.7	42

If we compare the particle size data of D2 and B1, we can hypothesize that there is one primary nucleation mechanism for B1, whilst for D2 there are probably more. The CHDF chromatogram of B1 is given in Figure 6.23 and should be compared to that of D2 in Figure 6.8 (A).

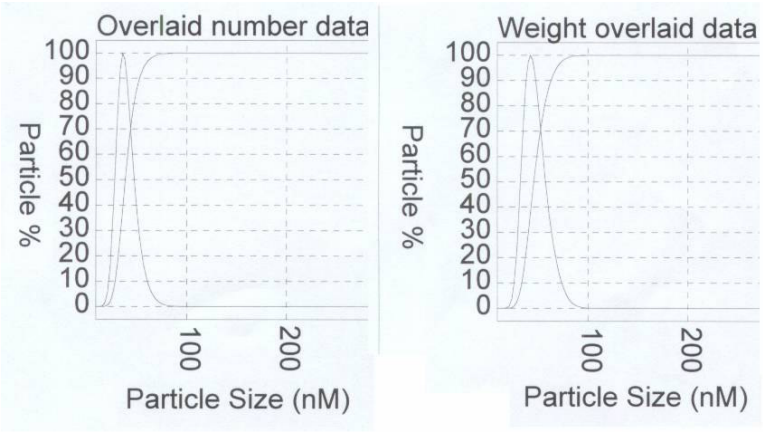

Figure 6.23: CHDF chromatograms of the final latex of polymerization B1.

In D4 and B3, an increase in *standard deviation* values indicates the possibility of multiple nucleation mechanisms in interval I. If we compare D2 and D4, we see that there is a larger spread

of particle sizes for D4. This is unexpected, since from GPC data it was deduced that there is less uncontrolled polymer formation in D4. This increase in PSD for D4 may be due to the increase in nucleation time and could also explain the increase in PSD of B3 when compared to B1. In this case however, the larger difference in particle size distribution can also (and probably primarily) be due to the different nucleation mechanisms in play.

6.2.1.3. Phenyl ethyl versus isobutyric acid: Conclusions

In Section 6.2.1 the difference in behaviour between the two RAFT agents DIBTC and DPTC, having two different leaving groups, was investigated. As mentioned in Chapter 4, the leaving group's ability to exit from the particles during the polymerization will greatly influence the behaviour of the miniemulsion. In section 6.2.1 it was speculated that there would be a substantial difference between the action of DIBTC and DPTC in the respective polymerizations due to the fact that DIBTC's leaving group is more hydrophilic that that of DPTC. From the data presented in the two sections 6.2.1.1 and 6.2.1.2 only slight differences between the behaviours of DPTC and DIBC were seen for certain miniemulsions, whilst for others there was a substantial reduction in uncontrolled behaviour. In Section 6.1.3, four main points were highlighted when comparing the RAFT-mediated polymerization to conventional FRP, namely rate retardation, unreacted RAFT agents and multiple nucleation mechanisms. These points are once again assessed when summarizing the eight polymerizations investigated in Section 6.2.1.

Pectora roborant cultus recti

1. **Rate retardation and inhibition.**

   The eight polymerizations investigated in Section 6.2.1 showed rate retardation. Slower z-mer formation for the styrene miniemulsions will lead to rate retardation, which was indeed seen when comparing respective polymerizations. In Chapter 4, with regard to conventional miniemulsion FRPs, it was speculated that the non-ionically stabilized miniemulsions did not suffer rate retardation due to a lower monomer droplet surface area and thick hydration layer. This rate retarding phenomenon could thus be eliminated as a reason for rate retardation when comparing miniemulsions stabilized with SDS and Igepal®CO-990. Two other possible reasons for rate retardation were the RAFT process and radical exit.

   The RAFT equilibrium that is established within the particles regulates the propagation rate and will also influence the rate retardation. The stability of the secondary 1-phenylethyl radical will be higher than that of the tertiary isobutyric acid radical, and thus it could be speculated that the

fragmentation step (k_{trans2}) for DPTC will be faster than DIBTC in the initialization step of the RAFT equilibrium. The weak stabilization of the intermediate radical formed during the initialization step of the RAFT equilibrium will be the same for DPTC and DIBTC. This instability will lead to a high rate of fragmentation and could even override the effect that the stability of the radical leaving group might impart on the equilibrium. This could mean that the fragmentation rates will be similar for DPTC and DIBTC, even though the radical stabilities of the leaving groups are different. Furthermore, this implies that any rate retardation differences between DPTC and DIBTC mediated miniemulsions are more likely to be due to radical desorption and secondary nucleations than the RAFT process itself.

The extent to which the radical exit occurs is largely dependent on the solubility, concentration and reactivity of the radicals. Butté *et al*. found that the larger the leaving group of the RAFT agent, the lower the probability of exit from the particle.[9] Between the two leaving groups under investigation there was a size difference, the 1-phenylethyl group being only slightly larger than the cyanovaleric acid group. The size difference was so slight that the influence on the exit rate was probably negligible. More importantly, the water solubility of the two groups is different. This implies that the group with higher water solubility will undergo more radical exit. Increased radical exit for any miniemulsion will result in substantial changes in the z-mer formation in the aqueous phase. The rate of z-mer formation will be higher, but the probability of radical termination (k_t) will also be higher. For DIBTC the leaving group is that of the water soluble isobutyric acid and, for this reason, it was speculated that radical leaving group exit might be higher for DIBTC mediated polymerizations. An inhibition period was observed for the DIBTC mediated butyl acrylate (B2) and styrene polymerization (B1). Increased radical exit (from newly nucleated droplets) will lead to a substantial increase in the radical concentration in the aqueous phase and thus increased termination. This termination will result in the inhibition period seen for B1 and B2. A steady-state of z-mer formation and termination will eventually be reached. For the butyl acrylate miniemulsions, fast z-mer formation (from radical leaving groups) implies that a steady-state will be reached in a shorter time period, leading to an earlier increase in the rate of polymerization. Thus the inhibition period will be shorter for B2, which is indeed the case. When the surfactant is changed to the non-ionic surfactant, the larger particles that result will cause a decrease in radical exit, leading to minimal termination and shorter inhibition periods. No inhibition is seen for any of the DPTC mediated miniemulsions, probably due to a very low exit rate. There does however appear to be slight rate retardation for the non-

ionically stabilized miniemulsions (D4 and D3). The net rate of polymerization is the summation of the rate of the RAFT-mediated polymerization and the rate of conventional FRP. Polymerizations in which substantial conventional FRP occurs are likely to show less rate retardation than RAFT-mediated polymerizations due to a higher net R_p rather than reduced radical exit or the RAFT process. This is true for many of the DPTC mediated polymerizations, when a slower polymerization can be linked to predominant RAFT-mediated polymerization.

2. Unreacted RAFT agents.

The presence of unreacted RAFT agents in a polymerization system indicates that the nucleation efficiency of the system is poor. The various concentrations of unreacted RAFT agents is linked directly to the movement of radicals from nucleated particles into unnucleated droplets i.e. nucleation efficiency. The nucleation efficiency will depend on the rate of z-mer formation in the aqueous phase. Increased radical concentrations in the aqueous phase due to radical leaving group exit from particles could increase the nucleation. A balance between z-mer formation and termination will ultimately determine the nucleation efficiency.

Increased radical leaving group exit for DIBTC mediated polymerizations theoretically leads to increased nucleation. This is always the case except for the ionically stabilized butyl acrylate miniemulsion (B2) where there is a high concentration of unreacted RAFT agent. A higher probability of secondary particle formation for the BA miniemulsion due to substantial radical exit leads to increased monomer diffusion out of unnucleated particles. Competition between the secondary particles and unnucleated droplets for radicals in the aqueous phase will result in less droplet nucleation. For the non-ionically stabilized butyl acrylate miniemulsions (B4), less exit results in less secondary particle formation and less extraction of z-mers from the aqueous phase. Increased droplet nucleation will follow. The reason why there is a lower concentration of unreacted RAFT agent in the ionically stabilized DIBTC mediated styrene miniemulsion (B1) resides in the fact that the influx of radical leaving groups into the aqueous phase will be lower due to slower droplet nucleation (z-mer formation). This leads to less secondary particle formation and less competition for aqueous phase radicals, which leads to increased nucleation (albeit slow nucleation).

For the DPTC mediated polymerizations, where exit is theoretically lower, there is evidence of unreacted RAFT agents. For the ionically stabilized butyl acrylate miniemulsion (D1), there is

unreacted RAFT agent, dormant RAFT end-capped z-mers and uncontrolled polymer. Exit still takes place, leading to micellar nucleation (uncontrolled polymer), but the particles from which radical exit does not take place are still growing and, in this process, abstracting free surfactant from the aqueous phase. This results in less uncontrolled polymer (fewer micelles) than in the case of the respective DIBTC mediated polymerization (B2). The growing particles also absorb more monomer from unnucleated droplets, leading to less radical entry into these particles (competition between growing particles and unnucleated droplets for z-mers), and this leads to higher concentrations of unreacted RAFT agents. The low concentration of RAFT end-capped oligomers leads to the high $\overline{M}_n$ values for the controlled chains. The non-ionically stabilized DPTC mediated butyl acrylate polymerization (D3) shows little unreacted RAFT agents due to less secondary particle nucleation. The M_p value for the controlled chains in D3 is higher than the predicted $\overline{M}_n$ value. This could imply poor RAFT agent consumption which is however not the case. Slow nucleation (slow radical leaving group exit) will lead to short RAFT end-capped chains, which is observed for D3. Both styrene miniemulsions (D2 and D4) have the highest concentrations of unreacted RAFT agents due to slower radical exit (slow nucleation), which results in chain lengths that are much longer than predicted (higher average molecular weights). Droplets that are nucleated later in the polymerization will have a lower monomer concentration due to Ostwald ripening of the growing particles. Short RAFT end-capped chains will result, giving strong UV traces in the GPC

Pectora roborant cultus recti

3. Multiple nucleation mechanisms.

Multiple nucleation mechanisms and long nucleation times lead to broader PSDs. From the tables of particle size analysis values given in this chapter, the following is observed: DIBTC mediated polymerizations generally lead to narrow PSD, the lowest PSDs being for the latexes stabilized with SDS (B1 and B2). From the GPC chromatograms for these polymerizations it is clear that most of the droplets were nucleated (due to little unreacted RAFT) but that very few of them continued growing, leading to $\overline{M}_n$ values far below the theoretically calculated values. The remaining polymer resides in particles formed via a secondary nucleation process. These particles will all grow simultaneously, leading to a narrow PSD. For the Igepal®CO-990 stabilized latexes (B3 and B4) the reduced aqueous phase radical concentrations, due to less radical exit, leads to less simultaneous particle formation and thus a larger spread of sizes. The same can be said for the DPTC mediated polymerizations, where wider PSDs are due to uncontrolled polymer residing in secondary particles.

These four points are all dependent on the movements of radicals in the miniemulsion during the polymerization. In conclusion, it can be said that the water-soluble leaving group leads to the most uncontrolled polymer, but also the least unnucleated droplets. This fact is independent of the type of monomer used. It has been seen that the non-ionic surfactant limits the movement of radicals.

6.2.2. 1-PHENYLETHYL VERSUS CYANOVALERIC ACID

The two RAFT agents compared in this section are PEDTB and CVADTB for which the stabilizing group is the phenyl group. The two leaving groups are the 1-phenylethyl and cyanovaleric acid groups respectively. In Section 6.2.2.1, PEDTB and CVADTB mediated butyl acrylate polymerizations stabilized with SDS and Igepal®CO-990 are investigated. Section 6.2.2.2 deals with PEDTB and DPTC mediated styrene polymerizations stabilized with SDS and Igepal®CO-990.

6.2.2.1. Butyl acrylate miniemulsion polymerization

Miniemulsions C1 (PEDTB) and A2 (CVADTB) were stabilized with SDS. The first-order rate plots for C1 and A2 are given in Figure 6.24:

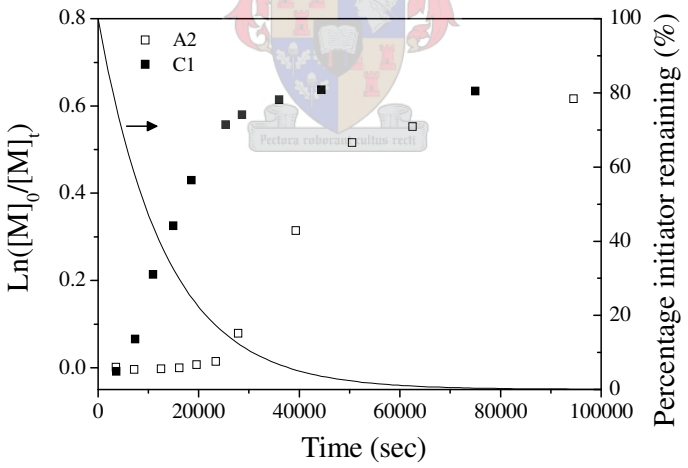

Figure 6.24: First-order rate plots for polymerizations C1 and A2.

The final conversions after 24 hours are 50% for C1 and 46% for A2. The reaction profile for A2 shows an inhibition period. After the inhibition period the rate at which R_p increases during interval I is similar for C1 and A2.

A GPC chromatogram overlay of a single sample at a conversion of 45% for C1 (PEDTB) and A2 (CVADTB) is given in Figure 6.25:

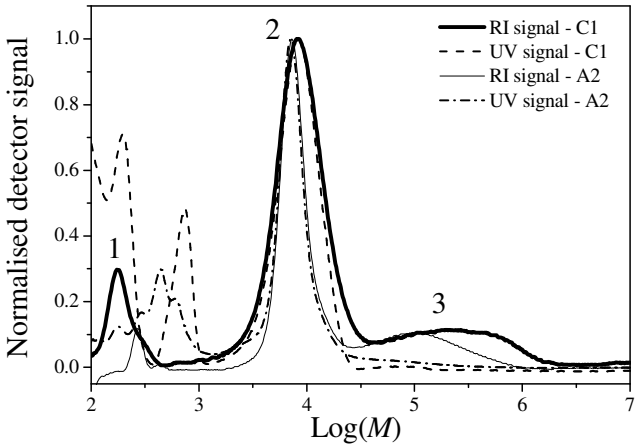

Figure 6.25: GPC chromatograms of samples of polymerizations C1 and A2.

Multiple molecular weight distributions are visible. The distribution labeled as 2 can be said to be controlled due to a neat RI-UV overlay. The distribution labeled as 3 is uncontrolled, and lacks the thio carbonyl thio functionality. The controlled distribution for A2 seems narrower than that in C1 (the polydispersity of the narrower peak is 1.3 for C1 and 1.17 for A2). The *number average molecular weight* of distribution 2 for C1 and A2 is 9 758 g.mol^{-1} and 7 260 g.mol^{-1} respectively, whilst the predicted $\overline{M}_n$ value at this conversion is 7 980 g.mol^{-1}. The concentration of uncontrolled polymer for A2 appears to be less. The distribution labeled as 1 has a distinct UV absorbance, which indicates unreacted RAFT agent at this molecular weight. There also appears to be a small distribution at the same molecular weight for A2, along with a peak in the UV trace. This implies that there are unconsumed RAFT agents in both systems.

The two corresponding polymerizations in which Igepal®CO-990 was used as the surfactant are C3 (PEDTB) and A4 (CVADTB). The first-order rate plots for C3 and A4 are given in Figure 6.26:

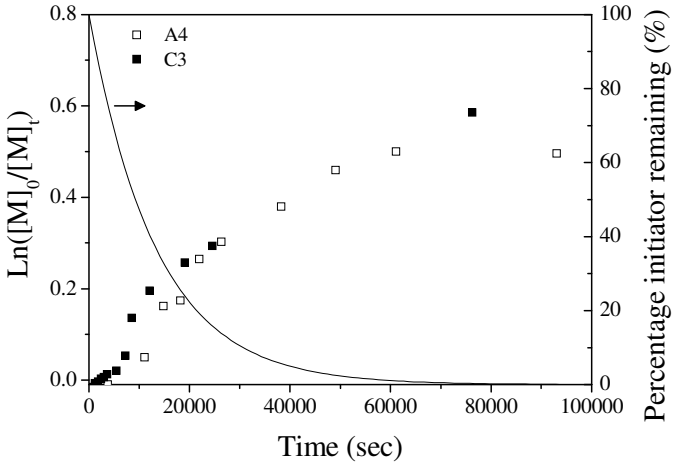

Figure 6.26: First-order rate plots for polymerizations C3 and A4.

The conversion after 24 hours for C3 is 44%, whilst for A4 it is 39%. The trends for both plots seem to be similar. It is apparent that A4 is slightly more retarded than C3 during interval I. This could be linked to the relative stabilities of the intermediate radical species for both RAFT agents or to any radical exit from the particles that might be taking place.

The GPC chromatogram of C3 is given in Figure 6.27 (A), as well as an overlay of a sample with a conversion of 42% from both A4 and C3:

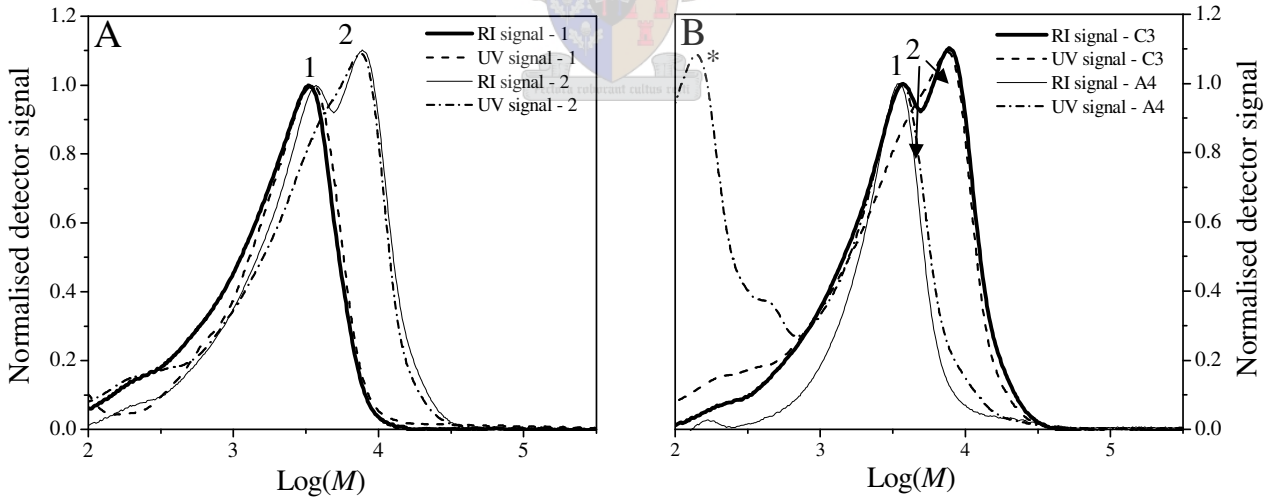

Figure 6.27: GPC chromatograms of (A) C3 and (B) an overlay of a single sample from C3 and A4. Sample conversions for C3 are: (1) – 22% and (2) – 44%.

Due to the low conversion of the samples used in the GPC analysis, there is a large degree of overlapping of the surfactant (labeled as 1) and polymer (labeled as 2) distributions. This can clearly been seen in Figure 6.27 (A), sample 1. There is only one distribution, which shows a

perfect RI-UV overlay. It would be natural to identify this as a controlled polymer distribution, but the GPC chromatogram for the surfactant indicates that this distribution will also include the surfactant. For sample 2 it is clearer that there are two distinct species in the latex and the UV overlay indicates that the growing distribution (labeled as 2) has the dithiobenzoate end group. From the overlay in Figure 6.27, chromatogram B, a distinct difference in the molecular weight of the polymer in each latex is visible. Both these samples are at the same conversion and, accordingly, it is assumed that the resultant molecular weight could be similar. An exact molecular weight for A4 cannot be established due to the overlay with the surfactant, but a rough estimate places the *peak molecular weight* at 3 523 g.mol^{-1}. This is much lower than that of C3, which is 7 740 g.mol^{-1}, as well as the predicted $\overline{M}_n$ value of 7 861 g.mol^{-1}.

Particle size analysis were performed on A2, A4, C1 and C3. The results are given in Tables 6.9 and 6.10.

Table 6.9: DLS results of the final latexes of polymerizations A2, A4, C1 and C3

Reaction	RAFT	Monomer	Surfactant	Z (average)	Polydispersity
C1	PEDTB	Butyl acrylate	SDS	72	X
A2	CVADTB			117.5	0.052
C3	PEDTB		Igepal®CO-990	206.3	0.135
A4	CVADTB			226.7	0.115

From these results it appears that the polymerizations mediated by PEDTB lead to latexes with smaller particle sizes. The particle size polydispersities of polymerizations C1 and A2 seem to be very low.

Table 6.10: CHDF results of the final latexes of polymerizations A2, A4, C1 and C3

Reaction	Z (Number average)			Z (Weight average)		
	Mean	**Max**	**Standard deviation**	**Mean**	**Max**	**Standard deviation**
C1	64.8	64.7	19.4	81.2	74.4	20
A2	68.8	33.1	30.3	102.8	89.6	28.3
C3	105.7	82.9	51.1	216.4	105.3	108.4
A4	121.9	92	55.8	230.7	133.9	109.9

The *weight average standard deviation values* are large for both C3 and A4. Looking back at the CHDF chromatogram for A4 that was given in Figure 5.16, we see that this is due to a few larger particles (> 250 nm). The same can be seen in the chromatogram of C3 that is given in Figure 6.28:

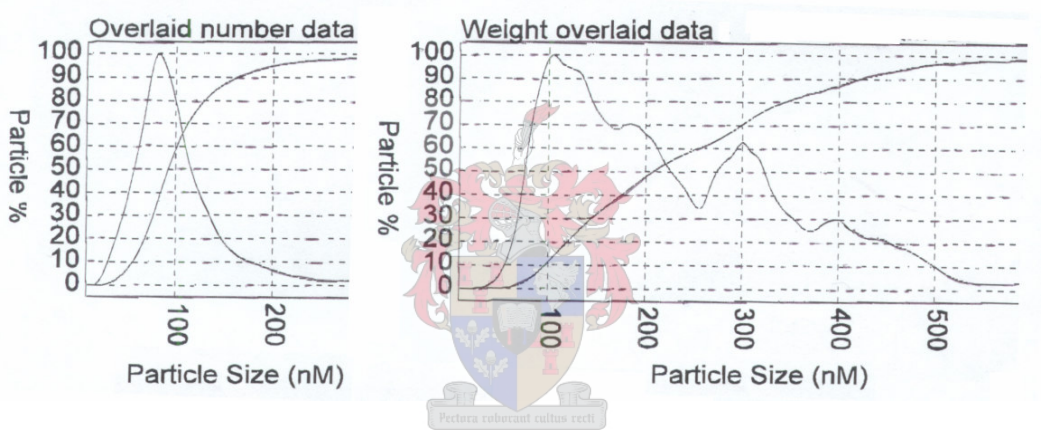

Figure 6.28: CHDF chromatograms of the final latex of polymerization C3.

It is evident that there are very large particles in the latex. This phenomenon has previously been seen in other butyl acrylate polymerizations and was discussed with reference to polymerizations D1 and D3 in Section 6.2.1.1. As was stated there, these large particles could be due to coalescence of smaller particles. From Table 6.14, we note that the *number average mean particle size* for A2 and C1 is similar. The chromatogram for A2 was given in Figure 5.15. It gave evidence of a species of particles of approximately 30 nm, as well as a species of particles of approximately 60 nm. The bimodality of the chromatogram for A2 is not evident in the chromatogram for C1 (Figure 6.5). For C1 we see a single, broad distribution. The difference between the chromatograms for C3 and A4 is not as stark; both show a single broad distribution.

6.2.2.2. Styrene miniemulsion polymerization

Polymerizations C2 (PEDTB) and A1 (CVADTB) in which SDS is used as surfactant were investigated. The first-order rate plots for C2 and A1 are given in Figure 6.2:.

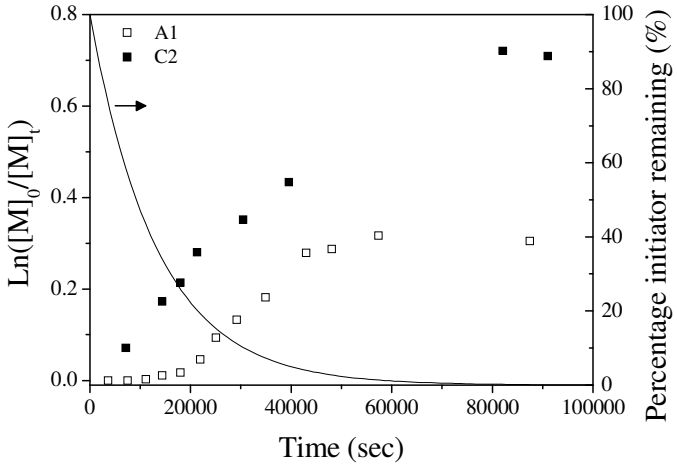

Figure 6.29: First-order rate plots for polymerizations C2 and A1.

The conversion after 24 hours for C2 is 50%, which is higher than the 30% for A1. The nucleation period for A1 is longer than that of C2 and the rate of reaction during this period is lower for A2. An inhibition period is observed for A1. The increase in reaction rate after the inhibition period of A2 is similar to that of C2 at the onset of interval I. Interval III appears to be much longer for C2.

A GPC chromatogram overlay of a single sample of a conversion of 50% from C2 and A1 is given in Figure 6.30:

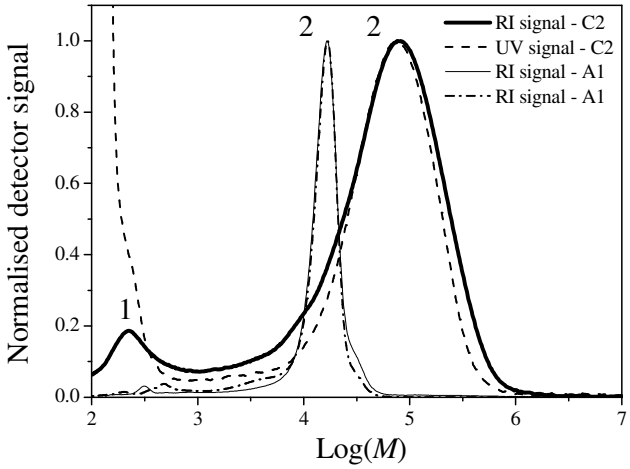

Figure 6.30: GPC chromatograms of a sample from polymerizations C2 and A1.

For both A1 and C2 the main distribution (labeled as 2) has a perfect RI-UV overlay, which indicates that it is a controlled polymerization. There is no distinct secondary, uncontrolled polymer growth. The polydispersity index for A1 is much lower than that for C2 (1.14 for A1 and 1.97 for C2). For C2 there is evidence of a smaller distribution (labeled as 1) that is probably unreacted RAFT agent, considering that there is a strong UV signal over this distribution. The *number average molecular weights* for both A1 and C2 are both higher than the predicted values: $\overline{M}_n$ for A1 is 13 494 g.mol^{-1} and for C2 is 71 609 g.mol^{-1}, versus the predicted weight of 8 664 g.mol^{-1}. The fact that the $\overline{M}_n$ value for C2 is extremely high can be linked to the fact that there appears to be large amounts of unreacted RAFT agent.

The two corresponding polymerizations in which Igepal®CO-990 was used as surfactant are C4 (PEDTB) and A3 (CVADTB). The first-order rate plots for polymerizations A3 and C4 are given in Figure 6.31:

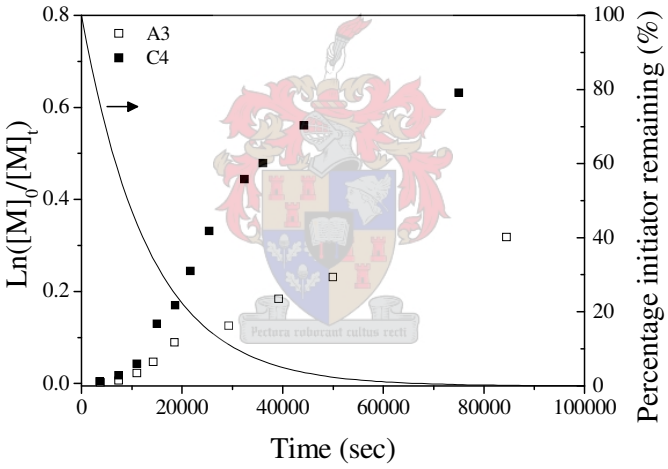

Figure 6.31: First-order rate plot for polymerizations C4 and A3.

The conversion after 24 hours for C4 is 46% whilst for A3 it is 27%. The rate of reaction during interval I is higher for C4 and the duration of this interval is similar for both polymerizations.

The GPC chromatogram of polymerization C4 is given in Figure 6.32 (A) as well as a single sample from C4 to show the RI-UV overlay (B):

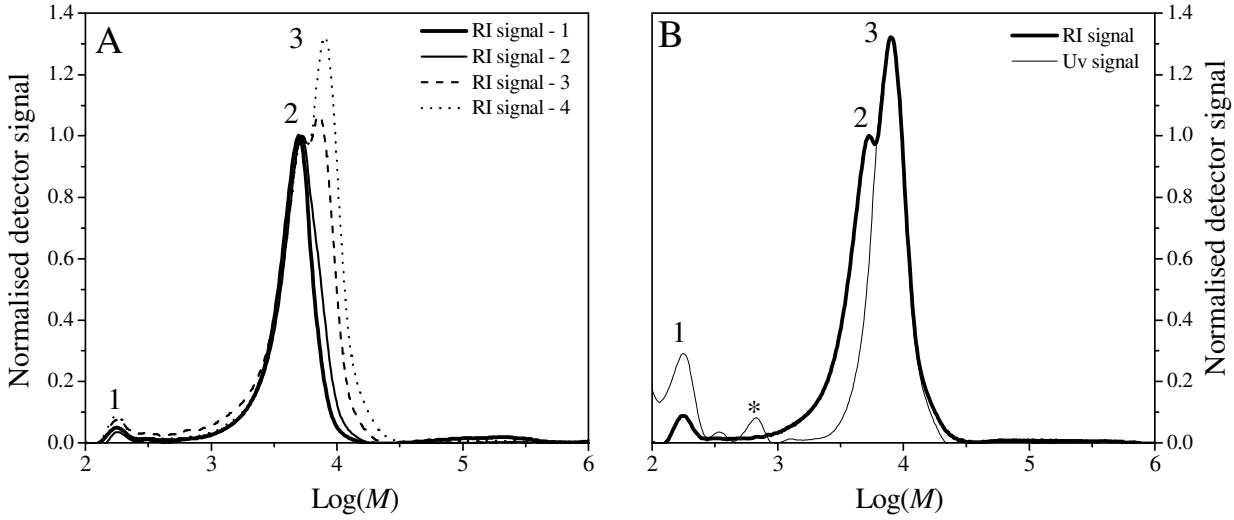

Figure 6.32: GPC chromatograms of A.) the polymerization C4 and B.) sample 4 of C4 showing the RI-UV overlay. Samples conversions for C4 are: (1) – 21%, (2) – 28%, (3) – 38% and (4) – 46%.

Figure 6.32 (A) shows two main distributions in the chromatogram. The most intense distribution (labeled as 3) is that of the controlled polymer. The first distribution is the surfactant (labeled as 2). Chromatogram A clearly shows the increasing molecular weight with conversion of the controlled distribution (3). The predicted $\overline{M}_n$ for the sample in chromatogram B is 8 088 g.mol^{-1} whilst the *peak molecular weight* (M_p) for the sample is 10 159 g.mol^{-1}. This value might well be different from the actual $\overline{M}_n$, but these values cannot accurately be determined due to extensive overlap of the two main distributions. The distribution labeled as 1 is at the molecular weight of the RAFT agent. In the single sample overlay in chromatogram B, the distribution marked with an asterisk is probably short RAFT end-capped chains. The most important observation is that there is no clear uncontrolled distribution in any of the samples analyzed.

A GPC chromatogram overlay of a single sample of 27% conversion from C4 and A3 is given in Figure 6.33:

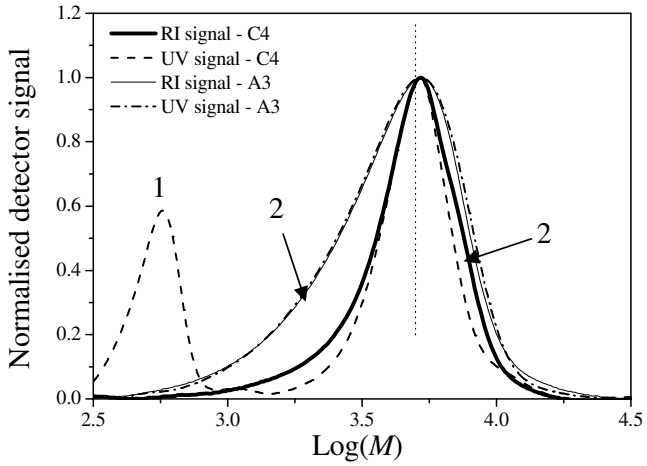

Figure 6.33: GPC chromatogram overlay of a sample from C4 and A3.

The overlay is similar to that seen in Figure 6.33 for polymerizations C3 and A4. One distinct distribution is visible. As was the problem in the comparison of the GPC chromatograms of C3 and A4, the fact that the molecular weights of the analyzed samples are so low make it impossible to distinguish between the surfactant and polymer in the system. The tail on the low molecular weight side of the RI signal (labeled as 2) for A3 is probably polymer. On the higher molecular weight side of the RI signal, a slight shoulder can be seen (labeled as 2), and this is probably the polymer distribution for C4. The predicted $\overline{M}_n$ for this conversion is indicated by the dotted vertical line (5 082 g.mol^{-1}). Accurate values for the $\overline{M}_n$ cannot be determined for either distribution. It appears that at this stage in the polymerization, the *polydispersity* of the polymer distribution for A3 is wider than for C4. The absorption (labeled as 1) in the UV signal for C4 is probably due to unreacted RAFT agents. The concentration of these chains is very low such that they are scarcely detected by the RI detector. The presence of the unreacted RAFT can explain the slight differences in theoretical and experimental $\overline{M}_n$ values.

Particle size analyses were performed on A1, A3, C2 and C4. The results are given in Tables 6.11 and 6.12.

Table 6.11: DLS results of the final latexes of polymerizations A1, A3, C2 and C4

Reaction	RAFT	Monomer	Surfactant	Z (average)	Polydispersity
C2	PEDTB	Styrene	SDS	107.9	0.044
A1	CVADTB			82.7	0.063
C4	PEDTB		Igepal®CO-990	226.8	X
A3	CVADTB			172.5	0.187

The trend observed for the butyl acrylate polymerizations in the section 6.2.2.1 (C1, A2, C3 and A4) is not observed here. The difference in particle size can be linked to the difference in conversion of the latex sample analyzed. The same is true for C4 and A3.

Table 6.12: CHDF results of the final latexes of polymerizations A1, A3, C2 and C4

Reaction	Z (Number average)			Z (Weight average)		
	Mean	Max	Standard deviation	Mean	Max	Standard deviation
C2	50.5	37.5	21	86.4	48.3	39.4
A1	60.4	56.9	17.6	74.5	74.7	17
C4	62	42.3	29.6	134.8	90.1	84.7
A3	79.3	73.9	29.3	130.8	89.4	77.1

The results determined by DLS and CHDF differ significantly. C2 and A1 have similar average particle sizes, but A1 has a slightly lower standard deviation, and thus PSD. The CHDF chromatogram for A1 is given in Figure 5.7 and that of C2 is given in Figure 6.10 (B). It appears that for C2 there are a few larger particles that are causing the PSD to increase. Control of the particle size is improved when using CVADTB. Comparing C4 and A3 we see little difference in average particle size and distribution, as was observed from the DLS data. Both systems show evidence of larger particles that cause the PSD to increase. If the *number average mean particle size* and *weight average mean particle size* for C2 and A1 as well as C4 and A3 are compared, it can be noted that for both C2 and C4 the largest majority of the particles are approximately 40 nm, but there are larger particles that cause the mean to increase. For A1 and A3, the particle distribution around the mean is more Gaussian like (i.e. forming a bell curve rather than a curve with one longer side, as can be seen for C2 as well as C4). A Gaussian shape is indicative of the operation of only one primary nucleation mechanism.

6.2.2.3. Phenyl ethyl versus cyanovaleric acid: Conclusions

In Section 6.2.2 the difference in the behaviour between the two RAFT agents CVADTB and PEDTB was investigated. Changing the Z- group and R- group structure will change the nature of the polymerization of the miniemulsions prepared here, with respect to those as discussed in Section 6.3.1.

The difference in behaviour between CVADTB and PEDTB can be linked to structural differences. The structure of the RAFT agent will affect the equilibrium that is established within the particles. For CVADTB and PEDTB, the leaving group after the initialization will be the only differing species in the equilibrium (i.e. in Scheme 2.9, the values of k_{trans2} and $k_{detrans2}$ will be different for the two agents). The tertiary cyanovaleric acid radical is theoretically more stable, but the resonance stability of the secondary phenylethyl radical could lead to similar stabilities and reactivities for both species. For this reason it could be speculated that the concentration of either leaving group after initialization will be similar. Assuming that the radical leaving group (R) can exit from the particles, the exit rate coefficient (k_{EXIT}) will be unique for the two leaving groups. The values of the rate coefficient of propagation within the aqueous phase (k_{Rp}) will be unique. Differing rates of propagation (R_p) and the rate of termination within the aqueous phase (R_t) can be expected due to differing radical concentrations. The radical exchange between the aqueous and oil phases will lead to differences in rate retardation, concentrations of unreacted RAFT agents and the nucleation mechanisms operating.

Pectora roborant cultus recti

1. Rate retardation and inhibition.

Rate retardation is linked either to radical loss from the locus of polymerization or the RAFT process. In the previous paragraph it was speculated that the RAFT equilibrium is similar for both PEDTB and CVADTB. When comparing the individual RAFT-mediated polymerizations in Section 6.2.2, slight differences in rate retardation, especially during interval I, can be linked to radical loss due to radical exit from the particles. An inhibition period is seen for the SDS stabilized CVADTB mediated polymerizations (A2 and A1). The water solubility of the leaving group increases the probability of exit, leading to increased termination within the aqueous phase. Rate retardation is decreased for the butyl acrylate polymerizations (C1, A2, C3 and A4) due to the increased rates of propagation for butyl acrylate polymerizations, and thus faster nucleation.[10]

2. Unreacted RAFT agents.

The concentration of unreacted RAFT agents is related to the radical movement between the two phases. Increased radical movement from the oil to the water phase increases the chance of nucleation. Increased termination will also follow from the influx of radicals but a steady-state will be reached and this state will define the nucleation efficiency. The PEDTB mediated, ionically stabilized polymerizations (C1 and C2) all show unreacted RAFT agents (which results in $\overline{M}_n$ values higher than predicted), which is due to few radical exit events. The non-ionically stabilized polymerizations (C3 and C4) show less unreacted RAFT agents due to fewer initial droplets in the miniemulsion that need to be nucleated. The consumption of the RAFT agent is so efficient in these two polymerizations that the $\overline{M}_n$ values are very close to the predicted values. The CVADTB mediated ionically stabilized miniemulsions (A2 and A1) show little unreacted RAFT agent. A higher radical flux, as well as faster Ostwald ripening of the growing particles, leads to increased concentrations of uncontrolled polymer and unreacted RAFT agents for the butyl acrylate polymerization (A2) compared to the styrene polymerization (A1). For A2, even though there are unreacted RAFT agents, the $\overline{M}_n$ is close to the predicted value. Competition between particles (droplet nucleation) and secondary particles for monomer could lead to the stability of the monomer:RAFT agent ratio, which will prevent unpredicted longer chain lengths. No such competition for the styrene polymerization (A1) as well as poor RAFT agent consumption leads to the longer (than predicted) chains lengths.

3. Multiple nucleation mechanisms.

The multitude of nucleation mechanisms will be reflected in the particle size analysis data. Very little uncontrolled polymer, and thus secondary particle formation, was observed for the PEDTB and CVADTB mediated polymerizations in Sections 6.2.2.1 and 6.2.2.2. Fewer radical exit events linked to slower fragmentation of the RAFT intermediate radical leads to less chance of secondary particle formation. Droplet nucleation is therefore the primary nucleation mechanism. Narrow, mono-modal PSD substantiates this.

The movement of radical leaving groups depends on various factors. In this section, it is shown that by changing the Z- group, the concentration of the propagating radical leaving groups is altered. The influence that this has on the radical behaviour was investigated. It was seen that radical exit still takes place, but at a much reduced rate. Similar dependence on monomer and surfactant as was

seen for the trithiocarbonates investigated in Section 6.2.1 was observed in Section 6.2.2. Conclusions on the differing behaviours of the dithiocarbonates and trithiocarbonates will be made in Section 6.2.3.

6.2.3. THE ROLE OF THE R- GROUP: CONCLUSIONS

When RAFT-mediated polymerizations were investigated in this chapter, it was found that large deviations from the conventional miniemulsions (discussed in chapter 4) were apparent. Substantial rate retardation as well as multiple nucleation mechanisms were found to varying degrees, depending on the type of miniemulsion (monomer and surfactant) and RAFT agent. Rate retardation was linked to the RAFT mechanism that operates within the oil-phase as well as radical exit from the polymerization loci. Multiple nucleation mechanisms and uncontrolled polymer growth was linked to the radical loss. The role of the RAFT mechanism in the retardation and behaviour of the polymerization was investigated in Section 6.2. It was found that varying the RAFT structure, which leads to a change in RAFT equilibrium, influences the radical movement between the oil and water phases to a large degree.

From the comparisons between the two trithiocarbonates and the two dithiobenzoates, it is clear that the solubility, reactivity and concentration of the radical leaving groups will greatly influence the radical movement. The trithiocarbonates' (DITBC and DPTC) RAFT agent structure results in higher concentrations of the radical leaving group within the particles. This increases the probability of radical exit into the aqueous phase. By changing to the dithiobenzoates, a lower probability of radical exit is evident, but radical exit cannot be ruled out completely. The more water-soluble the leaving group, the higher the probability of exit events occurring, leading to an increased probability of aqueous phase (and thus uncontrolled) propagation, termination and nucleation. The more water-soluble the monomer, the faster the aqueous phase propagation and the faster the nucleation. Higher values of C_W^{sat} also lead to substantial Ostwald ripening that can cause monomer starvation of certain particles as well as an increased probability of micellar nucleation (less growing particles results in less free surfactant absorption and increased micelle concentrations). The non-ionic surfactant does not appear to substantially decrease the ability of radicals to exit, but the resultant larger sized particles (when using this surfactant) do lead to a net decrease in radical exit events.

To optimize a RAFT-mediated miniemulsion, a balance between monomer reactivity and solubility is needed. Added to this is the balance between the addition-fragmentation rate of the RAFT agent and the solubility of the radical leaving groups. Lastly, the surfactant plays a large role when highly reactive RAFT agents and monomers are used.

6.3. REFERENCES

(1) Lansalot, M.; Davis, T. P.; Heuts, J. P. A. *Macromolecules* **2002**, *35*, 7582

(2) Le, T. P.; Moad, G.; Rizzardo, E.; Thang, S. H. In World Patent 98/01478;,**1998**

(3) Wu, X. Q.; Schork, F. J. *Journal of Applied Polymer Science* **2000**, *81*, 1691

(4) Monteiro, M. J.; de Brouwer, H. *Macromolecules* **2000**, *34*, 349

(5) Barner-Kowollik, C.; Quinn, J. F.; Nguyen, T. L. U.; Heuts, J. P. A.; Davis, T. P. *Macromolecules* **2001**, *34*, 7849

(6) Ferguson, C. J.; Hughes, R. J.; Pham, B. T. T.; Hawkett, B. S.; Gilbert, R. G.; Serelis, A. K.; Such, C. H. *Macromolecules* **2002**, *35*, 9243

(7) Lide, D. R., Ed. *CRC Handbook of Chemistry and Physics*; CRC Press: Boca Raton, **2004**

(8) Pham, B. T. T.; Gilbert, R. G.; Fellows, C. M. *Australian. Journal of Chemistry* **2004**, *57*, 765

(9) Butte´, A.; Storti, G.; Morbidelli, M. *Macromolecules* **2001**, *34*, 5885

(10) Gilbert, R. G. In *Emulsion Polymerization and Emulsion Polymers*; El-Aasser, M. S., Ed.; John Wiley & Sons Ltd: Chichester, **1997**

Chapter 7. : *The introduction of aqueous phase radical traps into RAFT-mediated miniemulsion polymerizations*.

ABSTRACT

Aqueous phase radical scavengers will eliminate aqueous phase radicals. The incorporation of these scavengers will lead to a substantial decrease in the aqueous phase radical concentration. It has been speculated that an abnormally high aqueous phase radical concentration could lead to substantial conventional FRP occurring. By reducing the radical concentration, the final latex should lack all conventionally formed polymers.

Aqueous phase radical traps or scavengers can be used to eliminate radicals that are present in the aqueous phase. Blythe *et al.*[1] and Luo *et al.*[2] used radical scavengers to investigate the mechanism of particle formation in miniemulsions initiated by oil-soluble initiators. By eliminating initiating radicals that might possibly form in the aqueous phase, it is possible to limit the source of radicals in the miniemulsion to the oil phase. Lacik *et al.*[3] studied the kinetic behaviour of free radical polymerizations in emulsions that utilized a radical spin trap, with special attention given to radical exit. Radical exit in these systems is equivalent to radical loss, removing re-entry as a possible consideration. In this thesis, the effect that radical scavengers have on RAFT-mediated miniemulsion polymerizations was investigated. The role of the radical scavenger in this scenario is to reduce the possible nucleation mechanisms. By eliminating radicals from the aqueous phase, droplet nucleation becomes the primary nucleation mechanism by default. This provides a means to test the proposed model of secondary particle formation. If it is true that any uncontrolled polymer must form within particles generated in the aqueous phase (secondary particles), then by eliminating any radicals within the aqueous phase, any secondary particle growth can be prevented.

The two aqueous phase radical traps utilized in this study were sodium nitrite ($NaNO_2$) and Fremy's salt (dipotassium nitrosodisulphonate). The structure of the latter is given in Figure 7.1:

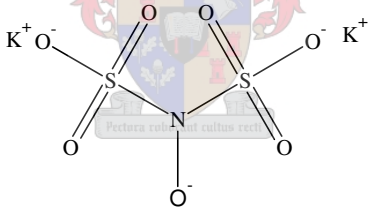

Figure 7.1: Structure of potassium nitrosodisulphonate (Fremy's salt).

The incorporation of an aqueous phase radical scavenger should theoretically lead to significant changes in the kinetics and mechanics of a radical polymerization due to the elimination of the probability of aqueous phase propagation. This is even more so in a living free radical polymerization. By investigating the behaviour of such a polymerization as compared to a control polymerization, in which there is no scavenger, we can obtain an understanding of the workings of the RAFT mechanism in miniemulsion with respect to aqueous phase radicals.

All miniemulsions were prepared as described in Section 3.2. The default RAFT agent was DIBTC. The reason for the choice of DIBTC as RAFT agent was that in the previous chapters (5 and 6) it was evident that the largest degree of control loss in the polymerization was observed in DIBTC-

mediated polymerizations. The incorporation of an ionic, aqueous phase radical trap into a miniemulsion stabilized with an ionic surfactant such as SDS has been found to lead to destabilization of the latex.[4] To circumvent this problem, all miniemulsions investigated in this section were stabilized with the non-ionic surfactant Igepal®CO-990. The concentration of the aqueous phase radical trap was equivalent to double the concentration of initiator (i.e. equal concentrations of initiating radicals and radical scavengers) in the miniemulsion. The miniemulsion procedure was as described in Section 3.2. As in the Chapter 4 and 5, the analyses of the polymerizations and analyses of the final latexes are supplied for each reaction. Kinetic analyses are given by first-order rate plots determined gravimetrically. The evolution of polymer characteristics such as molecular weight and polydispersity are given by size exclusion chromatography. Particle size analyses were performed by TEM, CHDF and DLS.

7.1. FREMY'S SALT

In this section, a range of polymerizations are investigated in which the aqueous phase radical trap dipotassium nitrodisulphonate was included. Styrene polymerizations are investigated in Section 7.1.1 followed by the butyl acrylate polymerizations in Section 7.1.2.

7.1.1. STYRENE MINIEMULSIONS

Polymerization B13 (including Fremy's salt) was compared to the control reaction B3. The first-order rate plots for B3 and B13 are given in Figure 7.2:

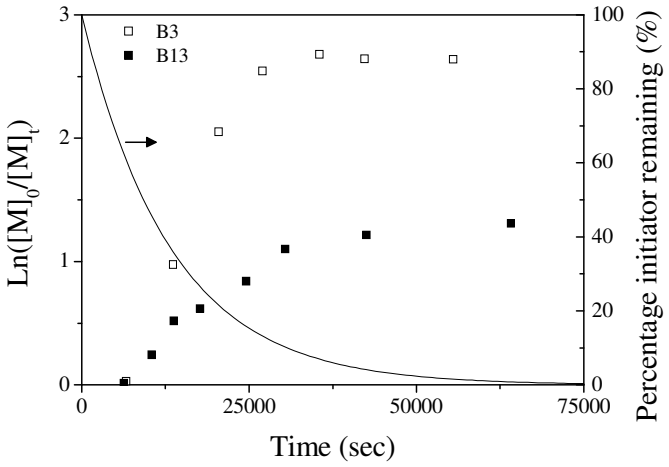

Figure 7.2: First-order rate plots for polymerizations B13 and B3.

The conversion in the presence of a radical scavenger after 24 hours is 80%, which is slightly less than the 93% for the control polymerization. The duration of interval I appears longer for B13 and the rate of reaction during this interval was also lower for B13. This retardation can explain the lower conversion after 24 hours for B13 when the radical initiator concentration is taken into account (solid line in Figure 7.2). Interval III was much shorter for the control polymerization (B3). This could be due to a lower radical concentration at the onset of interval III for B13, which leads to a lower rate of termination. There appears to be an inhibition period for B3; this was discussed in Section 5.1 and is linked to increased termination in the aqueous phase.

It was speculated that the incorporation of the radical scavenger would lead to the elimination of uncontrolled polymer growth. The validity of this assumption is revealed with dual detector GPC analysis. The GPC chromatograms for both reactions B3 (control) and B13 (scavenger) are given in Figure 7.3:

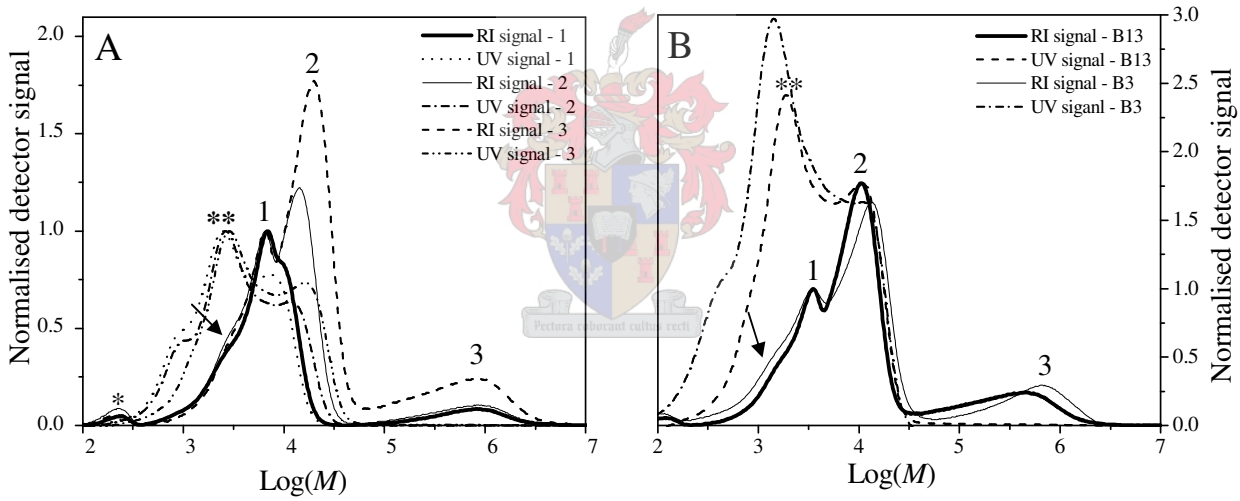

Figure 7.3: GPC chromatograms of A.) B13 and B.) samples with conversions of 60% for B3 and B13. Sample conversions for B13 are: (1) – 21%, (2) – 40% and (3) – 66%.

From the slight retardation of the reaction rate seen for B13 in the first-order rate plots, it appears consistent to infer that the presence of the radical scavenger decreases the rate of reaction. The elimination of aqueous phase radicals could lead to substantial changes in the polymer within the final latex. The RI trace in the chromatogram for B13 (scavenger) in Figure 7.3 (A) shows three clear distributions. The first distribution (labeled as 1) is that of the polymeric surfactant. On the low molecular weight side of the surfactant distribution, a small shoulder is evident for the three samples (marked with an arrow). This shoulder also corresponds with a strong UV absorbance

(marked with a double asterisk). These appear to be short, RAFT end-capped polymer chains. The second distribution (labeled as 2) increases in peak molecular weight and intensity with conversion. A neat RI-UV overlay of this peak indicates that these are RAFT end-capped chains. The ratio between the intensity of the UV signal marked with the double asterisk and the signal corresponding to the second distribution indicates that there is a higher concentration of shorter, RAFT end-capped chains. The concentration of the UV absorbing RAFT species will be much higher if the chains are shorter. The fact that the UV signal (**) shows a distinct peak and not a broad absorbance over the low molecular weight side of the second distribution does indicate that there are a distinct species of chains that have an *number average molecular weight* $\approx$2 900 g.mol^{-1}. The intensity of the UV peak will not provide quantative information viz the relative concentrations of chains. An important observation is that fact that the *peak molecular weight* of the controlled distribution (2) (the *number average* value cannot accurately be determined due to distribution overlap) is higher than the predicted value (20 290 versus 11 983 g.mol^{-1}). The third distribution (labeled as 3) increases in intensity with conversion, but the same cannot be said for the peak molecular weight. There is no UV absorbance in this region, which indicates that distribution 3 formed via conventional FRP. There is a small distribution (marked with an asterisk) at an elution volume similar to that of the RAFT agent. This distribution is probably unreacted RAFT agents in particles that were not nucleated.

In Figure 7.3 (B), chromatograms at identical conversions for the reactions in the presence and absence of the radical scavenger are overlaid and it is clear that there are no significant differences between the two polymer latexes. The first distribution (labeled as 1) is the polymeric surfactant distribution. The main differences between the two spectra (A and B) are as follows:

- The intensity of the UV signal marked with the double asterisk is much lower in the presence of the radical scavenger.

- The controlled distribution (labeled as 2) has a higher peak molecular weight in the absence of the radical scavenger, although it does appear that the polydispersity of this peak is smaller in the presence of the scavenger (an accurate value cannot be calculated due to the overlap of the controlled distribution with the surfactant distribution).

- The intensity and the peak molecular weight of the uncontrolled distribution (labeled as 3) are substantially higher for the control polymerization.

The results from particle size analysis for both B13 and B3 are given in Table 7.1:

Table 7.1: DLS results of the final latexes of polymerizations B3 and B13

Reaction	RAFT	Monomer	Surfactant	Radical trap	Z (average)	Polydispersity
B3	DIBTC	Styrene	Igepal®CO-990	-	163.6	0.017
B13				Fremy's salt	152.2	X

The particle sizes for both the latexes appear to be similar.

7.1.2. BUTYL ACRYLATE

Polymerization B11 (including Fremy's salt) and control polymerization B4 were investigated. The first-order rate plots for B4 and B11 are given in Figure 7.4:

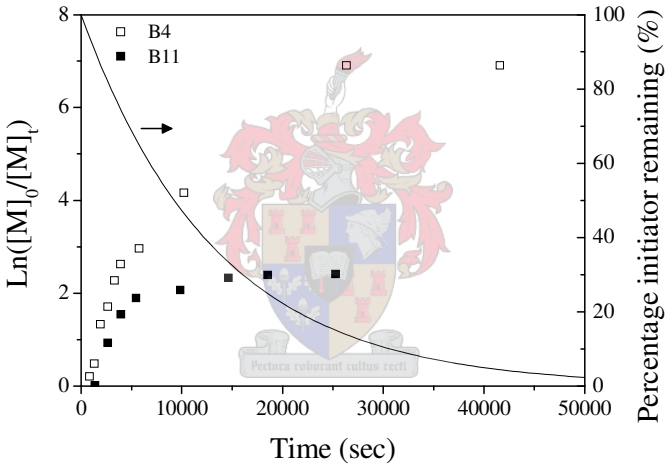

Figure 7.4: First-order rate plots for polymerizations B11 and B4.

The conversion after 24 hours for B11 (scavenger) is 93% whilst that for B4 (control) is 100%. The nucleation period is similar in the absence and presence of the radical scavenger. The rate of reaction appears to decrease at a greater rate during interval III in the presence of the scavenger. There is not as large a difference between the conversions of the butyl acrylate polymerizations, as was observed in Section 7.1.1 when the styrene polymerizations in the absence and presence of the scavenger were compared.

The GPC data for the butyl acrylate polymerizations give evidence of substantial uncontrolled polymer growth in the presence of the scavenger.

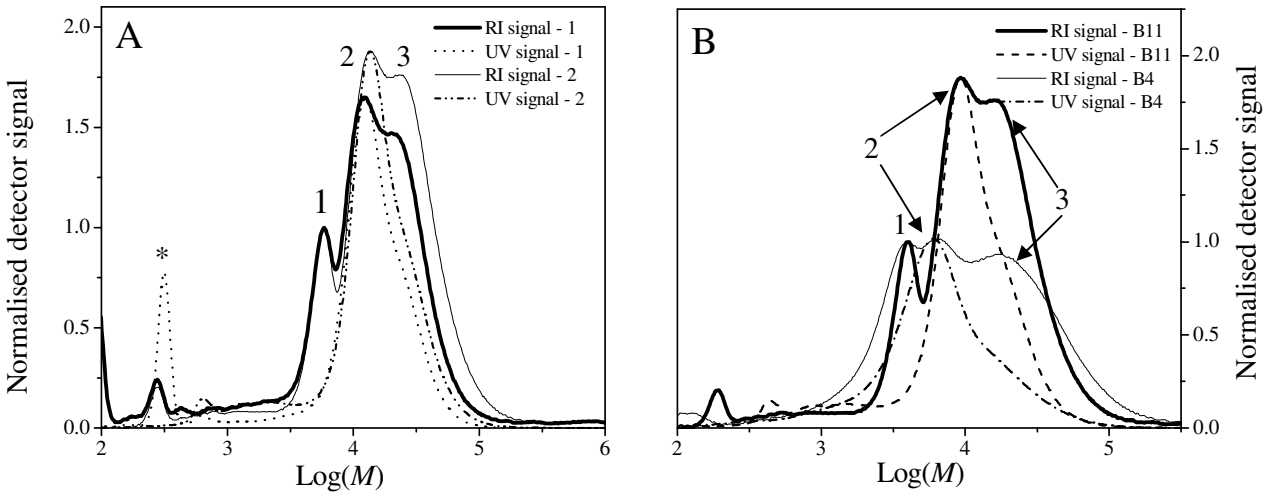

Figure 7.5: GPC chromatograms for A.) B11 and B.) a sample with a conversion of 95% for B4 and B11. Sample conversions for B11 are: (1) – 78% and (2) – 93%.

Chromatogram (A) in Figure 7.5 shows four distributions. The smallest distribution (marked with an asterisk) at a molecular weight of approximately 350 g.mol^{-1} is unreacted RAFT agent that is still present in the latex. The distribution labeled as 1 is that of the polymeric surfactant. The second distribution (labeled as 2) at a slightly higher peak molecular weight shows a perfect RI-UV overlay. This indicates that this distribution is formed by a RAFT-mediated polymerization and is potentially controlled. Between samples 1 and 2 for polymerization B11, there is a slight increase in peak molecular weight and an increase in intensity. The third distribution (labeled as 3) shows no UV absorbance and is identified as uncontrolled polymer. The overlay given in chromatogram B of Figure 7.5 indicates that the incorporation of Fremy's salt into the polymerization led to a substantial change in the final latex. Both the traces were normalised to the surfactant distribution (labeled as 1). The second distribution for B4 is much broader and overlaps with the surfactant distribution to a large extent, causing the surfactant distribution to appear wider. The second distribution (labeled as 2) for polymerization B11 has a greater intensity than the corresponding distribution in polymerization B4. The *peak molecular weight* for the second, controlled distribution is slightly higher for B11 (scavenger) (6 005 g.mol^{-1}) and for B4 (3 800g.mol^{-1}). The predicted *number average molecular weight* for both polymerizations at 95% conversion is 20 892 g.mol^{-1}. The same increase in M_p is observed for the third, uncontrolled distribution (labeled as 3) for polymerizations B4 and B11 (*peak molecular weight* is 23 949 g.mol^{-1} for B11 versus 16 680 g.mol^{-1} for B4). In general it can be said that both the second and third distribution for B4 are much broader than those of polymerization B11.

The results from particle size analysis of the final latexes of polymerization B4 and B11 are given in Tables 7.2 and 7.3:

Table 7.2: DLS results of the final latexes of polymerizations B4 and B11

Reaction	RAFT	Monomer	Surfactant	Radical trap	Z (average)	Polydispersity
B4	DIBTC	Butyl acrylate	Igepal®CO-990	-	163.1	0.056
B11				Fremy's salt	180.2	X

The average particle size and polydispersity values for B4 and B11 are similar. This suggests that the mechanistic behaviour of the two miniemulsion polymerizations could be similar in many aspects. Similar first-order kinetic plots and GPC chromatograms also imply similar mechanistic behaviour.

Table 7.3: CHDF results of the final latexes of polymerization B4 and B11

Reaction	Z (Number average)			Z (Weight average)		
	Mean	**Max**	**Standard deviation**	**Mean**	**Max**	**Standard deviation**
B4	109.9	101.1	35.7	167.5	130.1	87.1
B11	116.3	105.9	41.9	187.5	132.8	93.2

The weight average mean particle size results correspond well to the Z (average) values obtained via DLS. The CHDF chromatograms for B4 were given in Figure 4.20. When the chromatograms for B4 are compared to those given in Figure 7.6, it is clear that there is little difference between the two final latexes in terms of particle size and distribution.

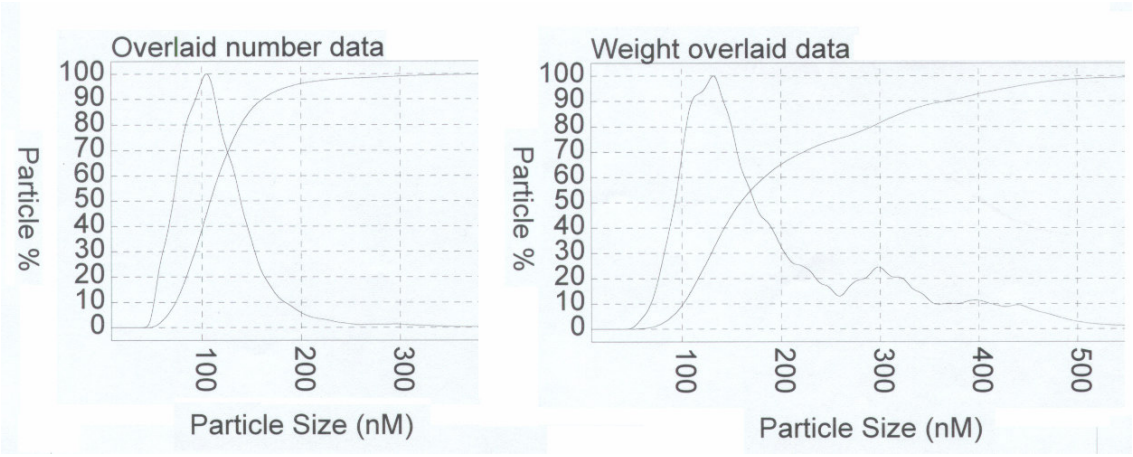

Figure 7.6: CHDF chromatograms of the final latex of polymerization B11.

The *number average* and *weight average* data show that there are primarily particles of roughly 110 nm in size. There is a lower concentration of larger particles. From the weight average chromatogram in Figure 7.6, it is evident that these particles range from 200 to 500 nm in size. The same phenomenon was reported earlier for other butyl acrylate polymerizations (Section 6.2.1.1). It was proposed that the larger particles are formed by possible coalescence of smaller particles. The fact that the larger particles are seen for both B4 and B11 eliminates the possibility that the coagulation might be due to the aqueous phase radical trap incorporation. The most important point that can be made in the comparison between the CHDF chromatograms for B4 and B11 is that there is little difference their profiles, which implies that there are few mechanistic differences between the two polymerizations.

7.1.3. THE ACTION OF FREMY'S SALT : SUMMARY AND CONCLUSIONS

Aqueous-phase radical scavengers ought to quench any radicals that are present in the aqueous phase. This implies that initiating radical fragments, propagating radical oligomers and even radicals that escape from the nucleated particles can be eliminated. The radical quenching action leads to rate retardation during the nucleation period. It will also influence the concentration of radicals in the two phases. In previous RAFT-mediated miniemulsions investigated in this study (Chapters 4-6), it was hypothesized that the radical leaving group created after the initialization step of the RAFT equilibrium could undergo exit from the particle. These radicals could undergo termination (causing rate retardation), propagation (leading to secondary particle growth) and even nucleation of previously unnucleated monomer droplets. The action of the radical scavenger will influence all these possible mechanistic pathways. The rate of aqueous phase radical quenching will depend on the concentration of the radical scavenger. In the previous two sections it is clearly seen that the styrene (7.1.1) and butyl acrylate (7.1.2) polymerizations behave uniquely in the presence of the radical scavenger.

The main differences between the control polymerizations and those incorporating the radical scavenger are highlighted.

1. Rate retardation.

The quenching of initiating fragments that partition into the aqueous phase will lead to a distinct retardation of the reaction rate during interval I. The largest difference in rate during interval I is seen for the styrene polymerizations. The higher concentration of butyl acrylate monomer in the

aqueous phase, as well as the increased propagation rate of BA, will lead to a higher rate of z-mer formation. An increased z-mer formation rate, coupled with an increased nucleation rate, will mean that the flux of radicals from the aqueous to oil phase will be higher for the BA polymerization. The action of the radical scavenger, with regards to termination of the initiating radicals, will thus be reduced. For the styrene polymerizations, a slow flux of radicals into the droplets implies an increased probability of termination of the initiating radicals in the aqueous phase before nucleation can take place. The same will hold true for any radicals that might desorb from the particles. The rate of radical exit will be similar for the two control polymerizations as well as those incorporating the radical scavenger. The fate of the radicals will depend on the ratio of the rates of termination and aqueous phase propagation. Therefore it can be speculated that in the BA polymerizations, aqueous phase propagation will be more probable whilst termination is more likely for the styrene polymerizations.

2. **Unreacted RAFT agents.**

The concentration of unreacted RAFT agent is very low for all four polymerizations investigated in Section 7.1. In Chapter 5 it was speculated that the concentration of the RAFT agents could be linked to the movement of radicals across the oil-water interface, especially after radicals begin to grow in length. The higher the radical flux between the two phases, the lower the concentration of unreacted RAFT agent. The existence of short RAFT end-capped chains in the styrene polymerizations as well as the absence of such a distribution in the butyl acrylate polymerizations indicates that the movement of radicals, that are nucleating droplets later in the polymerization, is dependent on the monomer. This was addressed when the roles of the surfactant and monomer were investigated in Chapter 5. The main point of interest here is that, although it appears that the radical scavenger is influencing the radical behaviour (from the rate retardation), little difference is observed in the GPC chromatograms, implying that the influence on the mechanism of polymer formation is minimal.

3. **Controlled versus uncontrolled polymer concentrations.**

The efficiency of the added aqueous phase radical trap can be deduced when comparing the GPC chromatograms of the respective polymerizations. Uncontrolled distributions in the control polymerizations, which show no UV absorbance at a wavelength of 320 nm, should theoretically not be visible in the polymerizations utilizing the trap. From the comparison

between polymerizations B13 and B3 (styrene) and B11 and B4 (butyl acrylate), it is evident that the complete removal of any uncontrolled distributions was not achieved. The GPC chromatograms for B13 and B11 still show a substantial concentration of uncontrolled polymer. The first-order rate plots for these polymerizations do provide evidence of some rate retardation, which is probably due to radical loss from the system. This radical loss could be due to the radical (initiating radical species or radical leaving groups) quenching action of the aqueous phase radical trap. The efficiency of the radical scavenger will vary with the rate of radical flux between the aqueous and oil phase. For the styrene polymerizations there appears to be little difference in molecular weight distribution, whilst for the butyl acrylate polymerizations there is considerable change in the relative concentration of controlled and uncontrolled polymer. It has been mentioned earlier (Chapters 4-7) that the reason that less uncontrolled polymer is seen for the styrene miniemulsions can be linked to the slower propagation of any radical species within the aqueous phase. Slower radical propagation will lead to increased termination via the radical scavenger. This implies that radical fragments that enter the aqueous phase later in the polymerization have a decreased probability of termination due to a lower radical scavenger concentration. For the butyl acrylate polymerizations it appears that the controlled and uncontrolled distributions are much narrower. For the controlled distribution this implies that most of the RAFT agent is consumed in a short time interval (fast nucleation). For many of the RAFT-mediated polymerizations investigated in this study, it has been proposed that nucleation of droplets by radicals other than that of the initiating fragments can take place. It is observed from the GPC chromatograms for B11 and B4 that the addition of a radical scavenger counteracts this phenomenon (more unreacted RAFT agents detected in the polymerizations, including the radical scavenger).

The action of the Fremy's salt radical scavenging appears limited. The fact that the molecular weight profile (or more specifically the concentration of uncontrolled polymer) does not change substantially in the presence of the aqueous phase radical scavenger implies that the efficiency of the radical scavenger is poor. Fremy's salt is a nitroxide that can reversibly react with carbon centered radicals,[5] but the reversible equilibrium can only be established at elevated temperatures (>100^{o}C). Radicals that react with the radical scavenger will thus be irreversibly terminated (reaction temperature is 75 ^{o}C). The poor radical scavenging ability exhibited by Fremy's salt could be linked to poor quality of the trap or degradation during the polymerization.

7.2. SODIUM NITRITE

The efficiency of the radical scavenger sodium nitrite is investigated. As was the case with Fremy's salt, sodium nitrite is a water soluble nitroxide. The rates of termination between the various radical species and the $NaNO_2$ will however be different. The styrene miniemulsions are investigated in Section 7.2.1, followed by the butyl acrylate miniemulsions in Section 7.2.2.

7.2.1. STYRENE MINIEMULSIONS

Polymerization B14, which includes the radical scavenger, and B3, the control, were investigated. The first-order rate plots for both are given in Figure 7.7:

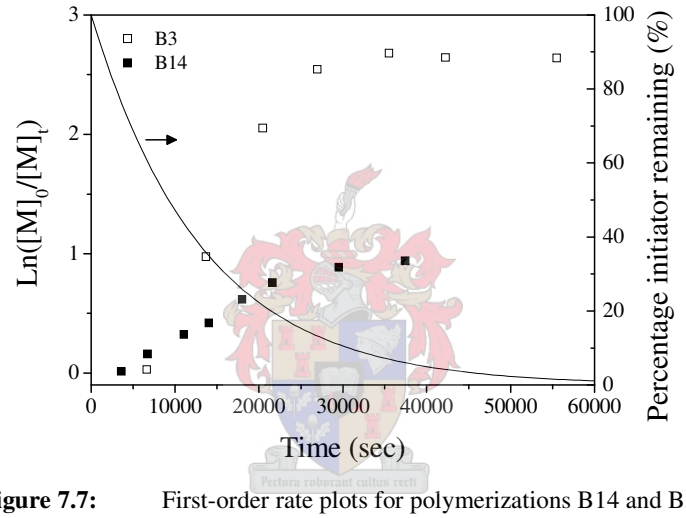

Figure 7.7: First-order rate plots for polymerizations B14 and B3.

The conversion after 24 hours for polymerization B14 is 60% and B3 is 93%. This overlay looks similar to that of the comparison of B13 and B3 given in Figure 7.2. It is apparent that there is rate retardation during interval I for B14. The inhibition period for B3 appears to be shorter than for B14. The length of interval I is similar for both reactions. The final conversion for B14 is much lower than that for B3, which implies that there is substantial loss of radicals during the polymerization.

The GPC chromatograms of B14 and an overlay of a sample with a conversion of 64% for both B14 and B3 are in Figure 7.8:

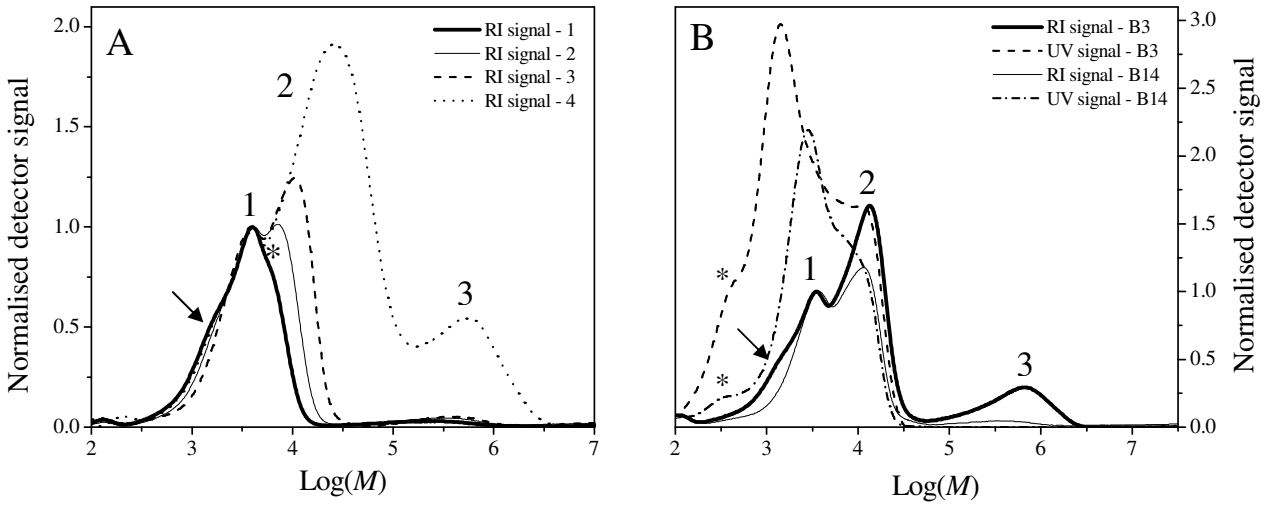

Figure 7.8: GPC chromatographs for A.) B14 and B.) a sample with a conversion of 64% for both B3 and B14. Sample conversions for B14 (A) are: (1) – 26%, (2) – 34%, (3) – 53% and (4) – 60%.

Chromatogram A shows two distinct distributions. The first distribution (labeled as 1) is that of the surfactant. There is a distinct shoulder on the low molecular weight side of the surfactant distribution (marked with an arrow). This shoulder decreases in intensity with an increase in conversion. The second distribution begins as a shoulder on the high molecular weight side of the surfactant distribution in sample 1 (marked with an asterisk). Distribution 2 increases in intensity and peak molecular weight with an increase in conversion, indicating controlled polymerization behaviour. The *peak molecular weight* of the controlled distribution in sample 4 is much higher than the predicted value (25 206 g.mol^{-1} versus 10 543 g.mol^{-1}). There also appears to be a broad polymer distribution at a peak molecular weight of 466 100 g.mol^{-1}.

The overlays of the samples from both B14 and B3 clearly indicate that there is a change in the latex with the incorporation of the aqueous phase radical trap. The surfactant distribution is labeled as 1. The low molecular weight shoulder (marked with an arrow) on this peak is of a greater intensity for B3 than B14. The RI-UV overlay indicates that this shoulder corresponds to a strong UV absorbance. There is also a shoulder on the low molecular weight side of the UV trace (marked with an asterisk), which corresponds to unreacted RAFT agent that is present in the miniemulsion. The UV trace overlays well with the second distribution for the samples from the polymerizations B14 and B3. This indicates that these are distributions with trithiocarbonate moieties in the polymer. The most important observation in chromatogram B in Figure 7.8 is that there is a large difference in the concentration of uncontrolled polymer between polymerizations B14 and B3. This

indicates that the aqueous phase radical trap may well have eliminated many of the aqueous phase radicals that could have initiated secondary, uncontrolled polymer growth.

The results of particle size analysis of the final latexes of polymerization B3 and B14 are given in Tables 7.4 and 7.5:

Table 7.4: DLS results of the final latexes of polymerizations B3 and B14

Reaction	RAFT	Monomer	Surfactant	Radical trap	Z (average)	Polydispersity
B3	DIBTC	Styrene	Igepal®CO-990	-	163.6	0.017
B14				$NaNO_2$	156.2	0.021

The average particle sizes of polymerizations B3 and B14 are similar. The similarity in *polydispersity value*s is unexpected since it is assumed that, due to the radical quenching action of the sodium nitrite, there would be vast mechanistic differences between the polymerization in or without the presence of the scavenger. These values are similar to those obtained for polymerizations B13 and B3, where Fremy's salt was used as the aqueous phase radical trap rather than sodium nitrite.

Table 7.5: CHDF results of the final latexes of polymerizations B3 and B14

Reaction	**Z (Number average)**			**Z (Weight average)**		
	Mean	**Max**	**Standard deviation**	**Mean**	**Max**	**Standard deviation**
B3	92.6	47	41.5	142.7	145.7	42
B14	109.9	101.1	35.7	167.5	130.1	87.1

The CHDF chromatograms for B3 are given in Figure 5.11. A comparison between the *number average* values for B3 and B14 indicates that the largest species of particles for both polymerizations is around 95 nm in size. The distribution of sizes is narrower for B14, which indicates that most of the particles are formed via the same process. The *weight average* data for B14 does show evidence of larger particles that will cause the *standard deviation* value to increase. A comparison between the *number average CHDF chromatograms* of B14 and B3 is given in Figure 7.9, so as to allow for a comparison between the two latexes.

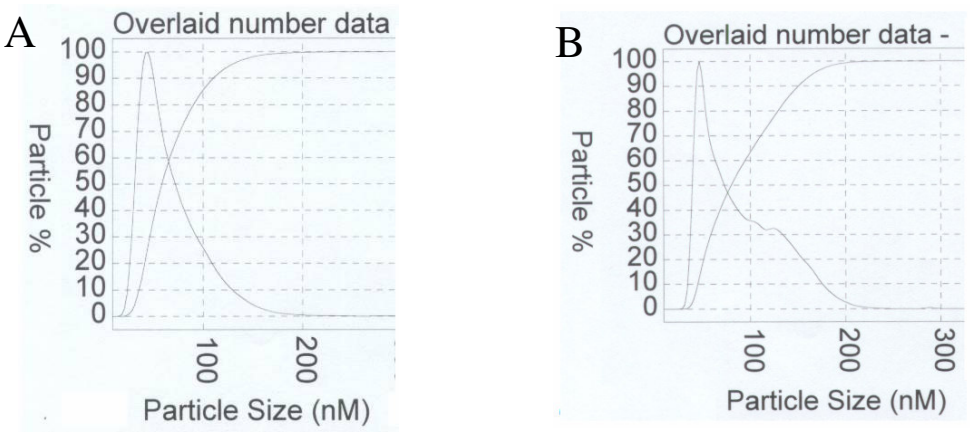

Figure 7.9: Number average CHDF chromatograms of the final latexes of polymerizations A.) B14 and B.) B3.

From Figure 7.9 it is clear that for B3 there is a definite species of particles around 130 nm in size. This species does not occur in the same concentration in polymerization B14. The primary distribution lies at a particle size of 45 nm for B14 and 47 nm for B3. It is possible that these particles are formed via a similar mechanism. A TEM micrograph of the final latex of polymerization B14 is given in Figure 7.10.

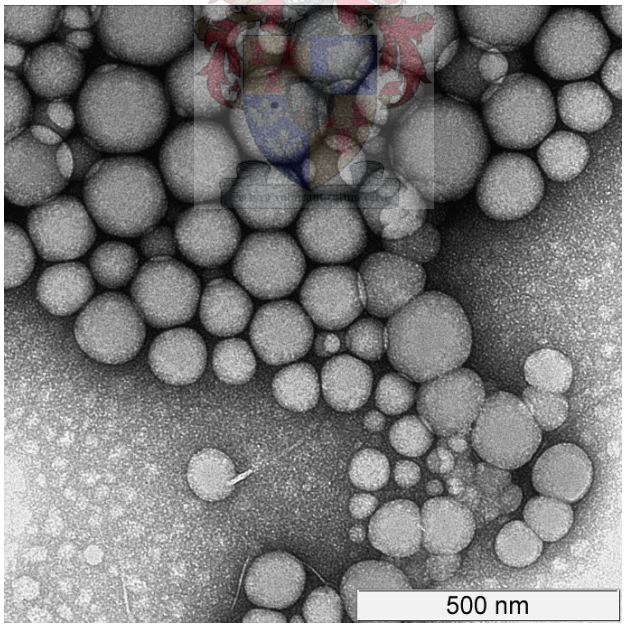

Figure 7.10: TEM micrograph of the final latex of polymerization B14.

Figure 7.10 shows a distribution of larger particles of around 120 nm. There are numerous particles that are about 40 nm. This wide distribution of sizes indicates that the duration of particle formation is fairly long.

7.2.2. BUTYL ACRYLATE MINIEMULSIONS

Polymerizations B12 and B4 are investigated in this section. The radical scavenger is present for polymerization B12. The first-order rate plots for B4 and B12 are given in Figure 7.11:

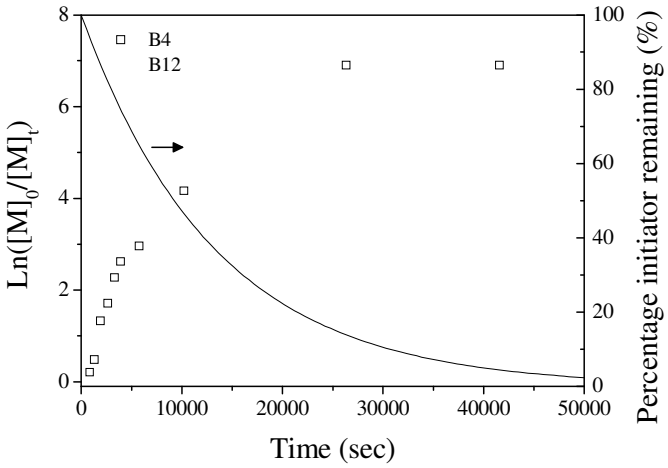

Figure 7.11: First-order rate plots for polymerizations B12 and B4.

The conversion after 24 hours for B12 is 93% whilst for B4 it is 100%. This reduction in conversion is similar to that observed in the comparison between B14 and B3. There is a distinct inhibition period for B12 that lasts for about 1.5 hours. After this, the rate of reaction increases. The duration of interval I is much shorter for B4.

The GPC chromatograms of B12 and an overlay of a sample with a conversion of 95% for both B4 and B12 are given in Figure 7.12:

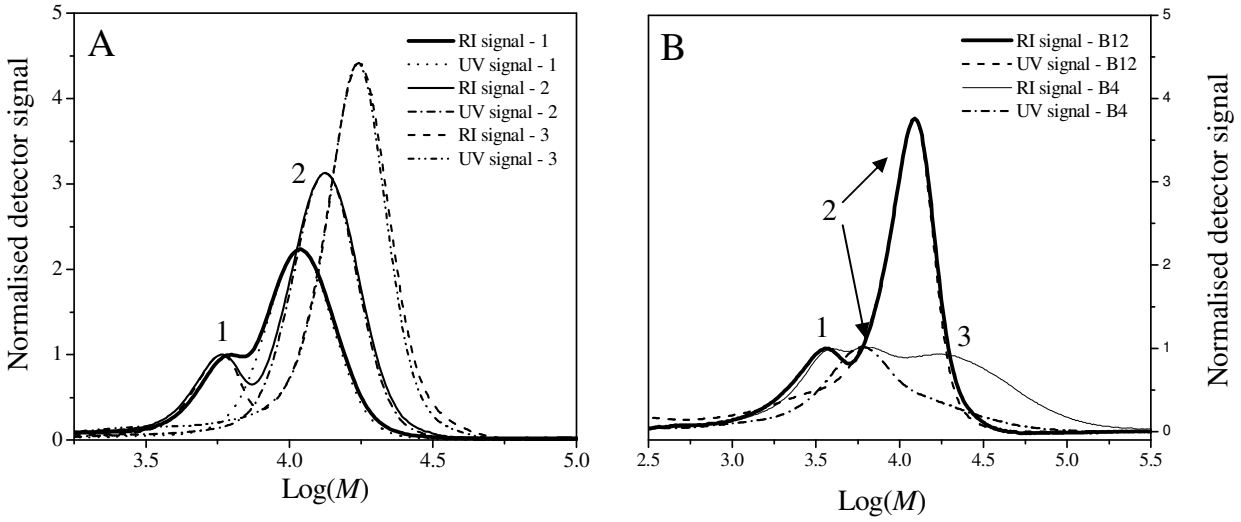

Figure 7.12: GPC chromatograms of A.) B12 and B.) a sample with 95% conversion for both B4 and B12. Sample conversions for B12 are: (1) – 49%, (2) – 60% and (3) – 93%.

From the chromatogram in Figure 7.12 it is clear that there are two distinct distributions. The first distribution labeled as 1 is the surfactant. The second distribution (labeled as 2) exhibits a perfect RI-UV overlay, which indicates that this distribution is controlled. The controlled distribution increases in intensity and peak molecular weight with an increase in conversion, implying controlled polymer growth. The peak molecular weight of the final sample is 17 443 g.mol^{-1}, which is very close to the targeted molecular weight for this polymerization (target $\overline{M}_n$ is 17 000 g.mol^{-1}). There are no visible uncontrolled distributions in the latex.

From the comparison in chromatogram B, it is clear that there are vast differences between the two latexes. The surfactant is labeled as 1. For B4, two distributions (other than the surfactant distribution) are clear, whereas for polymerization B12 there is only one distribution other than the surfactant. The RI-UV overlay for the sample for B4 indicates that the second distribution (labeled as 2) is controlled. This distribution is at a slightly lower peak molecular weight in B4 compared to that in B12. The most important observation from this comparison is that there is a definite elimination of any uncontrolled polymer growth in polymerization B12.

The results of particle size analysis of the final latexes of polymerizations B4 and B12 are given in Tables 7.6 and 7.7:

Table 7.6: DLS results of the final latexes of polymerizations B4 and B12

Reaction	RAFT	Monomer	Surfactant	Radical trap	Z (average)	Polydispersity
B4	DIBTC	Butyl acrylate	Igepal®CO-990	-	163.1	0.056
B12				$NaNO_2$	226.1	X

The average particle size for B12 is much larger than that of B4. This large difference was not seen when comparing B4 and B11.

Table 7.7: CHDF results of the final latexes of polymerizations B4 and B12

Reaction	Z (Number average)			Z (Weight average)		
	Mean	**Max**	**Standard deviation**	**Mean**	**Max**	**Standard deviation**
B4	109.9	101.1	35.7	167.5	130.1	87.1
B12	126.3	111.9	63.1	236.4	172.8	99.5

The chromatogram of B4 was given in Figure 5.20 and that of B12 is given in Figure 7.12:

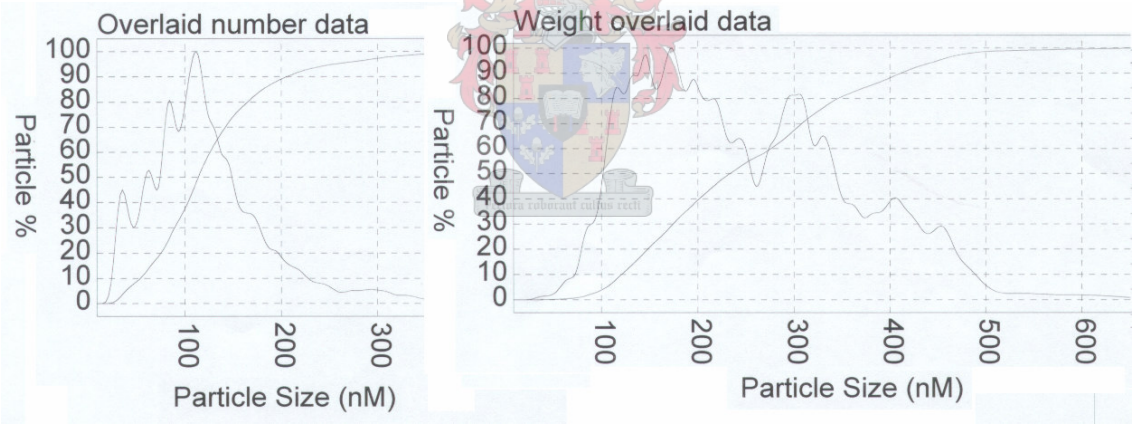

Figure 7.13: CHDF chromatograms of the final latex for polymerization B12.

From the chromatogram shown in Figure 7.13, it is clear that there is a wide range of particle sizes. From the number overlaid chromatogram for B12 it is evident that most particles are roughly 110 nm in size. The strange profile of the chromatogram indicates that there is a spread of smaller particles in the latex. A TEM micrograph of B12 is given in Figure 7.14.

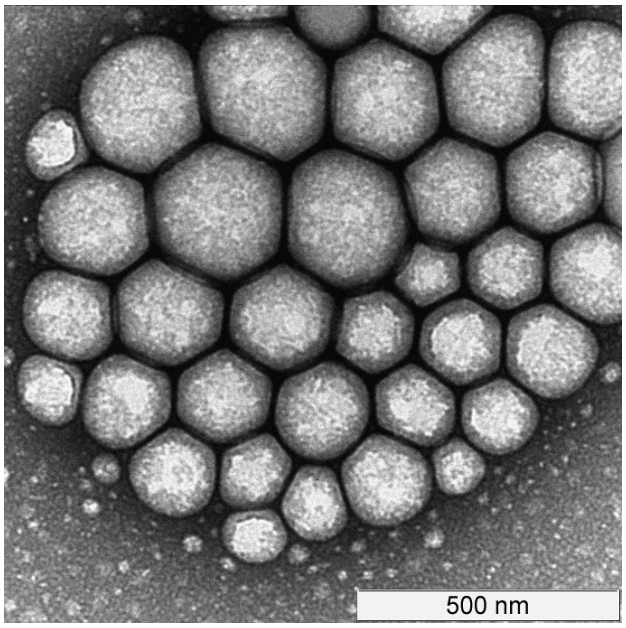

Figure 7.14: TEM micrograph of the final latex of polymerization B12.

The particles shown in the micrograph in Figure 7.14 have a larger average particle size than those observed in the TEM micrograph for the styrene polymerization B14 in Figure 7.10. This corresponds well with the DLS and CHDF data for both latexes. There appear to be fewer small particles in B12 than in B14. A narrower distribution of particle sizes implies that the duration of interval I (nucleation time) is shorter. When comparing the standard deviation values of the CHDF data for B14 and B12, it is evident that the particle size distribution for B14 is much narrower.

7.2.3. THE ACTION OF SODIUM NITRITE: SUMMARY AND CONCLUSIONS

The use of sodium nitrite as an effective agent against the growth of uncontrolled polymer within a RAFT-mediated miniemulsion polymerization was considered in this section. From the GPC data collected for B14 and B12 (sodium nitrite) as compared to data for B3 and B4 (controls) respectively, it is clear that with the addition of the aqueous phase radical trap there was a significant gain in control over the polymerization. Very little uncontrolled polymer was observed in the GPC chromatograms. First-order rate plots for these two polymerizations showed substantial rate retardation due to radical loss from the system. Similar points to those addressed for the Fremy's salt polymerizations will be addressed with respect to the sodium nitrite polymerizations.

1. **Inhibition and rate retardation.**

The quenching of initiating radicals within the aqueous phase will lead to the retardation of the reaction rate during interval I. This was seen to a greater degree for the styrene polymerization (B14). This was linked to the slower nucleation and thus increased concentration of initiating radicals within the aqueous phase that can potentially undergo termination. The inhibition period observed for the butyl acrylate polymerization (B12) was not seen in the control styrene polymerization (B4). The GPC chromatogram for B12 indicated the absence of any uncontrolled polymer. This implies that the radical scavenger successfully eliminated (terminated) the radicals that may have initiated secondary particle formation. This termination would lead to the inhibition period.

2. **Consumption of RAFT agents.**

A low concentration of unreacted RAFT agent was observed for the butyl acrylate polymerizations in the presence of sodium nitrite as well as without. This was linked to increased nucleation for the BA polymerizations. One important point is that there is still substantial nucleation even though the concentration of initiating radicals in the aqueous phase was reduced by the radical scavenging action of the sodium nitrite.

3. **Concentration of uncontrolled versus controlled polymer.**

The main focus of this section is the ratio of the concentrations of uncontrolled to controlled polymer. The action of the radical scavenger will eliminate aqueous phase radicals, which could be initiating radical fragments, z-mers, and/or radical leaving groups. If aqueous phase initiation is assumed to be the dominant initiating mechanism, any radicals that are formed within the aqueous phase will be eliminated (equal concentrations of radical scavenger and initiating radicals). Oil-phase initiation will not be affected by the presence of the radical scavenger. It was apparent that for the styrene miniemulsion in the presence of the radical scavenger (B14) there was evidence of conventionally formed polymer. The rate of reaction was however retarded, implying that radical termination was taking place. The slower formation of z-mers for the styrene miniemulsions corresponds to greater termination in the aqueous phase (and thus retardation). This implies that the radical scavenger concentration will constantly decrease from the onset of the polymerization. The aqueous phase radical scavenger concentration will decrease linearly with time due to the steady influx of initiating radicals into the aqueous phase.

Radicals (initiating fragments or radical leaving groups) that exit into the aqueous phase at a later stage in the polymerization, thus have an ever decreasing probability of termination, leading to increased uncontrolled polymerization. This hypothesis is corroborated by the fact that the conventionally polymerized polymer for B14 was only detected at 60% conversion (which corresponds to 20 hours into the polymerization).

The faster z-mer formation and droplet nucleation for the butyl acrylate polymerizations (B12) lead to decreased radical termination within the aqueous phase. The control polymerization (B4) showed substantial uncontrolled polymerization, which was linked (in Section 5.1) to the increased radical concentration due to the exit of radical leaving groups from nucleated droplets. This would have occurred in B12 and would have resulted in the inhibition period that can be observed (radicals terminated by the sodium nitrite). The faster propagation of the exited radicals would however lead to substantial radical entry. Thus, if the aqueous phase radical scavenger concentrations for the butyl acrylate (B12) and styrene polymerization (B14) are compared, then the former will probably be greater. This implies that any radicals that could exit later in polymerization B12 would have been efficiently eliminated, leading to optimal control of the polymerization.

The action of sodium nitrite in RAFT-mediated polymerizations is monomer dependent. This is linked mainly to the rate of z-mer formation in the aqueous phase. A faster rate leads to less termination of these oligomeric radicals by the radical scavenger resulting in a slower consumption of the scavenger. Achieving maximum control of the polymerization will result.

7.3. FREMY'S SALT VERSUS SODIUM NITRITE.

The addition of an aqueous phase radical trap allows simplification of the possible mechanistic pathways operating within the miniemulsion polymerization by eliminating aqueous phase initiation. The mechanistic model of miniemulsion polymerizations given in Section 2.2.2 starts with the formation of z-mers within the aqueous phase. It has been shown that the initiation of polymerization can proceed even if z-mers are unable to form within the aqueous phase.[2] The main purpose of the polymerization comparisons constructed in this chapter was to investigate whether the initiation location of uncontrolled polymerization is in the aqueous phase. In this study it has been proposed that any uncontrolled polymerization taking place within the miniemulsion originates from radical species that desorb from the nucleated particles into the aqueous phase or

radicals that form in the aqueous phase. These radicals may be radical leaving groups formed after the fragmentation of the RAFT agent during the initialization step. If this is true, then by eliminating the desorbed radical by means of a radical scavenger we should see a distinct decrease in the uncontrolled polymer growth.

The action of the radical scavenger in retarding the rate of polymerization is apparent as can be seen in Sections 7.1 and 7.2. This implies that radicals are continuously being terminated within the aqueous phase. The oddity in the behaviour of the aqueous phase radical traps lies in the dependence of the behaviour on the monomer utilized. Very different behaviour was observed when the monomer was changed. It appears that the radical scavengers are more effective if butyl acrylate is used as the monomer. This might be due to the higher rate of z-mer formation (as compared to styrene) within the aqueous phase for butyl acrylate or due to faster exit of z-mers from particles. The increased rate of z-mer formation leads to a shorter nucleation time. This in turn will lead to a short time between the onset of the polymerization and the first interaction between the radical oligomer and RAFT agent within the particle. The shorter this time, the higher is the concentration of the radical trap within the aqueous phase that has not yet reacted with any initiating radicals. This implies that if any radicals do exit from the particles, they will, with the greatest probability, terminate within the aqueous phase. This hypothesis can successfully explain why, in the styrene miniemulsions, there is a less prominent reduction of uncontrolled polymer growth when an aqueous phase radical trap is utilized, yet this only occurs at 60% conversion.

The efficiency of the two radical traps is linked to the ability of the trap to prevent secondary particle formation. GPC data revealed that the Fremy's salt was less efficient. This can be linked either to poor scavenging for the radicals in the aqueous phase or to degradation of the scavenger during the polymerizations. From the GPC chromatograms for the two styrene polymerizations with their respective radical scavengers, it was clear that for Fremy's salt, the onset of secondary particle formation was approximately 40% conversion, whilst for sodium nitrite it was 60%. For this reason, it could be proposed that the only reason that the Fremy's salt appeared to be less efficient was due to an earlier depletion of the scavenger or degradation. The same was not true for the butyl acrylate polymerizations where it was observed that the retardation was slightly lower for the sodium nitrite. This could indicate that the efficiency of the sodium nitrite as a radical scavenger is higher. In conclusion, it can be said that incorporating an aqueous phase radical scavenger such as Fremy's salt or sodium nitrite can eliminate secondary particle formation. The efficiency and extent of this

elimination is dependent on the miniemulsion system utilized as well as the scavenger concentration. An optimal formulation will need to be determined for each specific monomer type.

7.4. REFERENCES

(1) Blythe, P. J.; Sudol, E. D.; El-Aasser, M. S. *Journal of Polymer Science Part A: Polymer Chemistry* **1997**, *35*, 807

(2) Luo, Y.; Schork, F. J. *Journal of Polymer Science Part A: Polymer Chemistry* **2002**, *40*, 3200

(3) Lacik, I.; Casey, B. S.; Sangster, D.; Gilbert, R.; Napper, D. H. *Macromolecules* **1992**, *25*, 4066

(4) McLeary, J. B.. In PhD thesis, University of Stellenbosch, **2004**

(5) Matyjaszewski, K.; Davis, T. P. *Handbook of Radical Polymerization*; John Wiley and Sons, Inc.: Hoboken **2002**

Chapter 8. : *Conclusions and recommendations*

8.1. CONCLUSIONS

The primary objective laid out in Section 1.6 focused on achieving RAFT-mediated miniemulsion polymerizations that exhibit living radical polymerization characteristics (laid out in Section 2.3) and produce stable latexes (shelf life-times of over one week). Whilst it was observed that for all RAFT-mediated miniemulsion polymerizations investigated stable latexes (shelf life-times of over one year) were produced, LRP characteristics were not achieved in all cases. The deviations were linked to the effects that the various reaction components of the miniemulsion (shown in Figure 1.2) have on the kinetic and mechanistic behaviour of the RAFT-mediated miniemulsion polymerizations.

Elementary kinetic information regarding conventional FRP miniemulsion polymerizations was gathered in Chapter 4. The kinetic model that would best describe the conventional FRP miniemulsions was established. This model could then act as a base upon which more complex descriptions of RAFT-mediated minemulsions can be built. The following conclusions can be made from the results given in Chapter 4:

- Z-mer entry rate is similar for both non-ionically and ionically stabilized styrene miniemulsions, and is slightly higher for butyl acrylate miniemulsions. This implies that even though there is a large difference in monomer droplet surface area (much less for the non-ionically stabilized droplets) and hydration layer (thicker for non-ionically stabilized droplets) when using the two surfactants, the resultant z-mer entry rate is unaffected. This could imply that the entry rate (k_{ENTRY}) is not rate-determining.

- The profile of the reaction rate can deliver information about the kinetic behaviour of the polymerization. It was speculated that the larger non-ionically stabilized miniemulsions exhibited typical *pseudo-bulk* kinetics whilst the smaller ionically stabilized miniemulsions follow *zero-one* kinetics.

The introduction of a RAFT agent into a miniemulsion formulation alters the kinetic and mechanistic behaviour of the miniemulsion due to the changed propagating radical concentrations and component locations in the reaction. Rate retardation and inhibition were observed for various RAFT-mediated miniemulsion polymerizations given in Chapters 5-7. This implies that the RAFT process influences the radical steady-state that is established in the miniemulsion. The following conclusions can be made to the results obtained in Chapter 5:

- Differences in reaction rates between styrene and butyl acrylate monomers can be linked to the differing rates of z-mer formation and z-mer entry into the droplets. One important observation is that these two rates will also influence the secondary particle formation. Increased uncontrolled polymerization is seen with the more water-soluble butyl acrylate monomer. This was contrary to what was expected as it was assumed that the fast nucleation of BA miniemulsions would lead to complete droplet nucleation and optimal control over the polymerization.

- Evidence of unreacted RAFT agents indicates poor droplet nucleation. An indirect relationship between the concentration of unreacted RAFT agents and inhibition periods was observed. The concentration of unreacted RAFT agent appeared to be less for styrene polymerizations. It is speculated that this is due to slower Ostwald ripening of nucleated particles leading to less competition between particles and unnucleated droplets for radicals in the aqueous phase.

- From reduced rate retardation and shorter inhibition periods for miniemulsions stabilized with Igepal®CO-990 (non-ionic surfactant), it was concluded that the extent to which the RAFT process influenced the radical steady-state was reduced. The larger size of the particles stabilized by the non-ionic surfactant implied that oil-phase initiation was more prominent and less radical movement across that water-oil phase interface was required for particle nucleation. This however should have lead to an increased consumption of RAFT agent, which was seen not to be the case. Extensive conclusions regarding the role of oil-phase initiation in the RAFT-mediated miniemulsion polymerizations cannot be drawn from the data obtained.

- Larger particles lead to less defined inhibition periods. The altered kinetics of the RAFT-mediated miniemulsions is linked to a changing radical flux (into the aqueous phase). The change in radical steady-state in the aqueous phase is limited for larger particles for which exit was less probable or oil-phase initiation is more probable.

- By increasing the aqueous phase radical concentration by using a water-soluble initiator, the steady-state radical equilibrium concentration is disturbed to a lesser degree by any additional radicals that may enter the aqueous phase from the particles i.e. the initiator acts as a type of radical scavenger.

Conventional FRP can occur in secondary particles, which are formed by the nucleation of a micelle by a z-mer formed in the aqueous phase. In Chapter 5 it was seen that this process occurred to varying extents when the RAFT agent was changed. A distinct relationship between the inhibition periods and concentrations of uncontrolled polymer could be constructed: increased inhibition implied increased concentration of uncontrolled polymer.

The RAFT process influences the radical concentration in the aqueous phase, leading to increased termination (inhibition) and secondary particle formation. From the investigations in Chapter 6, it can be concluded that, due to the fact that RAFT agents with fast addition/fast fragmentation equilibria were shown to lead to substantial inhibition and secondary particle formation and RAFT agents with fast addition/slow fragmentation equilibria were shown to lead to substantial rate retardation and minimal inhibition and secondary particle formation:

- The radical leaving group can undergo exit, and the extent to which it exits would depend on its concentration in the particles. RAFT agents that show substantial intermediate radical stabilization thus lead to minimal radical exit and disturbance of the steady-state equilibrium.

- Decreased radical exit leads to less rate inhibition and reduced secondary particle formation when the non-ionic surfactant is utilized. This can be related to effect of particle size and hydration layer structure.

A reduction in radical exit can be achieved by decreasing the radical leaving group's water solubility. This implies that to optimize the control over the polymerization, the RAFT structure is of great importance. The RAFT equilibrium (intermediate radical stability) must be taken into consideration as well as the structure of the radical leaving group.

For many of the RAFT-mediated miniemulsions, high concentrations of unreacted RAFT agents were detected in the final latexes. It can be concluded that droplet nucleation was inefficient in these polymerizations. For polymerizations in which substantial radical leaving group exit took place, very low concentrations of unreacted RAFT agents were observed. This implies that radical exit should not be seen in a negative light. In an ideal miniemulsion, the aqueous phase surfactant concentration is kept as low as possible, whilst still maintaining latex stability, such that there are few micelles. If this is indeed the case, then leaving group radical exit could be harnessed to increase the droplet nucleation efficiency of the miniemulsion.

An effective means of avoiding secondary particle formation is by utilizing aqueous phase radical traps that will "mop up" excess radicals in the aqueous phase that could otherwise initiate secondary particle formation. The use of these radical scavengers was addressed in Chapter 7. The varying abilities of these radical scavengers to eliminate substantial rate retardation and secondary particles were linked to scavenging ability and concentration depletion rate. Slower polymerizations (styrene polymerizations) lead to increased consumption of the radical scavenger by the conventional radical steady-state rather than the new radical influx (into the aqueous phase) due to particle nucleation. Furthermore, it implied that secondary particle formation actually increased after a point where the radical scavenger was substantially depleted.

In conclusion it can be stated that formulations which allow RAFT agents with fast addition / fast fragmentation equilibria to be used in miniemulsion polymerization stabilized by high surfactant concentrations while maintaining defined living radical polymerization characteristics in the resultant latexes were developed. The fine control over the radical flux that is required was achieved by understanding that the RAFT agent structure, initiator hydrophobicity and particle size all influence the radical flux and determining suitable conditions based on this understanding. The latexes were formed rapidly and had excellent shelf life.

8.2. RECOMMENDATIONS

The application of the RAFT process in miniemulsion polymerization requires a clear understanding of the numerous experimental variables and their potential impact on the polymerization. Various LRP techniques have failed in miniemulsion polymerizations due to poor partitioning of active species between the two phases. It has been speculated that the nature of the RAFT process is such that it could effortlessly be applied in miniemulsions. In this thesis it has been shown that regardless of the improvements that the RAFT process inherently brings to a partitioned system, an understanding of the fundamental aspects of the RAFT and miniemulsion processes is required for successful implementation. In an optimal RAFT-mediated miniemulsion polymerization, little secondary particle formation should occur. All the active RAFT agents should remain in the particles, and radical exit should be at a minimum. Selection of an appropriate monomer, surfactant, initiator and RAFT agent is crucial in obtaining a functional miniemulsion that will deliver the desired product. The dual formation of secondary particles and primary particles (droplets) could be used in applications where bimodal molecular weight distributions are required.

Further study into the various kinetic aspects of RAFT-mediated miniemulsions is therefore required. The role of oil-phase initiation and the thick hydration layer of the non-ionic surfactant are still not adequately clear. Stronger analytical tools like 2D GPC and CHDF coupling; and dual detector CHDF and RI (or even UV) could provide further insight into nucleation mechanisms operating in these complex polymerizations.

In conclusion, as can be stated in many fields of science: quality and quantity often do not walk hand in hand. A defined product often requires fine control, which cannot be rushed. In order to scale up and intensify the application of RAFT-mediated miniemulsions, much research is still required to optimize its speed and efficiency.

Appendixes. : *Addendums to Chapter 3*

Appendix A: Cyanovaleric acid dithiobenzoate (CVADTB)

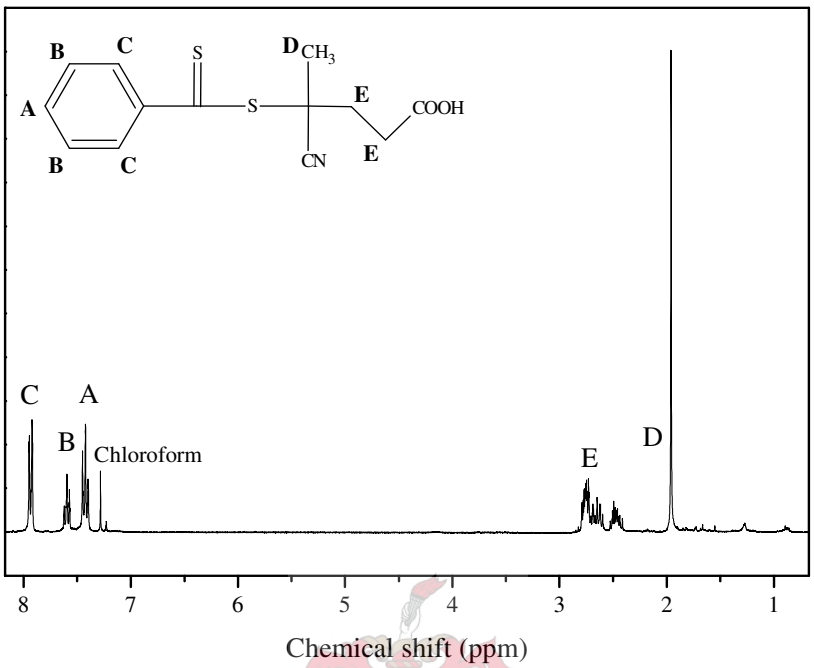

Figure A1: ^{1}H-NMR spectrum of cyanovaleric acid dithiobenzoate in $CDCl_3$.

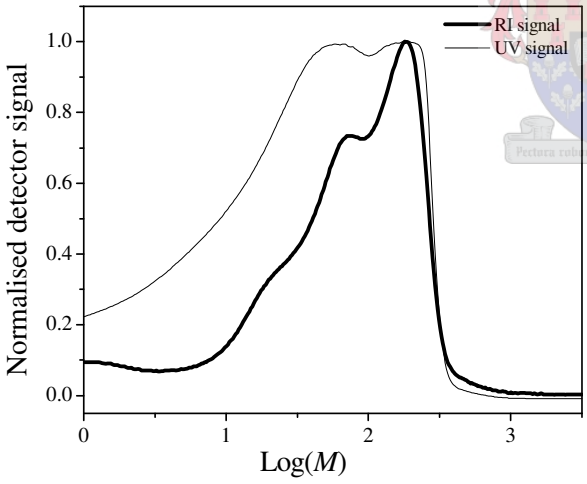

Figure A2: GPC chromatogram of CVADTB.

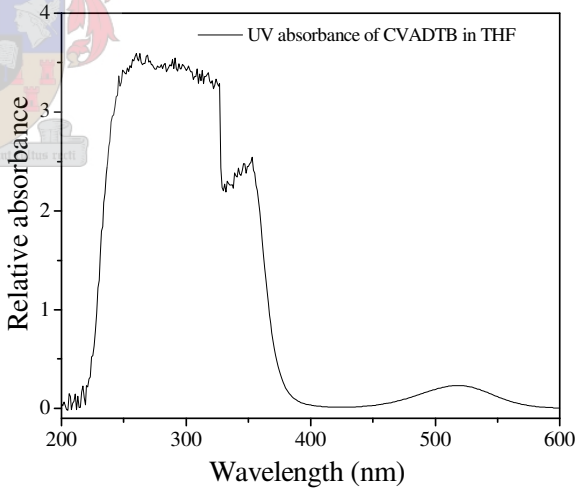

Figure A3: UV absorbance spectrum of CVADTB in THF.

Appendix B: 1-Phenylethyl dithiobenzoate (PEDTB)

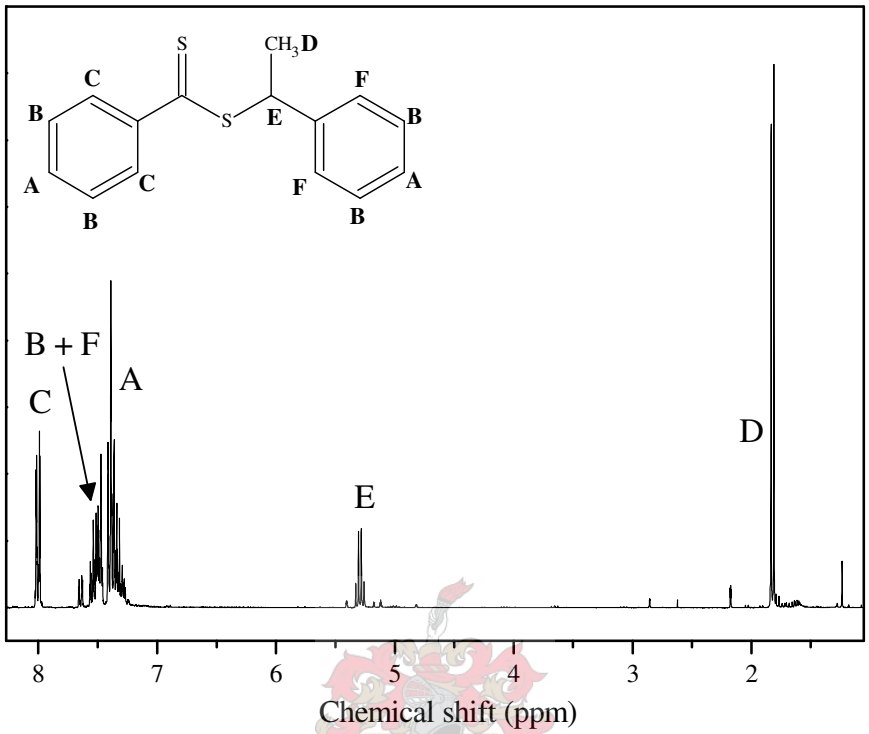

Figure B1: ^{1}H-NMR spectrum of 1-phenylethyl dithiobenzoate in $CDCl_3$.

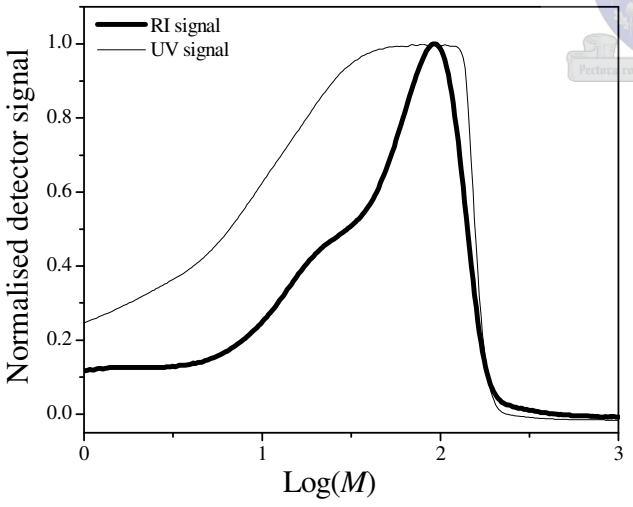

Figure B2: GPC chromatogram of PEDTB

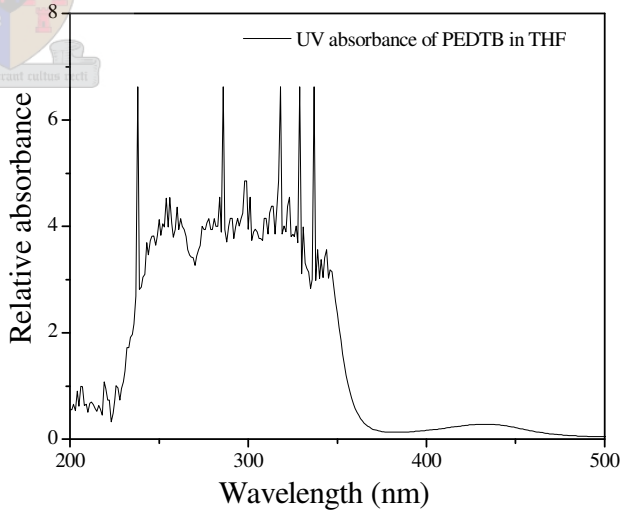

Figure B3: UV absorbance spectrum of PEDTB in THF.

Appendix C: S-Dodecyl-S'-isobutyric acid trithiocarbonate (DIBTC)

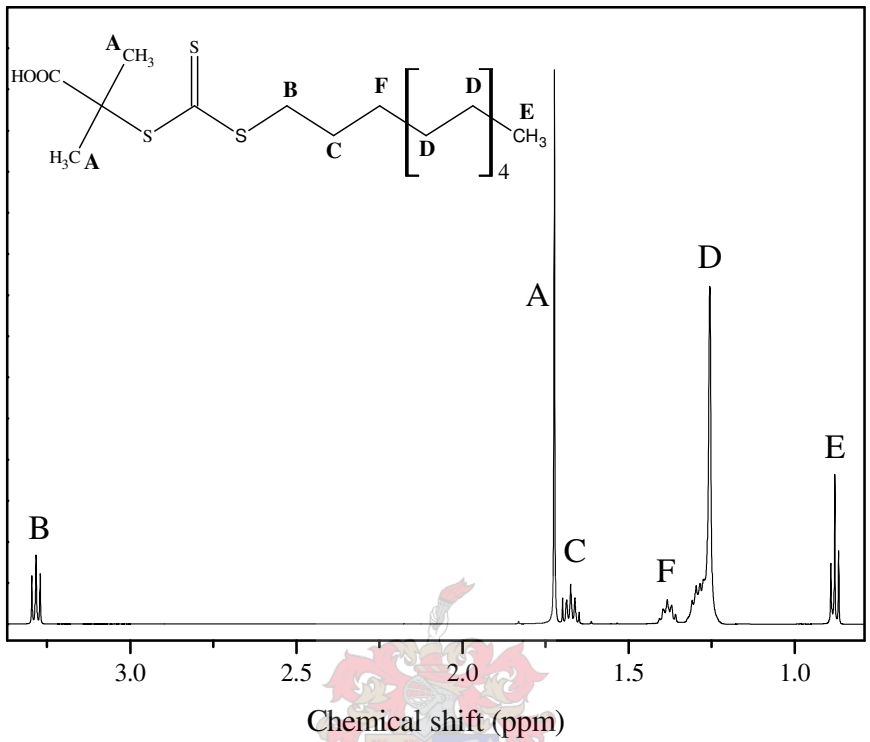

Figure C1: ^{1}H-NMR spectrum of S-dodecyl-S'-isobutyric acid trithiocarbonate in $CDCl_3$.

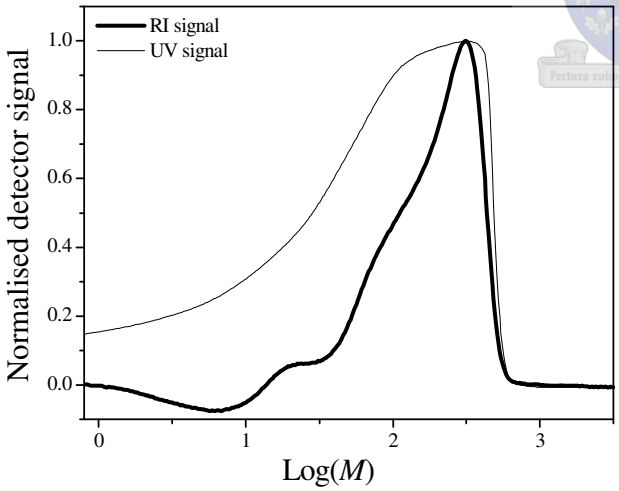

Figure C2: GPC chromatogram of DIBTC.

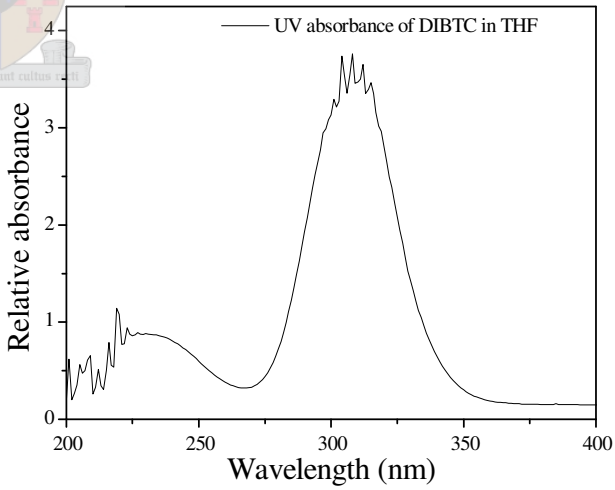

Figure C3: UV absorbance spectrum of DIBTC in THF.

Appendix D: S-Dodecyl-S'-phenylethyl trithiocarbonate (DPTC)

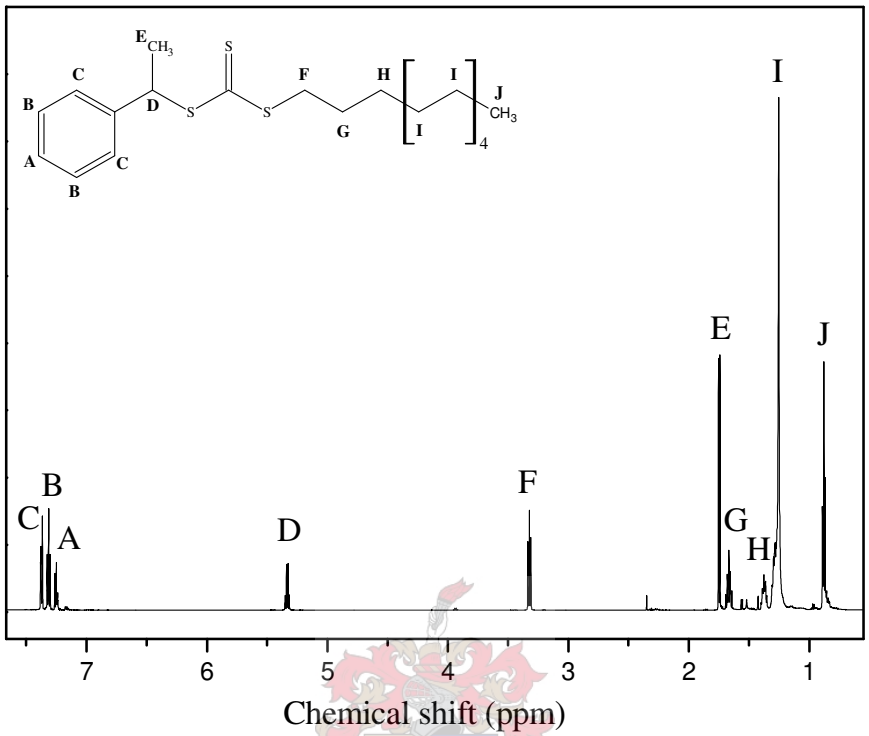

Figure D1: ^{1}H- NMR spectrum of S-dodecyl-S'-phenylethyl trithiocarbonate in $CDCl_3$.

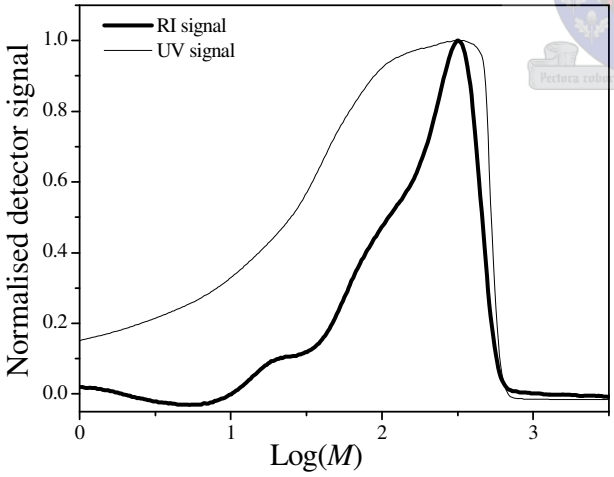

Figure D2: GPC chromatogram of DPTC.

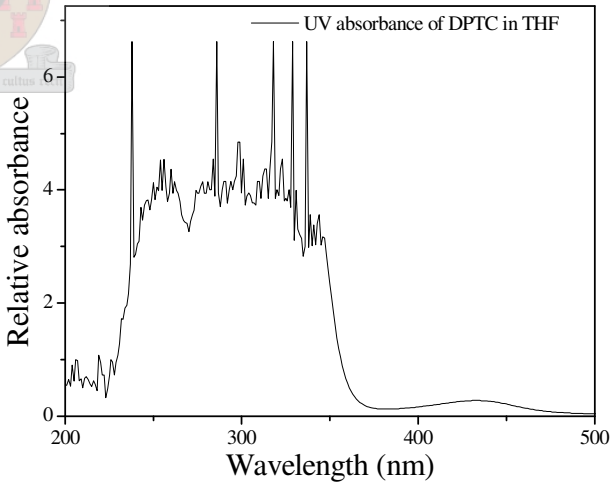

Figure D3: UV absorbance spectrum of DPTC in THF.

Pectora roborant cultus recti